METASTASIS: FROM CELL ADHESION AND BEYOND
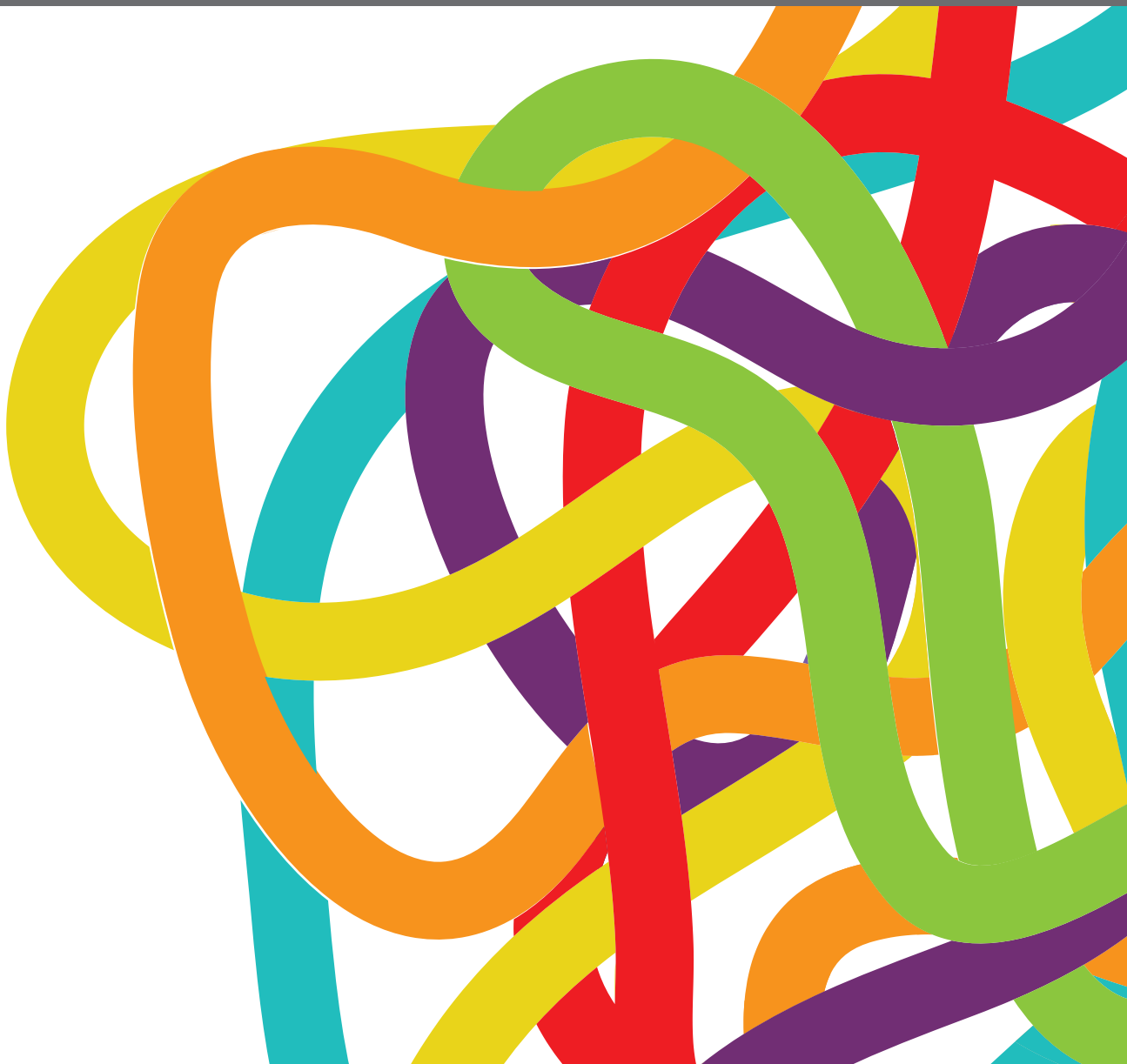
EDITED BY: Vasiliki Gkretsi and Triantafyllos Stylianopoulos

frontiers Research Topics

About Frontiers

Frontiers is more than just an open-access publisher of scholarly articles: it is a pioneering approach to the world of academia, radically improving the way scholarly research is managed. The grand vision of Frontiers is a world where all people have an equal opportunity to seek, share and generate knowledge. Frontiers provides immediate and permanent online open access to all its publications, but this alone is not enough to realize our grand goals.

Frontiers Journal Series

The Frontiers Journal Series is a multi-tier and interdisciplinary set of open-access, online journals, promising a paradigm shift from the current review, selection and dissemination processes in academic publishing. All Frontiers journals are driven by researchers for researchers; therefore, they constitute a service to the scholarly community. At the same time, the Frontiers Journal Series operates on a revolutionary invention, the tiered publishing system, initially addressing specific communities of scholars, and gradually climbing up to broader public understanding, thus serving the interests of the lay society, too.

Dedication to Quality

Each Frontiers article is a landmark of the highest quality, thanks to genuinely collaborative interactions between authors and review editors, who include some of the world's best academicians. Research must be certified by peers before entering a stream of knowledge that may eventually reach the public - and shape society; therefore, Frontiers only applies the most rigorous and unbiased reviews.
Frontiers revolutionizes research publishing by freely delivering the most outstanding research, evaluated with no bias from both the academic and social point of view. By applying the most advanced information technologies, Frontiers is catapulting scholarly publishing into a new generation.

What are Frontiers Research Topics?

Frontiers Research Topics are very popular trademarks of the Frontiers Journals Series: they are collections of at least ten articles, all centered on a particular subject. With their unique mix of varied contributions from Original Research to Review Articles, Frontiers Research Topics unify the most influential researchers, the latest key findings and historical advances in a hot research area! Find out more on how to host your own Frontiers Research Topic or contribute to one as an author by contacting the Frontiers Editorial Office: researchtopics@frontiersin.org

METASTASIS: FROM CELL ADHESION AND BEYOND

Topic Editors:
Vasiliki Gkretsi, European University Cyprus, Cyprus
Triantafyllos Stylianopoulos, University of Cyprus, Cyprus

This eBook consists of a collection of articles focused on fundamental processes of cancer cell metastasis, such as cell-Extracellular matrix adhesions, epithelial-to-mesenchymal transition (EMT) and lymph node metastasis as well as on upcoming research fields including the effects of biomechanical factors, the use of analytical and statistical tools and experimental techniques to further understand and characterize the invasive and metastatic potential of tumors.

Citation: Gkretsi, V., Stylianopoulos, T., eds. (2019). Metastasis: From Cell Adhesion and Beyond. Lausanne: Frontiers Media. doi: 10.3389/978-2-88945-953-7

Table of Contents

Editorial: Metastasis: From Cell Adhesion and Beyond

Vasiliki Gkretsi [1,2]* and Triantafyllos Stylianopoulos [1]*

[1] Cancer Biophysics Laboratory, Department of Mechanical and Manufacturing Engineering, University of Cyprus, Nicosia, Cyprus, [2] Biomedical Sciences Program, Department of Life Sciences, School of Sciences, European University Cyprus, Nicosia, Cyprus

Editorial on the Research Topic

Metastasis: From Cell Adhesion and Beyond

METASTASIS

Metastasis is a complex multistep process during which cancer cells within a tumor dissociate from one another, migrate, and invade through surrounding tissues to finally enter the circulation or the lymphatic system, being thus transported to other sites of the body where they establish a new metastatic tumor. Many different approaches have been followed so far to study this process and find ways to prevent it. The collection of articles in this Frontiers Research Topic depicts exactly that.

CELL ADHESION

Firstly, a pivotal role in the metastatic process is played by the cell-extracellular matrix (ECM) adhesion proteins as well as their interaction with actin cytoskeleton. Gkretsi and Stylianopoulos provide a concise review of the recent literature on important determinants of the cell's adhesome at cell–ECM adhesion sites that affect its invasive properties. Multiple protein-protein interactions define this adhesome linking the ECM directly or indirectly with the actin cytoskeleton (1, 2) and downstream effectors such as RhoGTPases (3) that collectively coordinate metastasis-related cellular processes. Furthermore, ECM accumulation within the tumor often leads to desmoplasia, an intense fibrotic response, causing tumor stiffening. Stiffening in turn, adds a biomechanical perspective to the whole concept of tumor growth and metastasis (4, 5). In that regard, Gkretsi and Stylianopoulos also emphasize the importance of keeping stiffness in mind when developing *in vitro* model systems.

THE MECHANICAL COMPONENT

Adding to the biomechanical aspect of metastasis and tumor growth, Kalli and Stylianopoulos, define the concepts of stiffness and solid stress in tumors, as so far it is not clear whether matrix stiffness and solid stress are interrelated or if they have distinct roles in tumor progression. Pointing out that increased solid stress and stiffness are two distinct biomechanical abnormalities of the

tumor microenvironment, they present a review of the different effects of these two parameters on the behavior of cancer and stromal cells. They also review and compare the *in vitro* experimental approaches that have been employed so far to analyze the effect of stiffness and solid stress providing a useful guide for similar studies.

TRIPLE-NEGATIVE BREAST CANCER METASTASIS AND METASTASIS TO THE LYMPH NODES (LN)

Along the same lines, Neophytou et al. focus on one of the most desmoplastic types of cancer, breast cancer, and triple negative breast cancer (TNBC), in particular, and provide a thorough analysis of the molecular mechanism involved during epithelial-to-mesenchymal transition (EMT), as well as the genes activated in this aggressive cancer type during the different stages of metastasis (metastasis promoting genes and metastasis suppressors). Moreover, they discuss recent advances on TNBC treatment, at the preclinical level, using agents that remodel tumor microenvironment and enhance the effects of chemotherapy delivery as well as advances emerging from novel molecular targets.

As with TNBC, in many cancer types, the first sites of metastasis for the original tumor are lymph nodes (LN). In fact, LN metastasis has been associated with worse prognosis although the mechanism is still vague. Jones et al. provide herein, an overview of the seeding, growth, and dissemination of LN metastases based on recent literature. Emphasis is given on how tumor cells and their secreted molecules decrease anti-tumor immunity and promote tumor growth in the LN.

CLUSTERS OF CIRCULATING TUMOR CELLS

Tripathi et al. focus on another aggressive type of breast cancer, which is also desmoplastic, inflammatory breast cancer (IBC). In this type of cancer, metastasis occurs not only through circulating tumor cells (CTCs) but rather via the generation of CTC clusters. CTC clusters may be rare and are thought to retain some epithelial characteristics, as they do not undergo a complete EMT, but account for more than 90% of metastases. Tripathi et al. based their work on a theory suggesting that the more hierarchically organized a physical system is, the more adaptable it can become. Thus, in the research article presented in this special issue, Tripathi et al. use the cophenetic correlation coefficient (CCC) to quantify the hierarchical organization in terms of gene expression of two different gene sets. They show that indeed high CCC, of both collective dissemination-associated genes and the IBC-associated genes, is associated with higher metastatic relapse rate in breast cancer patients.

A HIGH-THROUGHPUT, FUNCTIONAL TECHNIQUE FOR ASSESSING CANCER CELL INVASION POTENTIAL

Interestingly, in a more applicable point of view, the research article by Weitz et al. introduces a novel high-throughput, functional method for assessing cancer cell invasion potential. This method takes advantage of the biophysical changes occurring during metastasis that enable a cancer cell to invade the surrounding tissue. Using this technique, prostate, and bladder cancer cells are labeled with a fluorescent calcium dye and imaged during stimulation with low-intensity focused ultrasound; invasive cell lines exhibit calcium elevation which is not true for non-invasive cells (Weitz et al.). Thus, this method provides a means of assessing tumor invasion potential which could prove useful in cytology studies and ultimately improve clinical management (Weitz et al.).

INTRATUMORAL IMMUNE CYTOLYTIC ACTIVITY

Last but not least, Roufas et al. provide us with a different view of dealing with metastasis focusing on immune checkpoint blockade therapy. Contrary to the approach taken by most anti-cancer immunotherapies, immune checkpoint blockade aims at blocking immune responses by inhibiting immune suppressor molecules, thus awakening the cytotoxic T lymphocytes from dormancy and enabling them to kill the cancer cells they infiltrate (6). Here, Roufas et al. conduct a comprehensive meta-analysis to evaluate the intratumoral immune cytolytic activity (CYT) in different cancer types, as judged by the expression of toxins granzyme A (GZMA) and perforin 1, and investigate differences between primary and metastatic tumors (data obtained from The Cancer Genome Atlas and Genotype-Tissue Expression project databases). They show that the cytolytic index among other associations with tumor-infiltrated immune cells promotes evasion from immunosurveillance in certain cancers Roufas et al..

CONCLUDING REMARKS

In this research topic, we presented a collection of articles focused on fundamental processes of cancer cell metastasis, such as cell-ECM adhesions, EMT and LN metastasis as well as on upcoming research fields including the effects of biomechanical factors, the use of analytical and statistical tools and experimental techniques to further understand and characterize the invasive and metastatic potential of tumors.

AUTHOR CONTRIBUTIONS

All authors listed have made a substantial, direct and intellectual contribution to the work, and approved it for publication.

REFERENCES

1. Horton ER, Astudillo P, Humphries MJ, Humphries JD. Mechanosensitivity of integrin adhesion complexes: role of the consensus adhesome. *Exp Cell Res.* (2016) 343:7–13. doi: 10.1016/j.yexcr.2015.10.025

2. Horton ER, Humphries JD, James J, Jones MC, Askari JA, Humphries MJ. The integrin adhesome network at a glance. *J Cell Sci.* (2016) 129:4159–63. doi: 10.1242/jcs.192054

3. Sahai E, Marshall CJ. Differing modes of tumour cell invasion have distinct requirements for Rho/ROCK signalling and extracellular proteolysis. *Nat Cell Biol.* (2003) 5:711–9. doi: 10.1038/ncb1019

4. Kai F, Laklai H, Weaver VM. Force matters: biomechanical regulation of cell invasion and migration in disease. *Trends Cell Biol.* (2016) 26:486–97. doi: 10.1016/j.tcb.2016.03.007

5. Oudin MJ, Weaver VM. Physical and Chemical gradients in the tumor microenvironment regulate tumor cell invasion, migration, and metastasis. *Cold Spring Harb Symp Quant Biol.* (2016) 81:189–205. doi: 10.1101/sqb.2016.81.030817

6. Wieder T, Eigentler T, Brenner E, Rocken M. Immune checkpoint blockade therapy. *J Allergy Clin Immunol.* (2018) 142:1403–14. doi: 10.1016/j.jaci.2018.02.042

Cell Adhesion and Matrix Stiffness: Coordinating Cancer Cell Invasion and Metastasis

Vasiliki Gkretsi[1]* and Triantafyllos Stylianopoulos[2]*

[1] *Department of Life Sciences, Biomedical Sciences Program, School of Sciences, European University Cyprus, Nicosia, Cyprus,* [2] *Cancer Biophysics Laboratory, Department of Mechanical and Manufacturing Engineering, University of Cyprus, Nicosia, Cyprus*

Metastasis is a multistep process in which tumor extracellular matrix (ECM) and cancer cell cytoskeleton interactions are pivotal. ECM is connected, through integrins, to the cell's adhesome at cell–ECM adhesion sites and through them to the actin cytoskeleton and various downstream signaling pathways that enable the cell to respond to external stimuli in a coordinated manner. Cues from cell-adhesion proteins are fundamental for defining the invasive potential of cancer cells, and many of these proteins have been proposed as potent targets for inhibiting cancer cell invasion and thus, metastasis. In addition, ECM accumulation is quite frequent within the tumor microenvironment leading in many cases to an intense fibrotic response, known as desmoplasia, and tumor stiffening. Stiffening is not only required for the tumor to be able to displace the host tissue and grow in size but also contributes to cell–ECM interactions and can promote cancer cell invasion to surrounding tissues. Here, we review the role of cell adhesion and matrix stiffness in cancer cell invasion and metastasis.

Keywords: extracellular matrix, cell–extracellular matrix adhesion, actin cytoskeleton, cell invasion, metastasis, stiffness, solid stress, desmoplasia

Cancer cells undergo certain fundamental changes in terms of cell physiology to attain a malignant phenotype. They acquire self-sufficiency in growth signals, insensitivity to growth-inhibitory signals, limitless replicative potential, evasion of apoptosis, sustained angiogenesis, and tissue invasion capacity that enables them to metastasize to distant sites of the body (1, 2). In fact, the latter is the unique "hallmark of cancer" that differentiates benign and malignant tumors and truly defines cancer (3).

Metastasis is a complex process in which cancer cells spread from a primary site to other organs in the body. It consists of several steps and the involvement of the extracellular matrix (ECM), and the cytoskeleton is indisputable. During this process, malignant cells dissociate from the original tumor mass, reorganize their attachment to the ECM though alterations in cell–ECM adhesion dynamics, and start degrading surrounding ECM to eventually invade through adjacent

tissues and/or intravasate into blood vessels and travel through the circulation to distant sites of the body (4). The establishment of a metastatic tumor at the new site is not random but rather seems to follow a pattern known as "metastatic tropism." Cancer cells that have managed to survive in the circulation find a metastatic niche that, based on the "seed and soil" theory, is suitable for their growth (5–7). Hence, some cancer types metastasize according to circulation patterns or based on the anatomical proximity of neighboring organs or the host–organ microenvironment. For instance, prostate cancer shows a preference toward the bone, pancreatic cancer forms metastases to the lung and liver, and breast cancer metastasizes to the bone, liver, lung, and the brain (6–8). Notably, biophysical and biochemical cues from the tumor ECM affect each one of the "hallmarks of cancer" (9) and control cell–cell and cell–ECM adhesions, which in turn determine cancer cell invasion and metastasis (7). Thus, integrins, ECM-related adhesion proteins and cell–cell adhesion proteins play a vital role in regulating the various stages of metastasis and defining the aggressiveness of cancer cells (10).

CELL–CELL AND CELL–ECM ADHESION PROTEINS IN CANCER CELL METASTASIS

Cancer cells are able to invade the surrounding ECM in the form of single cells or as collective groups of cells moving together, depending on whether cell–cell adhesion proteins, such as E-cadherin, are completely or partially lost in the original tumor, respectively (11). Although integrin-independent migration has also been described (12), both modes of invasion are considered to be heavily dependent on integrin-mediated adhesion to the ECM, whereas collective invasion also requires dynamic cell–cell adhesions so that loosening of cell junctions becomes sufficient for invasion. Thus, E-cadherin expression or its localization in cell–cell junctions is often lost in advanced cancers and has been linked to higher incidence of metastasis (11).

However, the actual outcome in terms of invasion is ultimately dependent upon the balance between E-cadherin-mediated adhesions and integrin cell–ECM adhesions (11). Integrins connect the ECM with the interior of the cell transmitting extracellular signals through the assembly of multiple protein complexes that act as adaptor proteins and also bear strong attachments to actin cytoskeleton (10). There are more than 180 cell–ECM proteins forming networks of protein–protein interactions at cell–ECM adhesion sites, which altogether comprise what is known as cell's *adhesome* (13). Critical determinants in cell–ECM adhesions that also link the ECM directly or indirectly with the actin cytoskeleton include talin, paxillin, kindlins, vinculin, integrin-linked kinase (ILK), parvins [parvin alpha (PARVA), parvin beta, and parvin gamma], particularly interesting new cysteine–histidine rich protein (PINCH)-1, Ras suppressor-1 (RSU-1), vasodilator-stimulated phosphoprotein (VASP) and its interactor Migfilin (14), and α-actinin (15–17). Upon integrin, activation protein tyrosine kinases Src and focal adhesion kinase (FAK) are also activated promoting further cytoskeletal changes as well as activation of downstream signaling pathways vital for cell adhesion, proliferation, survival, migration,

and invasion (**Figure 1**) (18). Small Rho GTPases, Rho, Rac, and Cdc42, as well as Rho-associated protein kinase (ROCK) are such downstream effectors known to coordinate cytoskeletal reorganization and cell migration. Interestingly, most of these components of the cell–ECM adhesions have been found to be significantly deregulated in most cancer types with their expression being associated with higher metastatic potential or lower survival rates (19–26). Moreover, increased levels of RhoA, RhoB, RhoC, Rac1, Cdc42, and ROCK, have been found in late-stage tumors and metastases with prognostic relevance in breast cancer (27, 28). This suggests a strong involvement of cell–ECM adhesion molecules in cancer cell metastasis, although the exact molecular mechanisms involved can be different depending on cell type, tumor location, or grade. In fact, research has shown that cancer cells can have different modes of invasion, and thus a different molecular mechanism activated every time (29, 30). For instance, Rho signaling through ROCK promotes a rounded bleb-associated mode of motility, whereas elongated cell motility is associated with Rac-dependent F-actin-rich protrusions and does not require Rho or ROCK (30).

DISRUPTION OF CELL–CELL ADHESION AND EPITHELIAL TO MESENCHYMAL TRANSITION (EMT)

All the above-described changes in cell–ECM and cell–cell adhesion components are important for the detachment of cancer cells from the original tumor mass and their invasion through adjacent tissues and contribute to the "epithelial to mesenchymal transition," also termed EMT. EMT refers to a transition of polarized epithelial cells toward cells exhibiting mesenchymal properties that enables them to metastasize. Thus, during EMT, epithelial cells reorganize their cytoskeleton, dissociate from one another, and begin expressing mesenchymal genes. These genes may vary significantly in different cells and tissues but there are certain transcription factors, such as TWIST1/2, SNAIL1/2, zinc finger E-box-binding homeobox, and forkhead box protein C2 that are indispensable for EMT in all cases (37–40). In fact, EMT-activating transcription factors have been proposed to have pleiotropic functions acting on all stages of cancer progression from initiation to metastasis (41). Also, several cytokines such as transforming growth factor-β (TGF-β), tumor necrosis factor-α, and interleukin-6, as well as ECM proteins such as collagen I, fibronectin, and hyaluronan are crucially involved in EMT in various tumors (37). Notably, several types of cancer cells have been found to acquire a more mesenchymal-like phenotype which also correlates with their resistance to cytotoxic drugs (38, 42), providing a link between EMT and cancer therapy. Moreover, expression of EMT markers has been also found in circulating tumor cells (CTCs) that are fundamental in the metastatic process. These markers facilitate detection of CTCs while also giving more insights into tumor diagnosis, treatment, and prognosis (43).

All in all, current studies have demonstrated the complexity of the EMT process which raises important and exciting questions for future investigation (41).

FIGURE 1 | Schematic representation of critical protein–protein interactions at cell–extracellular matrix (ECM) adhesion sites in cancer cells grown in low (left) and high (right) stiffness conditions. Several important protein complexes are formed at the cell–ECM sites that are vital for normal cell function. More specifically, integrin-linked kinase (ILK) binds to the cytoplasmic domain of integrins and also interacts with particularly interesting new cysteine–histidine rich protein (PINCH)-1 and parvin alpha (PARVA) forming a stable ternary complex at cell–ECM adhesions known as PIP (PINCH–ILK–PARVA) or IPP (ILK–PINCH–PARVA) complex (31). PARVA, in turn, binds directly to actin connecting the complex to the cytoskeleton of the cell. ILK has also been shown to interact with Kindlin-2 (also known as mitogen-inducible gene-2 or Mig-2) which again forms a protein complex with Migfilin and filamin A (FLNA) (32), an actin-crosslinking protein. Interestingly, Migfilin has been shown to interact with vasodilator-stimulated phosphoprotein (VASP) (14), regulating cell migration. Equally important is the interaction of integrins with talin (33) and paxillin, which in turn binds to focal adhesion kinase (FAK) (34) while FAK binds to Src (35), which has been also shown to interact with Migfilin regulating cell–ECM mediated survival (36). Note that all cell–ECM adhesion proteins have direct or indirect connection to the actin cytoskeleton, while they activate downstream effectors such as the RhoGTPases, and matrix metalloproteinases (MMPs) eventually leading to regulation of vital cellular functions (proliferation, survival, migration, and invasion). Notably, higher stiffness conditions are associated with marked increase in the amount of stress fibers as well as increased migration and invasion.

TUMOR MICROENVIRONMENT AND DESMOPLASIA

Apart from cancer cells and the ECM, tumors exhibit an additional aspect of complexity that accounts for the heterogeneity attributed to them and plays an important role in metastasis. They contain a number of allegedly normal cells that comprise the "tumor microenvironment" (1, 44). Hence, structural components of the tumor microenvironment are the tumor blood and lymphatic vessels, and the stromal cell constituents of the tumor that can be subdivided into three categories: (a) angiogenic vascular cells, which include endothelial cells and pericytes, (b) infiltrating immune cells, which include platelets, mast cells, neutrophils, inflammatory monocytes, myeloid-derived suppressor cells (45), macrophages (46), CD8^{+} T-cells, NK T-cells, CD4^{+} T-cells (47), and B cells, and (c) cancer-associated fibroblasts (CAF) cells, which include activated tissue fibroblasts, activated adipocytes, α-smooth muscle actin (α-SMA) positive myofibroblasts, and mesenchymal stem cells (48). As expected, the exact composition

of a tumor's microenvironment varies depending on the tumor type and its location, which justifies the observed heterogeneity among tumors, rendering every tumor unique.

The ECM is a fundamental constituent of the tumor microenvironment that closely interacts with cancer cells for the transmission of signals in and out of the cell through integrins (10), while also providing the necessary growth factors for tumor growth (49). Moreover, upregulation of ECM remodeling molecules, such as TGF-β, are considered to be responsible for the development of *desmoplasia* in tumors (50). Desmoplasia is an intense fibrotic response characterized by the formation of dense ECM consisting of increased levels of total fibrillar collagen, fibronectin, proteoglycans, and tenascin C that accumulates within the tumor. It is associated with increased production and secretion of inflammatory and tumorigenic growth factors, and it is also characterized by an abnormally large population of stromal cells. Moreover, a large percentage of tissue fibroblasts are transformed to CAFs that contain high levels of α-SMA. Therefore, it is proposed that TGF-β activates fibroblasts to

become CAFs, which in turn produce more ECM fibers leading to desmoplasia (50). Apart from that, molecules that remodel the ECM, such as matrix metalloproteinases and lysyl oxidase, are also critical for desmoplasia development (51). Collectively, desmoplastic tumors are considered to be more aggressive and are, in fact, associated with worse prognosis in several cancer types (52, 53).

ROLE OF TUMOR STIFFNESS IN CANCER CELL INVASION AND METASTASIS

Desmoplasia is highly related to tumor *stiffening*, which is perhaps the only mechanical property of tumors that clinicians can really appreciate. Stiffness, which defines how rigid a material is or the extent to which a material resists deformation in response to an applied force (54), depends on the composition and organization of the structural components of a material and describes the extent to which it deforms in response to an applied force or the magnitude of the developed force when the material is subject to a specific strain. Therefore, the stiffer a material is, the more resistant to deformations and more prone to develop higher stresses (i.e., force per unit area) becomes. In tumors, in particular, which are known to grow at the expense of the host tissue, the stress exerted from the tumor on the host should balance the reciprocal stress applied from the host to the tumor. Therefore, the developed stresses within a tumor depend on the relative stiffness between the two tissues and from a biomechanical point of view, stiffening is required for a tumor to be able to displace the host tissue and grow in size (55, 56). Using mathematical modeling, we have previously estimated that tumors should be at least 1.5 times stiffer than their surrounding normal tissue, otherwise confinement by the host prevails to tumor expansion (57).

As mentioned earlier, tumor stiffness is mainly determined by the amount of ECM, particularly collagen and hyaluronan contained in the tumor. Given the fact that the interior of the tumor is subject to compression (58), its stiffness is mainly determined by hyaluronan, which owing to its fixed negative charges creates hydrated, gel-like regions within the tumor capable of resisting compressive stresses (59–62). At the tumor periphery, tumor growth can remodel the collagen fibers and change their orientation toward the tumor circumference. As a result, collagen fibers can be stretched and develop tensile stresses. Therefore, stiffness at the periphery should also depend on the amount of collagen (63, 64).

For the study of ECM stiffness, cancer cells usually grow in three dimensions (3D) within a collagen, hyaluronan, or similar gel that mimics the ECM and parameters that most often vary to modulate stiffness are either the gel's concentration or the degree of collagen crosslinking for gels that contain collagen. Cancer cell spheroids are also employed for the study of cell invasion through the matrix (65–70). Increasing ECM stiffness has been shown to induce malignant phenotype (71–73) characterized by Rho-dependent cytoskeletal tension that leads to enhanced cell–ECM adhesions, disruption of cell–cell junctions and increased growth (69) (**Figure 1**) and is actually associated with activated FAK and extracellular signal-regulated kinase signaling (69). Finally, another proof that stiffness is crucially involved in cancer cell metastasis comes from preclinical studies showing that disruption of tumor ECM integrity halts metastasis (74).

Cells can sense ECM stiffening through integrins by cytoskeletal filaments that coordinate cell migration and induce changes within the cell. As that, a stiffer ECM can induce production of fibronectin, a glycoprotein of the ECM that binds from one side to extracellular collagen, fibrin, and heparan sulfate proteoglycans and from the other side to integrins. ECM stiffening can also enhance cell–ECM adhesions that connect the ECM to the cytoskeleton through local adhesion proteins, and increase cytoskeletal tension by Rho/ROCK signaling activation (69, 75). Therefore, integrin clustering can initiate the recruitment of focal adhesion signaling molecules such as FAK, ILK, PARVA, Src, paxillin, as well as Rac, Rho, and Ras that cause cell contractility and can promote tumor progression (**Figure 1**) (76, 77). In addition, stiffening of the ECM can enhance phosphatidylinositide 3-kinases activity, which regulates tumor invasion (78–80). Furthermore, the cell–ECM adhesion protein RSU-1 was found to be significantly upregulated in increased stiffness conditions in a 3D collagen-based *in vitro* culture system, while tumor spheroids made of cells lacking RSU-1 lost their invasive capacity through the 3D matrix in all stiffness conditions (65). Moreover, lack of the actin polymerization regulator VASP, also inhibited tumor spheroid invasion through matrix of increasing stiffness indicating that both actin cytoskeleton and cell–ECM adhesions play pivotal role in tumor spheroid invasion through 3D matrix (81), an *in vitro* property that mimics tumor invasion in a real tumor setting.

In addition, in pancreatic tumors with mutant SMAD4, matrix stiffening was associated with elevated ROCK activity that in turn stimulated increased production of ECM, assembly of focal adhesions and signal transducer, and activator of transcription-3 (STAT-3) signaling driving tumor progression (82). Matrix stiffening can also induce EMT, leading to the acquisition of a more aggressive phenotype that promotes cancer cell invasion owing to a loss of intercellular adhesions (83), and it is hypothesized to contribute to the transformation of cancer cells to stem cell-like cancer cells that can survive under the harsh hypoxic conditions of the tumor microenvironment, are more resistant to cytotoxic drugs, and can migrate and invade through surrounding tissues (84).

EFFECTS OF SOLID STRESS ON CANCER CELL BEHAVIOR

It should be noted, however, that even though ECM stiffness can be related to the magnitude of solid stress, the two quantities are distinct and thus, one should not be used to replace the other (85). Solid stress is defined as the force per unit area of the structural components of a tissue, which can cause either compaction (compression) or expansion (tension) of the material, whereas stiffness refers to the extent to which the tissue can resist deformations or external forces (54).

Different experimental procedures have been also developed to study the effects of solid stress and ECM stiffness on cancer cell behavior. For the study of solid stress, transmembrane pressure devices, cancer cell spheroids, or modifications of these are most often used. In transmembrane pressure devices,

cells grow as single cells embedded in a matrix or as a monolayer on a transwell insert membrane, and a piston with adjustable weight is placed on the top to apply a predefined stress (86–89). This method has been used to study stress induced changes in gene expression, invasion, and migration. In the tumor spheroid model, cancer cell aggregates form spheroids that are embedded in a matrix that mimics tumor ECM, such as agarose, collagen, or matrigel. The matrix exerts an external stress to the cells and pertinent studies focus on the effect of solid stress on cancer cell proliferation and apoptosis (87, 90–93). This method is limited, however, in that the applied by the matrix stress cannot be directly quantified. When applied to compress cancer cells, solid stress can inhibit proliferation, induce apoptosis, and increase cancer cell invasive and metastatic potential (87, 88, 90). Compressive solid stress can also activate fibroblasts to become CAFs (similarly to TGF-β), which in turn can facilitate not only development of desmoplasia but also cancer cell invasion to the surrounding, normal tissues (89, 94).

CONCLUDING REMARKS AND PERSPECTIVES

Cell–ECM adhesion proteins, actin cytoskeleton, and ECM stiffness evidently play a major role in driving cancer cell invasion and metastasis being involved in virtually all steps of the metastatic process from cell dissociation from the original tumor, to invasion through surrounding ECM until the final step of cancer cell homing in the new metastasis site. For this to happen, ECM is connected through integrins to the cell's adhesome at cell–ECM adhesion sites where multiple protein–protein interactions take place connecting the ECM to the actin cytoskeleton so that response to external stimuli is well coordinated. In fact, signals from these cell-adhesion proteins appear to be crucial for defining the invasive potential of cancer cells, while evidence shows that they may also prove potent targets for inhibiting cancer cell invasion and thus, metastasis (65, 81). Moreover, as ECM stiffness is also a driving force in metastasis (72, 73), it also needs to be taken into account when studying cancer cell metastasis both *in vitro* and *in vivo* in an attempt to better recapitulate tumor

microenvironment in a physiologically relevant manner. Thus, the development of appropriate and physiologically relevant *in vitro* systems is needed to define the molecular determinants in the process and open new avenues in the discovery of novel therapeutic candidates to block metastasis.

From another point of view, solid stress is a distinct parameter that affects cancer cell behavior and should be also considered in *in vitro* tumor models. Furthermore, solid stress is exerted not only on cancer cells but also on the endothelial cells that form the tumor micro-vessels. As a result, blood vessels can be compressed or totally collapsed, creating large avascular regions within the tumor thus causing hypo-perfusion and hypoxia (58, 95) which ultimately inhibit systemic administration of drugs to the tumors (55, 60) and can promote tumor progression in multiple ways (96). Notably, recent *in vivo* evidence has shown that modulating the tumor microenvironment through administration of drugs that alleviate intratumoral solid stress (such as anti-fibrotic agents) reduces mechanical stresses, decompresses tumor vessels, and improves tumor drug delivery (60–62, 97), once again suggesting that modulation of ECM is of fundamental significance for tumor biology and cancer therapeutics.

AUTHOR CONTRIBUTIONS

Both authors contributed equally to writing, editing, and approving the final version of this article.

ACKNOWLEDGMENTS

FUNDING

REFERENCES

1. Hanahan D, Weinberg RA. The hallmarks of cancer. *Cell* (2000) 100:57–70. doi:10.1016/S0092-8674(00)81683-9

2. Hanahan D, Weinberg RA. Hallmarks of cancer: the next generation. *Cell* (2011) 144:646–74. doi:10.1016/j.cell.2011.02.013

3. Lazebnik Y. What are the hallmarks of cancer? *Nat Rev Cancer* (2010) 10:232–3. doi:10.1038/nrc2827

4. Wei SC, Yang J. Forcing through tumor metastasis: the interplay between tissue rigidity and epithelial-mesenchymal transition. *Trends Cell Biol* (2016) 26:111–20. doi:10.1016/j.tcb.2015.09.009

5. Mueller MM, Fusenig NE. Friends or foes – bipolar effects of the tumour stroma in cancer. *Nat Rev Cancer* (2004) 4:839–49. doi:10.1038/nrc1477

6. Budczies J, von Winterfeld M, Klauschen F, Bockmayr M, Lennerz JK, Denkert C, et al. The landscape of metastatic progression patterns across major human cancers. *Oncotarget* (2015) 6:570–83. doi:10.18632/oncotarget.2677

7. Valastyan S, Weinberg RA. Tumor metastasis: molecular insights and evolving paradigms. *Cell* (2011) 147:275–92. doi:10.1016/j.cell.2011.09.024

8. Barney LE, Jansen LE, Polio SR, Galarza S, Lynch ME, Peyton SR. The predictive link between matrix and metastasis. *Curr Opin Chem Eng* (2016) 11:85–93. doi:10.1016/j.coche.2016.01.001

9. Pickup MW, Mouw JK, Weaver VM. The extracellular matrix modulates the hallmarks of cancer. *EMBO Rep* (2014) 15:1243–53. doi:10.15252/embr.201439246

10. Hynes RO. Integrins: bidirectional, allosteric signaling machines. *Cell* (2002) 110:673–87. doi:10.1016/S0092-8674(02)00971-6

11. Canel M, Serrels A, Frame MC, Brunton VG. E-cadherin-integrin crosstalk in cancer invasion and metastasis. *J Cell Sci* (2013) 126:393–401. doi:10.1242/jcs.100115

12. Schmidt S, Friedl P. Interstitial cell migration: integrin-dependent and alternative adhesion mechanisms. *Cell Tissue Res* (2010) 339:83–92. doi:10.1007/s00441-009-0892-9

13. Horton ER, Humphries JD, James J, Jones MC, Askari JA, Humphries MJ. The integrin adhesome network at a glance. *J Cell Sci* (2016) 129:4159–63. doi:10.1242/jcs.192054

14. Zhang Y, Tu Y, Gkretsi V, Wu C. Migfilin interacts with vasodilator-stimulated phosphoprotein (VASP) and regulates VASP localization to cell-matrix

adhesions and migration. *J Biol Chem* (2006) 281:12397–407. doi:10.1074/jbc.M512107200

15. Bottcher RT, Lange A, Fassler R. How ILK and kindlins cooperate to orchestrate integrin signaling. *Curr Opin Cell Biol* (2009) 21:670–5. doi:10.1016/j.ceb.2009.05.008

16. Horton ER, Astudillo P, Humphries MJ, Humphries JD. Mechanosensitivity of integrin adhesion complexes: role of the consensus adhesome. *Exp Cell Res* (2016) 343:7–13. doi:10.1016/j.yexcr.2015.10.025

17. Horton ER, Byron A, Askari JA, Ng DH, Millon-Fremillon A, Robertson J, et al. Definition of a consensus integrin adhesome and its dynamics during adhesion complex assembly and disassembly. *Nat Cell Biol* (2015) 17:1577–87. doi:10.1038/ncb3257

18. Legate KR, Fassler R. Mechanisms that regulate adaptor binding to beta-integrin cytoplasmic tails. *J Cell Sci* (2009) 122:187–98. doi:10.1242/jcs.041624

19. Cai HX, Yang LC, Song XH, Liu ZR, Chen YB, Dong GK. Expression of paxillin and FAK mRNA and the related clinical significance in esophageal carcinoma. *Mol Med Rep* (2012) 5:469–72. doi:10.3892/mmr.2011.664

20. Chen D, Zhang B, Kang J, Ma X, Lu Y, Gong L. Expression and clinical significance of FAK, ILK, and PTEN in salivary adenoid cystic carcinoma. *Acta Otolaryngol* (2013) 133:203–8. doi:10.3109/00016489.2012.728295

21. Gkretsi V, Papanikolaou V, Zacharia LC, Athanassiou E, Wu C, Tsezou A. Mitogen-inducible Gene-2 (MIG2) and migfilin expression is reduced in samples of human breast cancer. *Anticancer Res* (2013) 33(5):1977–81.

22. Ozkal S, Paterson JC, Tedoldi S, Hansmann ML, Kargi A, Manek S, et al. Focal adhesion kinase (FAK) expression in normal and neoplastic lymphoid tissues. *Pathol Res Pract* (2009) 205:781–8. doi:10.1016/j.prp.2009.07.002

23. Papachristou DJ, Gkretsi V, Rao UN, Papachristou GI, Papaefthymiou OA, Basdra EK, et al. Expression of integrin-linked kinase and its binding partners in chondrosarcoma: association with prognostic significance. *Eur J Cancer* (2008) 44:2518–25. doi:10.1016/j.ejca.2008.07.021

24. Papachristou DJ, Gkretsi V, Tu Y, Shi X, Chen K, Larjava H, et al. Increased cytoplasmic level of migfilin is associated with higher grades of human leiomyosarcoma. *Histopathology* (2007) 51:499–508. doi:10.1111/j.1365-2559.2007.02791.x

25. Li R, Liu B, Yin H, Sun W, Yin J, Su Q. Overexpression of integrin-linked kinase (ILK) is associated with tumor progression and an unfavorable prognosis in patients with colorectal cancer. *J Mol Histol* (2013) 44:183–9. doi:10.1007/s10735-012-9463-6

26. Giotopoulou N, Valiakou V, Papanikolaou V, Dubos S, Athanassiou E, Tsezou A, et al. Ras suppressor-1 promotes apoptosis in breast cancer cells by inhibiting PINCH-1 and activating p53-upregulated-modulator of apoptosis (PUMA); verification from metastatic breast cancer human samples. *Clin Exp Metastasis* (2015) 32:255–65. doi:10.1007/s10585-015-9701-x

27. Fritz G, Brachetti C, Bahlmann F, Schmidt M, Kaina B. Rho GTPases in human breast tumours: expression and mutation analyses and correlation with clinical parameters. *Br J Cancer* (2002) 87:635–44. doi:10.1038/sj.bjc.6600510

28. Lane J, Martin TA, Watkins G, Mansel RE, Jiang WG. The expression and prognostic value of ROCK I and ROCK II and their role in human breast cancer. *Int J Oncol* (2008) 33(3):585–93.

29. Sahai E. Erik Sahai: getting the whole picture of metastasis. Interview by Sedwick Caitlin. *J Cell Biol* (2011) 193:428–9. doi:10.1083/jcb.1933pi

30. Sahai E, Marshall CJ. Differing modes of tumour cell invasion have distinct requirements for Rho/ROCK signalling and extracellular proteolysis. *Nat Cell Biol* (2003) 5:711–9. doi:10.1038/ncb1019

31. Zhang Y, Chen K, Tu Y, Velyvis A, Yang Y, Qin J, et al. Assembly of the PINCH-ILK-CH-ILKBP complex precedes and is essential for localization of each component to cell-matrix adhesion sites. *J Cell Sci* (2002) 115:4777–86. doi:10.1242/jcs.00166

32. Tu Y, Wu S, Shi X, Chen K, Wu C. Migfilin and Mig-2 link focal adhesions to filamin and the actin cytoskeleton and function in cell shape modulation. *Cell* (2003) 113:37–47. doi:10.1016/S0092-8674(03)00163-6

33. Tadokoro S, Shattil SJ, Eto K, Tai V, Liddington RC, de Pereda JM, et al. Talin binding to integrin beta tails: a final common step in integrin activation. *Science* (2003) 302:103–6. doi:10.1126/science.1086652

34. Scheswohl DM, Harrell JR, Rajfur Z, Gao G, Campbell SL, Schaller MD. Multiple paxillin binding sites regulate FAK function. *J Mol Signal* (2008) 3:1. doi:10.1186/1750-2187-3-1

35. Bolos V, Gasent JM, Lopez-Tarruella S, Grande E. The dual kinase complex FAK-Src as a promising therapeutic target in cancer. *Onco Targets Ther* (2010) 3:83–97. doi:10.2147/OTT.S6909

36. Zhao J, Zhang Y, Ithychanda SS, Tu Y, Chen K, Qin J, et al. Migfilin interacts with Src and contributes to cell-matrix adhesion-mediated survival signaling. *J Biol Chem* (2009) 284:34308–20. doi:10.1074/jbc.M109.045021

37. Jung HY, Fattet L, Yang J. Molecular pathways: linking tumor microenvironment to epithelial-mesenchymal transition in metastasis. *Clin Cancer Res* (2015) 21:962–8. doi:10.1158/1078-0432.CCR-13-3173

38. Lambert AW, Pattabiraman DR, Weinberg RA. Emerging biological principles of metastasis. *Cell* (2017) 168:670–91. doi:10.1016/j.cell.2016.11.037

39. Kim DH, Xing T, Yang Z, Dudek R, Lu Q, Chen YH. Epithelial mesenchymal transition in embryonic development, tissue repair and cancer: a comprehensive overview. *J Clin Med* (2017) 7:E1. doi:10.3390/jcm7010001

40. Scheel C, Weinberg RA. Cancer stem cells and epithelial-mesenchymal transition: concepts and molecular links. *Semin Cancer Biol* (2012) 22:396–403. doi:10.1016/j.semcancer.2012.04.001

41. Brabletz T, Kalluri R, Nieto MA, Weinberg RA. EMT in cancer. *Nat Rev Cancer* (2018) 18:128–34. doi:10.1038/nrc.2017.118

42. Kurrey NK, Jalgaonkar SP, Joglekar AV, Ghanate AD, Chaskar PD, Doiphode RY, et al. Snail and slug mediate radioresistance and chemoresistance by antagonizing p53-mediated apoptosis and acquiring a stem-like phenotype in ovarian cancer cells. *Stem Cells* (2009) 27:2059–68. doi:10.1002/stem.154

43. Jie XX, Zhang XY, Xu CJ. Epithelial-to-mesenchymal transition, circulating tumor cells and cancer metastasis: mechanisms and clinical applications. *Oncotarget* (2017) 8:81558–71. doi:10.18632/oncotarget.18277

44. Gkretsi V, Stylianou A, Papageorgis P, Polydorou C, Stylianopoulos T. Remodeling components of the tumor microenvironment to enhance cancer therapy. *Front Oncol* (2015) 5:214. doi:10.3389/fonc.2015.00214

45. Gabrilovich DI, Nagaraj S. Myeloid-derived suppressor cells as regulators of the immune system. *Nat Rev Immunol* (2009) 9:162–74. doi:10.1038/nri2506

46. Chow A, Brown BD, Merad M. Studying the mononuclear phagocyte system in the molecular age. *Nat Rev Immunol* (2011) 11:788–98. doi:10.1038/nri3087

47. Mantovani A, Cassatella MA, Costantini C, Jaillon S. Neutrophils in the activation and regulation of innate and adaptive immunity. *Nat Rev Immunol* (2011) 11:519–31. doi:10.1038/nri3024

48. Hanahan D, Coussens LM. Accessories to the crime: functions of cells recruited to the tumor microenvironment. *Cancer Cell* (2012) 21:309–22. doi:10.1016/j.ccr.2012.02.022

49. Briquez PS, Hubbell JA, Martino MM. Extracellular matrix-inspired growth factor delivery systems for skin wound healing. *Adv Wound Care (New Rochelle)* (2015) 4:479–89. doi:10.1089/wound.2014.0603

50. Papageorgis P, Stylianopoulos T. Role of TGFbeta in regulation of the tumor microenvironment and drug delivery (review). *Int J Oncol* (2015) 46:933–43. doi:10.3892/ijo.2015.2816

51. Egeblad M, Rasch MG, Weaver VM. Dynamic interplay between the collagen scaffold and tumor evolution. *Curr Opin Cell Biol* (2010) 22:697–706. doi:10.1016/j.ceb.2010.08.015

52. Cardone A, Tolino A, Zarcone R, Borruto Caracciolo G, Tartaglia E. Prognostic value of desmoplastic reaction and lymphocytic infiltration in the management of breast cancer. *Panminerva Med* (1997) 39:174–7.

53. Ueno H, Shinto E, Hashiguchi Y, Shimazaki H, Kajiwara Y, Sueyama T, et al. In rectal cancer, the type of desmoplastic response after preoperative chemoradiotherapy is associated with prognosis. *Virchows Arch* (2015) 466:655–63. doi:10.1007/s00428-015-1756-1

54. Kalli M, Stylianopoulos T. Defining the role of solid stress and matrix stiffness in cancer cell proliferation and metastasis. *Front Oncol* (2018) 8:55. doi:10.3389/fonc.2018.00055

55. Jain RK, Martin JD, Stylianopoulos T. The role of mechanical forces in tumor growth and therapy. *Annu Rev Biomed Eng* (2014) 16:321–46. doi:10.1146/annurev-bioeng-071813-105259

56. Stylianopoulos T. The solid mechanics of cancer and strategies for improved therapy. *J Biomech Eng* (2017) 139. doi:10.1115/1.4034991

57. Voutouri C, Mpekris F, Papageorgis P, Odysseos AD, Stylianopoulos T. Role of constitutive behavior and tumor-host mechanical interactions in the state of stress and growth of solid tumors. *PLoS One* (2014) 9:e104717. doi:10.1371/journal.pone.0104717

58. Stylianopoulos T, Martin JD, Snuderl M, Mpekris F, Jain SR, Jain RK. Coevolution of solid stress and interstitial fluid pressure in tumors during progression: implications for vascular collapse. *Cancer Res* (2013) 73:3833–41. doi:10.1158/0008-5472.CAN-12-4521

59. Netti PA, Berk DA, Swartz MA, Grodzinsky AJ, Jain RK. Role of extracellular matrix assembly in interstitial transport in solid tumors. *Cancer Res* (2000) 60(9):2497–503.

60. Papageorgis P, Polydorou C, Mpekris F, Voutouri C, Agathokleous E, Kapnissi-Christodoulou CP, et al. Tranilast-induced stress alleviation in solid tumors improves the efficacy of chemo- and nanotherapeutics in a size-independent manner. *Sci Rep* (2017) 7:46140. doi:10.1038/srep46140

61. Polydorou C, Mpekris F, Papageorgis P, Voutouri C, Stylianopoulos T. Pirfenidone normalizes the tumor microenvironment to improve chemotherapy. *Oncotarget* (2017) 8:24506–17. doi:10.18632/oncotarget.15534

62. Mpekris F, Papageorgis P, Polydorou C, Voutouri C, Kalli M, Pirentis AP, et al. Sonic-hedgehog pathway inhibition normalizes desmoplastic tumor microenvironment to improve chemo- and nanotherapy. *J Control Release* (2017) 261:105–12. doi:10.1016/j.jconrel.2017.06.022

63. Stylianopoulos T, Martin JD, Chauhan VP, Jain SR, Diop-Frimpong B, Bardeesy N, et al. Causes, consequences, and remedies for growth-induced solid stress in murine and human tumors. *Proc Natl Acad Sci U S A* (2012) 109:15101–8. doi:10.1073/pnas.1213353109

64. Pirentis AP, Polydorou C, Papageorgis P, Voutouri C, Mpekris F, Stylianopoulos T. Remodeling of extracellular matrix due to solid stress accumulation during tumor growth. *Connect Tissue Res* (2015) 56:345–54. doi:10.3109/03008207.2015.1047929

65. Gkretsi V, Stylianou A, Louca M, Stylianopoulos T. Identification of Ras suppressor-1 (RSU-1) as a potential breast cancer metastasis biomarker using a three-dimensional in vitro approach. *Oncotarget* (2017) 8:27364–79. doi:10.18632/oncotarget.16062

66. Lutolf MP, Lauer-Fields JL, Schmoekel HG, Metters AT, Weber FE, Fields GB, et al. Synthetic matrix metalloproteinase-sensitive hydrogels for the conduction of tissue regeneration: engineering cell-invasion characteristics. *Proc Natl Acad Sci U S A* (2003) 100:5413–8. doi:10.1073/pnas.0737381100

67. Mason BN, Starchenko A, Williams RM, Bonassar LJ, Reinhart-King CA. Tuning three-dimensional collagen matrix stiffness independently of collagen concentration modulates endothelial cell behavior. *Acta Biomater* (2013) 9:4635–44. doi:10.1016/j.actbio.2012.08.007

68. Zaman MH, Trapani LM, Sieminski AL, Mackellar D, Gong H, Kamm RD, et al. Migration of tumor cells in 3D matrices is governed by matrix stiffness along with cell-matrix adhesion and proteolysis. *Proc Natl Acad Sci U S A* (2006) 103:10889–94. doi:10.1073/pnas.0604460103

69. Paszek MJ, Zahir N, Johnson KR, Lakins JN, Rozenberg GI, Gefen A, et al. Tensional homeostasis and the malignant phenotype. *Cancer Cell* (2005) 8:241–54. doi:10.1016/j.ccr.2005.08.010

70. Pedersen JA, Lichter S, Swartz MA. Cells in 3D matrices under interstitial flow: effects of extracellular matrix alignment on cell shear stress and drag forces. *J Biomech* (2010) 43:900–5. doi:10.1016/j.jbiomech.2009.11.007

71. Acerbi I, Cassereau L, Dean I, Shi Q, Au A, Park C, et al. Human breast cancer invasion and aggression correlates with ECM stiffening and immune cell infiltration. *Integr Biol (Camb)* (2015) 7:1120–34. doi:10.1039/c5ib00040h

72. Kai F, Laklai H, Weaver VM. Force matters: biomechanical regulation of cell invasion and migration in disease. *Trends Cell Biol* (2016) 26:486–97. doi:10.1016/j.tcb.2016.03.007

73. Oudin MJ, Weaver VM. Physical and chemical gradients in the tumor microenvironment regulate tumor cell invasion, migration, and metastasis. *Cold Spring Harb Symp Quant Biol* (2016) 81:189–205. doi:10.1101/sqb.2016.81.030817

74. Venning FA, Wullkopf L, Erler JT. Targeting ECM disrupts cancer progression. *Front Oncol* (2015) 5:224. doi:10.3389/fonc.2015.00224

75. Samuel MS, Lopez JI, McGhee EJ, Croft DR, Strachan D, Timpson P, et al. Actomyosin-mediated cellular tension drives increased tissue stiffness and beta-catenin activation to induce epidermal hyperplasia and tumor growth. *Cancer Cell* (2011) 19:776–91. doi:10.1016/j.ccr.2011.05.008

76. Shi Q, Boettiger D. A novel mode for integrin-mediated signaling: tethering is required for phosphorylation of FAK Y397. *Mol Biol Cell* (2003) 14:4306–15. doi:10.1091/mbc.E03-01-0046

77. Lawson CD, Burridge K. The on-off relationship of Rho and Rac during integrin-mediated adhesion and cell migration. *Small GTPases* (2014) 5:e27958. doi:10.4161/sgtp.27958

78. Friedland JC, Lee MH, Boettiger D. Mechanically activated integrin switch controls alpha5beta1 function. *Science* (2009) 323:642–4. doi:10.1126/science.1168441

79. Leventhal KR, Yu H, Kass L, Lakins JN, Egeblad M, Erler JT, et al. Matrix crosslinking forces tumor progression by enhancing integrin signaling. *Cell* (2009) 139:891–906. doi:10.1016/j.cell.2009.10.027

80. Rubashkin MG, Cassereau L, Bainer R, DuFort CC, Yui Y, Ou G, et al. Force engages vinculin and promotes tumor progression by enhancing PI3K activation of phosphatidylinositol (3,4,5)-triphosphate. *Cancer Res* (2014) 74:4597–611. doi:10.1158/0008-5472.CAN-13-3698

81. Gkretsi V, Stylianou A, Stylianopoulos T. Vasodilator-Stimulated Phosphoprotein (VASP) depletion from breast cancer MDA-MB-231 cells inhibits tumor spheroid invasion through downregulation of Migfilin, beta-catenin and urokinase-plasminogen activator (uPA). *Exp Cell Res* (2017) 352(2):281–92. doi:10.1016/j.yexcr.2017.02.019

82. Laklai H, Miroshnikova YA, Pickup MW, Collisson EA, Kim GE, Barrett AS, et al. Genotype tunes pancreatic ductal adenocarcinoma tissue tension to induce matricellular fibrosis and tumor progression. *Nat Med* (2016) 22:497–505. doi:10.1038/nm.4082

83. Potenta S, Zeisberg E, Kalluri R. The role of endothelial-to-mesenchymal transition in cancer progression. *Br J Cancer* (2008) 99:1375–9. doi:10.1038/sj.bjc.6604662

84. Northey JJ, Przybyla L, Weaver VM. Tissue force programs cell fate and tumor aggression. *Cancer Discov* (2017) 7:1224–37. doi:10.1158/2159-8290.CD-16-0733

85. Nia HT, Liu H, Seano G, Datta M, Jones D, Rahbari N, et al. Solid stress and elastic energy as measures of tumour mechanopathology. *Nat Biomed Eng* (2016) 1:0004. doi:10.1038/s41551-016-0004

86. Demou ZN. Gene expression profiles in 3D tumor analogs indicate compressive strain differentially enhances metastatic potential. *Ann Biomed Eng* (2010) 38:3509–20. doi:10.1007/s10439-010-0097-0

87. Cheng G, Tse J, Jain RK, Munn LL. Micro-environmental mechanical stress controls tumor spheroid size and morphology by suppressing proliferation and inducing apoptosis in cancer cells. *PLoS One* (2009) 4:e4632. doi:10.1371/journal.pone.0004632

88. Tse JM, Cheng G, Tyrrell JA, Wilcox-Adelman SA, Boucher Y, Jain RK, et al. Mechanical compression drives cancer cells toward invasive phenotype. *Proc Natl Acad Sci U S A* (2012) 109:911–6. doi:10.1073/pnas.1118910109

89. Kalli M, Papageorgis P, Gkretsi V, Stylianopoulos T. Solid stress facilitates fibroblasts activation to promote pancreatic cancer cell migration. *Ann Biomed Eng* (2018) 46(5):657–69. doi:10.1007/s10439-018-1997-7

90. Helmlinger G, Netti PA, Lichtenbeld HC, Melder RJ, Jain RK. Solid stress inhibits the growth of multicellular tumor spheroids. *Nat Biotechnol* (1997) 15:778–83. doi:10.1038/nbt0897-778

91. Kaufman LJ, Brangwynne CP, Kasza KE, Filippidi E, Gordon VD, Deisboeck TS, et al. Glioma expansion in collagen I matrices: analyzing collagen concentration-dependent growth and motility patterns. *Biophys J* (2005) 89:635–50. doi:10.1529/biophysj.105.061994

92. Delarue M, Montel F, Vignjevic D, Prost J, Joanny JF, Cappello G. Compressive stress inhibits proliferation in tumor spheroids through a volume limitation. *Biophys J* (2014) 107:1821–8. doi:10.1016/j.bpj.2014.08.031

93. Desmaison A, Frongia C, Grenier K, Ducommun B, Lobjois V. Mechanical stress impairs mitosis progression in multi-cellular tumor spheroids. *PLoS One* (2013) 8:e80447. doi:10.1371/journal.pone.0080447

94. Wipff PJ, Hinz B. Myofibroblasts work best under stress. *J Bodyw Mov Ther* (2009) 13:121–7. doi:10.1016/j.jbmt.2008.04.031

95. Padera TP, Stoll BR, Tooredman JB, Capen D, di Tomaso E, Jain RK. Pathology: cancer cells compress intratumour vessels. *Nature* (2004) 427:695. doi:10.1038/427695a

96. Jain RK. Antiangiogenesis strategies revisited: from starving tumors to alleviating hypoxia. *Cancer Cell* (2014) 26:605–22. doi:10.1016/j.ccell.2014.10.006

97. Chauhan VP, Martin JD, Liu H, Lacorre DA, Jain SR, Kozin SV, et al. Angiotensin inhibition enhances drug delivery and potentiates chemotherapy by decompressing tumor blood vessels. *Nat Commun* (2013) 4:2516. doi:10.1038/ncomms3516

Defining the Role of Solid Stress and Matrix Stiffness in Cancer Cell Proliferation and Metastasis

Maria Kalli and Triantafyllos Stylianopoulos*

Cancer Biophysics Laboratory, Department of Mechanical and Manufacturing Engineering, University of Cyprus, Nicosia, Cyprus

Solid tumors are characterized by an abnormal stroma that contributes to the development of biomechanical abnormalities in the tumor microenvironment. In particular, these abnormalities include an increase in matrix stiffness and an accumulation of solid stress in the tumor interior. So far, it is not clearly defined whether matrix stiffness and solid stress are strongly related to each other or they have distinct roles in tumor progression. Moreover, while the effects of stiffness on tumor progression are extensively studied compared to the contribution of solid stress, it is important to ascertain the biological outcomes of both abnormalities in tumorigenesis and metastasis. In this review, we discuss how each of these parameters is evolved during tumor growth and how these parameters are influenced by each other. We further review the effects of matrix stiffness and solid stress on the proliferative and metastatic potential of cancer and stromal cells and summarize the *in vitro* experimental setups that have been designed to study the individual contribution of these parameters.

Keywords: extracellular matrix, fibroblasts, externally applied stress, growth-induced stress, *in vitro* models

UNRAVELING THE TUMOR MICROENVIRONMENT

Tumor stroma and biomechanical abnormalities developed during tumor growth comprise dominant regulators of cancer progression (1–3). The tumor stroma is composed of an extracellular matrix (ECM), which consists of immune cells, fibroblasts, capillaries, and fibrillar proteins, such as collagen I, elastin, and fibronectin, as well as hyaluronan and other sulfated glycosaminoglycans (4). Fibroblasts are key regulators of ECM composition and organization and physiologically remain in the quiescent state with negligible metabolic and transcriptomic activities (5, 6). In response to tissue damage, fibroblasts become activated and are characterized by the expression of alpha-smooth muscle actin (α-SMA). In this activated state, fibroblasts overproduce ECM proteins, mainly collagen I and fibronectin, secrete cytokines and growth factors, and exert contractile forces modifying tissue architecture (5, 6).

In tumors, fibroblasts tend to acquire a constantly activated phenotype as a response to several growth factors secreted from the highly proliferative cancer cells, including transforming growth factor-β (TGFβ), epidermal growth factors (EGFs), and bone morphogenetic proteins (BMPs) (5, 6). Activated fibroblasts, which are commonly known as cancer-associated fibroblasts (CAFs), start a chronic wound healing-like response toward cancer cells, leading to an excessive accumulation of fibrillar ECM proteins, a condition known as desmoplasia (5). Under this desmoplastic reaction, CAFs continuously produce and remodel the tumor ECM increasing tumor stiffness (1, 5). Desmoplasia and ECM stiffening characterize many tumor types, especially breast and pancreatic cancers, and it usually promotes tumor progression (1, 7, 8).

As the density of cancer cells, stromal cells, and ECM constituents increase within the restricted environment of the host tissue, it leads to the development of mechanical stress (i.e., force per unit area) within the tumor (1, 3, 9–11). This stress, derived from the structural components of a tumor, is known as solid stress and can be divided into two parts. A part of it, known as growth-induced (or residual) stress, is accumulated during tumor growth by microscopic interactions among structural components of the tumor microenvironment, and it remains within the tumor even if the tumor is removed (3). These interactions might include collagen stretching by cancer cells and CAFs, and hyaluronan and cancer cell swelling to resist compression (12–15). Moreover, as tumors grow and exert forces on the adjacent host tissue, a reciprocal compressive stress is applied from the host tissue to the tumor, to resist tumor expansion (1). This stress is known as externally applied stress, and it diminishes after tumor excision (1). The total solid stress in a tumor interior is compressive (i.e., tends to reduce the size of an object), while near the interface between the tumor and normal tissue, the stress is tensile (i.e., tends to increase the size of an object) (16, 17).

THE DEFINITION OF ECM STIFFNESS AND SOLID STRESS

It is not clearly defined in the pertinent literature whether matrix stiffness and solid stress refer to the same term or they are two distinct biomechanical abnormalities of a tumor that are related to each other. By definition, stiffness is a material property, which describes the extent to which a material resists deformation in response to an applied force, while solid stress is a force per unit area, which can cause either compaction (compression) or expansion (tension) of a material. In solid tumors, the stiffness is mainly determined by ECM composition and organization, while solid stress arises by the sum of the physical forces exerted during tumor growth. These forces can be generated in the subcellular level by cytoskeletal filaments that control cellular processes such as filopodia formation and extension. At the cellular level, forces are exerted by cell contractions (such as in CAFs) and cell–ECM interactions during migration of cancer and stromal cells, while at the tissue level, forces are exerted between the tumor and the host tissue (18–21).

The relationship between tumor stiffness and solid stress can be described using the analogy of a spring of specific elastic modulus (E) that obeys Hooke's law (**Figure 1**). According to the equation of Hooke's law for linear elastic materials, $\sigma = E \cdot \varepsilon$, when a tumor of elastic modulus E grows and pushes the surrounding host tissue of elastic modulus E′, it causes a deformation ε_1 and a subsequent stress σ_1. As a consequence, the host tissue returns an equal and opposite stress σ_1', the so-called externally applied solid stress. At the same time, growth-induced solid stress is accumulated in the tumor interior owing to interactions among tumor components (**Figure 1A**). Thus, the total solid stress accumulated intratumorally is the sum of the externally applied and the growth-induced solid stress. In the case that the stiffness of the tumor E_2 is greater than E_1, then the tumor can displace the host tissue with a greater deformation and the externally applied solid stress σ_2 can be greater than σ_1 (**Figure 1B**). Therefore, in

FIGURE 1 | Solid stress and stiffness are two distinct biomechanical abnormalities present in the tumor microenvironment. **(A)** According to the simple analogy of a spring that obeys Hooke's law $\sigma = E \cdot \varepsilon$, when a tumor grows and pushes the surrounding host tissue of elastic modulus E′, it results in a deformation ε_1 and a stress, σ_1. As a consequence, the host tissue returns an equal and opposite stress σ_1', which is defined as externally applied solid stress ($\sigma_1 = \sigma_1'$). This externally applied stress, in combination with the growth-induced stress (σ_g), generated from mechanical interactions within the tumor, constitutes the total solid stress transmitted in the tumor interior. **(B)** In the case that the tumor stiffens so that E_2 is greater than E_1 ($E_2 > E_1$), the tumor can increase in size and the deformation ε_2 is greater than ε_1 ($\varepsilon_2 > \varepsilon_1$). The externally applied stress (σ_2') and finally the total solid stress accumulated in the tumor interior are greater than that in **(A)** without any change in the growth-induced stress. **(C)** The growth-induced solid stress, however, increases during growth, while tumor stiffening might remain the same (16). In this case, the externally applied solid stress σ_3' can be equal to σ_1', but total solid stress increases. Therefore, the resultant stress transmitted in the tumor interior is greater than that in **(A)** without any change in tumor stiffness.

this case, a solid tumor creates a stiffer matrix to push against the normal tissue and grow in size. Indeed, it has been demonstrated using mathematical modeling that the stiffness of a solid tumor should be at least 1.5 times greater than that of the host tissue, in order for the tumor to displace the tissue and grow (14).

As for the growth-induced solid stress, it increases during tumor growth, while the matrix stiffness might stop changing (16, 17). In this case, the further increase in total solid stress accumulated intratumorally can become less depended on matrix stiffness (**Figure 1C**). This hypothesis was confirmed by an elegant study by Nia et al. (16), showing that the total solid stress transmitted into the cells can depend only in part on tumor stiffness, and thus, the two terms should not be used without a distinction. Specifically, Nia et al. found that primary pancreatic tumors exhibited larger stresses compared to those in metastatic sites, while the opposite effect was observed for colon tumors (16). Interestingly, tumor stiffness was similar in the primary and metastatic tumor for both the pancreatic and colon cancer models, showing that tumor stiffness and solid stress are not necessarily coupled to each other. In addition, they found that solid stress increased in breast tumors of larger size despite the fact that stiffness did not change with tumor size. In line with our analysis, these observations can be explained by the fact that growth-induced solid stress generated owing to microscopic interactions among structural components in the tumor interior contributes to the accumulation of an additional to the externally applied solid stress. Therefore, the effects of matrix stiffness and solid stress on tumorigenesis and metastasis should be studied separately (22). Following, we provide a summary of these effects on cancer and stromal cell behavior, elaborating on the less studied contribution of solid stress and the pertinent experimental setups.

EFFECTS OF MATRIX STIFFNESS ON CANCER AND STROMAL CELLS

The effect of ECM stiffness on cancer and stromal cells has been studied using *in vitro* two-dimensional substrates (2D) and three-dimensional tumor analogs (3D). In 2D models, cells are seeded on coating substrates such as collagen or fibronectin (23–26), while the 3D models include single cells or tumor spheroids embedded in gels composed of collagen or matrigel (27–34) (**Figure 2A**). In both cases, stiffness is increased by changing the protein density or the degree of crosslinking of the matrix to study the effects of ECM-originating mechanical cues on cancer and stromal cells.

Matrix stiffness can activate intracellular signaling pathways to regulate cellular behavior. Cancer cells recognize the increase in ECM stiffness and respond by generating increased traction forces on their surroundings through actomyosin and cytoskeleton contractility (9, 35, 36). Moreover, the changes in matrix rigidity are sensed and transmitted intracellularly through mechanosensors such as p130 CRK-associated proteins, growth factor receptors, or integrin-ECM adhesion plaques (9, 10, 23, 35, 37–40). These mechanosensors can recruit focal adhesion molecules such as FAK, SRC, paxillin, RAC, RHO/RAS GTPases, and Rho-associated kinase to trigger signaling cascades and cytoskeleton organization (9, 10, 35, 36, 39, 41–44). These

cascades finally regulate gene expression and induce quantifiable changes in cell shape, survival, migration, and invasion (9, 35, 39, 42). For example, it has been shown that tissue stiffness activates the nuclear translocation of the transcription factor TWIST1 in breast cancer cells, which inhibits the expression of E-cadherin and promotes cell invasion (35, 45). Furthermore, in a 3D model consisting of breast tumor spheroids growing in collagen matrix, the Ras suppressor-1 (RSU-1), a cell-ECM adhesion protein, was shown to be upregulated as a response to increasing stiffness. Interestingly, tumor spheroids knockdown for RSU-1 or actin polymerization regulator (VASP) lost their invasiveness through the 3D matrix (46, 47). Matrix stiffening is also shown to induce fibroblast activation and migration, which leads to a fibrotic response setting a positive feedback to matrix stiffness (13, 15, 35, 48, 49). However, in these studies, it cannot be distinguished explicitly whether the observed effects are emerged by increased cell-ECM adhesion sites owing to increased ECM density or by stiffness-induced solid stress generation.

EFFECTS OF SOLID STRESS ON CANCER AND STROMAL CELLS

While the role of ECM stiffness in cancer and stromal cells is actively studied, data regarding the effect of solid stress on tumor progression are elusive. There are several experimental setups mimicking the solid stress developed in the tumor microenvironment. These setups include models consisting of tumor spheroids growing in a confined environment that causes the development of solid stress (50–57) and models employing a transmembrane pressure device that applies a mechanical compression on a cell monolayer or on single cells embedded in a matrix (51, 58–60) (**Figure 2B**).

Regarding the first method, cancer cells are grown as spheroids in a polymer gel (e.g., agarose), which leads to the development of solid stress that resists to spheroid expansion (**Figure 2B**, i). Helmlinger et al. (55) using spheroids of colon adenocarcinoma cells estimated that the accumulated solid stress was in the range of 45–120 mmHg (6–16 kPa), depending on the concentration of the agarose gel and the size of the spheroid. In an analogous study, Cheng et al. (51) estimated the solid stress to be ~28 mmHg (~3.73 kPa) when mammary carcinoma cell spheroids were growing in a 0.5% agarose matrix. Recent *in vivo* measurements of breast, colon, pancreatic, and brain tumors estimated that the growth-induced stress is in the range of 1.56–142.4 mmHg (0.21–20 kPa) (3, 11, 16, 54). Differences in the magnitude of solid stress among *in vitro* studies and between *in vitro* and *in vivo* methods should depend on the tumor model and the experimental procedure used in each study. However, the conclusion that increasing compressive stress inhibits tumor growth is common (51, 52, 55, 57), while this effect was reversed when loads were removed (51, 55). It was also observed that solid stress can regulate tumor morphology since mechanical loads can induce apoptotic cell death in regions with high compressive stress and allow proliferation in low-stress regions of the tumor spheroid, suggesting that anisotropic loads result in anisotropic tumor growth (51).
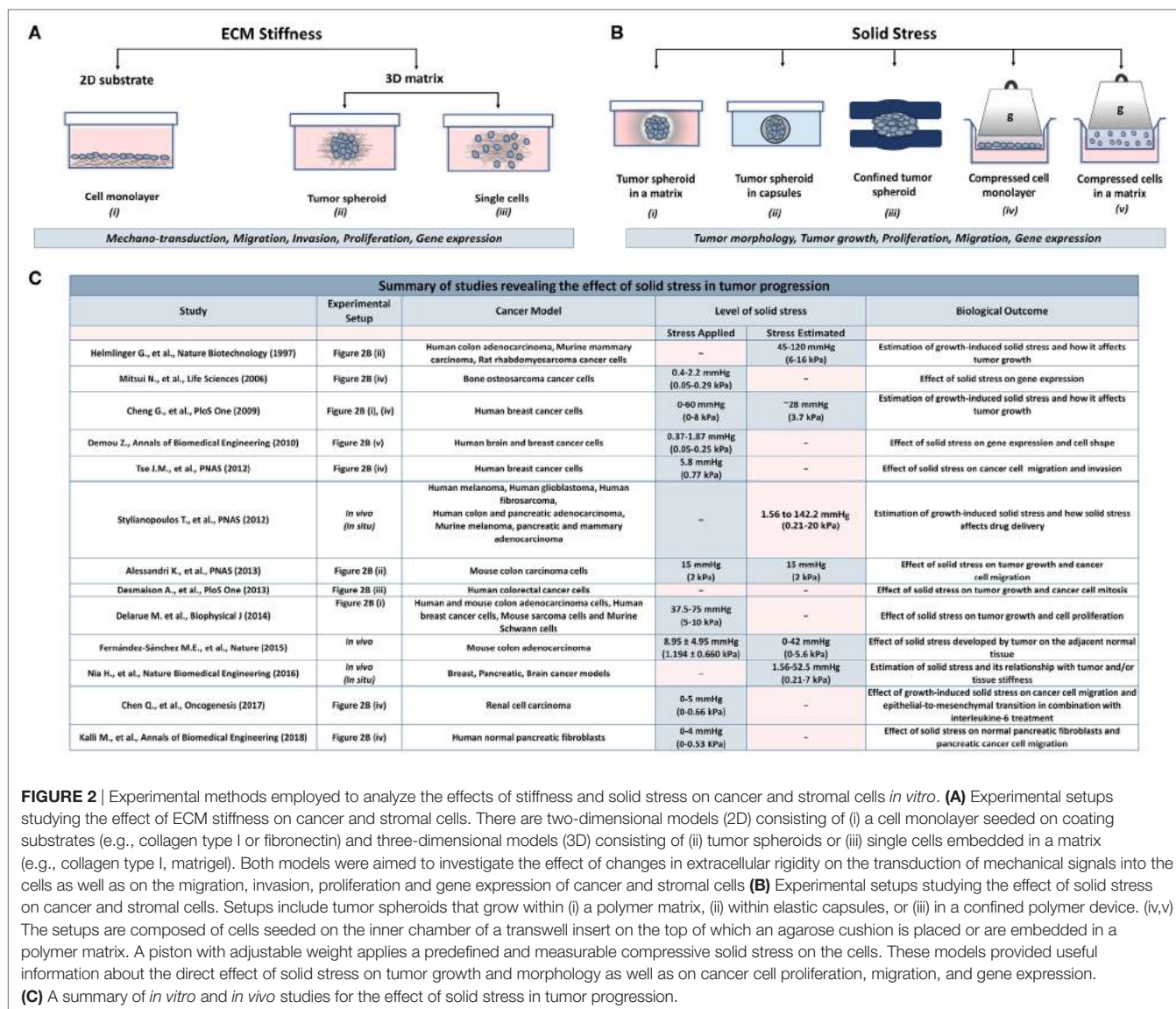
FIGURE 2 | Experimental methods employed to analyze the effects of stiffness and solid stress on cancer and stromal cells *in vitro*. **(A)** Experimental setups studying the effect of ECM stiffness on cancer and stromal cells. There are two-dimensional models (2D) consisting of (i) a cell monolayer seeded on coating substrates (e.g., collagen type I or fibronectin) and three-dimensional models (3D) consisting of (ii) tumor spheroids or (iii) single cells embedded in a matrix (e.g., collagen type I, matrigel). Both models were aimed to investigate the effect of changes in extracellular rigidity on the transduction of mechanical signals into the cells as well as on the migration, invasion, proliferation and gene expression of cancer and stromal cells **(B)** Experimental setups studying the effect of solid stress on cancer and stromal cells. Setups include tumor spheroids that grow within (i) a polymer matrix, (ii) within elastic capsules, or (iii) in a confined polymer device. (iv,v) The setups are composed of cells seeded on the inner chamber of a transwell insert on the top of which an agarose cushion is placed or are embedded in a polymer matrix. A piston with adjustable weight applies a predefined and measurable compressive solid stress on the cells. These models provided useful information about the direct effect of solid stress on tumor growth and morphology as well as on cancer cell proliferation, migration, and gene expression. **(C)** A summary of *in vitro* and *in vivo* studies for the effect of solid stress in tumor progression.

More recent studies developed novel techniques to mimic solid stress during tumor growth in the absence of a matrix. Alessandri et al. (50) employed a microfluidic method based on the encapsulation and growth of cells inside permeable, elastic, and hollow microspheres (**Figure 2B**, ii). This approach offered the ability to produce size-controlled multicellular spheroids growing in confined conditions. They found that the confined spheroids exhibited a necrotic core compared with the unconfined spheroids. In contrast, peripheral cells were more proliferative and migratory, suggesting that mechanical cues from the surrounding microenvironment may trigger cell invasion from a growing tumor (50). Desmaison et al. (53) designed polymer polydimethylsiloxane microdevices to restrict the growth of spheroids and subsequently to induce the development of mechanical stress (**Figure 2B**, iii). They showed that the mitosis of mechanically confined spheroids was suppressed compared to spheroids grown in suspension (53). Furthermore, it was demonstrated that a population of cells within the confined tumor spheroids was arrested at mitosis, which was due to the inhibition of bipolar spindle assembly (53). Later, Fernández-Sánchez et al. (54) developed a method that allows the delivery of a defined mechanical pressure *in vivo* by subcutaneously inserting a magnet close to the mouse colon. The implanted magnet generates a magnetic force on ultramagnetic liposomes stabilized in the mesenchymal cells of the connective tissue surrounding colonic crypts after intravenous injection (54). The induced pressure was similar in magnitude to the endogenous stress (54), in the order of 9.0 mmHg (1.2 kPa), without affecting tissue stiffness, as monitored by ultrasound strain imaging and shear wave elastography (54). The magnetic pressure stimulated Ret activation and the subsequent β-catenin phosphorylation, impairing its interaction with E-cadherin in adherens junctions (54). These data suggested that tumor progression could be driven by signaling pathways that are directly activated by mechanical pressure.

To study the effect of a predefined solid stress on cancer cells, the transmembrane pressure device has been introduced (**Figure 2B**, iv). Setups employed consist of a transwell insert that fits in a well of a 6-well culture plate. The insert is separated in the lower chamber containing culture medium and the upper chamber containing the cell monolayer. A piston of a preferable weight is applied on the cell monolayer, while water, nutrients, and oxygen from the culture media are diffused through the pores of the transmembrane. This device provides a tool to mimic solid stress in a predefined manner according to the stress magnitudes measured in native tumor tissues.

Cheng et al. (51) used this device to study the effect of solid stress on murine mammary carcinoma cells. In this study, they applied a stress ranging from 0 to 60 mmHg (0–8 kPa), and they observed increased apoptosis with increased stress levels. In a following study, they used the same experimental setup to study the migration of cancer cells using a scratch wound assay (60). They applied a stress of 5.8 mmHg (0.77 kPa), and concluded that in these levels of compression, cancer cells stopped proliferating and started to create a leader cell formation, which allowed them to move toward the scratch having an invasive phenotype. Mitsui et al. (59) used a similar device for bone osteosarcoma cells to identify the effect of compressive stress on the expression of matrix metalloproteinases and plasminogen activators. They observed enhanced protein and mRNA levels of these molecules under low mechanical compression of bone cells (0–2.20 mmHg/0–0.29 kPa) (59). Recently, Chen et al. (61) observed increased migration and mesenchymal-like phenotype of renal carcinoma cells that were compressed by 0–5.0 mmHg (0–0.66 kPa), while Kalli et al. (62) found that normal fibroblasts become activated as a response to solid stress to promote pancreatic cancer cell migration.

Another device that was developed to study the effect of solid stress in a more realistic way involved the use of single cancer cells growing in an agarose matrix (**Figure 2B**, v). This device was composed of two custom-made parts, the well pressor and the optic pressor (58). Both devices consisted of a chamber containing a 3D gel with single cells embedded, a screw and a nut for pressure application, and their housing support. Specifically, the well pressor applied a strain that compressed the cell-contained agarose gels to 50% of their original volume. This stress was estimated to be ~0.37 mmHg (~0.05 kPa), much smaller than loads measured by other studies (3, 51, 55, 58). However, this stress was sufficient to cause differential expression profiles of metastasis-associated genes in glioblastoma and breast cancer cells. In addition, the optic pressor provided quantifiable changes in cell circularity and orientation with respect to the direction of the applied force (58).

Collectively, these *in vitro* studies suggest that mechanical forces can regulate tumor morphology, tumor growth, and metastatic potential of cancer cells in the absence of matrix stiffness. However, as indicated in **Figure 2C**, there is a discrepancy among the levels of solid stress applied or estimated in the pertinent studies due to the variability of the experimental procedures and the cancer models used. Therefore, it should be given special attention when performing experiments to study the effect of solid stress on tumor progression, taking into account the estimations derived from *in vivo* studies.

CONCLUSION AND FUTURE PERSPECTIVES

In light of recent studies showing that increased matrix stiffness and elevated solid stress are two distinct tumor abnormalities, and given the fact that most pertinent studies are focused on the effects of stiffness, it becomes clear that scientific efforts need to focus on the implications of solid stress in tumor progression and metastasis (16, 22).

Regarding the implications of tumor stiffness in tumor progression, most pertinent *in vitro* models include only cancer cells and ECM matrix. However, tumor stiffness might also depend on the presence of stromal CAFs that continuously interact with the fibrillar proteins. CAFs-ECM interactions remodel the ECM organization and fibers orientation for cancer cells to migrate and invade into the matrix (1, 63, 64). Regarding the effects of solid stress on tumor progression, further studies are required to shed light upon the mechanisms by which solid stress is transmitted and guides cellular behavior of both cancer cells and CAFs. Moreover, CAFs exert contractile forces that contribute to the accumulation of solid stress in the tumor interior. Therefore, it is necessary to include both cell types when solid stress and ECM stiffness are being studied.

It has been also shown that CAFs dynamically interact with cancer cells to promote tumor progression (62, 64). In fact, CAFs mediate the invasiveness of colon, pancreatic, and breast cancer cells when co-injected into mice (64–68), while breast and prostate tumors containing CAFs grew faster than tumors injected with normal fibroblasts (69, 70). Nevertheless, there is no pertinent study taking into account the effect of ECM stiffness and solid stress on the interaction of cancer cells and CAFs and *vice versa* the implication of tumor-stromal interactions in ECM stiffening and solid stress accumulation.

Concerning the complexity of the tumor microenvironment, new experimental setups consisting of cancer cells, CAFs, and changes in matrix stiffness and solid stress, in combination or separately, should be introduced to broaden our knowledge about the role of each component in the evolution and malignancy of cancer.

AUTHOR CONTRIBUTIONS

MK and TS planned and wrote the manuscript of this mini review.

FUNDING

REFERENCES

1. Jain RK, Martin JD, Stylianopoulos T. The role of mechanical forces in tumor growth and therapy. *Annu Rev Biomed Eng* (2014) 16:321–46. doi:10.1146/annurev-bioeng-071813-105259

2. Spill F, Reynolds DS, Kamm RD, Zaman MH. Impact of the physical microenvironment on tumor progression and metastasis. *Curr Opin Biotechnol* (2016) 40:41–8. doi:10.1016/j.copbio.2016.02.007

3. Stylianopoulos T, Martin JD, Chauhan VP, Jain SR, Diop-Frimpong B, Bardeesy N, et al. Causes, consequences, and remedies for growth-induced solid stress in murine and human tumors. *Proc Natl Acad Sci U S A* (2012) 109:15101–8. doi:10.1073/pnas.1213353109

4. Quail DF, Joyce JA. Microenvironmental regulation of tumor progression and metastasis. *Nat Med* (2013) 19:1423–37. doi:10.1038/nm.3394

5. Kalluri R. The biology and function of fibroblasts in cancer. *Nat Rev Cancer* (2016) 16:582–98. doi:10.1038/nrc.2016.73

6. Kalluri R, Zeisberg M. Fibroblasts in cancer. *Nat Rev Cancer* (2006) 6:392–401. doi:10.1038/nrc1877

7. Acerbi I, Cassereau L, Dean I, Shi Q, Au A, Park C, et al. Human breast cancer invasion and aggression correlates with ECM stiffening and immune cell infiltration. *Integr Biol (Camb)* (2015) 7:1120–34. doi:10.1039/c5ib00040h

8. Rath N, Olson MF. Regulation of pancreatic cancer aggressiveness by stromal stiffening. *Nat Med* (2016) 22:462–3. doi:10.1038/nm.4099

9. Butcher DT, Alliston T, Weaver VM. A tense situation: forcing tumour progression. *Nat Rev Cancer* (2009) 9:108–22. doi:10.1038/nrc2544

10. Paszek MJ, Weaver VM. The tension mounts: mechanics meets morphogenesis and malignancy. *J Mammary Gland Biol Neoplasia* (2004) 9:325–42. doi:10.1007/s10911-004-1404-x

11. Voutouri C, Polydorou C, Papageorgis P, Gkretsi V, Stylianopoulos T. Hyaluronan-derived swelling of solid tumors, the contribution of collagen and cancer cells, and implications for cancer therapy. *Neoplasia* (2016) 18:732–41. doi:10.1016/j.neo.2016.10.001

12. McGrail DJ, McAndrews KM, Brandenburg CP, Ravikumar N, Kieu QM, Dawson MR. Osmotic regulation is required for cancer cell survival under solid stress. *Biophys J* (2015) 109:1334–7. doi:10.1016/j.bpj.2015.07.046

13. Tomasek JJ, Gabbiani G, Hinz B, Chaponnier C, Brown RA. Myofibroblasts and mechano-regulation of connective tissue remodelling. *Nat Rev Mol Cell Biol* (2002) 3:349–63. doi:10.1038/nrm809

14. Voutouri C, Mpekris F, Papageorgis P, Odysseos AD, Stylianopoulos T. Role of constitutive behavior and tumor-host mechanical interactions in the state of stress and growth of solid tumors. *PLoS One* (2014) 9:e104717. doi:10.1371/journal.pone.0104717

15. Wipff PJ, Rifkin DB, Meister JJ, Hinz B. Myofibroblast contraction activates latent TGF-beta1 from the extracellular matrix. *J Cell Biol* (2007) 179:1311–23. doi:10.1083/jcb.200704042

16. Nia HT, Liu H, Seano G, Datta M, Jones D, Rahbari N, et al. Solid stress and elastic energy as measures of tumour mechanopathology. *Nat Biomed Eng* (2016) 1:0004. doi:10.1038/s41551-016-0004

17. Stylianopoulos T, Martin JD, Snuderl M, Mpekris F, Jain SR, Jain RK. Coevolution of solid stress and interstitial fluid pressure in tumors during progression: implications for vascular collapse. *Cancer Res* (2013) 73:3833–41. doi:10.1158/0008-5472.CAN-12-4521

18. Chen CS. Mechanotransduction – a field pulling together? *J Cell Sci* (2008) 121:3285. doi:10.1242/jcs.023507

19. De Pascalis C, Etienne-Manneville S. Single and collective cell migration: the mechanics of adhesions. *Mol Biol Cell* (2017) 28:1833–46. doi:10.1091/mbc.E17-03-0134

20. Polacheck WJ, Chen CS. Measuring cell-generated forces: a guide to the available tools. *Nat Methods* (2016) 13:415–23. doi:10.1038/nmeth.3834

21. Stylianopoulos T. The solid mechanics of cancer and strategies for improved therapy. *J Biomech Eng* (2017) 139(2):021004. doi:10.1115/1.4034991

22. Gilkes DM, Wirtz D. Tumour mechanopathology: cutting the stress out. *Nat Biomed Eng* (2017) 1:0012. doi:10.1038/s41551-016-0012

23. Friedland JC, Lee MH, Boettiger D. Mechanically activated integrin switch controls alpha5beta1 function. *Science* (2009) 323:642–4. doi:10.1126/science.1168441

24. Li Z, Dranoff JA, Chan EP, Uemura M, Sévigny J, Wells RG. Transforming growth factor-beta and substrate stiffness regulate portal fibroblast activation in culture. *Hepatology* (2007) 46:1246–56. doi:10.1002/hep.21792

25. Ulrich TA, de Juan Pardo EM, Kumar S. The mechanical rigidity of the extracellular matrix regulates the structure, motility, and proliferation of glioma cells. *Cancer Res* (2009) 69:4167–74. doi:10.1158/0008-5472.CAN-08-4859

26. Yeung T, Georges PC, Flanagan LA, Marg B, Ortiz M, Funaki M, et al. Effects of substrate stiffness on cell morphology, cytoskeletal structure, and adhesion. *Cell Motil Cytoskeleton* (2005) 60:24–34. doi:10.1002/cm.20041

27. Kaufman LJ, Brangwynne CP, Kasza KE, Filippidi E, Gordon VD, Deisboeck TS, et al. Glioma expansion in collagen I matrices: analyzing collagen concentration-dependent growth and motility patterns. *Biophys J* (2005) 89:635–50. doi:10.1529/biophysj.105.061994

28. Kraning-Rush CM, Reinhart-King CA. Controlling matrix stiffness and topography for the study of tumor cell migration. *Cell Adh Migr* (2012) 6:274–9. doi:10.4161/cam.21076

29. Mason BN, Starchenko A, Williams RM, Bonassar LJ, Reinhart-King CA. Tuning three-dimensional collagen matrix stiffness independently of collagen concentration modulates endothelial cell behavior. *Acta Biomater* (2013) 9:4635–44. doi:10.1016/j.actbio.2012.08.007

30. Paszek MJ, Zahir N, Johnson KR, Lakins JN, Rozenberg GI, Gefen A, et al. Tensional homeostasis and the malignant phenotype. *Cancer Cell* (2005) 8:241–54. doi:10.1016/j.ccr.2005.08.010

31. Pedersen JA, Swartz MA. Mechanobiology in the third dimension. *Ann Biomed Eng* (2005) 33:1469–90. doi:10.1007/s10439-005-8159-4

32. Szot CS, Buchanan CF, Freeman JW, Rylander MN. 3D in vitro bioengineered tumors based on collagen I hydrogels. *Biomaterials* (2011) 32:7905–12. doi:10.1016/j.biomaterials.2011.07.001

33. Van Goethem E, Poincloux R, Gauffre F, Maridonneau-Parini I, Le Cabec V. Matrix architecture dictates three-dimensional migration modes of human macrophages: differential involvement of proteases and podosome-like structures. *J Immunol* (2010) 184:1049–61. doi:10.4049/jimmunol.0902223

34. Zaman MH, Trapani LM, Sieminski AL, Mackellar D, Gong H, Kamm RD, et al. Migration of tumor cells in 3D matrices is governed by matrix stiffness along with cell-matrix adhesion and proteolysis. *Proc Natl Acad Sci U S A* (2006) 103:10889–94. doi:10.1073/pnas.0604460103

35. Northey JJ, Przybyla L, Weaver VM. Tissue force programs cell fate and tumor aggression. *Cancer Discov* (2017) 7:1224–37. doi:10.1158/2159-8290.CD-16-0733

36. Samuel MS, Lopez JI, McGhee EJ, Croft DR, Strachan D, Timpson P, et al. Actomyosin-mediated cellular tension drives increased tissue stiffness and beta-catenin activation to induce epidermal hyperplasia and tumor growth. *Cancer Cell* (2011) 19:776–91. doi:10.1016/j.ccr.2011.05.008

37. Defilippi P, Di Stefano P, Cabodi S. p130Cas: a versatile scaffold in signaling networks. *Trends Cell Biol* (2006) 16:257–63. doi:10.1016/j.tcb.2006.03.003

38. Gehler S, Baldassarre M, Lad Y, Leight JL, Wozniak MA, Riching KM, et al. Filamin A-beta1 integrin complex tunes epithelial cell response to matrix tension. *Mol Biol Cell* (2009) 20:3224–38. doi:10.1091/mbc.E08-12-1186

39. Kharaishvili G, Simkova D, Bouchalova K, Gachechiladze M, Narsia N, Bouchal J. The role of cancer-associated fibroblasts, solid stress and other microenvironmental factors in tumor progression and therapy resistance. *Cancer Cell Int* (2014) 14:41. doi:10.1186/1475-2867-14-41

40. Levental KR, Yu H, Kass L, Lakins JN, Egeblad M, Erler JT, et al. Matrix crosslinking forces tumor progression by enhancing integrin signaling. *Cell* (2009) 139:891–906. doi:10.1016/j.cell.2009.10.027

41. Lawson CD, Burridge K. The on-off relationship of Rho and Rac during integrin-mediated adhesion and cell migration. *Small GTPases* (2014) 5:e27958. doi:10.4161/sgtp.27958

42. Polacheck WJ, Zervantonakis IK, Kamm RD. Tumor cell migration in complex microenvironments. *Cell Mol Life Sci* (2013) 70:1335–56. doi:10.1007/s00018-012-1115-1

43. Ross TD, Coon BG, Yun S, Baeyens N, Tanaka K, Ouyang M, et al. Integrins in mechanotransduction. *Curr Opin Cell Biol* (2013) 25:613–8. doi:10.1016/j.ceb.2013.05.006

44. Shi Q, Boettiger D. A novel mode for integrin-mediated signaling: tethering is required for phosphorylation of FAK Y397. *Mol Biol Cell* (2003) 14:4306–15. doi:10.1091/mbc.E03-01-0046

45. Wei SC, Fattet L, Tsai JH, Guo Y, Pai VH, Majeski HE, et al. Matrix stiffness drives epithelial-mesenchymal transition and tumour metastasis through a TWIST1-G3BP2 mechanotransduction pathway. *Nat Cell Biol* (2015) 17:678–88. doi:10.1038/ncb3157

46. Gkretsi V, Stylianou A, Louca M, Stylianopoulos T. Identification of Ras suppressor-1 (RSU-1) as a potential breast cancer metastasis biomarker using a three-dimensional in vitro approach. *Oncotarget* (2017) 8:27364–79. doi:10.18632/oncotarget.16062

47. Gkretsi V, Stylianou A, Stylianopoulos T. Vasodilator-stimulated phosphoprotein (VASP) depletion from breast cancer MDA-MB-231 cells inhibits tumor spheroid invasion through downregulation of Migfilin, beta-catenin and urokinase-plasminogen activator (uPA). *Exp Cell Res* (2017) 352:281–92. doi:10.1016/j.yexcr.2017.02.019

48. Wipff PJ, Hinz B. Myofibroblasts work best under stress. *J Bodyw Mov Ther* (2009) 13:121–7. doi:10.1016/j.jbmt.2008.04.031

49. Zhang K, Grither WR, Van Hove S, Biswas H, Ponik SM, Eliceiri KW, et al. Mechanical signals regulate and activate SNAIL1 protein to control the fibrogenic response of cancer-associated fibroblasts. *J Cell Sci* (2016) 129:1989–2002. doi:10.1242/jcs.180539

50. Alessandri K, Sarangi BR, Gurchenkov VV, Sinha B, Kießling TR, Fetler L, et al. Cellular capsules as a tool for multicellular spheroid production and for investigating the mechanics of tumor progression in vitro. *Proc Natl Acad Sci U S A* (2013) 110:14843–8. doi:10.1073/pnas.1309482110

51. Cheng G, Tse J, Jain RK, Munn LL. Micro-environmental mechanical stress controls tumor spheroid size and morphology by suppressing proliferation and inducing apoptosis in cancer cells. *PLoS One* (2009) 4:e4632. doi:10.1371/journal.pone.0004632

52. Delarue M, Montel F, Vignjevic D, Prost J, Joanny JF, Cappello G. Compressive stress inhibits proliferation in tumor spheroids through a volume limitation. *Biophys J* (2014) 107:1821–8. doi:10.1016/j.bpj.2014.08.031

53. Desmaison A, Frongia C, Grenier K, Ducommun B, Lobjois V. Mechanical stress impairs mitosis progression in multi-cellular tumor spheroids. *PLoS One* (2013) 8:e80447. doi:10.1371/journal.pone.0080447

54. Fernández-Sánchez ME, Barbier S, Whitehead J, Béalle G, Michel A, Latorre-Ossa H, et al. Mechanical induction of the tumorigenic β-catenin pathway by tumour growth pressure. *Nature* (2015) 523:92. doi:10.1038/nature14329

55. Helmlinger G, Netti PA, Lichtenbeld HC, Melder RJ, Jain RK. Solid stress inhibits the growth of multicellular tumor spheroids. *Nat Biotechnol* (1997) 15:778–83. doi:10.1038/nbt0897-778

56. Koike C, McKee TD, Pluen A, Ramanujan S, Burton K, Munn LL, et al. Solid stress facilitates spheroid formation: potential involvement of hyaluronan. *Br J Cancer* (2002) 86:947–53. doi:10.1038/sj.bjc.6600158

57. Roose T, Netti PA, Munn LL, Boucher Y, Jain RK. Solid stress generated by spheroid growth estimated using a linear poroelasticity model. *Microvasc Res* (2003) 66:204–12. doi:10.1016/S0026-2862(03)00057-8

58. Demou ZN. Gene expression profiles in 3D tumor analogs indicate compressive strain differentially enhances metastatic potential. *Ann Biomed Eng* (2010) 38:3509–20. doi:10.1007/s10439-010-0097-0

59. Mitsui N, Suzuki N, Koyama Y, Yanagisawa M, Otsuka K, Shimizu N, et al. Effect of compressive force on the expression of MMPs, PAs, and their inhibitors in osteoblastic Saos-2 cells. *Life Sci* (2006) 79:575–83. doi:10.1016/j.lfs.2006.01.040

60. Tse JM, Cheng G, Tyrrell JA, Wilcox-Adelman SA, Boucher Y, Jain RK, et al. Mechanical compression drives cancer cells toward invasive phenotype. *Proc Natl Acad Sci U S A* (2012) 109:911–6. doi:10.1073/pnas.1118910109

61. Chen Q, Yang D, Zong H, Zhu L, Wang L, Wang X, et al. Growth-induced stress enhances epithelial-mesenchymal transition induced by IL-6 in clear cell renal cell carcinoma via the Akt/GSK-3beta/beta-catenin signaling pathway. *Oncogenesis* (2017) 6:e375. doi:10.1038/oncsis.2017.74

62. Kalli M, Papageorgis P, Gkretsi V, Stylianopoulos T. Solid stress facilitates fibroblasts activation to promote pancreatic cancer cell migration. *Ann Biomed Eng* (2018). doi:10.1007/s10439-018-1997-7

63. Egeblad M, Rasch MG, Weaver VM. Dynamic interplay between the collagen scaffold and tumor evolution. *Curr Opin Cell Biol* (2010) 22:697–706. doi:10.1016/j.ceb.2010.08.015

64. Karagiannis GS, Poutahidis T, Erdman SE, Kirsch R, Riddell RH, Diamandis EP. Cancer-associated fibroblasts drive the progression of metastasis through both paracrine and mechanical pressure on cancer tissue. *Mol Cancer Res* (2012) 10:1403–18. doi:10.1158/1541-7786.MCR-12-0307

65. Dimanche-Boitrel MT, Vakaet L Jr, Pujuguet P, Chauffert B, Martin MS, Hammann A, et al. In vivo and in vitro invasiveness of a rat colon-cancer cell line maintaining E-cadherin expression: an enhancing role of tumor-associated myofibroblasts. *Int J Cancer* (1994) 56:512–21. doi:10.1002/ijc.2910560410

66. Hwang RF, Moore T, Arumugam T, Ramachandran V, Amos KD, Rivera A, et al. Cancer-associated stromal fibroblasts promote pancreatic tumor progression. *Cancer Res* (2008) 68:918–26. doi:10.1158/0008-5472.CAN-07-5714

67. Masamune A, Shimosegawa T. Pancreatic stellate cells: a dynamic player of the intercellular communication in pancreatic cancer. *Clin Res Hepatol Gastroenterol* (2015) 39(Suppl 1):S98–103. doi:10.1016/j.clinre.2015.05.018

68. Trimis G, Chatzistamou I, Politi K, Kiaris H, Papavassiliou AG. Expression of p21waf1/Cip1 in stromal fibroblasts of primary breast tumors. *Hum Mol Genet* (2008) 17:3596–600. doi:10.1093/hmg/ddn252

69. Olumi AF, Grossfeld GD, Hayward SW, Carroll PR, Tlsty TD, Cunha GR. Carcinoma-associated fibroblasts direct tumor progression of initiated human prostatic epithelium. *Cancer Res* (1999) 59:5002–11.

70. Orimo A, Gupta PB, Sgroi DC, Arenzana-Seisdedos F, Delaunay T, Naeem R, et al. Stromal fibroblasts present in invasive human breast carcinomas promote tumor growth and angiogenesis through elevated SDF-1/CXCL12 secretion. *Cell* (2005) 121:335–48. doi:10.1016/j.cell.2005.02.034

Conflict of Interest Statement: The authors declare that the research was conducted in the absence of any potential conflict of interest.

Molecular Mechanisms and Emerging Therapeutic Targets of Triple-Negative Breast Cancer Metastasis

Christiana Neophytou[1], Panagiotis Boutsikos[2] and Panagiotis Papageorgis[2]*

[1] Department of Biological Sciences, School of Pure and Applied Sciences, University of Cyprus, Nicosia, Cyprus,
[2] Department of Life Sciences, European University Cyprus, Nicosia, Cyprus

Breast cancer represents a highly heterogeneous disease comprised by several subtypes with distinct histological features, underlying molecular etiology and clinical behaviors. It is widely accepted that triple-negative breast cancer (TNBC) is one of the most aggressive subtypes, often associated with poor patient outcome due to the development of metastases in secondary organs, such as the lungs, brain, and bone. The molecular complexity of the metastatic process in combination with the lack of effective targeted therapies for TNBC metastasis have fostered significant research efforts during the past few years to identify molecular "drivers" of this lethal cascade. In this review, the most current and important findings on TNBC metastasis, as well as its closely associated basal-like subtype, including metastasis-promoting or suppressor genes and aberrantly regulated signaling pathways at specific stages of the metastatic cascade are being discussed. Finally, the most promising therapeutic approaches and novel strategies emerging from these molecular targets that could potentially be clinically applied in the near future are being highlighted.

Keywords: triple-negative breast cancer, metastasis, targeted therapy, tumor microenvironment, dormancy

INTRODUCTION: TUMOR HETEROGENEITY AND CURRENT CHALLENGES IN TRIPLE-NEGATIVE BREAST CANCER (TNBC) TREATMENT

Breast cancer is the most frequently diagnosed cancer among women in the United States and Europe (1, 2). Despite the relative improvement in patient survival rates, breast cancer remains the most commonly diagnosed cancer and the second leading cause of cancer deaths in women worldwide. One of major challenges for the effective treatment of breast cancer is its intertumoral and intratumoral heterogeneity (3). Breast cancer can be initially classified into three different types based on the presence or absence of estrogen receptors (ERs), progesterone receptors (PRs), and the human epidermal growth factor receptor 2 (Her2/neu) (4). Hormone receptor-positive breast cancers that express ER and/or PR constitute approximately 60% of all breast cancers (5). The Her2/neu receptor is overexpressed in approximately 20% of all breast cancer cases; while TNBC constitute approximately 20% of breast cancer cases and are negative for the expression of ER, PR, and Her2/neu (6, 7).

Based on their molecular profile, breast cancers may also be clustered into basal-like and luminal subsets. Luminal breast cancers are more heterogeneous compared to basal cancers in terms of gene expression, mutation spectrum, copy number changes, and patient outcomes and can be further subdivided into luminal A and B subtypes (8, 9). The luminal A subtype represents 50–60% of breast cancer cases and is characterized by low histological grade and good prognosis. Luminal A cancers express ER and PR and have a low frequency of P53 mutations (9). Luminal B represents 10–20% of all breast cancers; compared with the luminal A subtype, these cancers are more aggressive; they have a higher grade, worse prognosis, and worse proliferative index. Luminal B display an increased expression of proliferation genes; they are ER+, PR+/−, Her-2+/−, and EGFR+ and have a higher frequency of P53 mutation (9). Because luminal cancers have a high frequency of PIK$_3$CA mutations, the gene that encodes the p110α catalytic subunit of the phosphatidylinositol 3-kinase (PI$_3$K), agents targeting the PI$_3$K/AKT/mammalian target of rapamycin pathway may be useful for their treatment (10).

The basal-like subtype represents 10–20% of breast cancer cases. They are characterized by high proliferation, high histological grade, and poor prognosis. Basal-like cancers can be triple negative and have a high frequency of P53 mutations combined with loss of Rb1 (9, 11). However, not all basal-like cancers are triple negative; studies have shown that 5–45% of basal-like cancers express ER while 14% express Her2/Neu (12, 13). TNBC is a diverse group of malignancies and can be further categorized to different subtypes. An analysis of 21 breast cancer data sets containing 587 TNBC cases identified seven subtypes based on differential expression of a set of 2,188 genes: two basal like (BL1 and BL2), a mesenchymal (M), a mesenchymal-stem cell-like, an immunomodulatory, a luminal androgen receptor/luminal-like, and an unclassified type (14).

The deregulation of adult mammary stem cells (aMaSC) during tumorigenesis is believed to contribute to the development of TNBC. aMaSCs give rise to common progenitor cells that can differentiate either to basal progenitors that develop mature basal cells, or luminal progenitors. Disruption in the homeostasis of luminal progenitor cells may lead to the development of TNBC. Contributors in the development of TNBC include aberrantly activated signaling pathways, such as Wnt/β-catenin and Notch, transcriptional factors, like Snail, and embryonic stem cell markers including Sox2, Nanog, and Oct4. These alterations allow the restoration of proliferation capacity as well as the de-differentiation of these progenitor cells, leading to the accumulation of mutations that give rise to TNBC (15).

Traditionally, due to the lack of ER, PR, and Her2/Neu expression, the ineffectiveness of current breast cancer targeted therapies as well as due to the challenges in identifying key molecular drivers of TNBC progression, chemotherapy has been the foundation of treatment for patients with this disease over the last decades. Despite its sensitivity to chemotherapy, TNBC is associated with a higher risk of distant recurrence, high rates of metastases, higher probability of relapse and worse overall survival (OS) compared to other subtypes (16, 17).

COMPLEXITY OF TNBC METASTASIS

The dissemination of breast cancer cells and eventual metastatic growth to distant organs—predominantly the bone, lungs, and brain—represents a significant clinical problem, as metastatic disease is incurable and is the primary cause of death for the vast majority of TNBC patients. Metastatic spread of tumor cells is a highly complex, yet poorly understood process, and consists of multiple steps, including acquisition of invasive properties through genetic and epigenetic alterations, angiogenesis, tumor–stroma interactions, intravasation through the basement membrane, survival in the circulation, and extravasation of some cancer cells to distal tissues (18). However, disseminated cells that survive pro-apoptotic signals in their new environment often remain quiescent in secondary organs undergoing long periods of latency, also known as the dormancy period (19). It is well established that the outgrowth of metastatic cells in a foreign tissue microenvironment is a highly inefficient process and is considered as the rate-limiting step of breast cancer metastasis (20) (**Figure 1**). During this stage, breast cancer cells are usually difficult to detect and exhibit resistance to chemotherapy due to lack of proliferation (19). This remains a major clinical problem since patients, often considered as "survivors," can develop metastatic disease years later. Disseminated tumor cells (DTCs) can enter a state of dormancy in secondary organs by exiting the proliferative cycle for an indefinite period or by achieving a balanced state of proliferation and apoptosis. Successful emergence from dormancy is the result of further evolution of surviving DTCs, by accumulating molecular alterations as well as *via* permissive interactions with the tumor microenvironment (19). By acquiring these characteristics, metastatic populations can optimally adapt to the host microenvironment and initiate colonization. While significant progress has been made to highlight some of the specific processes required for the breast tumor initiation, efforts have recently been focused on elucidating the roles of critical genes, the underlying molecular mechanisms and signaling pathways involved in the fatal late stages of metastatic dissemination. These studies are of outmost importance for the development of novel effective treatments against metastasis of TNBC.

GENES IMPLICATED IN MULTISTEP TNBC METASTASIS

Local Invasion/Intravasation

Upon accumulation of genetic and/or epigenetic alterations, breast cancer cells at the primary tumor initially acquire properties, such as self-renewal, ability to migrate, and invade the surrounding normal tissues. During local invasion, breast cancer cells undergo epithelial-to-mesenchymal transition (EMT), a highly orchestrated transcriptional program, initially described during embryonic development, associated with dramatic remodeling of cytoskeleton, loss of apico-basolateral polarity, dissolution of cell–cell junctions, concomitant with downregulation of epithelial markers and upregulation of mesenchymal genes (21). This process is triggered by EMT-master regulators,
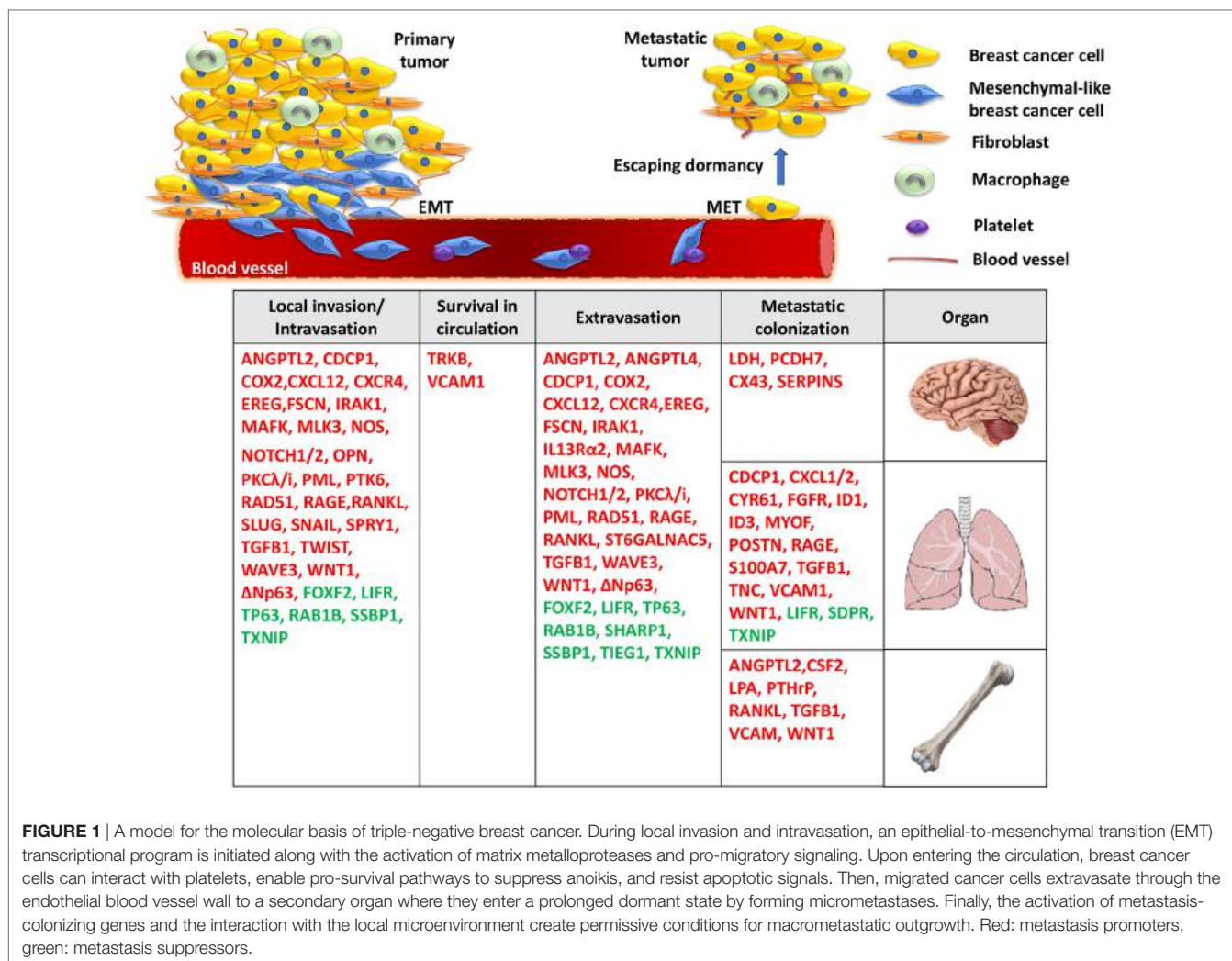
FIGURE 1 | A model for the molecular basis of triple-negative breast cancer. During local invasion and intravasation, an epithelial-to-mesenchymal transition (EMT) transcriptional program is initiated along with the activation of matrix metalloproteases and pro-migratory signaling. Upon entering the circulation, breast cancer cells can interact with platelets, enable pro-survival pathways to suppress anoikis, and resist apoptotic signals. Then, migrated cancer cells extravasate through the endothelial blood vessel wall to a secondary organ where they enter a prolonged dormant state by forming micrometastases. Finally, the activation of metastasis-colonizing genes and the interaction with the local microenvironment create permissive conditions for macrometastatic outgrowth. Red: metastasis promoters, green: metastasis suppressors.

such as the transcription factors Slug, Snail, and Twist to promote TNBC cell migration and intravasation in the circulation (22–24). The TGFβ pathway plays a critical role in regulating this early metastatic event. During intravasation, TGFβ promotes overexpression of musculoaponeurotic fibrosarcoma oncogene family protein K (MAFK) to induce EMT and enhance tumor formation and invasion *in vivo* (25). The TGFβ-Smad signaling axis controls the EMT step in the malignant progression of breast cancer cells either by inducing the expression of master transcriptional regulators of EMT, as described above, or by epigenetic silencing of epithelial genes, including CDH1 (26). The EMT program regulated by TGFβ/Smad signaling also involves WAVE3, a WASP/WAVE family actin-binding protein. In TNBC cells, depletion of WAVE3 expression prevented TGFβ-induced EMT phenotype (27). However, despite numerous studies using cell lines and animal models suggesting a functional role of EMT and EMT-inducing transcription factors in promoting breast cancer metastasis, the *in vivo* role and clinical relevance of this process remains controversial (28–31).

Moreover, the majority of genes implicated in TNBC metastasis have been reported to play a major role at the initial stages of cancer cell dissemination which include migration, invasion, and intravasation. This is not surprising given the fact that cancer cell dissemination is thought to be an early event during breast cancer evolution and that primary and metastatic tumor growth is likely to progress in parallel (32). For example, activation of CXCR4 receptor *via* its ligand CXCL12 or ANGPTL2 was found to induce MLK3 and Erk1/2 signaling and promote intravasation which leads to the development of lung and bone metastases (33–39). This hyperactive signaling axis may also function in multiple stages of the metastatic cascade, including angiogenesis, extravasation, and osteolysis at the secondary organ. At the same time, it is becoming increasingly clear that trans-endothelial migration and invasion of breast cancer cells in the vasculature is inhibited by metastasis suppressors, including TP63, LIFR, lysyl oxidase-like 4 (LOXL4), FOXF2, SSBP1, RAB1B, and TIEG1 (25, 40–47), suggesting that the migratory and invasive potential of breast cancer cells is ultimately determined by the balance in the activity of these molecules. The identification of numerous genes implicated in the initial stages of TNBC metastasis highlights the significant challenges for early molecular diagnosis and therapy.

Survival in Circulation

Upon entering the blood vessels, circulating tumor cells express proteins that have antiapoptotic and pro-survival functions which allow them to attach to and infiltrate specific secondary sites. Neurotrophic tyrosine kinase receptor TRKB was shown to inhibit anoikis, a form of cell death caused by lack of adhesion, *via* the PI₃K/Akt pathway. These studies indicated that TRKB induces survival and proliferation of breast cancer cells to promote infiltration in the lymphatic and blood vessels and colonization in distant organs (48). In TNBC cells, brain-derived neurotrophic factor (BDNF) binds and activates TRKB receptor to regulate a network consisting of metalloproteases and calmodulin and thus modulate cancer–endothelial cells interaction. Importantly, Erk1/2 inhibitors were able to block the BDNF-induced phenotype, suggesting that blocking this pathway may be explored for therapeutic purposes against TNBC metastasis (49). In addition, the binding of platelets with circulating breast cancer cells has been shown to essential for their survival, evasion of pro-apoptotic signals, whereas interfering with this interaction inhibits the development of lung metastasis in TNBC mouse models (50, 51).

Extravasation in Distal Sites

Many of the genetic alterations found to be involved in intravasation are also implicated in extravasation (**Table 1**) since, in large part, these two processes are considered "mirrored" to each other. The TGFβ pathway plays an important role in regulating both these metastatic steps. More specifically, TGFβ induces the assembly of a mutant-p53/Smad protein complex to inhibit the function of the metastasis suppressor TP63 and promote cell migration and invasion (40). During extravasation, TGFβ induces angiopoietin-like 4 (ANGPTL4) expression *via* the Smad signaling pathway; the increased levels of ANGPTL4 enhance the retention of cancer cells in the lungs by disrupting vascular endothelial cell–cell junctions, thus increasing the permeability of lung capillaries to facilitate trans-endothelial passage of breast cancer cells (52). Moreover, targeting the decoy interleukin-13 receptor alpha 2 (IL13Ra2) upregulates the metastasis suppressor TP63 in an IL13-mediated, STAT6-dependent manner and impairs extravasation of basal-like breast cancer cells to the lungs (41). Several reports also highlight the importance of the synergistic effects of genes in promoting metastasis by regulating specific stages of the process. For example, EREG, COX2, MMP1, and MMP2 can collectively promote metastatic extravasation to the lungs. These four genes were found to be overexpressed in TNBC cells independently of VEGF. Individual reduction of each gene or their silencing in different combinations produced limited effects on tumor growth *in vivo* while concurrent silencing of all four achieved nearly complete growth abrogation (53).

Metastatic Colonization

Following extravasation and infiltration at the secondary site, a genetic program is initiated so that cancer cells can escape dormancy and form micro and macrometastatic tumors. Initially, EMT plasticity and the reversal to MET phenotype have been shown to be important for metastatic colonization (113). During this process, epithelial phenotype becomes re-established through miR-200-mediated downregulation of ZEB1, SIP1 to promote metastatic colonization (114, 115). Also, breast DTCs in the bone marrow gain the ability to form typical osteolytic metastases by producing parathyroid hormone-related protein (PTHLH), tumor necrosis factor-α (TNFα), interleukin-6 and/or interleukin-11. These factors stimulate the release of receptor activator of nuclear factor-κB ligand (RANKL) from osteoblasts which induces osteoclast formation (33, 58, 83, 116). Furthermore, inflammation in the lung microenvironment could also be responsible for triggering the escape of metastatic breast cancer cells from latency leading to metastatic colonization (117). A subset of genes contributing to primary tumor growth can also promote survival and growth at the secondary site. Chemokines CXCL1/2 mediate chemoresistance and lung metastasis by attracting myeloid cells into the tumor, which produce low molecular weight calcium-binding proteins S100A8/9 that enhance cancer cell survival by binding to the receptor for advanced glycation end products (RAGE) (59). Another calcium binding protein, S100A7 has been found to enhance tumor growth and metastasis, by binding to RAGE and activating Erk and NFκB signaling (88, 90). Furthermore, fibroblast growth factor receptor (FGFR) was shown to trigger pro-survival signals through PI₃K/Akt signaling and promote outgrowth of metastatic breast cancer cells to the lungs (62). However, it needs to be highlighted that cellular and genetic context among cancers influences whether proteins act as tumor suppressors or metastasis promoters. One controversial example is LOXL4 which has been shown to recruit bone marrow-derived cells and facilitate colonization of TNBC to the lungs *via* a HIF1α-dependent mechanism (118). However, in another study, knockdown of LOXL4 expression in TNBC cells promoted primary tumor growth and lung metastasis which was associated with thickening of collagen bundles and remodeling of the extracellular matrix (ECM) within tumors (25). Overall, it is noteworthy that while some genes have been associated only with TNBC metastasis so far (i.e., TIEG1, MAFK, MLK3, SDPR), the majority is also involved in other tumor types, suggesting a more fundamental role in cancer progression.

CONCLUDING REMARKS ON CURRENT AND FUTURE PERSPECTIVES ON TNBC METASTASIS THERAPY

Due to their molecular heterogeneity, there are no drugs that can target the entire spectrum of TNBC tumors and each subtype is vulnerable to specific therapeutic approaches. Despite the lack of FDA-approved targeted therapies for TNBC to date, ongoing clinical trials are assessing the efficacy of single or combinatorial approaches that tackle different TNBC molecular alterations. Up to 20% of TNBC have been associated with germ-line mutations in BRCA1 (119). TNBC tumors with loss of function of BRCA1 or BRCA2 are sensitive to poly(ADP-ribose) polymerase inhibitors and alkylating agents that induce DNA double-strand breaks (120). Olaparib has been the most successful PARP inhibitor

TABLE 1 | List of genes involved triple-negative breast cancer metastasis.

Metastasis-promoting genes

Gene	Function	Signaling pathway	Gene ontology	Stage	Organ site	Reference
ANGPTL2	Promotes osteolysis Migration Angiogenesis	Activates CXCR4 and Erk1/2 signaling	Receptor binding, extracellular space	Intravasation, extravasation Angiogenesis Micro- to macrometastasis colonization	Bone	(37)
ANGPTL4	Promotes trans-endothelial cancer cell migration by disrupting lung capillary cell junctions	Activated by TGFβ signaling	Angiogenesis	Extravasation	Lungs	(52)
CDCP1	Reduces lipid droplets, stimulates fatty acid oxidization and oxidative phosphorylation	Interacts with and inhibits acyl-CoA-synthetase ligase	Plasma membrane, protein binding	Intravasation, extravasation Metastatic colonization and growth	Lungs	(54)
COX2	Migration, invasion Promotes cancer stem cell maintenance	Mediates TGFβ-induced cancer cell stemness	Prostaglandin biosynthetic process, angiogenesis	Intravasation, extravasation Self-renewal	Bone	(53, 55–57)
CSF2	Osteoclast activation	Activated by NFκB signaling	Granulocyte macrophage colony-stimulating factor receptor binding	Micro- to macrometastasis colonization	Bone	(58)
CXCL1/2	Recruitment of myeloid cells	Activated by tumor necrosis factor-α/NFκB pathway	Receptor binding, extracellular region	Cancer cell survival at primary and metastatic sites	Lungs	(59, 60)
CXCL12	Binds CXCR4 to initiate downstream signaling	Activates CXCR4 signaling	Response to hypoxia, migration, endothelial cell proliferation, receptor binding	Intravasation, extravasation Angiogenesis	Lungs	(34)
CXCR4	Mediates actin polymerization and formation of lamellopodia Migration, Invasion Angiogenesis	Activated by ANGPTL2	Activation of MAPK activity, response to hypoxia, chemotaxis, G-protein coupled receptor activity	Intravasation, extravasation Angiogenesis	Lungs	(33–36)
CYR61	Vascularization	Activated by Sonic-Hedgehog/Gli1 signaling	Regulation of cell growth, angiogenesis	Angiogenesis Micro- to macrometastasis colonization	Lungs	(61)
EREG	Promotes vessel remodeling and invasion	VEGF-independent	MAPK cascade, angiogenesis	Intravasation Extravasation Angiogenesis	Lungs	(53)
FGFR	Suppresses apoptosis and promotes survival	Activates PI₃K/Akt signaling	MAPK cascade, angiogenesis	Survival Primary tumor growth Micro- to macrometastasis colonization	Lungs	(62)
FSCN	Migration, invasion	Activates NFκB signaling Increases MMP2, MMP9 expression	Stress fiber, podosome, actin binding	Intravasation, extravasation	Lungs	(63, 64)
ID1, ID3	Promotes tumor re-initiation	Induced by NFκB-mediated IGF2/PI₃K signaling	DNA binding transcription factor activity, angiogenesis	Micro- to macrometastasis colonization	Lungs	(65–67)
IL13Ra2	Migration	Suppresses IL13–STAT6–P63 signaling	Cytokine receptor activity, signal transducer activity	Extravasation	Lungs	(41, 60)

(*Continued*)

25

TABLE 1 | Continued

Metastasis-promoting genes

IRAK1	Invasion Promotes cancer stem cell maintenance	Activates NFκB and p38 signaling	Activation of MAPK activity, regulation of cytokine-mediated signaling	Intravasation, extravasation Self-renewal	Lungs	(68)
LDH	Catalyzes final reactions of glycolysis	Activates glycolytic pathway	Response to hypoxia, lactate dehydrogenase activity, lactate/pyruvate metabolism	Metastatic growth and colonization	Brain	(69, 70)
LPA	Produced by platelets to promote osteolysis	Induces interleukin-6 and IL8 secretion by breast cancer cells	Fibronectin binding, endopeptidase activity	Micro- to macrometastasis colonization	Bone	(71)
MAFK	Promotes epithelial-to-mesenchymal transition (EMT)	Activated by TGFβ pathway	DNA binding transcription factor activity	Intravasation, extravasation	Lungs	(72)
MLK3	Drives invasion and trans-endothelial migration	Mediates CXCL12/CXCR4 signaling to promote paxillin phosphorylation Increases FRA1, MMP1 and MMP9 levels	Activation of MAPK activity, protein serine/threonine kinase activity	Intravasation Extravasation	Lungs	(38, 39)
MYOF	Regulates lipid metabolism and mitochondrial function and promotes vesicle trafficking	Loss of MYOF suppresses AMPK phosphorylation and HIF1α stabilization due to metabolic stress	Phospholipid binding, plasma membrane, caveola	Metastatic growth and colonization	Lungs	(73)
NOS	Promotes EMT, self-renewal, migration, invasion	Activates TGFβ and hypoxia signaling	Response to hypoxia, nitric-oxide synthase activity	Intravasation, extravasation Self-renewal	Lungs	(74)
NOTCH1/ NOTCH2	Migration, invasion Promotes cancer stem cell maintenance	Activate Notch signaling	Golgi membrane, cell fate determination, receptor activity	Intravasation, extravasation Tumor initiation and self-renewal	Lungs Bone	(75)
OPN	Mediates MSC-to-cancer-associated fibroblast transformation, tumor growth and invasion	Mediate TGFβ1 signaling to increase MMP2 and uPA levels	Osteoblast differentiation, cytokine activity	Tumor growth Invasion	Lung Liver	(76, 77)
PCDH7/CX43	Promotes cancer cell-astrocyte interaction	Activates IFNγ, NFκB pathway	Calcium ion binding, plasma membrane, cell adhesion	Micro- to macrometastasis colonization	Brain	(78)
PKCλ/ι	Migration, invasion	Activated by TGFβ/IL1β Activates NFκB	Golgi membrane, protein serine/threonine kinase activity	Intravasation, extravasation	Lungs	(79)
PML	Migration, invasion	Activated by hypoxia/HIF1α signaling	Response to hypoxia	Intravasation, extravasation	Lungs	(80)
POSTN	Expressed by stromal or cancer cells Promotes cancer stem cell maintenance	Activates Wnt1 and Wnt3A signaling Activates NFκB and Erk signaling	Negative regulation of cell–matrix adhesion, response to hypoxia	Micro- to macrometastasis colonization	Lungs	(81, 82)
PTHLH	Osteoclast activation	Activated by TGFβ signaling Induced by miR-218-5p	Osteoblast development, hormone activity	Micro- to macrometastasis colonization	Bone	(83, 84)
PTK6	Promotes EMT *via* Snail upregulation	Activates EGF and PI3K/Akt signaling	Protein tyrosine kinase activity	Local invasion Intravasation	Lungs	(85, 86)
RAD51	Promotes aberrant DNA repair	Double-strand break repair pathway	Double-strand break repair *via* homologous recombination	Intravasation, extravasation	Lungs	(87)
RAGE	Binds S100A7 to promote recruitment of tumor-associated macrophages and migration	Activates Erk and NFκB pathways	Cytokine production, inflammatory responses	Primary and metastatic tumor growth Intravasation, extravasation	Lungs	(88)

(*Continued*)

TABLE 1 | Continued

Metastasis-promoting genes

RANKL	Migration Osteoclast activation	Activates NFκB signaling Induced by miR-218-5p	Osteoblast proliferation, cytokine activity, monocyte chemotaxis	Intravasation, extravasation Micro- to macrometastasis colonization	Bone	(84, 89)
S100A7	Promotes inflammation, recruitment of tumor-associated macrophages and angiogenesis	Activates STAT3, Akt and Erk pathways	Response to ROS, angiogenesis	Primary and metastatic tumor growth	Lungs	(90)
SERPINS (NS, B2, D1)	Inhibit plasminogen activation Promote vascular co-option	Inhibits FasL-mediated apoptotic pathway	Serine-type endopeptidase inhibitor activity, chemotaxis, blood coagulation	Survival Micro- to macrometastasis colonization	Brain	(91)
SLUG	Promotes EMT Migration Invasion Survival by suppressing Puma-induced apoptosis	Activated by Erk, FGF signaling Activates TGFβ signaling	EMT	Local invasion Intravasation Metastatic colonization	Lungs	(22, 92–94)
SNAIL	Promotes EMT Migration Invasion	Activated by EGF signaling Activates TGFβ signaling	EMT, Mesoderm formation	Local invasion Intravasation	Lungs	(23, 94–96)
SPRY1	Promotes EGFR stability Promotes EMT, migration, invasion	Activates EGFR signaling	Mitotic spindle orientation	Intravasation, extravasation	Lungs	(97)
ST6GALNAC5	Mediates brain infiltration across the blood–brain barrier	Catalyzes cell-surface sialylation	Golgi membrane, sialytransferase activity	Extravasation	Brain	(98)
TGFβ1	EMT Migration Invasion Promotes osteoclastic bone resorption	Activates AP1- and Smad4-dependent interleukin-11 and CTGF expression. Maintains Smad2-dependent, DNMT1 mediated DNA methylation and silencing of CDH1	EMT, vasculogenesis, neural tube closure, response to hypoxia	Intravasation, extravasation Colonization	Lungs Bone	(26, 99, 100)
TNC	Promotes survival and outgrowth of macrometastases	Activates Notch and Wnt signaling	Osteoblast differentiation, extracellular region	Micro- to macrometastasis colonization	Lungs	(101)
TRKB	Suppresses anoikis to promote survival in circulation Modulates breast cancer-endothelial cell interaction	Interacts with brain-derived neurotrophic factor ligand Activates Erk and PI3K signaling	Vasculogenesis, neuron migration	Survival in circulation	Lungs Bone	(48, 49)
TWIST	Promotes EMT Migration Invasion	Induced by Wnt signaling	Neuron migration, neural tube closure, morphogenesis	Local invasion Intravasation	Lungs	(24, 102)
VCAM1	Osteoclast activation through interaction with integrin α4β1 Binds metastasis-associated macrophages via α4 integrins	Activated by NFκB pathway Activates PI3K/Akt pathway	Inflammatory response, integrin binding, extracellular space	Survival Micro- to macrometastasis colonization	Bone Lungs	(60, 103, 104)
WAVE3	Promotes EMT	Activates TGFβ signaling	Actin binding, cytoskeleton organization, lamellipodium	Intravasation, extravasation	Lungs	(27)

(*Continued*)

27

TABLE 1 | Continued

Metastasis-promoting genes

Wnt1	Maintains CSC renewal Migration Invasion	Activates Wnt/β-catenin signaling Induced by miR-218-5p	Embryonic axis specification, frizzled binding, cytokine activity	Intravasation, extravasation Colonization	Lungs Bone	(84, 105–107)
ΔNp63	Promotes migration, invasion EMT	Activates PI3K signaling and CD44v6 expression	Transcription factor activity, p53 binding	Intravasation, extravasation	Lungs Bone	(108)

Metastasis suppressor genes

FOXF2	Inhibits migration, invasion	Blocks EMT by suppressing Twist	Transcription factor activity, EMT	Intravasation, extravasation	Lungs	(44)
LIFR	Inhibits migration, invasion	Targeted by miR-9 Activates Hippo/YAP pathway	Regulation of cytokine-mediated signaling pathway	Intravasation, extravasation Metastatic colonization	Lungs	(43)
LOXL4	Inhibits migration, invasion, primary and metastatic tumor growth	Suppresses collagen synthesis	Scavenger receptor activity, oxidoreductase activity	Intravasation, extravasation	Lungs	(25)
TP63	Inhibits migration, invasion Regulates miRNA processing	Inhibited by TGFβ-induced Smad/ mutant-p53 complex Induced by IL13 Upregulates Dicer to control miRNA processing	Transcription factor activity, p53 binding	Intravasation, extravasation	Lungs	(40–42)
RAB1B	Inhibits migration, invasion	Activates TGFβ/Smad signaling	Golgi membrane	Intravasation, extravasation	Lungs	(46)
SDPR	Inhibits extravasation, Apoptosis	Silenced by DNA methylation Suppresses NFκB, Erk	Phosphatidylserine binding	Extravasation Apoptosis at secondary organ	Lungs	(109)
SHARP1	Promotes degradation of hypoxia-inducible factors Inhibits migration, invasion	Suppresses hypoxia-inducible pathway	DNA binding transcription factor activity	Extravasation	Lungs	(110)
SSBP1	Inhibits TGFβ-induced EMT	Regulates mitochondrial retrograde signaling	Single-stranded DNA binding, RNA binding, mitochondrial matrix	Intravasation, extravasation	Lungs	(45)
TIEG1	Inhibits migration, invasion	Downregulates EGFR expression to suppress EGF signaling	DNA binding transcription factor activity	Intravasation, extravasation	Lungs	(47)
TXNIP	Blocks glucose uptake and aerobic glycolysis Suppresses EMT	Suppressed by Myc oncogene and miR-373	Mitochondrial intermembrane space, enzyme inhibitor activity	Intravasation, extravasation Metastatic colonization and growth	Lungs	(111, 112)

A comprehensive list of genes implicated in various stages of the metastatic cascade, their reported functions, upstream or downstream regulatory signaling pathways involved, gene ontology, as well as the secondary organs which become affected.

against BRCA-mutated TNBC, inducing partial responses in 54% of patients when administered as a single agent (121) and an overall response rate of 88% when combined with carboplatin (122). Anti-androgens as well as FGFR inhibitors have been tested in clinical trials against TNBCs that are androgen receptor-positive or harbor FGFR amplification, respectively (123, 124). Gamma-secretase inhibitors that block the NOTCH pathway are currently in clinical trials for TNBC patients with upregulated NOTCH signaling (125). All together clinical trials have shown that each agent alone provides small or no benefit in TNBC patients suggesting that further effort is needed to discover novel targets of TNBC and to identify each patient's molecular profile that will lead to a more individualized treatment.

Toward this goal, some of the metastasis-promoting genes reported here could be further exploited for the future development of promising targeted therapies. Since local invasion, intravasation and possibly extravasation are thought to occur relatively early in the metastatic process (32), a plausible strategy would be to target dormancy and the outgrowth of macrometastatic tumors in distal organs. Since this final stage is considered the critical "rate-limiting" step of the "invasion-metastasis" cascade requiring even years to be completed, it provides a window of opportunity for effective therapy. Therefore, different approaches could aim against "druggable" molecules that facilitate metastatic colonization, such as overexpressed receptors or secreted molecules (i.e., CXCL1/2, FGFR, TGFβ1, WNT1, ANGPTL2, CSF2, RANKL), which target commonly deregulated signaling networks at this late-stage (**Table 1**). Ongoing clinical trials are evaluating the efficacy of the TGFβR1 inhibitor LY2157299 with paclitaxel (NCT02672475), whereas the FGFR inhibitor Lucitanib is also under testing (NCT02202746) for patients with metastatic TNBC. The ultimate goal would be, if not to completely eliminate dormant metastatic breast cancer cells, to prolong dormancy period and hopefully transform this stage into a chronic inactive cancer cell state.

Importantly, recent studies have shown that tumor cells are able to evade immune responses by activating negative regulatory pathways, also known as immune checkpoints, that block T-cell activation through cytotoxic T-lymphocyte protein 4 (CTLA4) or *via* binding of the programmed cell death protein 1 (PD1) receptor expressed on T-cell surface to the PDL1 ligand expressed by cancer cells in response to various cytokines (126). The recent development and FDA approval of anti-CTLA4, anti-PDL1, and anti-PDL1 monoclonal antibodies that elicit

antitumor clinical responses in a variety of solid cancers created enthusiasm for cancer therapy (127). Currently, several clinical trials are underway to evaluate the efficacy of this approach in TNBC as well (128).

However, a major clinical problem is that breast cancer is considered one of the most desmoplastic tumor types due to the production of excessive amounts of ECM components, such as collagen and hyaluronan, which generate mechanical stresses within the growing tumor (129). This results in blood vessel compression, hypoperfusion, and hypoxia which promote cancer progression and metastasis as well as hinder drug delivery (130). Therefore, targeting components of the tumor microenvironment has also been recently proposed as another promising strategy for TNBC therapy by improving tumor penetration and delivery of cytotoxic drugs (131). For example, targeting of cancer-associated fibroblasts using pirfenidone, an FDA-approved drug for idiopathic pulmonary fibrosis, has been shown to suppress metastasis of TNBC in combination with doxorubicin (132). This effect is likely to be mediated through remodeling of tumor microenvironment which reduces ECM components through suppression of TGFβ signaling, improves perfusion and delivery of chemotherapy (133). Similar effects have also been demonstrated using the anti-fibrotic drug Tranilast or the anti-hypertensive drug Losartan in combination with chemotherapy or nanotherapy in mouse models for TNBC (134–136).

In conclusion, this evidence suggests that efforts in the near future should be focused toward the development and testing of novel anti-metastatic targeted therapies for late-stage TNBC that could be used in combination with existing chemotherapies, immunotherapies as well as with microenvironment-remodeling agents that can improve drug penetration and overall therapeutic efficacy.

AUTHOR CONTRIBUTIONS

CN and PB wrote the paper and helped with illustrations. PP conceived the theme, wrote the paper, and prepared illustrations.

FUNDING

REFERENCES

1. Ferlay J, Steliarova-Foucher E, Lortet-Tieulent J, Rosso S, Coebergh JW, Comber H, et al. Cancer incidence and mortality patterns in Europe: estimates for 40 countries in 2012. *Eur J Cancer* (2013) 49(6):1374–403. doi:10.1016/j.ejca.2012.12.027
2. Siegel RL, Miller KD, Jemal A. cancer statistics, 2017. *CA Cancer J Clin* (2017) 67(1):7–30. doi:10.3322/caac.21387
3. Polyak K. Heterogeneity in breast cancer. *J Clin Invest* (2011) 121(10):3786–8. doi:10.1172/JCI60534
4. Carlson RW, Allred DC, Anderson BO, Burstein HJ, Carter WB, Edge SB, et al. Breast cancer. clinical practice guidelines in oncology. *J Natl Compr Canc Netw* (2009) 7(2):122–92. doi:10.6004/jnccn.2009.0012

5. Buzdar AU. Role of biologic therapy and chemotherapy in hormone receptor- and HER2-positive breast cancer. *Ann Oncol* (2009) 20(6):993–9. doi:10.1093/annonc/mdn739
6. Slamon DJ, Leyland-Jones B, Shak S, Fuchs H, Paton V, Bajamonde A, et al. Use of chemotherapy plus a monoclonal antibody against HER2 for metastatic breast cancer that overexpresses HER2. *N Engl J Med* (2001) 344(11):783–92. doi:10.1056/NEJM200103153441101
7. Anders CK, Carey LA. Biology, metastatic patterns, and treatment of patients with triple-negative breast cancer. *Clin Breast Cancer* (2009) 9(Suppl 2):S73–81. doi:10.3816/CBC.2009.s.008
8. Hu Z, Fan C, Oh DS, Marron JS, He X, Qaqish BF, et al. The molecular portraits of breast tumors are conserved across microarray platforms. *BMC Genomics* (2006) 7:96. doi:10.1186/1471-2164-7-96

9. Cancer Genome Atlas Network. Comprehensive molecular portraits of human breast tumours. *Nature* (2012) 490(7418):61–70. doi:10.1038/nature11412

10. De Abreu FB, Wells WA, Tsongalis GJ. The emerging role of the molecular diagnostics laboratory in breast cancer personalized medicine. *Am J Pathol* (2013) 183(4):1075–83. doi:10.1016/j.ajpath.2013.07.002

11. Perou CM. Molecular stratification of triple-negative breast cancers. *Oncologist* (2011) 16(Suppl 1):61–70. doi:10.1634/theoncologist.2011-S1-61

12. Rakha E, Ellis I, Reis-Filho J. Are triple-negative and basal-like breast cancer synonymous? *Clin Cancer Res* (2008) 14(2):618. doi:10.1158/1078-0432.CCR-07-1943

13. Rouzier R, Perou CM, Symmans WF, Ibrahim N, Cristofanilli M, Anderson K, et al. Breast cancer molecular subtypes respond differently to preoperative chemotherapy. *Clin Cancer Res* (2005) 11(16):5678–85. doi:10.1158/1078-0432.CCR-04-2421

14. Lehmann BD, Jovanovic B, Chen X, Estrada MV, Johnson KN, Shyr Y, et al. Refinement of triple-negative breast cancer molecular subtypes: implications for neoadjuvant chemotherapy selection. *PLoS One* (2016) 11(6):e0157368. doi:10.1371/journal.pone.0157368

15. Rangel MC, Bertolette D, Castro NP, Klauzinska M, Cuttitta F, Salomon DS. Developmental signaling pathways regulating mammary stem cells and contributing to the etiology of triple-negative breast cancer. *Breast Cancer Res Treat* (2016) 156(2):211–26. doi:10.1007/s10549-016-3746-7

16. Early Breast Cancer Trialists' Collaborative Group (EBCTCG). Effects of chemotherapy and hormonal therapy for early breast cancer on recurrence and 15-year survival: an overview of the randomised trials. *Lancet* (2005) 365(9472):1687–717. doi:10.1016/S0140-6736(05)66544-0

17. Ovcaricek T, Frkovic SG, Matos E, Mozina B, Borstnar S. Triple negative breast cancer – prognostic factors and survival. *Radiol Oncol* (2011) 45(1):46–52. doi:10.2478/v10019-010-0054-4

18. Nguyen DX, Massague J. Genetic determinants of cancer metastasis. *Nat Rev Genet* (2007) 8(5):341–52. doi:10.1038/nrg2101

19. Giancotti FG. Mechanisms governing metastatic dormancy and reactivation. *Cell* (2013) 155(4):750–64. doi:10.1016/j.cell.2013.10.029

20. Valastyan S, Weinberg RA. Tumor metastasis: molecular insights and evolving paradigms. *Cell* (2011) 147(2):275–92. doi:10.1016/j.cell.2011.09.024

21. De Craene B, Berx G. Regulatory networks defining EMT during cancer initiation and progression. *Nat Rev Cancer* (2013) 13(2):97–110. doi:10.1038/nrc3447

22. Ferrari-Amorotti G, Chiodoni C, Shen F, Cattelani S, Soliera AR, Manzotti G, et al. Suppression of invasion and metastasis of triple-negative breast cancer lines by pharmacological or genetic inhibition of slug activity. *Neoplasia* (2014) 16(12):1047–58. doi:10.1016/j.neo.2014.10.006

23. Tran HD, Luitel K, Kim M, Zhang K, Longmore GD, Tran DD. Transient SNAIL1 expression is necessary for metastatic competence in breast cancer. *Cancer Res* (2014) 74(21):6330–40. doi:10.1158/0008-5472.CAN-14-0923

24. Yang J, Mani SA, Donaher JL, Ramaswamy S, Itzykson RA, Come C, et al. Twist, a master regulator of morphogenesis, plays an essential role in tumor metastasis. *Cell* (2004) 117(7):927–39. doi:10.1016/j.cell.2004.06.006

25. Choi SK, Kim HS, Jin T, Moon WK. LOXL4 knockdown enhances tumor growth and lung metastasis through collagen-dependent extracellular matrix changes in triple-negative breast cancer. *Oncotarget* (2017) 8(7):11977–89. doi:10.18632/oncotarget.14450

26. Papageorgis P, Lambert AW, Ozturk S, Gao F, Pan H, Manne U, et al. Smad signaling is required to maintain epigenetic silencing during breast cancer progression. *Cancer Res* (2010) 70(3):968–78. doi:10.1158/0008-5472.CAN-09-1872

27. Taylor MA, Davuluri G, Parvani JG, Schiemann BJ, Wendt MK, Plow EF, et al. Upregulated WAVE3 expression is essential for TGF-beta-mediated EMT and metastasis of triple-negative breast cancer cells. *Breast Cancer Res Treat* (2013) 142(2):341–53. doi:10.1007/s10549-013-2753-1

28. Cheung SY, Boey YJ, Koh VC, Thike AA, Lim JC, Iqbal J, et al. Role of epithelial-mesenchymal transition markers in triple-negative breast cancer. *Breast Cancer Res Treat* (2015) 152(3):489–98. doi:10.1007/s10549-015-3485-1

29. Jang MH, Kim HJ, Kim EJ, Chung YR, Park SY. Expression of epithelial-mesenchymal transition-related markers in triple-negative breast cancer: ZEB1 as a potential biomarker for poor clinical outcome. *Hum Pathol* (2015) 46(9):1267–74. doi:10.1016/j.humpath.2015.05.010

30. Fischer KR, Durrans A, Lee S, Sheng J, Li F, Wong ST, et al. Epithelial-to-mesenchymal transition is not required for lung metastasis but contributes to chemoresistance. *Nature* (2015) 527(7579):472–6. doi:10.1038/nature15748

31. Ye X, Brabletz T, Kang Y, Longmore GD, Nieto MA, Stanger BZ, et al. Upholding a role for EMT in breast cancer metastasis. *Nature* (2017) 547(7661):E1–3. doi:10.1038/nature22816

32. Klein CA. Parallel progression of primary tumours and metastases. *Nat Rev Cancer* (2009) 9(4):302–12. doi:10.1038/nrc2627

33. Kang Y, Siegel PM, Shu W, Drobnjak M, Kakonen SM, Cordon-Cardo C, et al. A multigenic program mediating breast cancer metastasis to bone. *Cancer Cell* (2003) 3(6):537–49. doi:10.1016/S1535-6108(03)00132-6

34. Muller A, Homey B, Soto H, Ge N, Catron D, Buchanan ME, et al. Involvement of chemokine receptors in breast cancer metastasis. *Nature* (2001) 410(6824):50–6. doi:10.1038/35065016

35. Liang Z, Yoon Y, Votaw J, Goodman MM, Williams L, Shim H. Silencing of CXCR4 blocks breast cancer metastasis. *Cancer Res* (2005) 65(3):967–71.

36. Orimo A, Gupta PB, Sgroi DC, Arenzana-Seisdedos F, Delaunay T, Naeem R, et al. Stromal fibroblasts present in invasive human breast carcinomas promote tumor growth and angiogenesis through elevated SDF-1/CXCL12 secretion. *Cell* (2005) 121(3):335–48. doi:10.1016/j.cell.2005.02.034

37. Masuda T, Endo M, Yamamoto Y, Odagiri H, Kadomatsu T, Nakamura T, et al. ANGPTL2 increases bone metastasis of breast cancer cells through enhancing CXCR4 signaling. *Sci Rep* (2015) 5:9170. doi:10.1038/srep09170

38. Rattanasinchai C, Llewellyn BJ, Conrad SE, Gallo KA. MLK3 regulates FRA-1 and MMPs to drive invasion and transendothelial migration in triple-negative breast cancer cells. *Oncogenesis* (2017) 6(6):e345. doi:10.1038/oncsis.2017.44

39. Chen J, Gallo KA. MLK3 regulates paxillin phosphorylation in chemokine-mediated breast cancer cell migration and invasion to drive metastasis. *Cancer Res* (2012) 72(16):4130–40. doi:10.1158/0008-5472.CAN-12-0655

40. Adorno M, Cordenonsi M, Montagner M, Dupont S, Wong C, Hann B, et al. A Mutant-p53/Smad complex opposes p63 to empower TGFbeta-induced metastasis. *Cell* (2009) 137(1):87–98. doi:10.1016/j.cell.2009.01.039

41. Papageorgis P, Ozturk S, Lambert AW, Neophytou CM, Tzatsos A, Wong CK, et al. Targeting IL13Ralpha2 activates STAT6-TP63 pathway to suppress breast cancer lung metastasis. *Breast Cancer Res* (2015) 17:98. doi:10.1186/s13058-015-0607-y

42. Su X, Chakravarti D, Cho MS, Liu L, Gi YJ, Lin YL, et al. TAp63 suppresses metastasis through coordinate regulation of Dicer and miRNAs. *Nature* (2010) 467(7318):986–90. doi:10.1038/nature09459

43. Chen D, Sun Y, Wei Y, Zhang P, Rezaeian AH, Teruya-Feldstein J, et al. LIFR is a breast cancer metastasis suppressor upstream of the Hippo-YAP pathway and a prognostic marker. *Nat Med* (2012) 18(10):1511–7. doi:10.1038/nm.2940

44. Wang QS, Kong PZ, Li XQ, Yang F, Feng YM. FOXF2 deficiency promotes epithelial-mesenchymal transition and metastasis of basal-like breast cancer. *Breast Cancer Res* (2015) 17:30. doi:10.1186/s13058-015-0531-1

45. Jiang HL, Sun HF, Gao SP, Li LD, Huang S, Hu X, et al. SSBP1 suppresses TGFbeta-driven epithelial-to-mesenchymal transition and metastasis in triple-negative breast cancer by regulating mitochondrial retrograde signaling. *Cancer Res* (2016) 76(4):952–64. doi:10.1158/0008-5472.CAN-15-1630

46. Jiang HL, Sun HF, Gao SP, Li LD, Hu X, Wu J, et al. Loss of RAB1B promotes triple-negative breast cancer metastasis by activating TGF-beta/SMAD signaling. *Oncotarget* (2015) 6(18):16352–65. doi:10.18632/oncotarget.3877

47. Jin W, Chen BB, Li JY, Zhu H, Huang M, Gu SM, et al. TIEG1 inhibits breast cancer invasion and metastasis by inhibition of epidermal growth factor receptor (EGFR) transcription and the EGFR signaling pathway. *Mol Cell Biol* (2012) 32(1):50–63. doi:10.1128/MCB.06152-11

48. Douma S, Van Laar T, Zevenhoven J, Meuwissen R, Van Garderen E, Peeper DS. Suppression of anoikis and induction of metastasis by the neurotrophic receptor TrkB. *Nature* (2004) 430(7003):1034–9. doi:10.1038/nature02765

49. Tsai YF, Tseng LM, Hsu CY, Yang MH, Chiu JH, Shyr YM. Brain-derived neurotrophic factor (BDNF) -TrkB signaling modulates cancer-endothelial cells interaction and affects the outcomes of triple negative breast cancer. *PLoS One* (2017) 12(6):e0178173. doi:10.1371/journal.pone.0178173

50. Wenzel J, Zeisig R, Fichtner I. Inhibition of metastasis in a murine 4T1 breast cancer model by liposomes preventing tumor cell-platelet interactions. *Clin Exp Metastasis* (2010) 27(1):25–34. doi:10.1007/s10585-009-9299-y

51. Gay LJ, Felding-Habermann B. Contribution of platelets to tumour metastasis. *Nat Rev Cancer* (2011) 11(2):123–34. doi:10.1038/nrc3004

52. Padua D, Zhang XH, Wang Q, Nadal C, Gerald WL, Gomis RR, et al. TGFbeta primes breast tumors for lung metastasis seeding through angiopoietin-like 4. *Cell* (2008) 133(1):66–77. doi:10.1016/j.cell.2008.01.046

53. DeJong RJ, Miller LM, Molina-Cruz A, Gupta L, Kumar S, Barillas-Mury C. Reactive oxygen species detoxification by catalase is a major determinant of fecundity in the mosquito *Anopheles gambiae*. *Proc Natl Acad Sci U S A* (2007) 104(7):2121–6. doi:10.1073/pnas.0608407104

54. Wright HJ, Hou J, Xu B, Cortez M, Potma EO, Tromberg BJ, et al. CDCP1 drives triple-negative breast cancer metastasis through reduction of lipid-droplet abundance and stimulation of fatty acid oxidation. *Proc Natl Acad Sci U S A* (2017) 114(32):E6556–65. doi:10.1073/pnas.1703791114

55. Larkins TL, Nowell M, Singh S, Sanford GL. Inhibition of cyclooxygenase-2 decreases breast cancer cell motility, invasion and matrix metalloproteinase expression. *BMC Cancer* (2006) 6:181. doi:10.1186/1471-2407-6-181

56. Singh B, Berry JA, Shoher A, Ayers GD, Wei C, Lucci A. COX-2 involvement in breast cancer metastasis to bone. *Oncogene* (2007) 26(26):3789–96. doi:10.1038/sj.onc.1210154

57. Tian J, Hachim MY, Hachim IY, Dai M, Lo C, Raffa FA, et al. Cyclooxygenase-2 regulates TGFbeta-induced cancer stemness in triple-negative breast cancer. *Sci Rep* (2017) 7:40258. doi:10.1038/srep40258

58. Park BK, Zhang H, Zeng Q, Dai J, Keller ET, Giordano T, et al. NF-kappaB in breast cancer cells promotes osteolytic bone metastasis by inducing osteoclastogenesis via GM-CSF. *Nat Med* (2007) 13(1):62–9. doi:10.1038/nm1519

59. Acharyya S, Oskarsson T, Vanharanta S, Malladi S, Kim J, Morris PG, et al. A CXCL1 paracrine network links cancer chemoresistance and metastasis. *Cell* (2012) 150(1):165–78. doi:10.1016/j.cell.2012.04.042

60. Minn AJ, Gupta GP, Siegel PM, Bos PD, Shu W, Giri DD, et al. Genes that mediate breast cancer metastasis to lung. *Nature* (2005) 436(7050):518–24. doi:10.1038/nature03799

61. Harris LG, Pannell LK, Singh S, Samant RS, Shevde LA. Increased vascularity and spontaneous metastasis of breast cancer by hedgehog signaling mediated upregulation of cyr61. *Oncogene* (2012) 31(28):3370–80. doi:10.1038/onc.2011.496

62. Dey JH, Bianchi F, Voshol J, Bonenfant D, Oakeley EJ, Hynes NE. Targeting fibroblast growth factor receptors blocks PI3K/AKT signaling, induces apoptosis, and impairs mammary tumor outgrowth and metastasis. *Cancer Res* (2010) 70(10):4151–62. doi:10.1158/0008-5472.CAN-09-4479

63. Chen L, Yang S, Jakoncic J, Zhang JJ, Huang XY. Migrastatin analogues target fascin to block tumour metastasis. *Nature* (2010) 464(7291):1062–6. doi:10.1038/nature08978

64. Al-Alwan M, Olabi S, Ghebeh H, Barhoush E, Tulbah A, Al-Tweigeri T, et al. Fascin is a key regulator of breast cancer invasion that acts via the modification of metastasis-associated molecules. *PLoS One* (2011) 6(11):e27339. doi:10.1371/journal.pone.0027339

65. Gupta GP, Perk J, Acharyya S, de Candia P, Mittal V, Todorova-Manova K, et al. ID genes mediate tumor reinitiation during breast cancer lung metastasis. *Proc Natl Acad Sci U S A* (2007) 104(49):19506–11. doi:10.1073/pnas.0709185104

66. Fong S, Itahana Y, Sumida T, Singh J, Coppe JP, Liu Y, et al. Id-1 as a molecular target in therapy for breast cancer cell invasion and metastasis. *Proc Natl Acad Sci U S A* (2003) 100(23):13543–8. doi:10.1073/pnas.2230238100

67. Tominaga K, Shimamura T, Kimura N, Murayama T, Matsubara D, Kanauchi H, et al. Addiction to the IGF2-ID1-IGF2 circuit for maintenance of the breast cancer stem-like cells. *Oncogene* (2017) 36(9):1276–86. doi:10.1038/onc.2016.293

68. Wee ZN, Yatim SM, Kohlbauer VK, Feng M, Goh JY, Bao Y, et al. IRAK1 is a therapeutic target that drives breast cancer metastasis and resistance to paclitaxel. *Nat Commun* (2015) 6:8746. doi:10.1038/ncomms9746

69. Dong T, Liu Z, Xuan Q, Wang Z, Ma W, Zhang Q. Tumor LDH-A expression and serum LDH status are two metabolic predictors for triple negative breast cancer brain metastasis. *Sci Rep* (2017) 7(1):6069. doi:10.1038/s41598-017-06378-7

70. Vergara D, Simeone P, del Boccio P, Toto C, Pieragostino D, Tinelli A, et al. Comparative proteome profiling of breast tumor cell lines by gel electrophoresis and mass spectrometry reveals an epithelial mesenchymal transition associated protein signature. *Mol Biosyst* (2013) 9(6):1127–38. doi:10.1039/c2mb25401h

71. Boucharaba A, Serre CM, Gres S, Saulnier-Blache JS, Bordet JC, Guglielmi J, et al. Platelet-derived lysophosphatidic acid supports the progression of osteolytic bone metastases in breast cancer. *J Clin Invest* (2004) 114(12):1714–25. doi:10.1172/JCI22123

72. Okita Y, Kimura M, Xie R, Chen C, Shen LT, Kojima Y, et al. The transcription factor MAFK induces EMT and malignant progression of triple-negative breast cancer cells through its target GPNMB. *Sci Signal* (2017) 10(474):eaak9397. doi:10.1126/scisignal.aak9397

73. Blomme A, Costanza B, de Tullio P, Thiry M, Van Simaeys G, Boutry S, et al. Myoferlin regulates cellular lipid metabolism and promotes metastases in triple-negative breast cancer. *Oncogene* (2017) 36(15):2116–30. doi:10.1038/onc.2016.369

74. Granados-Principal S, Liu Y, Guevara ML, Blanco E, Choi DS, Qian W, et al. Inhibition of iNOS as a novel effective targeted therapy against triple-negative breast cancer. *Breast Cancer Res* (2015) 17:25. doi:10.1186/s13058-015-0527-x

75. Azzam DJ, Zhao D, Sun J, Minn AJ, Ranganathan P, Drews-Elger K, et al. Triple negative breast cancer initiating cell subsets differ in functional and molecular characteristics and in gamma-secretase inhibitor drug responses. *EMBO Mol Med* (2013) 5(10):1502–22. doi:10.1002/emmm.201302558

76. Weber CE, Kothari AN, Wai PY, Li NY, Driver J, Zapf MA, et al. Osteopontin mediates an MZF1-TGF-beta1-dependent transformation of mesenchymal stem cells into cancer-associated fibroblasts in breast cancer. *Oncogene* (2015) 34(37):4821–33. doi:10.1038/onc.2014.410

77. Mi Z, Guo H, Russell MB, Liu Y, Sullenger BA, Kuo PC. RNA aptamer blockade of osteopontin inhibits growth and metastasis of MDA-MB231 breast cancer cells. *Mol Ther* (2009) 17(1):153–61. doi:10.1038/mt.2008.235

78. Chen Q, Boire A, Jin X, Valiente M, Er EE, Lopez-Soto A, et al. Carcinoma-astrocyte gap junctions promote brain metastasis by cGAMP transfer. *Nature* (2016) 533(7604):493–8. doi:10.1038/nature18268

79. Paul A, Gunewardena S, Stecklein SR, Saha B, Parelkar N, Danley M, et al. PKClambda/iota signaling promotes triple-negative breast cancer growth and metastasis. *Cell Death Differ* (2014) 21(9):1469–81. doi:10.1038/cdd.2014.62

80. Ponente M, Campanini L, Cuttano R, Piunti A, Delledonne GA, Coltella N, et al. PML promotes metastasis of triple-negative breast cancer through transcriptional regulation of HIF1A target genes. *JCI Insight* (2017) 2(4):e87380. doi:10.1172/jci.insight.87380

81. Malanchi I, Santamaria-Martinez A, Susanto E, Peng H, Lehr HA, Delaloye JF, et al. Interactions between cancer stem cells and their niche govern metastatic colonization. *Nature* (2011) 481(7379):85–9. doi:10.1038/nature10694

82. Lambert AW, Wong CK, Ozturk S, Papageorgis P, Raghunathan R, Alekseyev Y, et al. Tumor cell-derived periostin regulates cytokines that maintain breast cancer stem cells. *Mol Cancer Res* (2016) 14(1):103–13. doi:10.1158/1541-7786.MCR-15-0079

83. Yin JJ, Selander K, Chirgwin JM, Dallas M, Grubbs BG, Wieser R, et al. TGF-beta signaling blockade inhibits PTHrP secretion by breast cancer cells and bone metastases development. *J Clin Invest* (1999) 103(2):197–206. doi:10.1172/JCI3523

84. Taipaleenmaki H, Farina NH, van Wijnen AJ, Stein JL, Hesse E, Stein GS, et al. Antagonizing miR-218-5p attenuates Wnt signaling and reduces metastatic bone disease of triple negative breast cancer cells. *Oncotarget* (2016) 7(48):79032–46. doi:10.18632/oncotarget.12593

85. Kamalati T, Jolin HE, Fry MJ, Crompton MR. Expression of the BRK tyrosine kinase in mammary epithelial cells enhances the coupling of EGF signalling to PI 3-kinase and Akt, via erbB3 phosphorylation. *Oncogene* (2000) 19(14):5471–6. doi:10.1038/sj.onc.1203931

86. Ito K, Park SH, Nayak A, Byerly JH, Irie HY. PTK6 inhibition suppresses metastases of triple-negative breast cancer via SNAIL-dependent E-cadherin regulation. *Cancer Res* (2016) 76(15):4406–17. doi:10.1158/0008-5472.CAN-15-3445

87. Wiegmans AP, Al-Ejeh F, Chee N, Yap PY, Gorski JJ, Da Silva L, et al. Rad51 supports triple negative breast cancer metastasis. *Oncotarget* (2014) 5(10):3261–72. doi:10.18632/oncotarget.1923

88. Nasser MW, Wani NA, Ahirwar DK, Powell CA, Ravi J, Elbaz M, et al. RAGE mediates S100A7-induced breast cancer growth and metastasis by modulating the tumor microenvironment. *Cancer Res* (2015) 75(6):974–85. doi:10.1158/0008-5472.CAN-14-2161

89. Jones DH, Nakashima T, Sanchez OH, Kozieradzki I, Komarova SV, Sarosi I, et al. Regulation of cancer cell migration and bone metastasis by RANKL. *Nature* (2006) 440(7084):692–6. doi:10.1038/nature04524

90. Nasser MW, Qamri Z, Deol YS, Ravi J, Powell CA, Trikha P, et al. S100A7 enhances mammary tumorigenesis through upregulation of inflammatory pathways. *Cancer Res* (2012) 72(3):604–15. doi:10.1158/0008-5472.CAN-11-0669

91. Valiente M, Obenauf AC, Jin X, Chen Q, Zhang XH, Lee DJ, et al. Serpins promote cancer cell survival and vascular co-option in brain metastasis. *Cell* (2014) 156(5):1002–16. doi:10.1016/j.cell.2014.01.040

92. Savagner P, Yamada KM, Thiery JP. The zinc-finger protein slug causes desmosome dissociation, an initial and necessary step for growth factor-induced epithelial-mesenchymal transition. *J Cell Biol* (1997) 137(6):1403–19. doi:10.1083/jcb.137.6.1403

93. Kim S, Yao J, Suyama K, Qian X, Qian BZ, Bandyopadhyay S, et al. Slug promotes survival during metastasis through suppression of puma-mediated apoptosis. *Cancer Res* (2014) 74(14):3695–706. doi:10.1158/0008-5472.CAN-13-2591

94. Dhasarathy A, Phadke D, Mav D, Shah RR, Wade PA. The transcription factors snail and slug activate the transforming growth factor-beta signaling pathway in breast cancer. *PLoS One* (2011) 6(10):e26514. doi:10.1371/journal.pone.0026514

95. Cano A, Perez-Moreno MA, Rodrigo I, Locascio A, Blanco MJ, del Barrio MG, et al. The transcription factor snail controls epithelial-mesenchymal transitions by repressing E-cadherin expression. *Nat Cell Biol* (2000) 2(2):76–83. doi:10.1038/35000025

96. Kim J, Kong J, Chang H, Kim H, Kim A. EGF induces epithelial-mesenchymal transition through phospho-Smad2/3-Snail signaling pathway in breast cancer cells. *Oncotarget* (2016) 7(51):85021–32. doi:10.18632/oncotarget.13116

97. He Q, Jing H, Liaw L, Gower L, Vary C, Hua S, et al. Suppression of Spry1 inhibits triple-negative breast cancer malignancy by decreasing EGF/EGFR mediated mesenchymal phenotype. *Sci Rep* (2016) 6:23216. doi:10.1038/srep23216

98. Bos PD, Zhang XH, Nadal C, Shu W, Gomis RR, Nguyen DX, et al. Genes that mediate breast cancer metastasis to the brain. *Nature* (2009) 459(7249):1005–9. doi:10.1038/nature08021

99. Tang B, Vu M, Booker T, Santner SJ, Miller FR, Anver MR, et al. TGF-beta switches from tumor suppressor to prometastatic factor in a model of breast cancer progression. *J Clin Invest* (2003) 112(7):1116–24. doi:10.1172/JCI18899

100. Kang Y, He W, Tulley S, Gupta GP, Serganova I, Chen CR, et al. Breast cancer bone metastasis mediated by the Smad tumor suppressor pathway. *Proc Natl Acad Sci U S A* (2005) 102(39):13909–14. doi:10.1073/pnas.0506517102

101. Oskarsson T, Acharyya S, Zhang XH, Vanharanta S, Tavazoie SF, Morris PG, et al. Breast cancer cells produce tenascin C as a metastatic niche component to colonize the lungs. *Nat Med* (2011) 17(7):867–74. doi:10.1038/nm.2379

102. Howe LR, Watanabe O, Leonard J, Brown AM. Twist is up-regulated in response to Wnt1 and inhibits mouse mammary cell differentiation. *Cancer Res* (2003) 63(8):1906–13.

103. Lu X, Mu E, Wei Y, Riethdorf S, Yang Q, Yuan M, et al. VCAM-1 promotes osteolytic expansion of indolent bone micrometastasis of breast cancer by engaging alpha4beta1-positive osteoclast progenitors. *Cancer Cell* (2011) 20(6):701–14. doi:10.1016/j.ccr.2011.11.002

104. Chen Q, Zhang XH, Massague J. Macrophage binding to receptor VCAM-1 transmits survival signals in breast cancer cells that invade the lungs. *Cancer Cell* (2011) 20(4):538–49. doi:10.1016/j.ccr.2011.08.025

105. Jang GB, Kim JY, Cho SD, Park KS, Jung JY, Lee HY, et al. Blockade of Wnt/beta-catenin signaling suppresses breast cancer metastasis by inhibiting CSC-like phenotype. *Sci Rep* (2015) 5:12465. doi:10.1038/srep12465

106. Dey N, Barwick BG, Moreno CS, Ordanic-Kodani M, Chen Z, Oprea-Ilies G, et al. Wnt signaling in triple negative breast cancer is associated with metastasis. *BMC Cancer* (2013) 13:537. doi:10.1186/1471-2407-13-537

107. Geyer FC, Lacroix-Triki M, Savage K, Arnedos M, Lambros MB, MacKay A, et al. beta-Catenin pathway activation in breast cancer is associated with triple-negative phenotype but not with CTNNB1 mutation. *Mod Pathol* (2011) 24(2):209–31. doi:10.1038/modpathol.2010.205

108. Di Franco S, Turdo A, Benfante A, Colorito ML, Gaggianesi M, Apuzzo T, et al. DeltaNp63 drives metastasis in breast cancer cells via PI3K/CD44v6 axis. *Oncotarget* (2016) 7(34):54157–73. doi:10.18632/oncotarget.11022

109. Ozturk S, Papageorgis P, Wong CK, Lambert AW, Abdolmaleky HM, Thiagalingam A, et al. SDPR functions as a metastasis suppressor in breast cancer by promoting apoptosis. *Proc Natl Acad Sci U S A* (2016) 113(3):638–43. doi:10.1073/pnas.1514663113

110. Montagner M, Enzo E, Forcato M, Zanconato F, Parenti A, Rampazzo E, et al. SHARP1 suppresses breast cancer metastasis by promoting degradation of hypoxia-inducible factors. *Nature* (2012) 487(7407):380–4. doi:10.1038/nature11207

111. Shen L, O'Shea JM, Kaadige MR, Cunha S, Wilde BR, Cohen AL, et al. Metabolic reprogramming in triple-negative breast cancer through Myc suppression of TXNIP. *Proc Natl Acad Sci U S A* (2015) 112(17):5425–30. doi:10.1073/pnas.1501551112

112. Chen D, Dang BL, Huang JZ, Chen M, Wu D, Xu ML, et al. MiR-373 drives the epithelial-to-mesenchymal transition and metastasis via the miR-373-TXNIP-HIF1alpha-TWIST signaling axis in breast cancer. *Oncotarget* (2015) 6(32):32701–12. doi:10.18632/oncotarget.4702

113. Gunasinghe NP, Wells A, Thompson EW, Hugo HJ. Mesenchymal-epithelial transition (MET) as a mechanism for metastatic colonisation in breast cancer. *Cancer Metastasis Rev* (2012) 31(3–4):469–78. doi:10.1007/s10555-012-9377-5

114. Gregory PA, Bert AG, Paterson EL, Barry SC, Tsykin A, Farshid G, et al. The miR-200 family and miR-205 regulate epithelial to mesenchymal transition by targeting ZEB1 and SIP1. *Nat Cell Biol* (2008) 10(5):593–601. doi:10.1038/ncb1722

115. Dykxhoorn DM, Wu Y, Xie H, Yu F, Lal A, Petrocca F, et al. miR-200 enhances mouse breast cancer cell colonization to form distant metastases. *PLoS One* (2009) 4(9):e7181. doi:10.1371/journal.pone.0007181

116. Mundy GR. Metastasis to bone: causes, consequences and therapeutic opportunities. *Nat Rev Cancer* (2002) 2(8):584–93. doi:10.1038/nrc867

117. De Cock JM, Shibue T, Dongre A, Keckesova Z, Reinhardt F, Weinberg RA. Inflammation triggers Zeb1-dependent escape from tumor latency. *Cancer Res* (2016) 76(23):6778–84. doi:10.1158/0008-5472.CAN-16-0608

118. Wong CC, Gilkes DM, Zhang H, Chen J, Wei H, Chaturvedi P, et al. Hypoxia-inducible factor 1 is a master regulator of breast cancer metastatic niche formation. *Proc Natl Acad Sci U S A* (2011) 108(39):16369–74. doi:10.1073/pnas.1113483108

119. Bosch A, Eroles P, Zaragoza R, Vina JR, Lluch A. Triple-negative breast cancer: molecular features, pathogenesis, treatment and current lines of research. *Cancer Treat Rev* (2010) 36(3):206–15. doi:10.1016/j.ctrv.2009.12.002

120. Okuma HS, Yonemori K. BRCA Gene Mutations and Poly(ADP-Ribose) Polymerase Inhibitors in Triple-Negative Breast Cancer. *Adv Exp Med Biol* (2017) 1026:271–86. doi:10.1007/978-981-10-6020-5_13

121. Tutt A, Robson M, Garber JE, Domchek SM, Audeh MW, Weitzel JN, et al. Oral poly(ADP-ribose) polymerase inhibitor olaparib in patients with BRCA1 or BRCA2 mutations and advanced breast cancer: a proof-of-concept trial. *Lancet* (2010) 376(9737):235–44. doi:10.1016/S0140-6736(10)60892-6

122. Dent RA, Lindeman GJ, Clemons M, Wildiers H, Chan A, McCarthy NJ, et al. Phase I trial of the oral PARP inhibitor olaparib in combination with paclitaxel for first- or second-line treatment of patients with metastatic triple-negative breast cancer. *Breast Cancer Res* (2013) 15(5):R88. doi:10.1186/bcr3484

123. Gucalp A, Tolaney S, Isakoff SJ, Ingle JN, Liu MC, Carey LA, et al. Cancer Research: Phase II trial of bicalutamide in patients with androgen receptor-positive, estrogen receptor-negative metastatic breast cancer. *Clin Cancer Res* (2013) 19(19):5505–12. doi:10.1158/1078-0432.CCR-12-3327

124. Gelmon K, Dent R, Mackey JR, Laing K, McLeod D, Verma S. Targeting triple-negative breast cancer: optimising therapeutic outcomes. *Ann Oncol* (2012) 23(9):2223–34. doi:10.1093/annonc/mds067

125. Locatelli MA, Aftimos P, Dees EC, LoRusso PM, Pegram MD, Awada A, et al. Phase I study of the gamma secretase inhibitor PF-03084014 in combination with docetaxel in patients with advanced triple-negative breast cancer. *Oncotarget* (2017) 8(2):2320–8. doi:10.18632/oncotarget.13727

126. Chen DS, Mellman I. Elements of cancer immunity and the cancer-immune set point. *Nature* (2017) 541(7637):321–30. doi:10.1038/nature21349

127. Zou W, Wolchok JD, Chen L. PD-L1 (B7-H1) and PD-1 pathway blockade for cancer therapy: Mechanisms, response biomarkers, and combinations. *Sci Transl Med* (2016) 8(328):328rv4. doi:10.1126/scitranslmed.aad7118

128. Bianchini G, Balko JM, Mayer IA, Sanders ME, Gianni L. Triple-negative breast cancer: challenges and opportunities of a heterogeneous disease. *Nat Rev Clin Oncol* (2016) 13(11):674–90. doi:10.1038/nrclinonc.2016.66

129. Walker RA. The complexities of breast cancer desmoplasia. *Breast Cancer Res* (2001) 3(3):143–5. doi:10.1186/bcr287

130. Jain RK, Martin JD, Stylianopoulos T. The role of mechanical forces in tumor growth and therapy. *Annu Rev Biomed Eng* (2014) 16:321–46. doi:10.1146/annurev-bioeng-071813-105259

131. Gkretsi V, Stylianou A, Papageorgis P, Polydorou C, Stylianopoulos T. Remodeling components of the tumor microenvironment to enhance cancer therapy. *Front Oncol* (2015) 5:214. doi:10.3389/fonc.2015.00214

132. Takai K, Le A, Weaver VM, Werb Z. Targeting the cancer-associated fibroblasts as a treatment in triple-negative breast cancer. *Oncotarget* (2016) 7(50):82889–901. doi:10.18632/oncotarget.12658

133. Polydorou C, Mpekris F, Papageorgis P, Voutouri C, Stylianopoulos T. Pirfenidone normalizes the tumor microenvironment to improve chemotherapy. *Oncotarget* (2017) 8(15):24506–17. doi:10.18632/oncotarget.15534

134. Papageorgis P, Polydorou C, Mpekris F, Voutouri C, Agathokleous E, Kapnissi-Christodoulou CP, et al. Tranilast-induced stress alleviation in solid tumors improves the efficacy of chemo- and nanotherapeutics in a size-independent manner. *Sci Rep* (2017) 7:46140. doi:10.1038/srep46140

135. Chauhan VP, Martin JD, Liu H, Lacorre DA, Jain SR, Kozin SV, et al. Angiotensin inhibition enhances drug delivery and potentiates chemotherapy by decompressing tumour blood vessels. *Nat Commun* (2013) 4:2516. doi:10.1038/ncomms3516

136. Diop-Frimpong B, Chauhan VP, Krane S, Boucher Y, Jain RK. Losartan inhibits collagen I synthesis and improves the distribution and efficacy of nanotherapeutics in tumors. *Proc Natl Acad Sci U S A* (2011) 108(7):2909–14. doi:10.1073/pnas.1018892108

Growth and Immune Evasion of Lymph Node Metastasis

Dennis Jones[1,2], Ethel R. Pereira[1,2] and Timothy P. Padera[1,2]*

[1] *Edwin L. Steele Laboratories for Tumor Biology, Department of Radiation Oncology, MGH Cancer Center, Massachusetts General Hospital, Boston, MA, United States,* [2] *Harvard Medical School, Boston, MA, United States*

Cancer patients with lymph node (LN) metastases have a worse prognosis than those without nodal disease. However, why LN metastases correlate with reduced patient survival is poorly understood. Recent findings provide insight into mechanisms underlying tumor growth in LNs. Tumor cells and their secreted molecules engage stromal, myeloid, and lymphoid cells within primary tumors and in the lymphatic system, decreasing anti-tumor immunity and promoting tumor growth. Understanding the mechanisms of cancer survival and growth in LNs is key to designing effective therapy for the eradication of LN metastases. In addition, uncovering the implications of LN metastasis for systemic tumor burden will inform treatment decisions. In this review, we discuss the current knowledge of the seeding, growth, and further dissemination of LN metastases.

Keywords: lymphatics, lymph node, tumor, metastasis, immunity

INTRODUCTION

Metastasis is the leading cause of death from cancer (1) and represents a challenging clinical problem. Lymph nodes (LNs) are common sites of metastasis and nodal disease predicts increased mortality in many cancer types. Meanwhile, LNs are critical for initiating antitumor immune responses. Thus, cancer cells that have metastasized to LNs must escape immune detection to avoid destruction. The process of lymphatic metastasis is regulated at several steps and by several different molecules (**Figures 1** and **2**, respectively), beginning with the orchestration of lymphangiogenesis and preparation of a LN microenvironment favorable for tumor growth (premetastatic niche). Cancer cells then invade tumor-associated lymphatic vessels at the primary site *en route* to tumor-draining LNs (TDLNs), where they survive and grow. In a metastatic node, immunological destruction of cancer cells depends on the degree of cancer cell immunogenicity and the extent of nodal immunosuppression. Similar to primary tumors, cancer cells in LNs shape their interactions with the host immune system by controlling the infiltration and reactivity of immune cells. The local microenvironment of the LN also dictates the growth and response of LN metastases to therapeutic intervention. For example, only a small fraction of drugs delivered systemically accumulate in LNs (2). Identifying effective therapy for LN metastases takes on new urgency as cancer cells in LNs have also been proposed to disseminate to other metastatic sites by lymphatic or hematogenous routes. In this review, we summarize recent progress in the understanding of lymphatic metastasis and metastatic outgrowth. We also discuss the consequences of lymphatic metastasis and therapeutic efforts to target LN lesions in experimental mouse models and humans.

LYMPHATIC ENDOTHELIAL CELLS (LECs) AND TUMOR IMMUNITY

Mediators of Immunosuppression

Recent studies suggest that in addition to serving as a portal for tumor dissemination, lymphatic vessels facilitate tumor growth through immune suppression (3). To generate an antitumor T cell response, migratory dendritic cells (DCs) from primary tumors cross-prime naïve T cells in TDLNs (4).

FIGURE 1 | Progression of lymphatic metastasis from primary tumor to tumor-draining LN (TDLN). Primary tumors induce lymphangiogenesis to facilitate lymphatic metastasis and release of immunomodulatory molecules, including exosomes, which lead to immunosuppression of TDLNs. Lymph node (LN) lymphatic endothelial cells (LECs) capture tumor antigen and tolerize T cells *via* programmed death-ligand 1 expression. Tumor-associated lymphatic vessels and tertiary lymphoid organs have been implicated in immune suppression and immune activation. High endothelial venules found in primary tumors can allow infiltration of naive T cells that may further differentiate into effector T cells. Tumor-associated lymphatic vessels recruit both cancer cells and immune cells by releasing chemoattractants (see **Figure 2**). Cancer cells, T cells, and dendritic cells enter lymphatic capillaries and migrate through collecting lymphatic vessels to LNs. Cancer cells in lymphatic vessels can attach to the lymphatic endothelium en route to LNs. Active mechanisms, such as CCL1/CCR8 signaling, control cancer cell entry into the LN. Polyclonal cancer cells proliferate to form a metastatic lesion that invades deeper into the LN parenchyma, where it can grow and replace LN tissue in the absence of new blood vessel growth. The immune response to a growing metastatic lesion is limited; some immune cells are excluded from LN lesions, while other immune cells are present, but unable to eliminate cancer cells (not shown). Some cancer cells may exit through the efferent lymphatic vessel and seed secondary draining LNs. Recent evidence suggests LEC sphingosine-1-phosphate (S1P) helps shape the antitumor immune response.

The adhesion ligand Mac-1 on DCs can bind to the adhesion molecule intercellular adhesion molecule-1 (ICAM-1), which is upregulated on endothelial cells of collecting lymphatic vessels in response to inflammation (5), including inflammation generated by the tumor microenvironment. This Mac-1/ICAM-1 interaction inhibits DC maturation (5) and may blunt the ability of DCs in an inflamed tumor microenvironment to prime antitumor T cells. LECs further inhibit antitumor T cell responses by inducing tolerance to tumor antigens. LECs can scavenge tumor and other peripheral antigens and cross-present them to CD8 T cells, but LECs lack co-stimulatory molecules needed for full activation of CD8 T cells (6). Programmed death-ligand 1 (PD-L1), a ligand for the T cell inhibitory receptor PD-1, is expressed on tumor-associated lymphatic vessels (7) and LN LECs (8). The engagement of PD-L1 on LECs with T cell PD-1 induces CD8 T cell tolerance to tumor antigens (7, 8). Given the paucity of antitumor T cells and functional lymphatic vessels within some tumors (9, 10), the degree of CD8 T cell interaction with tumor-associated lymphatic vessels and their degree of inhibiting antitumor immunity is unclear. Recent studies show that the presence of LECs inside tumors make the tumors more responsive to anti-PD-1 therapy, suggesting lymphatics can have a potent inhibitory effect on T cell function (11).

In normal physiology, LECs produce sphingosine-1-phosphate (S1P), which is secreted into lymph and controls lymphocyte exit from LNs (12). Neutralization of systemic S1P with a therapeutic antibody suppresses lung metastasis (13). More recently, a genome-wide functional screen identified the S1P transporter spinster homolog 2 (*Spns2*) as a regulator of metastatic colonization in animals with experimental lung metastases (14). Spns2 is expressed on LECs and is critical for LEC release of S1P (15). Global and lymphatic-specific deletion of *Spns2* decreased pulmonary metastases following intravenous tumor cell injection, with fewer total T cells present in lungs relative to WT mice (14). However, a higher proportion of effector memory T cells to regulatory T cells (Tregs) were found in the lungs of *Spns2* deficient animals (14). Coupled with enhanced KLRG1$^+$, CD69$^+$CXCR3$^+$ T cell activation, these findings were suggestive of an adaptive immune response against lung metastases (14). In addition, the natural killer (NK) cell population in the lungs of *Spns2* deficient animals was increased and limited the growth of lung metastases, even after CD8 T cell depletion (16). By contrast, S1P signaling has the potential to promote antitumor T cell responses. LEC-produced S1P appears to function not only as a regulator of lymphocyte circulation, but also supports naïve CD4 T cell survival by maintaining their mitochondrial content through an S1P$_1$ receptor-dependent mechanism (16). Targeting S1P signaling to

FIGURE 2 | Tumor-associated lymphatic vessels promote metastasis and cancer progression. (i) Tumor-associated macrophages and cancer cells secrete VEGF-C and VEGF-D, which binds to VEGFR-2/3 on lymphatic capillaries to mediate lymphangiogenesis. VEGF-C upregulates CCL21 production by lymphatic endothelial cells (LECs). CCL21 attracts cancer cells, T cells, and dendritic cells (DCs), which express CCR7, a receptor for CCL21. VEGF-C has also been shown to upregulate CXCR4 expression on LECs. The CXCL12–CXCR4 axis can stimulate lymphangiogenesis to promote cancer cell migration. Alternatively, LECs promote the migration of CXCR4-positive cancer cells by secretion of CXCL12. Tumor antigen is delivered to the tumor-draining lymph nodes, where it is presented to T cells by DCs and LECs. (ii) Binding of LEC programmed death-ligand 1 (PD-L1) with T cell PD-1 receptor induces CD8 T cell tolerance to tumor antigens.

decrease metastatic burden requires a better understanding of its temporal and spatial role in shaping antitumor T cell responses.

The chemokine CCL21 is produced by LECs and mobilizes DCs to LNs (17). Although CCL21 can also establish an immunosuppressive tumor microenvironment (18), it was recently shown that tumor-associated lymphatic vessels also facilitate naïve T cell recruitment into melanoma tumors through CCL21 production (11). The presence of T cells allows local immune priming and the ability to unleash potent antitumor activity in response to vaccination or immune checkpoint blockade (11). So while LECs and CCL21 themselves help suppress antitumor immune responses, their ability to recruit T cells sensitizes lymphangiogenic tumors to immunotherapy. Cancer patients with elevated VEGF-C (indicative of increased lymphangiogenesis and lymphatic metastasis) typically have poor prognosis. Based on recent data, VEGF-C [which upregulates CCL21 (19)] may now be used as a biomarker in these patients to predict their response to immunotherapy. The ability of T cells with effector function to leave primary tumors and travel to TDLNs through afferent lymphatic vessels also suggests that tumor-associated lymphatic vessels may assist in dampening tumor growth (20).

The above examples illustrate the potential for context-dependent benefit of inhibiting, altering or utilizing intrinsic properties of LECs to maximize effective antitumor immune responses.

Lymphangiogenesis

Lymphangiogenesis is a hallmark of many solid tumors. The expansion of the lymphatic network is primarily mediated by VEGF-C and its receptors VEGFR-2/3 (21). VEGF-D also binds VEGFR-2/3 and potently induces lymphangiogenesis (22, 23). Both VEGF-C and VEGF-D expression correlate with increased LN metastasis (24). Furthermore, *Vegf-d* deficient mice displayed less lymphatic metastasis relative to tumor-bearing wild type mice (25). Many preclinical studies have shown prevention of lymphatic metastasis by blocking VEGF-C or VEGF-D-mediated lymphangiogenesis (26–28). Clinically, this point of intervention is challenging as lymphangiogenesis is an early event in the natural history of cancer progression and many patients will already have LN metastases on initial presentation. However, additional opportunities may exist to target lymphangiogenesis. For example, lymphangiogenesis was identified as a mechanism of tumor resistance to paclitaxel chemotherapy in mice (29). In response to paclitaxel in mouse models, tumor-infiltrating macrophages secrete cathepsin, which activates heparanase. Active heparanase, by unknown mechanisms, increases both VEGF-C transcription and tumor invasiveness (30). In another study, VEGFR-3 reporter mice were used to image lymphangiogenesis in distant LNs, liver, lungs, and spleens in tumor-bearing mice. Following tumor resection, VEGFR-3 levels declined but reemerged before tumor relapse, suggesting a defined window of

opportunity to inhibit lymphangiogenesis in distal premetastatic organs (31).

Although there are a plethora of targets that exist to inhibit lymphangiogenesis (32), many studies find that VEGF-C/-D-VEGFR-2/3 signaling directly or indirectly promotes lymphangiogenesis in response to a wide range of stimuli (22, 24, 25). Surprisingly, few clinical trials targeting the lymphatic endothelium in cancer are ongoing, although several small molecules that non-selectively target VEGFR-3-mediated lymphangiogenesis are approved for cancer indications (33). A Phase I study was recently completed that assessed the effect of LY3022856 (IMC-3C5), a monoclonal antibody targeting human VEGFR-3, on colorectal cancer (CRC) (34). While LY3022856 was well tolerated at the given dose, minimal antitumor benefit was noted in patients with CRC. The impact of LY3022856 on tumor lymphangiogenesis and lymphatic metastasis was not assessed. As mentioned earlier, inhibiting lymphangiogenesis through targeting VEGF-C/D or VEGFR-3 is also complicated by the uncertainty of the effect that lymphatic vessels have on antitumor T cell responses (11).

Independent of lymphatic vessel growth and lymphangiogenesis, VEGF-C can promote cancer metastasis by disruption of the vascular endothelial cadherin/β-catenin complex at intercellular junctions of LECs (35). The authors concluded that enhanced permeability of intestinal lymphatic vessels caused by VEGF-C can increase CRC transmigration and metastasis. Thus, how therapies targeting VEGF-C/D signaling will impact cancer progression will depend on the specific context of the disease as well as other therapies being used in conjunction.

ESTABLISHMENT OF PREMETASTATIC NICHE IN TDLNs

Extracellular Vesicles (EVs)

In addition to the delivery of cells, lymphatic vessels deliver primary tumor-derived soluble and vesicle-associated factors to condition TDLNs before the arrival of cancer cells. Exosomes, a type of EV, were shown to modulate the immune and stromal response in TDLNs (36, 37). Melanoma cells injected into the footpad and taken up by local lymphatic vessels had a similar distribution pattern as premetastatic melanoma-derived exosomes previously injected into the footpad, suggesting exosomes influence the recruitment of cancer cells to the LN (38). Mechanistically, exosomes upregulated host genes that promoted the retention, recruitment, and progression of LN metastases (38). It is unclear what components of exosomal cargo (e.g., mRNA, miRNA, or proteins) were necessary for changes in nodal gene expression. Melanoma exosomes have also been shown to enhance metastasis by "educating" and mobilizing bone marrow-derived cells to metastatic sites (36), including LNs, where they facilitated cancer cell invasion. Melanoma-derived EVs were identified in afferent lymphatic vessels of patients (39). Cocultures of EVs from human melanoma cells with DCs resulted in inhibition of DC maturation (39). In premetastatic LNs, CD169+ subcapsular sinus (SCS) macrophages capture tumor-derived extracellular vesicles (TeVs) (40) and protect host LNs from TeV-mediated immunosuppression. TeV release was

required to accelerate tumor progression after the investigators depleted host macrophages. It is, however, unclear how TeVs can escape capture by SCS macrophages to deliver their payload under normal conditions. In contrast to the pro-tumor effects of EVs, migratory DCs acquire tumor-secreted vesicles released by circulating tumor cells in the lung (41). From here, the vesicle-loaded DCs migrate to mediastinal LNs to interact with and potentially activate antitumor T cells to limit metastatic growth. Taken together, these data suggest that TeVs have immune regulatory functions as well as help initiate and support the growth of LN metastases.

Lymphatics in a Premetastatic LN

It is known that lymphangiogenesis occurs in premetastatic LNs (42, 43). Nodal lymphangiogenesis has been shown to be tumor antigen independent and B cell dependent (42, 44) through production of VEGF-A and VEGF-C (43–46). Recently, midkine, a heparin-binding factor produced by tumor cells, was identified as a critical factor for mTOR-dependent lymphangiogenesis in premetastatic sites including skin, LN, spleen, and lung (31). Furthermore, midkine mediated tumor cell adhesion to LECs and promoted tumor colonization in distant organs.

It is unclear how LN lymphangiogenesis results in metastasis. One hypothesis is that LN lymphangiogenesis may lead to more efficient delivery of cancer cells to LNs and distant organs (47). This may be facilitated by the increased lymph flow that accompanies increased LN lymphangiogenesis (42). Increased lymphatic drainage from primary tumors was also associated with LN enlargement (48) and nodal remodeling, which may alter the distribution of antigen and soluble factors. Increased lymphatic drainage also coincided with collagen and hyaluronic acid deposition in premetastatic TDLNs of B16F10 tumors. Parental B16 melanoma cells failed to increase TDLN matrix remodeling and were inefficient at metastasis, suggesting that in addition to lymphangiogenesis, an increase in TDLN matrix may be a prerequisite for formation of LN metastases (48, 49).

Fibroblast Reticular Cells

The LN contains an array of stromal cells, including fibroblastic reticular cells (FRCs). Much is known about the tumor-promoting effects of cancer-associated fibroblasts, but few reports have characterized the FRC response to cancer cells. Transcriptional profiling of FRCs from non-tumor-bearing animals revealed abundant expression of chemokines critical for lymphocyte recruitment, including *CCL19*, *CCL21*, *CXCL12*, and *CXCL13* (50). FRCs also produce several forms of collagen (50), indicative of their role in forming the conduit system that delivers small antigens deep into the LN for antigen presentation (51). FRCs express genes necessary for MHC class 1/2 presentation (50) and can present peripheral antigens to T cells (52). Similar to LECs, FRCs contribute to peripheral tolerance by facilitating deletional tolerance (52, 53) and dampening effector T cell proliferation (54, 55). A recent transcriptional analysis revealed FRCs in premetastatic LNs are "reprogrammed" to favor tumor growth (56). In spontaneous and orthotopic models of melanoma, TDLN FRCs proliferated, but produced less *IL-7* and *CCL21*,

which are critical for T cell survival and guidance, respectively. The reduction in *IL-7* and *CCL21* resulted in disruption of the TDLN architecture, with loss of clear delineation between B and T cell zones. In a separate study, the loss of FRC *CCL21* in the TDLN was associated with disorganized T cell and B cell zones in premetastatic LNs (57). The perturbation of LN architecture due to altered FRC signaling molecules suggests altered immune responses to tumors. Since LNs are priming sites for adaptive immune responses, the disordered LN architecture may fail to elicit systemic protection from subsequent heterogeneous cancer cell clones that arrive in the TDLN (56). In metastatic LNs, collagen production was increased relative to tumor-free LNs (58). Although unclear whether recruited fibroblasts, FRCs, or cancer cells are the source of additional collagen, the investigators speculate that the increased density of collagen fibers may allow cancer cells to adhere and migrate within metastatic LNs. It is unknown how tumor cells influence FRC transcriptional status.

TUMOR CELL MIGRATION TO LNs

Cancer cells enter lymphatic vessels and travel with the lymph to establish LN metastasis (59). Cancer cells may actively migrate into lymphatic capillaries in response to molecular cues (19, 60) or they may passively enter into lymphatic capillaries (19, 60). Metastasis to the LN likely depends on a combination of intrinsic cancer cell properties and signals in the tumor microenvironment. VEGF-C and lymphatic flow both upregulate CCL21 in lymphatic endothelium (19, 61), attracting CCR7+ tumor cells (62). In a triple-negative breast cancer model, CCL21 was sufficient to recruit RORγt+ innate lymphoid cells (ILCs) into the primary tumor and promote metastasis to LNs (63). Furthermore, CXCL13 was required for clustering of ILCs and induction of epithelial–mesenchymal transition, likely driving invasion of cancer cells. In breast cancer patients, the presence of ILCs was significantly associated with lymphatic invasion at the primary tumor.

Several studies have shown that another chemokine, CXCL12, facilitates lymphatic metastasis of CXCR4+ tumor cells (64–66). CXCL12 expression is found on lymphatic vessels within primary tumors and guides CXCR4+ melanoma cells toward lymphatic vessels. Migration and invasion of CXCR4+ papillary thyroid carcinoma cells are dependent on CXCL12, which was produced by senescent cancer cells at the invasive border (67). These senescent cells invaded lymphatic vessels and persisted in metastatic foci, suggesting that they may promote lymphatic metastases. CXCR4 is also expressed on the surface of LECs (68) and is critical for lymphangiogenesis through CXCL12 stimulation, independent of the VEGFR-3 pathway (68). Thus, targeting the CXCR4/CXCL12 may provide a dual benefit of inhibiting cancer cell migration and lymphangiogenesis to curb lymphatic metastasis.

After entry of cancer cells into lymphatic vessels, it is thought that lymph flow allows cancer cells to traverse the collecting lymphatic vessel network until they reach TDLNs (59). Based on 3D modeling, it was predicted that smaller breast cancer cells may have a survival advantage over larger breast cancer cells in the lymphatic circulation because of the lower wall shear stress that

they encounter (69). Several studies have shown that inflammation causes dilation and inhibits contractile ability of collecting lymphatic vessels (70, 71). More work needs to be done to determine if tumor-induced collecting lymphatic dilation (10, 22, 59) or reduced contraction (72) enhances tumor cell dissemination by decreasing the shear stress on cancer cells. It is known that tumor cells can arrest within lymphatic vessels while "in-transit" to LNs (73). Compromised barrier integrity of lymphatic vessels may allow arrested cancer cells to escape lymphatic vessels and form metastases (74, 75). Additional characterization of the mechanism of how tumor cells attach to lymphatic endothelium and grow within lymphatic vessels is needed to treat in-transit metastases.

Recently, the chemokine CCL1 and its receptor CCR8 were demonstrated to be important for melanoma cell entry into TDLNs. CCL1 is produced by SCS LECs and mediated entry of CCR8+ melanoma cells into LNs (60). Tumor cells in the SCS can also bypass the LN parenchyma and drain through cortical and medullary sinuses to exit LNs *via* efferent lymphatic vessels (76). The enzyme lipoxygenase 15 (ALOX15) metabolizes arachidonic acid to 12(S)-hydroxyeicosatetraenoic acid [12(S)-HETE] and 15(S)-hydroxyeicosatetraenoic acid [15(S)-HETE]. Cancer cell-derived 12(S)-HETE forms discontinuities in the walls of lymphatic vessels, allowing LN metastases to invade nodal lymphatic vessels (77). The fate of these cancer cells is unclear, although TDLN lymphangiogenesis has been reported to be involved in further lymphatic spread of human breast cancer (78) and the presence of lymphatic vessel invasion by LN metastases is associated with worse survival (79). It is possible that cancer cells circulate to additional nodes through lymphatic vessels and eventually enter the systemic circulation through the thoracic duct.

IMMUNE EVASION IN TDLNs

Macrophages

Lymph node SCS macrophages are the first line of defense against tumor cells entering the LN. SCS macrophages capture microbes, antigen–antibody complexes and dead cancer cells for delivery of these antigens to nearby immune cells (80, 81). In premetastatic LNs, an experimental antigen (a fluorescent protein overexpressed in tumor cells) from the primary tumor was captured by SCS macrophages and distributed to follicular DCs, resulting in antibody production against the antigen (82). SCS macrophages can also directly cross-present tumor antigens to CD8 T cells (81). Sinus macrophages in regional LNs of CRC patients made direct contact with CD8 T cells and a high density of sinus macrophages is associated with increased overall survival (83). On the other hand, tumor-associated macrophages are often associated with poor prognosis and promotion of tumor growth (84). Strategies to deplete TAMs include targeting colony-stimulating factor 1-receptor (CSF1-R) (85), which controls macrophage chemotaxis. Interestingly, an increase in the burden of LN metastases was found following treatment with an anti-CSF1-R antibody (86). This increase in metastatic burden was associated with the loss of SCS macrophages due to anti-CSF1-R therapy (86).

Tumor-promoting (M2) macrophage depletion strategies should examine the effect on SCS macrophages to avoid unintended growth of LN metastases.

Neutrophils

Neutrophils, such as macrophages, are heterogeneous and have been reported to have either pro-tumor or antitumor phenotypes in primary tumors (87). High levels of tumor-associated neutrophils are associated with LN metastasis and poor prognosis (88). Granulocyte colony-stimulating factor was necessary to expand and polarize neutrophils to an immunosuppressive phenotype in mice bearing mammary tumors (89). The immunosuppressive neutrophils, whose expansion was also driven by IL-17, were able to suppress cytotoxic T cells and facilitate the establishment of LN metastases. Neutrophils can also secrete pro-inflammatory leukotrienes and initiate LN metastases *via* leukotriene receptors (LTR) on cancer cells (90). LTR expression was found in a cohort of primary and LN tumors from breast cancer patients. More research is needed to characterize the phenotype of neutrophils found in LN metastases and their role in metastatic progression.

T Cells

The TDLN often fails to produce effective antitumor immunity and instead tolerizes the patient to tumor antigens (91). The mechanisms that induce systemic tolerance include cross-presentation of tumor antigen by tolerogenic antigen-presenting cells, apoptosis of antigen-presenting cells (92), and suppression of antitumor T cells by an expanded pool of Tregs. Experimentally, subcutaneous injection of B16 melanoma resulted in tolerized CD8 T cells and lethal metastatic outgrowth (93). However, B16 cells implanted directly into LNs—without a primary tumor—were rejected, supporting previous evidence (94) that showed the primary tumor exerts a tolerogenic effect on the TDLN (94). However, initial metastatic deposits in lymphoid organs are important for the induction of antitumor CD8 T cells and tumor rejection (94). Notably, tumor cells injected into LNs using different cancer models have been shown to persist and disseminate to distant organs (95). These differences may be explained by factors such as the immunogenicity and antigen presentation capabilities of different cancer cells. Increased LN metastasis was found in cancer patients with tumor downregulation of MHC I (96).

NK Cells

Natural killer cells are cytotoxic lymphocytes of the innate immune system that are often recruited to tumors including prostate (97), melanoma, kidney, liver, and breast (98). NK cells are able to recognize and eliminate cells with aberrant ligand or altered/absent MHC expression (99, 100). However, NK cell infiltration into primary tumors is limited; NK cells that enter tumors are often found in primary tumor stroma and lack direct contact with cancer cells (98). Likewise, NK cells in metastatic LNs were adjacent to metastatic melanoma lesions (101). Moreover, NK cells isolated from metastatic human LNs showed significantly reduced cytotoxicity (101, 102). NK cells that were isolated from metastatic LN lesions and stimulated with IL-2 or IL-15 displayed more efficient lysis of cancer cells (101), suggesting that the LN

tumor microenvironment suppresses NK cell function. Thus, despite their presence in the TDLN, immunosuppressed NK cells may lack the ability to eliminate cancer cells.

B Cells

The number of B cells in premetastatic TDLNs is significantly increased (42). EVs from tumor cells increased immunosuppressive B cells in premetastatic LNs (40). Depletion of SCS macrophages in tumor-bearing animals permitted interactions of TeVs with B cells and led to increased antibody production. Although the tumor antigen specificity of the antibodies are unknown, transfer of these antibodies to wild-type recipient mice correlated with enhanced tumor growth compared with antibody transfer from tumor-bearing animals without disruption of SCS macrophages. Regulatory B cells (Bregs) were recently identified in mouse and human blood and secondary lymphoid organs (103). Bregs can secrete immunosuppressive cytokines, such as TGF-β and IL-10 (104), to dampen the effector activity of antitumor T cells. However, the data conflict on whether Bregs support or suppress tumor growth (105). The phenotypic markers that identify Bregs also remain unclear.

Together, these data suggest that multiple immune cell types in premetastatic and metastatic LNs have suboptimal killing activity for cancer cells. Identifying molecular targets to reverse immune suppression of several cell types will be of therapeutic benefit in treating metastatic cancer.

ECTOPIC LN IMMUNITY

High endothelial venules (HEVs) and their homeostatically associated chemokines are crucial for entry of naïve lymphocytes into LNs (106). Ectopic HEVs in primary human breast cancer and melanoma tumors allow lymphocytic intravasation and predict a favorable prognosis (106, 107). LTα₃–TNFR signaling, not LTβR, was critical for the generation of HEV-like vasculature expressing peripheral node addressin (PNAd) in models of lung cancer and melanoma (108) studied by Peske et al. The PNAd⁺ vasculature was critical for infiltration of naïve T cell into tumors. Growth of HEV-containing tumors was delayed although treatment with the S1P antagonist FTY720 retained tumor-specific T cells in secondary lymphoid organs (108). These data suggest that naïve T cells can differentiate into effector T cells within primary tumors.

Tertiary lymphoid organs (TLOs) are aggregates of immune cells that mimic the structure and function of LNs. They are formed in several diseases associated with chronic inflammation, including cancer (109). TLOs include lymphocytes, lymphatic vessels, and HEVs (110). TLOs within tumors are associated with improved outcomes for patients and function as sites of immune priming for the generation of antitumor lymphocytes. In animal models of pancreatic and breast cancer, tumor-associated blood vessels developed HEV markers and formed TLO-like structures in response to a combination of antiangiogenic (DC101) and immune checkpoint (PD-L1) therapy (111). Formation of LTβR signaling-dependent HEVs resulted in enhanced infiltration and activation of antitumor T cells, and better antitumor responses (111). By contrast, the presence of TLOs and ectopic HEVs has

been shown to promote tumor growth in other experimental conditions. Finkin et al. found that the cytokine-rich environment of liver TLOs promoted the growth of hepatocellular carcinoma progenitor cells in a hepatocellular carcinoma model (112). From studies using a murine model of lung cancer, Joshi et al., found that TLOs in tumor-bearing lungs were a site of antigen presentation (113). However, the abundant Tregs within the TLOs presumably suppressed antitumor T cell responses. The use of immune checkpoint inhibitors, such as the anti-CTLA-4 antibody ipilimumab, can lead to the depletion of Tregs (114) and may enhance the antitumor function of effector lymphocytes in tumors and TLOs with a high Treg: effector T cell ratio. In a separate study, depletion of Tregs resulted in intratumoral HEV formation and higher numbers of activated CD4 and CD8 T cells in carcinogen-induced fibrosarcomas, resulting in reduced tumor burden (115, 116). TNF-producing T cells that signaled through TNFR were critical for intratumoral HEV neogenesis (116).

Given the context-dependent benefit of TLOs, it is unclear whether induction of TLOs is a viable therapeutic strategy to limit tumor progression. TLO formation might need to be accompanied by a strategy to prevent Treg formation to generate an effective antitumor response. Moreover, the signaling mechanisms to induce TLO formation appear to be dependent on various cytokines and receptors of the lymphotoxin/TNF family as well as the local microenvironment, requiring further research to build our understanding.

GROWTH OF CANCER CELLS IN LNs

LN Vasculature

In primary tumors, hypoxia is associated with expression of VEGF, which in turn leads to the sprouting of nascent blood vessels. Primary tumor hypoxia has been shown to increase the frequency of LN metastasis (117) by upregulating the integrin α_5 subunit, which is required for 3D cell migration *in vitro* (117). We, and others, have found hypoxic tumor cells in the LN (118, 119). It is unclear whether these hypoxic cancer cells in the LN sinus maintain this status from their state in the primary tumor or if tumor cells become hypoxic on arrival and proliferation in the avascular LN sinus.

Angiogenic and non-angiogenic-dependent metastases have been found in LNs and other metastatic tissues, such as the lung and liver (120–123). The presence of hypoxic cancer cells correlates with endothelial cell proliferation in some LN metastases, a pattern that could be predicted by the characteristics of the primary tumor (124). We found elevated VEGF and angiogenesis in primary tumors but did not find the same in metastatic LNs, despite the presence of hypoxic cancer cells (118). In agreement with the findings of the lack of angiogenesis in LN metastasis from our laboratory, other studies have shown that the vascular density of metastatic LNs is lower than that of non-metastatic nodes (121, 125, 126).

Although overexpression of VEGF leads to the expansion of the LN lymphatic vessel network (43–45, 127), a limited number of studies suggest VEGF, or other growth factors, have an effect on the number of blood vessels within the LN. Overexpression of VEGF has been reported to increase the number of HEVs

(45). By contrast, other reports demonstrate that VEGF only increases the diameter of LN blood vessels, perhaps through proliferation of endothelial cells of existing vessels (43, 127). The scarcity of evidence concerning VEGF and inflammation-induced sprouting angiogenesis relative to lymphangiogenesis raises questions about the mechanistic control of the LN vasculature. During the progression of LN metastases, the existing LN vasculature may be sufficient to support tumor growth. It has been proposed that angiogenesis is redundant for tumor growth in the LN due to the rich native vascularity of LNs; the vessel density of the LN is comparable to that of the primary tumor (125). It has also been proposed that remodeled HEVs in TDLNs can nurture established metastatic lesions in LNs (128). Although studies of VEGF in other metastatic organs require investigation, the unresponsiveness of LN metastases to antiangiogenic therapy (59, 118) adds another explanation for the poor outcomes of anti-VEGF therapy in adjuvant settings.

Recent studies have investigated mechanisms of resistance to antiangiogenesis therapy in metastatic disease. The tyrosine kinase inhibitor sunitinib, whose targets include VEGF receptors, stimulated transcription and mRNA stabilization of *VEGF-C* in a xenograft model of renal cell carcinoma (129). As a result, lymphangiogenesis and lymphatic metastasis were increased. A recent study identified vascular cooption in breast cancer liver metastases as another resistance mechanism to anti-VEGF therapy (123). In a "replacement" pattern of growth, liver metastases replaced hepatocytes and were physically associated with liver sinusoidal blood vessels. Silencing of Actin Related Proteins 2/3 (ARP 2/3), which mediate breast cancer cell motility, effectively inhibited vascular cooption of these liver metastases. It remains to be determined if this mechanism of vascular cooption is active in LN metastases. As multiple modes of growth were seen in liver metastases, metastatic growth and vascularization may depend on multiple factors, including the tumor type. Further investigation is needed to tailor treatments targeting the growth of metastases, including LN metastases.

CLINICAL MANAGEMENT AND TREATMENT OF LN METASTASIS

Lymph node metastasis is a critical prognostic indicator for patients with solid tumors including melanoma, breast, and gastric cancers. However, the role LN metastasis plays in cancer progression has been debated in the clinic for decades (130). The guidelines and treatment strategies for patients with nodal disease are evolving as clinical trials are conducted to improve the ability to contain and treat metastases. Until recently, axillary LN dissection (ALND) had been the standard of care for breast cancer patients with sentinel-node involvement. However, recent clinical trials designed to define the benefit of ALND has changed the way breast cancer patients are being treated. The International Breast Cancer Study Group Trial 23-01 (IBCSG 23-01) clinical trial was conducted to determine the benefit of ALND in patients with limited sentinel-node involvement (1–2 micrometastatic nodes) and tumors less than 5 cm (131). Five-year follow-up showed no disease-free survival benefit in patients that underwent ALND compared with those that did

not. These findings are consistent with the ACOSOG Z0011 trial involving patients with limited sentinel-node involvement undergoing breast-conserving surgery, in which these patients were assigned randomly to receive either ALND or no further axillary surgery (132, 133). Both trials suggest that ALND in early-stage breast cancer patients with limited nodal involvement do not have a survival benefit compared with patients that do not undergo ALND. These trials have led to a reduction in the number of breast cancer patients undergoing ALND, which has also reduced the morbidities associated with ALND. However, all of these patients received traditional systemic adjuvant therapy and radiation that potentially eliminated any residual disease in the LNs (132). Thus, radiation and systemic therapies may be sufficient to control nodal disease, making ALND unnecessary for breast cancer patients with limited LN involvement.

To test this hypothesis, recent clinical trials have assessed the benefit of axillary radiation therapy (ART) in early-stage breast cancer patients as an alternate treatment strategy to ALND. Although ALND provides excellent regional control of the disease, patients experience debilitating side effects such as lymphedema. The After Mapping of the Axilla: Radiotherapy or Surgery (AMAROS) randomized phase III trial compared sentinel-node-positive T1-2 breast cancer patients who received either ART or ALND as adjuvant treatment after systemic therapy (134). The results from this trial showed that ART provided excellent local control of disease and the outcomes were comparable to ALND. Furthermore, ART patients had fewer complications compared with those receiving ALND.

For melanoma patients, the Multicenter Selective Lymphadenectomy Trial-I (MSLT-I) provided evidence that patients who undergo sentinel LN (SLN) biopsy have an increased survival rate (135). In this trial, patients were randomized to either (i) wide excision of the melanoma with SLN procedure, followed by complete nodal dissection in patients with a positive SLN or (ii) wide excision and nodal observation, with lymphadenectomy at the time of LN recurrence. However, the importance of complete LN dissection remained controversial, as the main difference between the treatments for patients with disease in LNs was the timing of when lymphadenectomy occurred, with patients having disease removed earlier (SLN patients) having better outcomes. More recently, results of the MSLT-II, a randomized, multicenter, phase-3 clinical trial conducted on 1,934 melanoma patients were reported (136). The MSLT-II trial evaluated the importance of complete LN dissection by randomizing patients with sentinel-node metastases to either immediate complete LN dissection or nodal observation with ultrasonography. Results from this trial showed that immediate complete LN dissection in patients with sentinel-node metastases was not associated with increased 3-year melanoma-specific survival. However, patients that underwent complete LN dissection had increased rates of local-disease control compared with the observation group at 3 years (92 + 1.0 vs. 77 + 1.5%) and a slightly higher rate of disease-free survival compared with the observation group at 3 years (68 + 1.7 and 63 + 1.7%, respectively). The results of the MSLT-I and MSLT-II trials show that removing positive SLNs improves outcomes, but that further LN removal does not improve 3-year overall survival. However, complete nodal dissection in positive SLN patients did improve disease recurrence. The importance of recurrent disease in cancer progression and ultimate patient survival is thus being called into question. It will be critical to address whether there is a difference in 5- and 10-year overall survival in the MSLT-II trial, as these data may be able to account for systemic progression from the recurrent disease. The risk of systemic progression from recurrent disease must be weighed against the very clear reduction in the rate of lymphedema in patients that did not undergo complete LN dissections.

Taken together, the results from these clinical trials have revolutionized the way clinicians manage cancer treatment. Current clinical practice has adopted the theory that less extensive LN dissections for patients with early-stage disease reduce complications without changing overall survival. In these cases, systemic adjuvant therapy and radiotherapy are able to manage any residual disease. Treating local disease in the LN that has not yet progressed to other locations with systemic therapies and radiation could decrease the long-term mortality rate in patients (137), potentially mitigating the impact of less extensive surgeries that leave some LNs with metastatic cancer cells in patients. However, fundamental questions in the biology of LN metastases still remain unanswered, including: What is the fate of cancer cells once they metastasize to the LN? Do LN metastases spread beyond the node and contribute to disease progression? Answers to these questions through continued research will give us better insights into the most effective strategy to manage the progression of solid tumors.

Although there is no direct experimental evidence to show that cancer cells can escape the LN, a few genetic studies provide evidence that nodal disease can colonize distant organs. A recent study used phylogenetic tracing to analyze tumor cell evolution in CRC patients. The analyses from this study revealed that 35% of distant liver metastasis has LN metastasis as the closest phylogenetic neighbor (138). An earlier study characterized the somatic evolution of mutations in cancer cells from primary and metastatic tumors by genome sequencing in a genetically modified mouse model of small cell lung carcinoma (SCLC) (139). This analysis suggested that multiple related primary tumor subclones can seed the LN and a single clone can then spread further from the node to the liver. From the experiments in the SCLC model, the authors were unable to conclude if LN metastases preceded systemic dissemination and if the LN microenvironment altered the genetic and epigenetic makeup of cancer cells before distant dissemination.

Even with radiation and systemic therapies, some patients still have LN recurrences. Systemic therapies that minimize toxicity while targeting disease in LNs represent a promising approach. Only a small fraction of systemically delivered chemotherapy drug accumulates in LNs (2). We have found that increased vascular permeability of LN blood vessels did not increase chemotherapy penetration into the LN parenchyma (140). Many current strategies focus on optimizing lymphatic delivery and retention properties of therapeutics that target tumor-associated lymphatic vessels (141). Targeted delivery of immunomodulatory agents or cancer cell-specific cytotoxic drugs into TDLNs can improve cancer vaccination strategies (142) and eradicate disease from LNs, respectively (141).

CONCLUSION

A growing interest and ability to study LEC biology has provided enormous insights into the role lymphatic vessels play in tumor metastasis and cancer progression. While it is known that tumor-associated lymphatic vessels are a route of metastasis, it is now appreciated that tumor cells also use these vessels to establish immunological tolerance in TDLNs. Although antitumor immune responses can be generated locally in primary tumors, TDLNs serve as critical sites for antitumor immune responses. It remains unknown how the systemic adaptive immune response to cancer is shaped by immunosuppressed LNs. Several additional important areas of exploration remain, including understanding the influence of the LN microenvironment on cancer cell behavior and determining the contribution of LN metastases to distant organ metastasis, which at present remains controversial. Therapies targeting LN metastases must also consider enhancing antigen presentation to tumor-specific T cells. Moreover, therapies to activate tumor-specific T cells should be considered in parallel with strategies to break tolerance and other immunosuppression mechanisms. With continued research focus on the LN, we will gain deeper insights into mechanisms of immune evasion by cancer cells. A more thorough understanding of the molecular signals that facilitate tumor metastasis to TDLNs and beyond may also provide therapeutic targets to control the further dissemination of lymphatic metastases. With these continued advances, patient survival from metastatic cancer will continue to improve.

AUTHOR CONTRIBUTIONS

DJ, EP, and TP contributed to the writing of the manuscript.

ACKNOWLEDGMENTS

REFERENCES

1. Chaffer CL, Weinberg RA. A perspective on cancer cell metastasis. *Science* (2011) 331:1559–64. doi:10.1126/science.1203543
2. Chen J, Wang L, Yao Q, Ling R, Li K, Wang H. Drug concentrations in axillary lymph nodes after lymphatic chemotherapy on patients with breast cancer. *Breast Cancer Res* (2004) 6:R474–7. doi:10.1186/bcr819
3. Lund AW, Wagner M, Fankhauser M, Steinskog ES, Broggi MA, Spranger S, et al. Lymphatic vessels regulate immune microenvironments in human and murine melanoma. *J Clin Invest* (2016) 126:3389–402. doi:10.1172/JCI79434
4. Spranger S, Bao R, Gajewski TF. Melanoma-intrinsic beta-catenin signalling prevents anti-tumour immunity. *Nature* (2015) 523:231–5. doi:10.1038/nature14404
5. Podgrabinska S, Kamalu O, Mayer L, Shimaoka M, Snoeck H, Randolph GJ, et al. Inflamed lymphatic endothelium suppresses dendritic cell maturation and function via Mac-1/ICAM-1-dependent mechanism. *J Immunol* (2009) 183:1767–79. doi:10.4049/jimmunol.0802167
6. Hirosue S, Vokali E, Raghavan VR, Rincon-Restrepo M, Lund AW, Corthesy-Henrioud P, et al. Steady-state antigen scavenging, cross-presentation, and CD8+ T cell priming: a new role for lymphatic endothelial cells. *J Immunol* (2014) 192:5002–11. doi:10.4049/jimmunol.1302492
7. Dieterich LC, Ikenberg K, Cetintas T, Kapaklikaya K, Hutmacher C, Detmar M. Tumor-associated lymphatic vessels upregulate PDL1 to inhibit T-cell activation. *Front Immunol* (2017) 8:66. doi:10.3389/fimmu.2017.00066
8. Tewalt EF, Cohen JN, Rouhani SJ, Guidi CJ, Qiao H, Fahl SP, et al. Lymphatic endothelial cells induce tolerance via PD-L1 and lack of costimulation leading to high-level PD-1 expression on CD8 T cells. *Blood* (2012) 120:4772–82. doi:10.1182/blood-2012-04-427013
9. Chen DS, Mellman I. Elements of cancer immunity and the cancer-immune set point. *Nature* (2017) 541:321–30. doi:10.1038/nature21349
10. Padera TP, Kadambi A, di Tomaso E, Carreira CM, Brown EB, Boucher Y, et al. Lymphatic metastasis in the absence of functional intratumor lymphatics. *Science* (2002) 296:1883–6. doi:10.1126/science.1071420
11. Fankhauser M, Broggi MAS, Potin L, Bordry N, Jeanbart L, Lund AW, et al. Tumor lymphangiogenesis promotes T cell infiltration and potentiates immunotherapy in melanoma. *Sci Transl Med* (2017) 9. doi:10.1126/scitranslmed.aal4712
12. Pham TH, Baluk P, Xu Y, Grigorova I, Bankovich AJ, Pappu R, et al. Lymphatic endothelial cell sphingosine kinase activity is required for lymphocyte egress and lymphatic patterning. *J Exp Med* (2010) 207:17–27. doi:10.1084/jem.20091619
13. Ponnusamy S, Selvam SP, Mehrotra S, Kawamori T, Snider AJ, Obeid LM, et al. Communication between host organism and cancer cells is transduced by systemic sphingosine kinase 1/sphingosine 1-phosphate signalling to regulate tumour metastasis. *EMBO Mol Med* (2012) 4:761–75. doi:10.1002/emmm.201200244
14. van der Weyden L, Arends MJ, Campbell AD, Bald T, Wardle-Jones H, Griggs N, et al. Genome-wide in vivo screen identifies novel host regulators of metastatic colonization. *Nature* (2017) 541:233–6. doi:10.1038/nature20792
15. Fukuhara S, Simmons S, Kawamura S, Inoue A, Orba Y, Tokudome T, et al. The sphingosine-1-phosphate transporter Spns2 expressed on endothelial cells regulates lymphocyte trafficking in mice. *J Clin Invest* (2012) 122:1416–26. doi:10.1172/JCI60746
16. Mendoza A, Fang V, Chen C, Serasinghe M, Verma A, Muller J, et al. Lymphatic endothelial S1P promotes mitochondrial function and survival in naive T cells. *Nature* (2017) 546:158–61. doi:10.1038/nature22352
17. Randolph GJ, Angeli V, Swartz MA. Dendritic-cell trafficking to lymph nodes through lymphatic vessels. *Nat Rev Immunol* (2005) 5:617–28. doi:10.1038/nri1670
18. Shields JD, Kourtis IC, Tomei AA, Roberts JM, Swartz MA. Induction of lymphoidlike stroma and immune escape by tumors that express the chemokine CCL21. *Science* (2010) 328:749–52. doi:10.1126/science.1185837
19. Issa A, Le TX, Shoushtari AN, Shields JD, Swartz MA. Vascular endothelial growth factor-C and C-C chemokine receptor 7 in tumor cell-lymphatic cross-talk promote invasive phenotype. *Cancer Res* (2009) 69:349–57. doi:10.1158/0008-5472.CAN-08-1875
20. Torcellan T, Hampton HR, Bailey J, Tomura M, Brink R, Chtanova T. In vivo photolabeling of tumor-infiltrating cells reveals highly regulated egress of T-cell subsets from tumors. *Proc Natl Acad Sci U S A* (2017) 114:5677–82. doi:10.1073/pnas.1618446114
21. Karpanen T, Egeblad M, Karkkainen MJ, Kubo H, Yla-Herttuala S, Jaattela M, et al. Vascular endothelial growth factor C promotes tumor lymphangiogenesis and intralymphatic tumor growth. *Cancer Res* (2001) 61:1786–90.
22. Karnezis T, Shayan R, Caesar C, Roufail S, Harris NC, Ardipradja K, et al. VEGF-D promotes tumor metastasis by regulating prostaglandins produced by the collecting lymphatic endothelium. *Cancer Cell* (2012) 21:181–95. doi:10.1016/j.ccr.2011.12.026

23. Stacker SA, Achen MG. Emerging roles for VEGF-D in human disease. *Biomolecules* (2018) 8:E1. doi:10.3390/biom8010001

24. Tammela T, Alitalo K. Lymphangiogenesis: molecular mechanisms and future promise. *Cell* (2010) 140:460–76. doi:10.1016/j.cell.2010.01.045

25. Koch M, Dettori D, Van Nuffelen A, Souffreau J, Marconcini L, Wallays G, et al. VEGF-D deficiency in mice does not affect embryonic or postnatal lymphangiogenesis but reduces lymphatic metastasis. *J Pathol* (2009) 219:356–64. doi:10.1002/path.2605

26. Zheng W, Aspelund A, Alitalo K. Lymphangiogenic factors, mechanisms, and applications. *J Clin Invest* (2014) 124:878–87. doi:10.1172/JCI71603

27. Stacker SA, Caesar C, Baldwin ME, Thornton GE, Williams RA, Prevo R, et al. VEGF-D promotes the metastatic spread of tumor cells via the lymphatics. *Nat Med* (2001) 7:186–91. doi:10.1038/84635

28. He Y, Kozaki K, Karpanen T, Koshikawa K, Yla-Herttuala S, Takahashi T, et al. Suppression of tumor lymphangiogenesis and lymph node metastasis by blocking vascular endothelial growth factor receptor 3 signaling. *J Natl Cancer Inst* (2002) 94:819–25. doi:10.1093/jnci/94.11.819

29. Alishekevitz D, Gingis-Velitski S, Kaidar-Person O, Gutter-Kapon L, Scherer SD, Raviv Z, et al. Macrophage-induced lymphangiogenesis and metastasis following paclitaxel chemotherapy is regulated by VEGFR3. *Cell Rep* (2016) 17:1344–56. doi:10.1016/j.celrep.2016.09.083

30. Cohen-Kaplan V, Naroditsky I, Zetser A, Ilan N, Vlodavsky I, Doweck I. Heparanase induces VEGF C and facilitates tumor lymphangiogenesis. *Int J Cancer* (2008) 123:2566–73. doi:10.1002/ijc.23898

31. Olmeda D, Cerezo-Wallis D, Riveiro-Falkenbach E, Pennacchi PC, Contreras-Alcalde M, Ibarz N, et al. Whole-body imaging of lymphovascular niches identifies pre-metastatic roles of midkine. *Nature* (2017) 546:676–80. doi:10.1038/nature22977

32. Jones D, Min W. An overview of lymphatic vessels and their emerging role in cardiovascular disease. *J Cardiovasc Dis Res* (2011) 2:141–52. doi:10.4103/0975-3583.85260

33. Dieterich LC, Detmar M. Tumor lymphangiogenesis and new drug development. *Adv Drug Deliv Rev* (2016) 99:148–60. doi:10.1016/j.addr.2015.12.011

34. Saif MW, Knost JA, Chiorean EG, Kambhampati SR, Yu D, Pytowski B, et al. Phase 1 study of the anti-vascular endothelial growth factor receptor 3 monoclonal antibody LY3022856/IMC-3C5 in patients with advanced and refractory solid tumors and advanced colorectal cancer. *Cancer Chemother Pharmacol* (2016) 78:815–24. doi:10.1007/s00280-016-3134-3

35. Tacconi C, Correale C, Gandelli A, Spinelli A, Dejana E, D'Alessio S, et al. Vascular endothelial growth factor C disrupts the endothelial lymphatic barrier to promote colorectal cancer invasion. *Gastroenterology* (2015) 148:1438–51.e8. doi:10.1053/j.gastro.2015.03.005

36. Peinado H, Aleckovic M, Lavotshkin S, Matei I, Costa-Silva B, Moreno-Bueno G, et al. Melanoma exosomes educate bone marrow progenitor cells toward a pro-metastatic phenotype through MET. *Nat Med* (2012) 18:883–91. doi:10.1038/nm.2753

37. Robbins PD, Morelli AE. Regulation of immune responses by extracellular vesicles. *Nat Rev Immunol* (2014) 14:195–208. doi:10.1038/nri3622

38. Hood JL, San RS, Wickline SA. Exosomes released by melanoma cells prepare sentinel lymph nodes for tumor metastasis. *Cancer Res* (2011) 71:3792–801. doi:10.1158/0008-5472.CAN-10-4455

39. Maus RLG, Jakub JW, Nevala WK, Christensen TA, Noble-Orcutt K, Sachs Z, et al. Human melanoma-derived extracellular vesicles regulate dendritic cell maturation. *Front Immunol* (2017) 8:358. doi:10.3389/fimmu.2017.00358

40. Pucci F, Garris C, Lai CP, Newton A, Pfirschke C, Engblom C, et al. SCS macrophages suppress melanoma by restricting tumor-derived vesicle-B cell interactions. *Science* (2016) 352:242–6. doi:10.1126/science.aaf1328

41. Headley MB, Bins A, Nip A, Roberts EW, Looney MR, Gerard A, et al. Visualization of immediate immune responses to pioneer metastatic cells in the lung. *Nature* (2016) 531:513–7. doi:10.1038/nature16985

42. Harrell MI, Iritani BM, Ruddell A. Tumor-induced sentinel lymph node lymphangiogenesis and increased lymph flow precede melanoma metastasis. *Am J Pathol* (2007) 170:774–86. doi:10.2353/ajpath.2007.060761

43. Hirakawa S, Kodama S, Kunstfeld R, Kajiya K, Brown LF, Detmar M. VEGF-A induces tumor and sentinel lymph node lymphangiogenesis and promotes lymphatic metastasis. *J Exp Med* (2005) 201:1089–99. doi:10.1084/jem.20041896

44. Angeli V, Ginhoux F, Llodra J, Quemeneur L, Frenette PS, Skobe M, et al. B cell-driven lymphangiogenesis in inflamed lymph nodes enhances dendritic cell mobilization. *Immunity* (2006) 24:203–15. doi:10.1016/j.immuni.2006.01.003

45. Shrestha B, Hashiguchi T, Ito T, Miura N, Takenouchi K, Oyama Y, et al. B cell-derived vascular endothelial growth factor A promotes lymphangiogenesis and high endothelial venule expansion in lymph nodes. *J Immunol* (2010) 184:4819–26. doi:10.4049/jimmunol.0903063

46. Hirakawa S, Brown LF, Kodama S, Paavonen K, Alitalo K, Detmar M. VEGF-C-induced lymphangiogenesis in sentinel lymph nodes promotes tumor metastasis to distant sites. *Blood* (2007) 109:1010–7. doi:10.1182/blood-2006-05-021758

47. Alitalo A, Detmar M. Interaction of tumor cells and lymphatic vessels in cancer progression. *Oncogene* (2012) 31:4499–508. doi:10.1038/onc.2011.602

48. Rohner NA, McClain J, Tuell SL, Warner A, Smith B, Yun Y, et al. Lymph node biophysical remodeling is associated with melanoma lymphatic drainage. *FASEB J* (2015) 29:4512–22. doi:10.1096/fj.15-274761

49. Lund AW, Duraes FV, Hirosue S, Raghavan VR, Nembrini C, Thomas SN, et al. VEGF-C promotes immune tolerance in B16 melanomas and cross-presentation of tumor antigen by lymph node lymphatics. *Cell Rep* (2012) 1:191–9. doi:10.1016/j.celrep.2012.01.005

50. Malhotra D, Fletcher AL, Astarita J, Lukacs-Kornek V, Tayalia P, Gonzalez SF, et al. Transcriptional profiling of stroma from inflamed and resting lymph nodes defines immunological hallmarks. *Nat Immunol* (2012) 13:499–510. doi:10.1038/ni.2262

51. Roozendaal R, Mempel TR, Pitcher LA, Gonzalez SF, Verschoor A, Mebius RE, et al. Conduits mediate transport of low-molecular-weight antigen to lymph node follicles. *Immunity* (2009) 30:264–76. doi:10.1016/j.immuni.2008.12.014

52. Fletcher AL, Lukacs-Kornek V, Reynoso ED, Pinner SE, Bellemare-Pelletier A, Curry MS, et al. Lymph node fibroblastic reticular cells directly present peripheral tissue antigen under steady-state and inflammatory conditions. *J Exp Med* (2010) 207:689–97. doi:10.1084/jem.20092642

53. Cohen JN, Guidi CJ, Tewalt EF, Qiao H, Rouhani SJ, Ruddell A, et al. Lymph node-resident lymphatic endothelial cells mediate peripheral tolerance via Aire-independent direct antigen presentation. *J Exp Med* (2010) 207:681–8. doi:10.1084/jem.20092465

54. Lukacs-Kornek V, Malhotra D, Fletcher AL, Acton SE, Elpek KG, Tayalia P, et al. Regulated release of nitric oxide by nonhematopoietic stroma controls expansion of the activated T cell pool in lymph nodes. *Nat Immunol* (2011) 12:1096–104. doi:10.1038/ni.2112

55. Siegert S, Huang HY, Yang CY, Scarpellino L, Carrie L, Essex S, et al. Fibroblastic reticular cells from lymph nodes attenuate T cell expansion by producing nitric oxide. *PLoS One* (2011) 6:e27618. doi:10.1371/journal.pone.0027618

56. Riedel A, Shorthouse D, Haas L, Hall BA, Shields J. Tumor-induced stromal reprogramming drives lymph node transformation. *Nat Immunol* (2016) 17:1118–27. doi:10.1038/ni.3492

57. Soudja SM, Henri S, Mello M, Chasson L, Mas A, Wehbe M, et al. Disrupted lymph node and splenic stroma in mice with induced inflammatory melanomas is associated with impaired recruitment of T and dendritic cells. *PLoS One* (2011) 6:e22639. doi:10.1371/journal.pone.0022639

58. Rizwan A, Bulte C, Kalaichelvan A, Cheng M, Krishnamachary B, Bhujwalla ZM, et al. Metastatic breast cancer cells in lymph nodes increase nodal collagen density. *Sci Rep* (2015) 5:10002. doi:10.1038/srep10002

59. Hoshida T, Isaka N, Hagendoorn J, di Tomaso E, Chen YL, Pytowski B, et al. Imaging steps of lymphatic metastasis reveals that vascular endothelial growth factor-C increases metastasis by increasing delivery of cancer cells to lymph nodes: therapeutic implications. *Cancer Res* (2006) 66:8065–75. doi:10.1158/0008-5472.CAN-06-1392

60. Das S, Sarrou E, Podgrabinska S, Cassella M, Mungamuri SK, Feirt N, et al. Tumor cell entry into the lymph node is controlled by CCL1 chemokine expressed by lymph node lymphatic sinuses. *J Exp Med* (2013) 210:1509–28. doi:10.1084/jem.20111627

61. Miteva DO, Rutkowski JM, Dixon JB, Kilarski W, Shields JD, Swartz MA. Transmural flow modulates cell and fluid transport functions of lymphatic endothelium. *Circ Res* (2010) 106:920–31. doi:10.1161/CIRCRESAHA.109.207274

62. Shields JD, Fleury ME, Yong C, Tomei AA, Randolph GJ, Swartz MA. Autologous chemotaxis as a mechanism of tumor cell homing to lymphatics via interstitial flow and autocrine CCR7 signaling. *Cancer Cell* (2007) 11:526–38. doi:10.1016/j.ccr.2007.04.020

63. Irshad S, Flores-Borja F, Lawler K, Monypenny J, Evans R, Male V, et al. RORgammat+ innate lymphoid cells promote lymph node metastasis of breast cancers. *Cancer Res* (2017) 77:1083–96. doi:10.1158/0008-5472.CAN-16-0598

64. Muller A, Homey B, Soto H, Ge N, Catron D, Buchanan ME, et al. Involvement of chemokine receptors in breast cancer metastasis. *Nature* (2001) 410:50–6. doi:10.1038/35065016

65. Uchida D, Onoue T, Tomizuka Y, Begum NM, Miwa Y, Yoshida H, et al. Involvement of an autocrine stromal cell derived factor-1/CXCR4 system on the distant metastasis of human oral squamous cell carcinoma. *Mol Cancer Res* (2007) 5:685–94. doi:10.1158/1541-7786.MCR-06-0368

66. Hirakawa S, Detmar M, Kerjaschki D, Nagamatsu S, Matsuo K, Tanemura A, et al. Nodal lymphangiogenesis and metastasis: role of tumor-induced lymphatic vessel activation in extramammary Paget's disease. *Am J Pathol* (2009) 175:2235–48. doi:10.2353/ajpath.2009.090420

67. Kim YH, Choi YW, Lee J, Soh EY, Kim JH, Park TJ. Senescent tumor cells lead the collective invasion in thyroid cancer. *Nat Commun* (2017) 8:15208. doi:10.1038/ncomms15208

68. Zhuo W, Jia L, Song N, Lu XA, Ding Y, Wang X, et al. The CXCL12-CXCR4 chemokine pathway: a novel axis regulates lymphangiogenesis. *Clin Cancer Res* (2012) 18:5387–98. doi:10.1158/1078-0432.CCR-12-0708

69. Morley ST, Newport DT, Walsh MT. Towards the prediction of flow-induced shear stress distributions experienced by breast cancer cells in the lymphatics. *Biomech Model Mechanobiol* (2017) 16:2051–62. doi:10.1007/s10237-017-0937-z

70. Liao S, Cheng G, Conner DA, Huang Y, Kucherlapati RS, Munn LL, et al. Impaired lymphatic contraction associated with immunosuppression. *Proc Natl Acad Sci U S A* (2011) 108:18784–9. doi:10.1073/pnas.1116152108

71. Liao S, von der Weid PY. Lymphatic system: an active pathway for immune protection. *Semin Cell Dev Biol* (2015) 38:83–9. doi:10.1016/j.semcdb.2014.11.012

72. Proulx ST, Luciani P, Christiansen A, Karaman S, Blum KS, Rinderknecht M, et al. Use of a PEG-conjugated bright near-infrared dye for functional imaging of rerouting of tumor lymphatic drainage after sentinel lymph node metastasis. *Biomaterials* (2013) 34:5128–37. doi:10.1016/j.biomaterials.2013.03.034

73. Tammela T, Saaristo A, Holopainen T, Yla-Herttuala S, Andersson LC, Virolainen S, et al. Photodynamic ablation of lymphatic vessels and intralymphatic cancer cells prevents metastasis. *Sci Transl Med* (2011) 3:69ra11. doi:10.1126/scitranslmed.3001699

74. Kwon S, Agollah GD, Wu G, Chan W, Sevick-Muraca EM. Direct visualization of changes of lymphatic function and drainage pathways in lymph node metastasis of B16F10 melanoma using near-infrared fluorescence imaging. *Biomed Opt Express* (2013) 4:967–77. doi:10.1364/BOE.4.000967

75. Thelmo MC, Morita ET, Treseler PA, Nguyen LH, Allen RE Jr, Sagebiel RW, et al. Micrometastasis to in-transit lymph nodes from extremity and truncal malignant melanoma. *Ann Surg Oncol* (2001) 8:444–8. doi:10.1007/s10434-001-0444-3

76. Jafarnejad M, Woodruff MC, Zawieja DC, Carroll MC, Moore JE Jr. Modeling lymph flow and fluid exchange with blood vessels in lymph nodes. *Lymphat Res Biol* (2015) 13:234–47. doi:10.1089/lrb.2015.0028

77. Kerjaschki D, Bago-Horvath Z, Rudas M, Sexl V, Schneckenleithner C, Wolbank S, et al. Lipoxygenase mediates invasion of intrametastatic lymphatic vessels and propagates lymph node metastasis of human mammary carcinoma xenografts in mouse. *J Clin Invest* (2011) 121:2000–12. doi:10.1172/JCI44751

78. Van den Eynden GG, Vandenberghe MK, van Dam PJ, Colpaert CG, van Dam P, Dirix LY, et al. Increased sentinel lymph node lymphangiogenesis is associated with nonsentinel axillary lymph node involvement in breast cancer patients with a positive sentinel node. *Clin Cancer Res* (2007) 13:5391–7. doi:10.1158/1078-0432.CCR-07-1230

79. Schiefer AI, Schoppmann SF, Birner P. Lymphovascular invasion of tumor cells in lymph node metastases has a negative impact on survival in esophageal cancer. *Surgery* (2016) 160:331–40. doi:10.1016/j.surg.2016.02.034

80. Junt T, Moseman EA, Iannacone M, Massberg S, Lang PA, Boes M, et al. Subcapsular sinus macrophages in lymph nodes clear lymph-borne viruses and present them to antiviral B cells. *Nature* (2007) 450:110–4. doi:10.1038/nature06287

81. Asano K, Nabeyama A, Miyake Y, Qiu CH, Kurita A, Tomura M, et al. CD169-positive macrophages dominate antitumor immunity by crosspresenting dead cell-associated antigens. *Immunity* (2011) 34:85–95. doi:10.1016/j.immuni.2010.12.011

82. Moalli F, Proulx ST, Schwendener R, Detmar M, Schlapbach C, Stein JV. Intravital and whole-organ imaging reveals capture of melanoma-derived antigen by lymph node subcapsular macrophages leading to widespread deposition on follicular dendritic cells. *Front Immunol* (2015) 6:114. doi:10.3389/fimmu.2015.00114

83. Ohnishi K, Komohara Y, Saito Y, Miyamoto Y, Watanabe M, Baba H, et al. CD169-positive macrophages in regional lymph nodes are associated with a favorable prognosis in patients with colorectal carcinoma. *Cancer Sci* (2013) 104:1237–44. doi:10.1111/cas.12212

84. Noy R, Pollard JW. Tumor-associated macrophages: from mechanisms to therapy. *Immunity* (2014) 41:49–61. doi:10.1016/j.immuni.2014.06.010

85. Ries CH, Cannarile MA, Hoves S, Benz J, Wartha K, Runza V, et al. Targeting tumor-associated macrophages with anti-CSF-1R antibody reveals a strategy for cancer therapy. *Cancer Cell* (2014) 25:846–59. doi:10.1016/j.ccr.2014.05.016

86. Hollmen M, Karaman S, Schwager S, Lisibach A, Christiansen AJ, Maksimow M, et al. G-CSF regulates macrophage phenotype and associates with poor overall survival in human triple-negative breast cancer. *Oncoimmunology* (2016) 5:e1115177. doi:10.1080/2162402X.2015.1115177

87. Fridlender ZG, Sun J, Kim S, Kapoor V, Cheng G, Ling L, et al. Polarization of tumor-associated neutrophil phenotype by TGF-beta: "N1" versus "N2" TAN. *Cancer Cell* (2009) 16:183–94. doi:10.1016/j.ccr.2009.06.017

88. Wang J, Jia Y, Wang N, Zhang X, Tan B, Zhang G, et al. The clinical significance of tumor-infiltrating neutrophils and neutrophil-to-CD8+ lymphocyte ratio in patients with resectable esophageal squamous cell carcinoma. *J Transl Med* (2014) 12:7. doi:10.1186/1479-5876-12-7

89. Coffelt SB, Kersten K, Doornebal CW, Weiden J, Vrijland K, Hau CS, et al. IL-17-producing gammadelta T cells and neutrophils conspire to promote breast cancer metastasis. *Nature* (2015) 522:345–8. doi:10.1038/nature14282

90. Wculek SK, Malanchi I. Neutrophils support lung colonization of metastasis-initiating breast cancer cells. *Nature* (2015) 528:413–7. doi:10.1038/nature16140

91. Munn DH, Mellor AL. The tumor-draining lymph node as an immune-privileged site. *Immunol Rev* (2006) 213:146–58. doi:10.1111/j.1600-065X.2006.00444.x

92. Ito M, Minamiya Y, Kawai H, Saito S, Saito H, Nakagawa T, et al. Tumor-derived TGFbeta-1 induces dendritic cell apoptosis in the sentinel lymph node. *J Immunol* (2006) 176:5637–43. doi:10.4049/jimmunol.176.9.5637

93. Preynat-Seauve O, Contassot E, Schuler P, Piguet V, French LE, Huard B. Extralymphatic tumors prepare draining lymph nodes to invasion via a T-cell cross-tolerance process. *Cancer Res* (2007) 67:5009–16. doi:10.1158/0008-5472.CAN-06-4494

94. Ochsenbein AF, Klenerman P, Karrer U, Ludewig B, Pericin M, Hengartner H, et al. Immune surveillance against a solid tumor fails because of immunological ignorance. *Proc Natl Acad Sci U S A* (1999) 96:2233–8. doi:10.1073/pnas.96.5.2233

95. Cho JK, Hyun SH, Choi N, Kim MJ, Padera TP, Choi JY, et al. Significance of lymph node metastasis in cancer dissemination of head and neck cancer. *Transl Oncol* (2015) 8:119–25. doi:10.1016/j.tranon.2015.03.001

96. Pantel K, Schlimok G, Kutter D, Schaller G, Genz T, Wiebecke B, et al. Frequent down-regulation of major histocompatibility class I antigen expression on individual micrometastatic carcinoma cells. *Cancer Res* (1991) 51:4712–5.

97. Pasero C, Gravis G, Granjeaud S, Guerin M, Thomassin-Piana J, Rocchi P, et al. Highly effective NK cells are associated with good prognosis in patients with metastatic prostate cancer. *Oncotarget* (2015) 6:14360–73. doi:10.18632/oncotarget.3965

98. Pampena MB, Levy EM. Natural killer cells as helper cells in dendritic cell cancer vaccines. *Front Immunol* (2015) 6:13. doi:10.3389/fimmu.2015.00013

99. Marcus A, Gowen BG, Thompson TW, Iannello A, Ardolino M, Deng W, et al. Recognition of tumors by the innate immune system and natural killer cells. *Adv Immunol* (2014) 122:91–128. doi:10.1016/B978-0-12-800267-4.00003-1

100. Ljunggren HG, Karre K. In search of the 'missing self': MHC molecules and NK cell recognition. *Immunol Today* (1990) 11:237–44. doi:10.1016/0167-5699(90)90097-S

101. Messaoudene M, Fregni G, Fourmentraux-Neves E, Chanal J, Maubec E, Mazouz-Dorval S, et al. Mature cytotoxic CD56(bright)/CD16(+) natural killer cells can infiltrate lymph nodes adjacent to metastatic melanoma. *Cancer Res* (2014) 74:81–92. doi:10.1158/0008-5472.CAN-13-1303

102. Kessler DJ, Mickel RA, Lichtenstein A. Depressed natural killer cell activity in cervical lymph nodes containing focal metastatic squamous cell carcinoma. *Arch Otolaryngol Head Neck Surg* (1988) 114:313–8. doi:10.1001/archotol.1988.01860150095022

103. Rosser EC, Mauri C. Regulatory B cells: origin, phenotype, and function. *Immunity* (2015) 42:607–12. doi:10.1016/j.immuni.2015.04.005

104. Schwartz M, Zhang Y, Rosenblatt JD. B cell regulation of the anti-tumor response and role in carcinogenesis. *J Immunother Cancer* (2016) 4:40. doi:10.1186/s40425-016-0145-x

105. Sarvaria A, Madrigal JA, Saudemont A. B cell regulation in cancer and anti-tumor immunity. *Cell Mol Immunol* (2017) 14:662–74. doi:10.1038/cmi.2017.35

106. Martinet L, Le Guellec S, Filleron T, Lamant L, Meyer N, Rochaix P, et al. High endothelial venules (HEVs) in human melanoma lesions: major gateways for tumor-infiltrating lymphocytes. *Oncoimmunology* (2012) 1:829–39. doi:10.4161/onci.20492

107. Martinet L, Filleron T, Le Guellec S, Rochaix P, Garrido I, Girard JP. High endothelial venule blood vessels for tumor-infiltrating lymphocytes are associated with lymphotoxin beta-producing dendritic cells in human breast cancer. *J Immunol* (2013) 191:2001–8. doi:10.4049/jimmunol.1300872

108. Peske JD, Thompson ED, Gemta L, Baylis RA, Fu YX, Engelhard VH. Effector lymphocyte-induced lymph node-like vasculature enables naive T-cell entry into tumours and enhanced anti-tumour immunity. *Nat Commun* (2015) 6:7114. doi:10.1038/ncomms8114

109. Drayton DL, Liao S, Mounzer RH, Ruddle NH. Lymphoid organ development: from ontogeny to neogenesis. *Nat Immunol* (2006) 7:344–53. doi:10.1038/ni1330

110. Ruddle NH. High endothelial venules and lymphatic vessels in tertiary lymphoid organs: characteristics, functions, and regulation. *Front Immunol* (2016) 7:491. doi:10.3389/fimmu.2016.00491

111. Allen E, Jabouille A, Rivera LB, Lodewijckx I, Missiaen R, Steri V, et al. Combined antiangiogenic and anti-PD-L1 therapy stimulates tumor immunity through HEV formation. *Sci Transl Med* (2017) 9. doi:10.1126/scitranslmed.aak9679

112. Finkin S, Yuan D, Stein I, Taniguchi K, Weber A, Unger K, et al. Ectopic lymphoid structures function as microniches for tumor progenitor cells in hepatocellular carcinoma. *Nat Immunol* (2015) 16:1235–44. doi:10.1038/ni.3290

113. Joshi NS, Akama-Garren EH, Lu Y, Lee DY, Chang GP, Li A, et al. Regulatory T cells in tumor-associated tertiary lymphoid structures suppress anti-tumor T cell responses. *Immunity* (2015) 43:579–90. doi:10.1016/j.immuni.2015.08.006

114. Liu C, Workman CJ, Vignali DA. Targeting regulatory T cells in tumors. *FEBS J* (2016) 283:2731–48. doi:10.1111/febs.13656

115. Hindley JP, Jones E, Smart K, Bridgeman H, Lauder SN, Ondondo B, et al. T-cell trafficking facilitated by high endothelial venules is required for tumor control after regulatory T-cell depletion. *Cancer Res* (2012) 72:5473–82. doi:10.1158/0008-5472.CAN-12-1912

116. Colbeck EJ, Jones E, Hindley JP, Smart K, Schulz R, Browne M, et al. Treg depletion licenses T cell-driven HEV neogenesis and promotes tumor destruction. *Cancer Immunol Res* (2017) 5:1005–15. doi:10.1158/2326-6066.CIR-17-0131

117. Cairns RA, Hill RP. Acute hypoxia enhances spontaneous lymph node metastasis in an orthotopic murine model of human cervical carcinoma. *Cancer Res* (2004) 64:2054–61. doi:10.1158/0008-5472.CAN-03-3196

118. Jeong HS, Jones D, Liao S, Wattson DA, Cui CH, Duda DG, et al. Investigation of the lack of angiogenesis in the formation of lymph node metastases. *J Natl Cancer Inst* (2015) 107. doi:10.1093/jnci/djv155

119. Zheng X, Wang X, Mao H, Wu W, Liu B, Jiang X. Hypoxia-specific ultrasensitive detection of tumours and cancer cells in vivo. *Nat Commun* (2015) 6:5834. doi:10.1038/ncomms6834

120. Guidi AJ, Berry DA, Broadwater G, Perloff M, Norton L, Barcos MP, et al. Association of angiogenesis in lymph node metastases with outcome of breast cancer. *J Natl Cancer Inst* (2000) 92:486–92. doi:10.1093/jnci/92.6.486

121. Pezzella F. Evidence for novel non-angiogenic pathway in breast-cancer metastasis. Breast Cancer Progression Working Party. *Lancet* (2000) 355:1787–8. doi:10.1016/S0140-6736(00)02268-6

122. Stessels F, Van den Eynden G, Van der Auwera I, Salgado R, Van den Heuvel E, Harris AL, et al. Breast adenocarcinoma liver metastases, in contrast to colorectal cancer liver metastases, display a non-angiogenic growth pattern that preserves the stroma and lacks hypoxia. *Br J Cancer* (2004) 90:1429–36. doi:10.1038/sj.bjc.6601727

123. Frentzas S, Simoneau E, Bridgeman VL, Vermeulen PB, Foo S, Kostaras E, et al. Vessel co-option mediates resistance to anti-angiogenic therapy in liver metastases. *Nat Med* (2016) 22:1294–302. doi:10.1038/nm.4197

124. Van den Eynden GG, Van der Auwera I, Van Laere SJ, Colpaert CG, Turley H, Harris AL, et al. Angiogenesis and hypoxia in lymph node metastases is predicted by the angiogenesis and hypoxia in the primary tumour in patients with breast cancer. *Br J Cancer* (2005) 93:1128–36. doi:10.1038/sj.bjc.6602828

125. Naresh KN, Nerurkar AY, Borges AM. Angiogenesis is redundant for tumour growth in lymph node metastases. *Histopathology* (2001) 38:466–70. doi:10.1046/j.1365-2559.2001.01061.x

126. Arapandoni-Dadioti P, Giatromanolaki A, Trihia H, Harris AL, Koukourakis MI. Angiogenesis in ductal breast carcinoma. Comparison of microvessel density between primary tumour and lymph node metastasis. *Cancer Lett* (1999) 137:145–50. doi:10.1016/S0304-3835(98)00343-7

127. Halin C, Tobler NE, Vigl B, Brown LF, Detmar M. VEGF-A produced by chronically inflamed tissue induces lymphangiogenesis in draining lymph nodes. *Blood* (2007) 110:3158–67. doi:10.1182/blood-2007-01-066811

128. Qian CN, Berghuis B, Tsarfaty G, Bruch M, Kort EJ, Ditlev J, et al. Preparing the "soil": the primary tumor induces vasculature reorganization in the sentinel lymph node before the arrival of metastatic cancer cells. *Cancer Res* (2006) 66:10365–76. doi:10.1158/0008-5472.CAN-06-2977

129. Dufies M, Giuliano S, Ambrosetti D, Claren A, Ndiaye PD, Mastri M, et al. Sunitinib stimulates expression of VEGFC by tumor cells and promotes lymphangiogenesis in clear cell renal cell carcinomas. *Cancer Res* (2017) 77:1212–26. doi:10.1158/0008-5472.CAN-16-3088

130. Nathanson SD, Shah R, Rosso K. Sentinel lymph node metastases in cancer: causes, detection and their role in disease progression. *Semin Cell Dev Biol* (2015) 38:106–16. doi:10.1016/j.semcdb.2014.10.002

131. Galimberti V, Cole BF, Zurrida S, Viale G, Luini A, Veronesi P, et al. Axillary dissection versus no axillary dissection in patients with sentinel-node micrometastases (IBCSG 23-01): a phase 3 randomised controlled trial. *Lancet Oncol* (2013) 14:297–305. doi:10.1016/S1470-2045(13)70035-4

132. Jagsi R, Chadha M, Moni J, Ballman K, Laurie F, Buchholz TA, et al. Radiation field design in the ACOSOG Z0011 (alliance) trial. *J Clin Oncol* (2014) 32:3600–6. doi:10.1200/JCO.2014.56.5838

133. Giuliano AE, Hunt KK, Ballman KV, Beitsch PD, Whitworth PW, Blumencranz PW, et al. Axillary dissection vs no axillary dissection in women with invasive breast cancer and sentinel node metastasis: a randomized clinical trial. *JAMA* (2011) 305:569–75. doi:10.1001/jama.2011.90

134. Donker M, van Tienhoven G, Straver ME, Meijnen P, van de Velde CJ, Mansel RE, et al. Radiotherapy or surgery of the axilla after a positive sentinel node in breast cancer (EORTC 10981-22023 AMAROS): a randomised, multicentre, open-label, phase 3 non-inferiority trial. *Lancet Oncol* (2014) 15:1303–10. doi:10.1016/S1470-2045(14)70460-7

135. Morton DL, Thompson JF, Cochran AJ, Mozzillo N, Nieweg OE, Roses DF, et al. Final trial report of sentinel-node biopsy versus nodal observation in melanoma. *N Engl J Med* (2014) 370:599–609. doi:10.1056/NEJMoa1310460

136. Faries MB, Thompson JF, Cochran AJ, Andtbacka RH, Mozzillo N, Zager JS, et al. Completion dissection or observation for sentinel-node metastasis in melanoma. *N Engl J Med* (2017) 376:2211–22. doi:10.1056/NEJMoa1613210

137. Punglia RS, Morrow M, Winer EP, Harris JR. Local therapy and survival in breast cancer. *N Engl J Med* (2007) 356:2399–405. doi:10.1056/NEJMra065241

138. Naxerova K, Reiter JG, Brachtel E, Lennerz JK, van de Wetering M, Rowan A, et al. Origins of lymphatic and distant metastases in human colorectal cancer. *Science* (2017) 357:55–60. doi:10.1126/science.aai8515

139. McFadden DG, Papagiannakopoulos T, Taylor-Weiner A, Stewart C, Carter SL, Cibulskis K, et al. Genetic and clonal dissection of murine small cell lung carcinoma progression by genome sequencing. *Cell* (2014) 156:1298–311. doi:10.1016/j.cell.2014.02.031

140. Meijer EFJ, Blatter C, Chen IX, Bouta E, Jones D, Pereira ER, et al. Lymph node effective vascular permeability and chemotherapy uptake. *Microcirculation* (2017) 24. doi:10.1111/micc.12381

141. Trevaskis NL, Kaminskas LM, Porter CJ. From sewer to saviour – targeting the lymphatic system to promote drug exposure and activity. *Nat Rev Drug Discov* (2015) 14:781–803. doi:10.1038/nrd4608

142. Maisel K, Sasso MS, Potin L, Swartz MA. Exploiting lymphatic vessels for immunomodulation: rationale, opportunities, and challenges. *Adv Drug Deliv Rev* (2017) 114:43–59. doi:10.1016/j.addr.2017.07.005

Check for updates

Analysis of Hierarchical Organization in Gene Expression Networks Reveals Underlying Principles of Collective Tumor Cell Dissemination and Metastatic Aggressiveness of Inflammatory Breast Cancer

Shubham Tripathi[1,2], Mohit Kumar Jolly[2], Wendy A. Woodward[3,4], Herbert Levine[1,2,5,6] and Michael W. Deem[1,2,5,6]*

[1] PhD Program in Systems, Synthetic, and Physical Biology, Rice University, Houston, TX, United States, [2] Center for Theoretical Biological Physics, Rice University, Houston, TX, United States, [3] Department of Radiation Oncology, The University of Texas MD Anderson Cancer Center, Houston, TX, United States, [4] MD Anderson Morgan Welch Inflammatory Breast Cancer Research Program and Clinic, The University of Texas MD Anderson Cancer Center, Houston, TX, United States, [5] Department of Bioengineering, Rice University, Houston, TX, United States, [6] Department of Physics and Astronomy, Rice University, Houston, TX, United States

Clusters of circulating tumor cells (CTCs), despite being rare, may account for more than 90% of metastases. Cells in these clusters do not undergo a complete epithelial-to-mesenchymal transition (EMT), but retain some epithelial traits as compared to individually disseminating tumor cells. Determinants of single cell dissemination versus collective dissemination remain elusive. Inflammatory breast cancer (IBC), a highly aggressive breast cancer subtype that chiefly metastasizes *via* CTC clusters, is a promising model for studying mechanisms of collective tumor cell dissemination. Previous studies, motivated by a theory that suggests physical systems with hierarchical organization tend to be more adaptable, have found that the expression of metastasis-associated genes is more hierarchically organized in cases of successful metastases. Here, we used the cophenetic correlation coefficient (CCC) to quantify the hierarchical organization in the expression of two distinct gene sets, collective dissemination-associated genes and IBC-associated genes, in cancer cell lines and in tumor samples from breast cancer patients. Hypothesizing that a higher CCC for collective dissemination-associated genes and for IBC-associated genes would be associated with retention of epithelial traits enabling collective dissemination and with worse disease progression in breast cancer patients, we evaluated the correlation of CCC with different phenotypic groups. The CCC of both the abovementioned gene sets, the collective dissemination-associated genes and the IBC-associated genes, was higher in (a) epithelial cell lines as compared to mesenchymal cell lines and (b) tumor samples from IBC patients as compared to samples from non-IBC breast cancer patients. A higher CCC of both gene sets was also correlated with a higher rate of metastatic relapse in breast cancer patients. In contrast, neither the levels of CDH1 gene expression nor gene set enrichment analysis (GSEA) of the abovementioned gene sets could provide similar insights. These results suggest

that retention of some epithelial traits in disseminating tumor cells as IBC progresses promotes successful breast cancer metastasis. The CCC provides additional information regarding the organizational complexity of gene expression in comparison to GSEA. We have shown that the CCC may be a useful metric for investigating the collective dissemination phenotype and a prognostic factor for IBC.

INTRODUCTION

Metastasis is responsible for 90% of deaths from solid tumors (1). It involves the escape of cancer cells from the site of the primary tumor, their entry into the circulatory system, and finally, colonization of and proliferation at a distant organ. However, this process is highly inefficient. Only an estimated 0.2% of the disseminated tumor cells are able to form a lesion at distant organ sites (2, 3). A well-studied mechanism of metastasis is single cell dissemination where carcinoma cells acquire migratory and invasive traits *via* an epithelial-to-mesenchymal transition (EMT) (4). These cells can then utilize blood or lymph circulation to reach distant organ sites, where they reacquire epithelial traits of cell–cell adhesion and apico-basal polarity *via* a mesenchymal-to-epithelial transition (MET) to establish metastases (4).

Recent studies have highlighted that EMT is not a binary process. Rather, cells *en route* to a mesenchymal phenotype can acquire a stable hybrid epithelial–mesenchymal (hybrid E/M) phenotype (5, 6). These observations have called into question the indispensability of a complete EMT followed by MET in metastasis (7). Instead, collective migration of tumor cells *via* clusters of circulating tumor cells (CTCs) has been suggested as an alternate mechanism of metastasis (8). Clusters of tumor cells had been detected in the bloodstream of cancer patients even before the characterization of EMT as a driver of cancer metastasis (9, 10). These clusters of tumor cells can efficiently seed secondary tumors, exhibiting up to 50 times the metastatic potential of individually migrating tumor cells (11). Tumor cell clusters accounted for >90% of metastases in a mouse model of breast cancer (12). Abundance of CTC clusters in the bloodstream has been associated with significantly poor prognosis in breast cancer and in small cell lung cancer (SCLC) (11, 13).

Multiple factors are believed to be responsible for the heightened metastatic potential of these CTC clusters. These include effective response to mechanical signals and chemical gradients by cells in CTC clusters as compared to migrating single tumor cells (14, 15), better evasion of the host immune system (16), and potential cooperation among heterogeneous cell types in CTC clusters (17, 18). Studies have shown that collectively invading tumor cells from the primary lesion often co-express epithelial and mesenchymal markers (19–21). Thus, cells in CTC clusters tend to manifest a hybrid epithelial–mesenchymal (hybrid E/M) phenotype and to retain cell–cell adhesion characteristics (8).

Inflammatory breast cancer (IBC) is a highly aggressive breast cancer subtype that has been reported to predominantly metastasize *via* CTC clusters (22). Characterized by breast erythema, edema, and *peau d'orange* presenting with or without a noticeable tumoral mass (23, 24), IBC involves tumoral infiltrate in the dermal lymphatics and about 30% of IBC patients have distant metastases at the time of diagnosis as compared to only 5% of non-IBC type breast cancer patients (25). Though only 2–4% of breast cancer cases each year in the United States are of the IBC type, IBC patients account for 10% of the annual breast cancer-related mortalities. A hallmark of IBC is the presence of cohesive clusters of tumor cells in the local lymph nodes (26) and IBC patients have larger and a higher frequency of CTC clusters as compared to non-IBC breast cancer patients (27). Abundance of CTC clusters has been shown to be associated with poor progression-free survival in IBC patients (27). Despite their great propensity to metastasize, tumor cells in the primary lesion and in metastatic lesions of IBC maintain a high expression E-cadherin, a hallmark of epithelial cells (26). IBC thus presents an exciting model for the study of collective dissemination of tumor cells *via* CTC clusters and of the prognostic potential of these clusters of migrating tumor cells. The results presented here strengthen the argument for investigating IBC to elucidate the mechanisms underlying collective dissemination of tumor cells.

Here, we invoke concepts from theoretical models of evolution to investigate cluster-based dissemination of tumor cells and analogous IBC characteristics. Theoretical studies suggest that systems with a more hierarchical structure are more adaptable (28–30) due to their ability to efficiently span the space of possible states. Hierarchical systems are also more robust to perturbations because a hierarchical network architecture has a buffering effect that hinders the propagation of local perturbations to a majority of nodes (30, 31). Hierarchical organization, thus, emerges over time in physical systems that are evolving in a changing environment with a rugged fitness landscape exhibiting numerous peaks and valleys (29). Given that tumor cells involved in metastasis and invasion progress through many different microenvironments (32–34), one can expect the expression of genes associated with a metastatic phenotype to be more hierarchically organized in instances of successful macrometastases as compared to instances with no metastasis.

We quantified the hierarchical organization in the expression of two distinct sets of genes, one associated with collective dissemination of tumor cells and the other related to IBC, in cancer cell lines and in breast cancer patients. For this purpose, we used the cophenetic correlation coefficient (CCC) metric. The CCC for a set of genes takes into consideration the collective expression of all genes within the given set and the correlations between the expression levels of different genes. It captures the level of hierarchical organization in the collective expression of genes in the given set. A higher CCC indicates greater hierarchical

organization in the expression of genes. The CCC was first used for comparing tree-like relationships represented by different dendrograms (35). It has been used previously to quantify the differences in expression of metastasis-associated genes in breast cancer patients with different clinical outcomes (36) and to quantify the differences in expression of genes predictive of clinical outcome in adult acute myeloid leukemia in patients belonging to different risk categories (37).

The goal of the present study was to determine whether the hierarchical organization in the expression of two sets of genes of interest is different in cell lines exhibiting different EMT-associated phenotypes and in tumor samples from breast cancer patients exhibiting features of IBC and non-IBC type disease. The first set of genes investigated here includes 87 genes reported to be associated with collective dissemination of tumor cells as CTC clusters: genes differentially expressed in cells forming CTC clusters as compared to individual CTCs (12). The second gene set includes 78 genes reported to be differentially expressed in tumor samples from IBC patients in comparison to tumor samples from non-IBC breast cancer patients (38). We observed that the CCC for both of these gene sets was higher in (a) epithelial cell lines as compared to mesenchymal cell lines and (b) tumor samples from IBC patients as compared to tumor samples from non-IBC breast cancer patients. A higher CCC further correlated with worse disease progression in breast cancer patients. In light of these observations, we propose that the metastatic aggressiveness of IBC potentially derives from the hierarchical organization in the expression of collective dissemination-associated genes in metastasizing tumor cells.

MATERIALS AND METHODS

Genes Associated With Collective Dissemination of Tumor Cells

Using multicolor lineage tracking, Cheung et al. showed that polyclonal seeding by disseminated clusters of tumor cells is the dominant mechanism for metastasis in a mouse model of breast cancer (12). These clusters accounted for more than 90% of distant organ metastases in mice. Circulating tumor cell clusters were observed to be enriched in expression of the epithelial protein keratin 14 (K14), and 87 genes with enriched or depleted expression in K14$^+$ primary tumor cells as compared to K14$^-$ primary tumor cells were identified. Broadly, expression of adhesion complex-associated genes was enriched and that of MHC Class II genes was depleted in K14$^+$ cells. We used this set of genes as a signature of the collective dissemination phenotype.

Genes Associated With the IBC Phenotype

Van Laere et al. obtained tumor samples from patients with breast adenocarcinoma: 137 samples from IBC patients and 252 samples from patients with non-IBC type breast cancer (non-IBC) (38). IBC patients were selected in accordance with the consensus diagnostic criteria described by Dawood et al. (23). RNA from the tumor samples was hybridized onto Affymetrix GeneChips (HGU133-series) to obtain the corresponding mRNA expression profiles. Linear regression models were employed to identify a

set of 78 IBC specific genes, which were differentially expressed in IBC tumor samples as compared to non-IBC tumor samples, independent of the molecular subtype of the tumor (38). We used this set of genes as a signature of the IBC phenotype in breast cancer patients. There were no genes common between this set of IBC-associated genes and the set of collective dissemination-associated genes described above. Both gene sets are available as Supplementary Material. The statistical methods used previously to obtain these gene sets are summarized in the Supplementary Material.

Gene Expression Data From Different Cell Lines

We used two different datasets of gene expression in cell lines, each cell line classified as epithelial (E), mesenchymal (M), or hybrid epithelial–mesenchymal (hybrid E/M). The first dataset was from the study by Grosse-Wilde et al. (39), Gene Expression Omnibus (GEO) accession number GSE66527. A total of 24 clones established from HMLER cell lines [normal human mammary epithelial cells immortalized and transformed with hTERT and the oncogenes *SV40LT* and *RAS* (40)] were sorted into 13 *CD24$^+$/CD44$^-$* E clones and 11 *CD24$^-$/CD44$^+$* M clones. The E clones and the M clones displayed cobble-stone like morphology and dispersed, fibroblast morphology, respectively.

The second dataset included gene expression from the National Cancer Institute 60 anticancer drug screen (NCI60), which includes panels of cell lines representing nine distinct types of cancer: leukemia, colon, lung, central nervous system, renal, melanoma, ovarian, breast, and prostate (41). The 60 cell lines have been classified into epithelial (E) ($n = 11$), mesenchymal (M) ($n = 36$), and hybrid epithelial-mesenchymal (hybrid E/M) ($n = 11$) categories on the basis of protein levels of E-cadherin and Vimentin (42). The gene expression data for these cell lines obtained using the Affymetrix Human Genome U133A array platform were downloaded from the CellMiner database (43, 44).

Gene Expression Data From Tumor Samples From IBC and Non-IBC Breast Cancer Patients

We used three different datasets of gene expression in tumor samples obtained from breast cancer patients. Each patient in the three datasets was diagnosed with either IBC or non-IBC type breast cancer (non-IBC). Iwamoto et al., GEO accession number GSE22597, collected tumor biopsies prospectively from 82 patients with locally advanced disease. A clinical diagnosis of IBC was made in 25 of these patients (45). Boersma et al., GEO accession number GSE5847, examined primary breast tumor samples from 50 patients, 15 of whom were diagnosed with IBC on the basis of the pathology and medical reports (46). Finally, Woodward et al., GEO accession number GSE45584, obtained tissue samples from core biopsies of breast tissue in 40 breast cancer patients, 20 IBC and 20 non-IBC (24).

In Iwamoto et al. and Woodward et al., IBC diagnosis was made in patients with clinical presentation of breast erythema and edema over more than one-third of the breast. In Boersma et al., nine IBC patients presented with erythema and edema,

while six IBC patients exhibited pathology indicating dermal lymphatic invasion and tumor emboli.

The microarray platforms and the normalization techniques used previously to obtain the gene expression profiles for different cell lines and for tumor samples from cancer patients have been outlined in the Supplementary Material.

Definition of Gene Network for Different Phenotypic Groups

For each phenotypic group, e.g., NCI60 cell lines labeled as epithelial (E) or patients in the Iwamoto et al. (45) dataset diagnosed with IBC, and gene set, e.g., the set of genes associated with IBC or the set of collective dissemination-associated genes, we defined a network with the genes as nodes and weighted edges between these nodes. The weight of the edge between gene i and gene j in the phenotypic group G was defined as

$$l_{ij}^{G} = \left| \sum_{k \in G} \frac{(e_i^k - \mu_i^G)(e_j^k - \mu_j^G)}{\sigma_i^G \sigma_j^G} \right| \quad (1)$$

Here, e_m^k is the expression of gene m in the sample k (patient/cell line), μ_m^G and σ_m^G are the mean and SD of the expression of gene m in the phenotypic group G, respectively, and the summation is over all patients or cell lines belonging to the group G. This definition resulted in a fully connected network for each phenotypic group and gene set. Since Eq. 1 is symmetric in i and j, the networks obtained were undirected.

We constructed such networks for the epithelial and mesenchymal cell lines in the Grosse-Wilde et al. (39) dataset and for the epithelial, mesenchymal, and hybrid epithelial–mesenchymal cell lines in the NCI60 dataset. Such networks were also constructed for IBC and non-IBC breast cancer patients in the three breast cancer datasets, Iwamoto et al. (45), Woodward et al. (24), and Boersma et al. (46), using each of the two gene sets described above, genes associated with collective dissemination of tumor cells and genes associated with the IBC phenotype.

Calculation of the CCC

To quantify the hierarchy in the expression of a set of genes in different groups of patients and cell lines, we used a metric called the CCC (35). The CCC is a measure of how well a hierarchical clustering of nodes in a network reproduces the distances between nodes in the original network. Intuitively, the CCC is a measure of how tree-like a network is. Since a tree topology is a prototypical hierarchical structure, a measure of the tree-like characteristic of a network allows us to aptly quantify the underlying hierarchy in the structure of the network.

For calculating the CCC of a given network, we defined the distance between nodes i and j as the Euclidean commute time distance (ECTD) between the two nodes, which is given by the square root of the mean first passage time taken by a random walker to travel from node i to node j and then back to node i. The ECTD between nodes i and j depends not only on the weight of the edge between nodes i and j but also on the number of different possible paths between the two nodes. The ECTD decreases as the number of possible paths between

the two nodes increases, and increases if any path between the two nodes becomes longer (47). This makes the ECTD suitable for clustering tasks. As described before, the network obtained for each phenotypic group and gene set was undirected and fully connected. This ensures that the ECTD between any pair of nodes will be finite. For a network with N nodes, we generated a $N \times N$ matrix D such that D_{ij} is the ECTD between nodes i and j (48). The matrix D was then used as an input to the average linkage hierarchical clustering algorithm (49), which generates a tree topology (T), i.e., a dendrogram, which best approximates the distances between the nodes of the network given by the matrix D. We then calculated the CCC as the correlation between the original pairwise distances and the corresponding distances in the tree topology:

$$CCC = \frac{\sum_{i<j}(D_{ij} - d)(T_{ij} - t)}{\sqrt{\sum_{i<j}(D_{ij} - d)^2 \sum_{i<j}(T_{ij} - t)^2}} \quad (2)$$

Here, $d = \langle D_{ij} \rangle$ is the mean of the original pairwise distances and $t = \langle T_{ij} \rangle$ is the mean of the pairwise distance in the tree topology. If the original network is hierarchical, the distances between nodes in the tree topology obtained *via* hierarchical clustering (T) will be highly correlated with the distances between nodes in the original network (D). Hence, the CCC will be high. However, if the original network lacks any hierarchical organization, this correlation will be weak, and the CCC will be low.

To test the sensitivity of the calculated CCC to the choice of ECTD as the network distance metric for hierarchical clustering, we alternatively defined the distance between node i and node j in the network as the resistance distance (50) between the two nodes. The resistance distance between any two nodes is given by the effective electrical resistance when a battery is connected across the two nodes. Like the ECTD, the resistance distance depends on all possible paths between nodes i and j and is, therefore, suited for clustering tasks. Using the resistance distance to create the matrix D where D_{ij} is the resistance distance between the nodes i and j, we calculated the CCC as described above.

The CCC calculated for a network was normalized with respect to the CCC of random networks with the same set of nodes but re-distributed edge weights. For this, we generated 10 such random networks by shuffling entries in the matrix D and then calculated the average of the CCCs of these random networks (CCC$_{rand}$). The normalized CCC was then defined as

$$CCC_{norm} = \frac{CCC - CCC_{rand}}{1 - CCC_{rand}} \quad (3)$$

Finally, to obtain the error in the estimate of CCC$_{norm}$, we used the bootstrap method (51). The method assumes that the distribution of gene expression in a patient or cell line group is the empirical distribution function of the observed expression in samples within the group. For a patient or cell line group with size n, we drew n samples from the group with replacement and calculated CCC$_{norm}$ for the sampled group. This sampling process was repeated 100 times to obtain 100 CCC$_{norm}$ values. The SE in the estimate of the CCC$_{norm}$ for the group was then given as the

sample SD of the 100 sampled CCC$_{norm}$ values. All p-values were also calculated using the bootstrap method.

The MATLAB code used for calculating the CCC is available at https://github.com/st35/gene-network-CCC.

RESULTS

Higher CCC for the Collective Dissemination-Associated Gene Network in Epithelial Cell Lines and in IBC Patients

We constructed networks with genes associated with collective dissemination of tumor cells (12), hereafter referred to as "collective dissemination-associated" genes, as nodes and the weight of the edge between nodes in a pair defined according to Eq. 1. Such networks were constructed for the E and M cell lines from the gene expression data from Grosse-Wilde et al. (39) and for the cell lines in the NCI60 anticancer drug screen (41) that have been categorized into E, M, and hybrid E/M classes (42). Representative networks for E and M cell lines from Grosse-Wilde et al. (39) are shown in Figures S1A,B in Supplementary Material. The normalized CCC for these networks was calculated using the method described above, and the results are shown in **Figure 1**. E cell lines exhibited a significantly higher CCC as compared to

M cell lines (p-value = 0.01) for the collective dissemination-associated gene network in the dataset from Grosse-Wilde et al. (39), **Figure 1A**. In the NCI60 dataset, the normalized CCC of the collective dissemination-associated gene network was higher for E cell lines as compared to the pooled M and hybrid E/M cell lines, **Figure 1B**. The bootstrap distribution of normalized CCC values for E cell lines was distinct from the distribution for M cell lines in the dataset from Grosse-Wilde et al. (39) and from the distribution for pooled M and hybrid E/M cell lines in the NCI60 dataset (Kolmogorov–Smirnov test, p-value < 0.01). We further calculated the CCC using the resistance distance instead of the ECTD and observed a similar trend in CCC values in the two datasets, Figures S2A,C in Supplementary Material.

We constructed similar networks for IBC and non-IBC patients using Affymetrix U133A profiles obtained by Iwamoto et al. (45). Representative networks for IBC and non-IBC breast cancer patients are shown in Figures S1C,D in Supplementary Material. Normalized CCC values for patients in the two groups are shown in **Figure 2A**. IBC patients exhibited a higher CCC for the network associated with collective dissemination of tumor cell clusters as compared to non-IBC breast cancer patients. The difference between the two groups in the dataset was significant (p-value < 0.02). Further, bootstrap distributions of the normalized CCC values for the two groups were

FIGURE 1 | Normalized cophenetic correlation coefficient of the collective dissemination-associated gene network for **(A)** 13 epithelial (E) and 11 mesenchymal cell lines from the study by Grosse-Wilde et al. (39), and **(B)** 11 epithelial (E) and 47 hybrid epithelial-mesenchymal (E/M) + mesenchymal (M) cell lines from the NCI60 dataset (41, 42). Error bars indicate the SE in the estimate of CCC$_{norm}$ calculated using the bootstrap method. *p-Value < 0.05.

FIGURE 2 | Normalized cophenetic correlation coefficient of the collective dissemination-associated gene network for tumor samples from inflammatory breast cancer (IBC) patients and non-IBC breast cancer patients for data from studies by **(A)** Iwamoto et al. (45) with 25 IBC and 57 non-IBC breast cancer patients, **(B)** Boersma et al. (46) with 13 IBC and 35 non-IBC breast cancer patients, and **(C)** Woodward et al. (24) with 20 IBC and 20 non-IBC breast cancer patients. Error bars indicate the SE in the estimate of CCC$_{norm}$ calculated using the bootstrap method. *p-Value < 0.05.

statistically distinct with *p*-value < 0.01 for the Kolmogorov–Smirnov test. The same trend in CCC values was observed from calculation of CCC using the resistance distance, Figure S2E in Supplementary Material. However, we did not observe a significant trend for the breast cancer samples characterized by Boersma et al. (46) and for the samples characterized by Woodward et al. (24), **Figures 2B,C**.
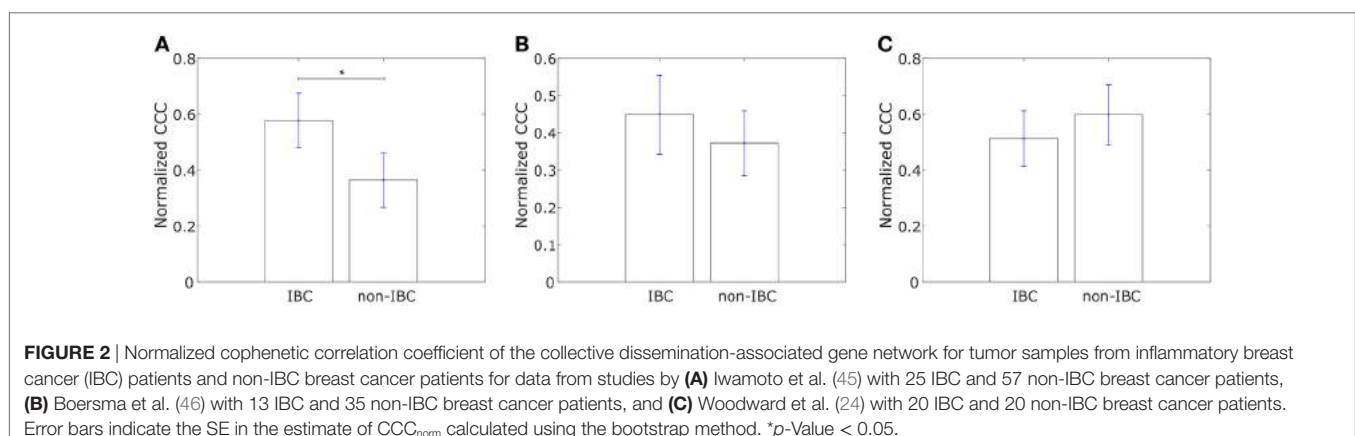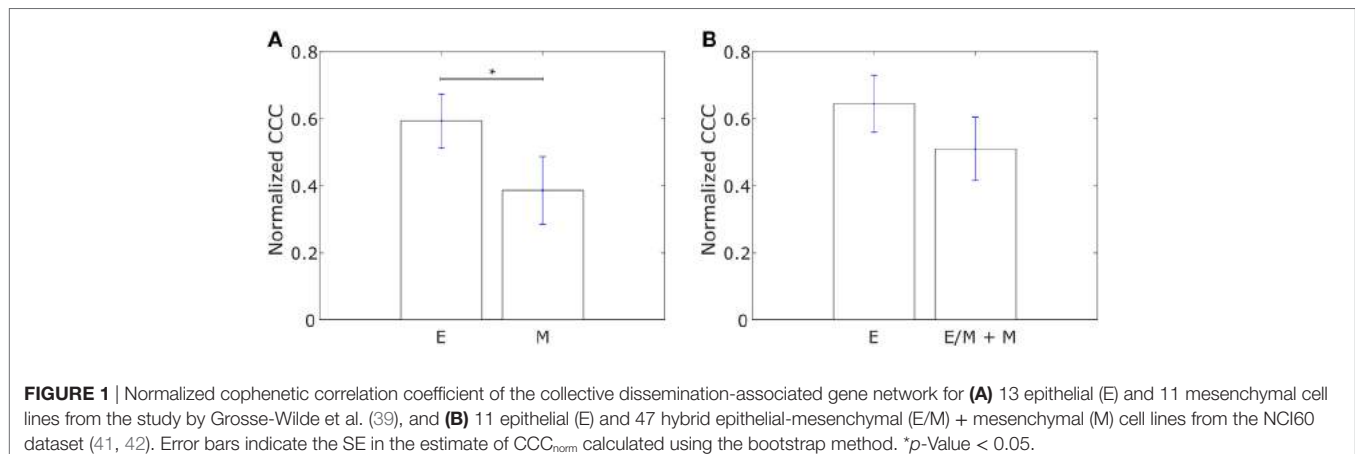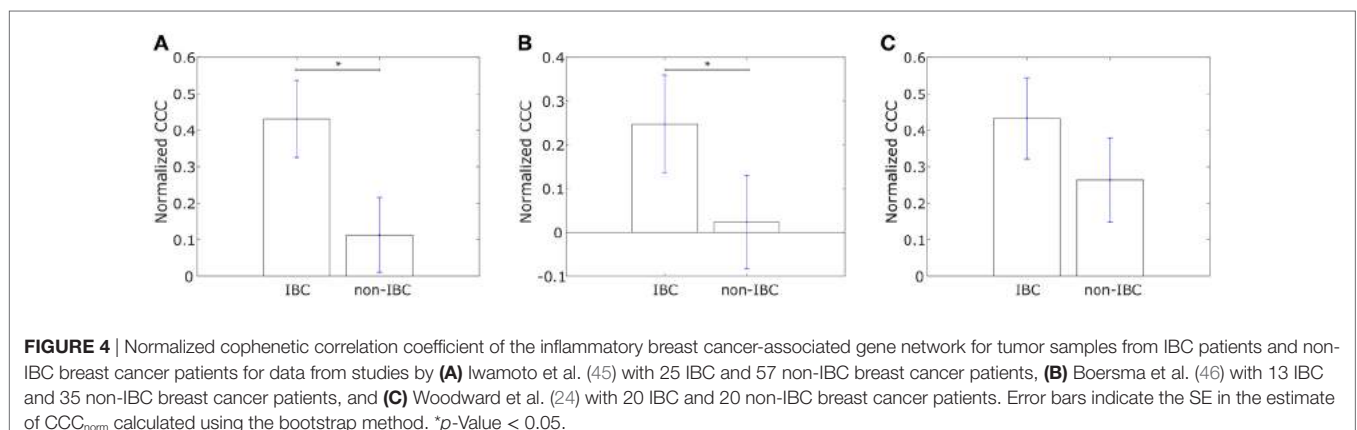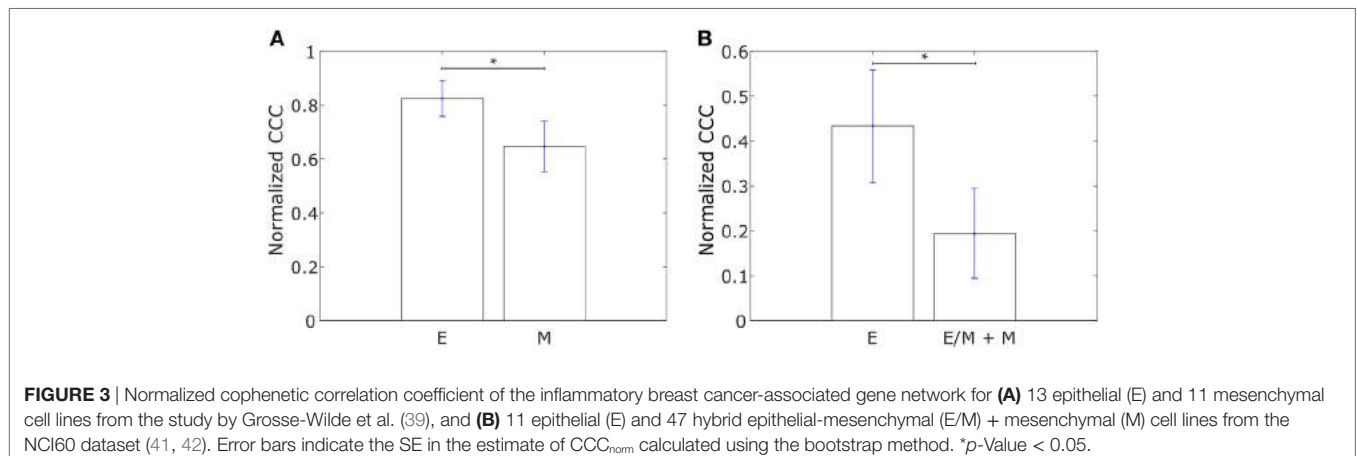
Higher CCC for the IBC-Associated Gene Network in Epithelial Cell Lines and in IBC Patients

We constructed networks with genes differentially expressed in tumor samples from IBC patients as compared to tumor samples from non-IBC breast cancer patients, hereafter referred to as "IBC-associated" genes, as nodes. The weight of the edge between nodes in a pair was defined using Eq. 1. Such networks were constructed for the E and M cell lines in the dataset from Gross-Wilde et al. (39) and for the E and pooled M + hybrid E/M cell lines in the NCI60 dataset. Normalized CCC values for these groups of cell lines calculated using the method described above are shown in **Figure 3**. E cell lines displayed a higher CCC for the IBC-associated gene network as compared to the other cell lines in both datasets [*p*-value = 0.03 for the cell lines in the study by Grosse-Wilde et al. (39) and *p*-value = 0.02 for the cell lines in the

NCI60 dataset]. The bootstrap distributions of normalized CCC values for the two groups of cell lines were statistically distinct for both datasets (*p*-value < 0.01 for the Kolmogorov–Smirnov test in each case). A higher CCC for the epithelial cell lines was also observed on using the resistance distance to calculate the CCC, Figures S2B,D in Supplementary Material.

Using Affymetrix U133A profiles from Iwamoto et al. (45), we constructed similar networks with IBC-associated genes as nodes for both IBC and non-IBC breast cancer patients. Normalized CCC values for the two breast cancer patient groups are shown in **Figure 4A**. The IBC group exhibited a significantly higher CCC for the IBC-associated gene network as compared to the non-IBC patient group (*p*-value = 0.01). Bootstrap distributions for the two groups were again statistically distinct (*p*-value < 0.01 for the Kolmogorov–Smirnov test). This trend in CCC values was also observed on using the resistance distance to calculate the CCC, Figure S2F in Supplementary Material. A similar trend in the CCC values for IBC and non-IBC patient groups was observed for breast cancer patients in the two other independent breast cancer datasets, Boersma et al. (46) (*p*-value = 0.02) and Woodward et al. (24) (*p*-value = 0.06), **Figures 4B,C**.

Saunders and McClay had used a well-understood gene regulatory network in the sea urchin embryo to identify transcription factors that control cell changes during EMT by perturbing individual transcription factors (52). They further determined 30

FIGURE 3 | Normalized cophenetic correlation coefficient of the inflammatory breast cancer-associated gene network for **(A)** 13 epithelial (E) and 11 mesenchymal cell lines from the study by Grosse-Wilde et al. (39), and **(B)** 11 epithelial (E) and 47 hybrid epithelial-mesenchymal (E/M) + mesenchymal (M) cell lines from the NCI60 dataset (41, 42). Error bars indicate the SE in the estimate of CCC$_{norm}$ calculated using the bootstrap method. *p-Value < 0.05.

FIGURE 4 | Normalized cophenetic correlation coefficient of the inflammatory breast cancer-associated gene network for tumor samples from IBC patients and non-IBC breast cancer patients for data from studies by **(A)** Iwamoto et al. (45) with 25 IBC and 57 non-IBC breast cancer patients, **(B)** Boersma et al. (46) with 13 IBC and 35 non-IBC breast cancer patients, and **(C)** Woodward et al. (24) with 20 IBC and 20 non-IBC breast cancer patients. Error bars indicate the SE in the estimate of CCC$_{norm}$ calculated using the bootstrap method. *p-Value < 0.05.

human transcription factors homologous to those identified in sea urchins. We calculated the CCC of a network with these transcription factors, hereafter referred to as "canonical drivers of EMT," as nodes for the IBC and non-IBC samples from each of the three breast cancer datasets, Iwamoto et al. (45), Boersma et al. (46), and Woodward et al. (24). The weight of the edge between any two transcription factors was defined using Eq. 1. We observed that the IBC patient group exhibited a lower CCC for the network composed of canonical EMT drivers as compared to the non-IBC patient group in data from each of the three studies, **Figure 5**.

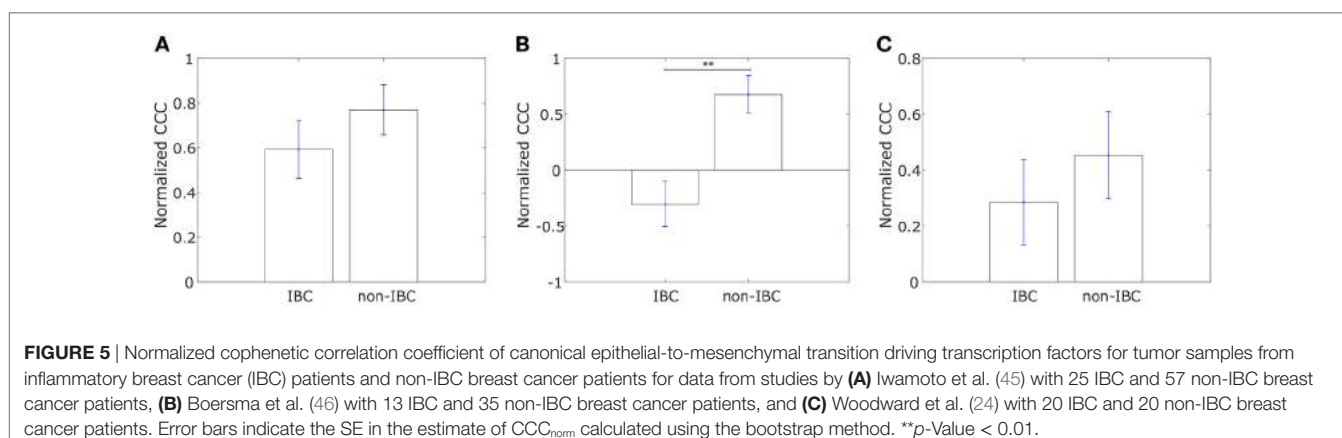## Higher CCC for the Two Networks Correlates With Early Metastasis Posttreatment

Having analyzed the differences in CCCs of collective dissemination-associated and IBC-associated gene sets in epithelial and mesenchymal cell lines and in tumor samples from IBC and non-IBC breast cancer patients, we next investigated if the CCC of these gene sets could provide insights into the metastatic propensity of tumors. We constructed networks with the two sets of genes, collective dissemination-associated and IBC-associated, as nodes for breast cancer patients who exhibited metastatic relapse within 5 years posttreatment (53). These patients were classified into two groups, those with metastatic relapse within 30 months posttreatment and those with metastasis between 30 and 60 months posttreatment, **Figures 6A,B**. Edge weights were defined, once again, using Eq. 1. For both collective dissemination-associated and IBC-associated gene sets, the CCC was significantly higher for the patient group with early metastatic relapse of breast cancer, i.e., relapse within 30 months of treatment, as compared to the patient group with relatively late relapse, i.e., metastatic relapse after 30 months posttreatment, **Figures 6A,B**. The p-values were 0.02 and 0.01 for the collective dissemination-associated gene network and the IBC-associated gene network, respectively. The same trend was observed upon considering only estrogen-receptor-positive patients, Figure S3 in Supplementary Material. There were too few samples from estrogen-receptor-negative patients for a similar analysis.

To investigate if the observation that a more hierarchical expression of collective dissemination-associated genes correlates with early relapse posttreatment can be generalized to other cancer types, we calculated the CCC of collective dissemination-associated and IBC-associated genes for SCLC patients. SCLC is a highly aggressive cancer subtype that is known to form tumor emboli and metastasize quickly, predominately *via* clusters of CTCs (55–57). SCLC patients with fewer than 10 months of disease-free survival posttreatment exhibited a higher CCC for both collective dissemination-associated and IBC-associated gene sets as compared to patients with greater than 10 months of disease-free survival posttreatment as computed from the data in the study by Rousseaux et al. (54), **Figures 6C,D**.

The metastasis of cancer to different organs is characterized by organ-specific bottlenecks (58). While tumor cells from the site of the primary lesion can easily migrate to the local lymph nodes by moving passively with the lymph flow, migration to other organs such as skin or liver is much more challenging. Given the benefits afforded to migrating cancer cells by collective dissemination, cells with a more hierarchical expression of collective dissemination-associated genes are likely to be over-represented in cancer metastases to distant organs as compared to metastases to local lymph nodes. Using the gene expression data from the study by Kimbung et al. (59), we calculated the CCC of collective disseminated-associated genes in samples from breast cancer metastases to different organs and observed a higher CCC for metastases to skin as compared to metastases to lymph nodes and liver, **Figure 7A**. A similar trend was observed on calculating the CCC of the IBC-associated gene network, **Figure 7B**.

We further explored whether the CCCs for the collective dissemination-associated gene network and the IBC-associated gene network were different in breast cancer patients with metastatic relapse within 5 years posttreatment and those with no metastasis during this follow-up period as computed from the data in the study by Wang et al. (53). Intriguingly, we observed that the CCCs of both networks were significantly higher, p-value = 0.03 in each case, for patients with no metastasis during the 5-year follow-up period as compared to the patients with metastatic relapse during the follow-up, **Figures 8A,B**. A similar trend was observed for breast tumor samples from The Cancer Genome Atlas (TCGA) for patients who exhibited relapse during the follow-up period and those who did not (60), **Figures 8C,D**. Given that healthy breast cells are inherently epithelial, a higher CCC for the patient

FIGURE 5 | Normalized cophenetic correlation coefficient of canonical epithelial-to-mesenchymal transition driving transcription factors for tumor samples from inflammatory breast cancer (IBC) patients and non-IBC breast cancer patients for data from studies by **(A)** Iwamoto et al. (45) with 25 IBC and 57 non-IBC breast cancer patients, **(B)** Boersma et al. (46) with 13 IBC and 35 non-IBC breast cancer patients, and **(C)** Woodward et al. (24) with 20 IBC and 20 non-IBC breast cancer patients. Error bars indicate the SE in the estimate of CCC$_{norm}$ calculated using the bootstrap method. **p-Value < 0.01.
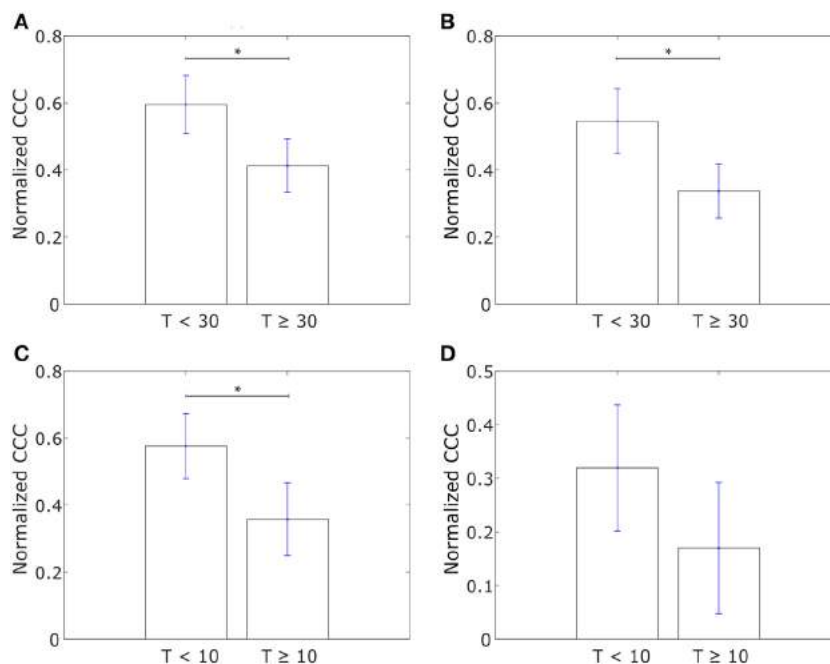
FIGURE 6 | (A) Normalized cophenetic correlation coefficient of the collective dissemination-associated gene network for breast cancer patients with metastatic relapse within a 30-month period posttreatment ($T < 30$; $n = 56$) or between 30 and 60 months posttreatment ($T \geq 30$; $n = 51$). Gene expression data from the study by Wang et al. (53). (B) Normalized CCC of the inflammatory breast cancer-associated gene network for the same groups of breast cancer patients as in (A). (C) Normalized CCC of the collective dissemination-associated gene network for small cell lung cancer (SCLC) patients with less than 10 months of disease-free survival posttreatment ($T < 10$; $n = 11$) and SCLC patients with longer than 10 months of disease-free survival posttreatment but death during the follow-up period ($T \geq 10$; $n = 10$). Gene expression data from the study by Rousseaux et al. (54). (D) Normalized CCC of the IBC-associated gene network for the same SCLC patient groups as in (C). Error bars indicate the SE in the estimate of CCC$_{norm}$ calculated using the bootstrap method. *p-Value < 0.05.

FIGURE 7 | Normalized cophenetic correlation coefficient for tumor samples from breast cancer metastases to skin ($n = 17$), lymph nodes ($n = 39$), and liver ($n = 16$): (A) normalized CCC of the collective dissemination-associated gene network and (B) normalized CCC of the IBC-associated gene network. Gene expression data from the study by Kimbung et al. (59). Error bars indicate the SE in the estimate of CCC$_{norm}$ calculated using the bootstrap method. *p-Value < 0.05.

group with no metastatic relapse during the follow-up period may be a consequence of the tumor being at initial stages of progression toward a metastatic phenotype at the time of diagnosis and sample collection in these patient groups. However, upon grouping the breast cancer patients by their estrogen-receptor status, no consistent trend was observed between patients with no relapse during the follow-up period and patients with metastatic relapse during the follow-up period for both gene sets, Figure S4 in Supplementary Material. These results indicate that the

collective dissemination pathway in breast cancer patients with differing receptor statuses warrants further study.

The CCC Provides Additional Information Regarding the Underlying Complexity of Collective Gene Expression

We next investigated if the insights described above can be obtained from an analysis of expression levels of collective

FIGURE 8 | (A) Normalized cophenetic correlation coefficient of the collective dissemination-associated gene network for tumor samples from 107 breast cancer patients who did not exhibit breast cancer relapse during the follow-up period and for tumor samples from 179 patients who exhibited metastatic relapse during the follow-up period. Gene expression data from the study by Wang et al. (53). **(B)** Normalized CCC of the Inflammatory breast cancer-associated gene network for the same patient groups as in **(A)**. **(C)** Normalized CCC of the collective dissemination-associated gene network for tumor samples from 527 breast cancer patients with no metastasis during the follow-up period and for tumor samples from 13 patients with breast cancer metastasis during the follow-up period. Gene expression data from the cancer genome atlas (TCGA) (60). **(D)** Normalized CCC of the IBC-associated gene network for the same patient groups as in **(C)**. Error bars indicate the SE in the estimate of CCC$_{norm}$ calculated using the bootstrap method. *p-value < 0.05 and **p-value < 0.01.
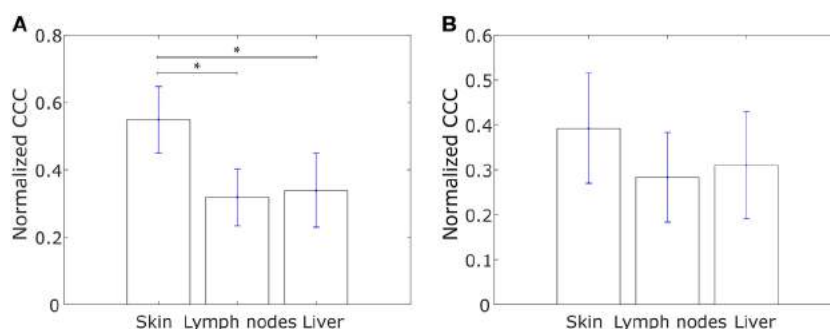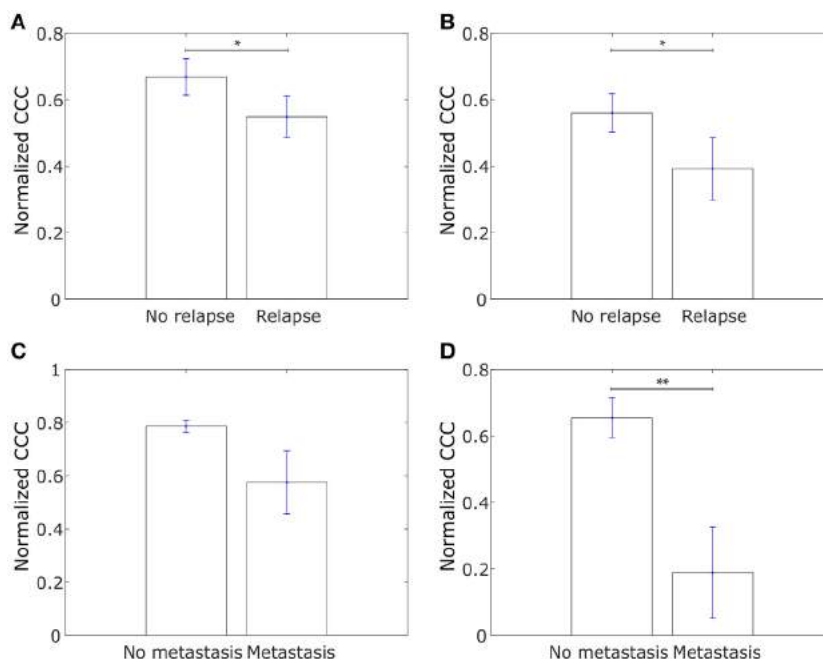
dissemination-associated and IBC-associated genes. To determine how the CCCs of different gene networks correlate with the expression levels of these genes in different phenotypic groups, we carried out gene set enrichment analysis (GSEA) for different sets of genes on the epithelial and mesenchymal cell lines from the study by Grosse-Wilde et al. (39) and on the tumor samples from IBC patients and non-IBC breast cancer patients from the study by Iwamoto et al. (45). Using the GSEA software provided by the Broad Institute (61), we tested for enrichment in the expression of collective dissemination-associated genes, IBC-associated genes, and the canonical drivers of EMT in different phenotypic groups, i.e., epithelial versus mesenchymal cell lines in the data from Grosse-Wilde et al. (39) and IBC versus non-IBC patients in the data from Iwamoto et al. (45). The results are shown in **Figures 9A–F**. The expression of collective dissemination-associated genes was significantly enriched in epithelial cell lines as compared to mesenchymal cell lines (p-value < 0.001), **Figure 9A**, while IBC-associated genes and canonical EMT drivers did not show any such significant enrichment when compared across these two phenotypic groups. On the other hand, expression of IBC-associated genes was significantly enriched in tumor samples from IBC patients (p-value = 0.035), **Figure 9E**, while the collective dissemination-associated genes and canonical EMT drivers did not show significant enrichment on comparing IBC tumor samples with non-IBC breast tumor samples. We further divided the set of collective dissemination-associated genes into

two groups, genes with enriched expression levels in K14+ cells and genes with depleted expression levels in K14+ cells. Neither of these two subsets exhibited significant enrichment when carrying out IBC tumor samples versus non-IBC breast tumor samples GSEA, Figure S5 in Supplementary Material.

Previous studies have suggested a strong association between expression of the E-cadherin protein in tumor cells and IBC (62, 63). To investigate if the level of *CDH1* (E-cadherin) gene expression in tumor samples from breast cancer patients is also associated with IBC, we compared the levels of *CDH1* gene expression in tumor samples from IBC and non-IBC patients. There was no significant difference in the expression levels of *CDH1* gene between the two patient groups in any of the three breast cancer patient datasets, Iwamoto et al. (45), Boersma et al. (46), and Woodward et al. (24), **Figures 9G–I**.

Finally, to test the specificity of the collective dissemination-associated and IBC-associated gene sets in characterizing IBC behavior, we generated 100 random gene sets. Each gene set consisted of 83 genes, average of the sizes of the collective dissemination-associated and IBC-associated gene sets. We calculated the normalized CCC of these gene sets in tumor samples from IBC and non-IBC breast cancer patients from the study by Iwamoto et al. (45). Only for 2 of the 100 randomly generated gene sets, the CCC was significantly higher for the IBC group as compared to the non-IBC group (p-value < 0.05), Figure S6 in Supplementary Material. This indicates that our hypothesis of a
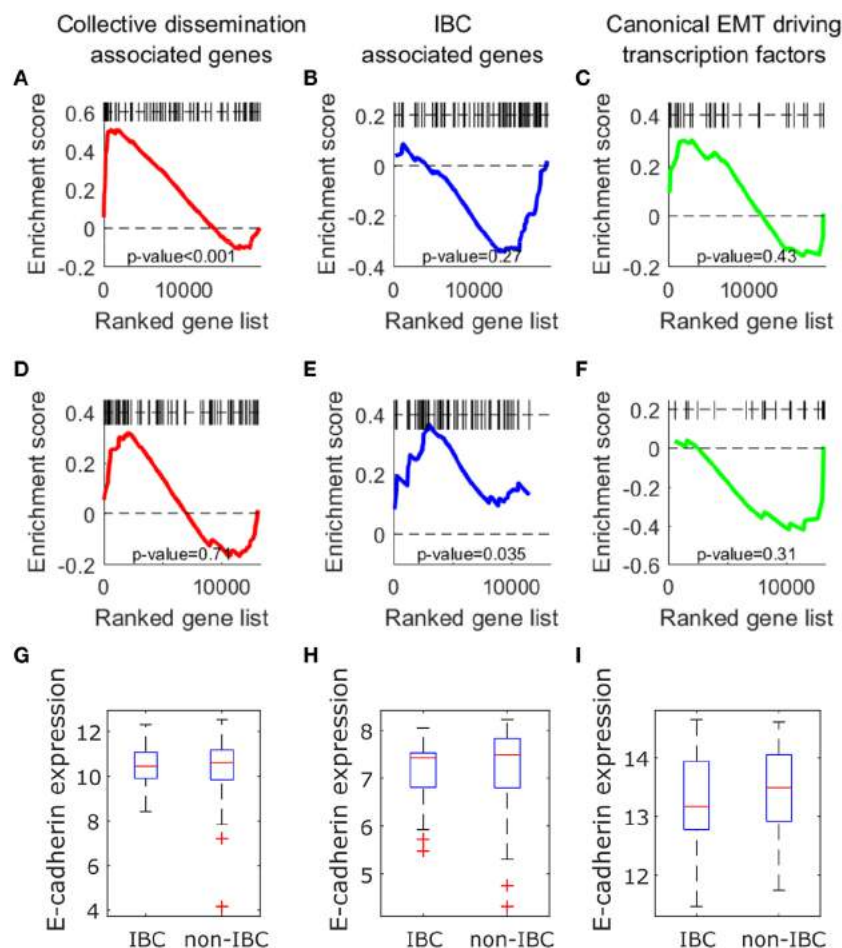
FIGURE 9 | **(A–F)** Gene set enrichment analysis using collective dissemination-associated genes **(A,D)**, inflammatory breast cancer (IBC)-associated genes **(B–E)**, and canonical epithelial-to-mesenchymal transition driving transcription factors **(C–F)** on: **(A–C)** gene expression data for epithelial and mesenchymal cell lines from the study by Grosse-Wilde et al. (39) and on **(D–F)** gene expression data for tumor samples from IBC and non-IBC breast cancer patients from the study by Iwamoto et al. (45). In **(A–C)**, genes are ordered from left to right in decreasing order of correlation of expression with the epithelial phenotype. In **(D–F)**, genes are ordered from left to right in decreasing order of correlation of expression with the IBC phenotype. Black bars along the top of each plot indicate the positions of hits to the gene set along the ordered list of genes. Nominal *p*-values of enrichment are indicated at the bottom of each plot. **(G–I)** Mean expression of *CDH1* (E-cadherin) gene in tumor samples from IBC and non-IBC breast cancer patients in studies by **(G)** Iwamoto et al. (45), **(H)** Boersma et al. (46), and **(I)** Woodward et al. (24).

more hierarchically organized gene expression in IBC samples as compared to non-IBC breast cancer samples is specific to collective dissemination-associated and IBC-associated gene sets and is not applicable to randomly chosen sets of genes.

DISCUSSION

Cancer metastasis *via* migrating clusters of CTCs has emerged as a critical mechanism of seeding secondary tumors in recent studies (9–12). Although rare in comparison with individually disseminated cancer cells, CTC clusters can efficiently seed secondary tumors at distant organ sites (11, 12), and their presence in the bloodstream of cancer patients has been shown to be associated with poor disease prognosis, i.e., worse overall survival and worse disease-free survival (11). Understanding the molecular mechanisms underlying collective dissemination of tumor cells is, therefore, important for predicting metastasis,

which remains the principal cause of cancer-associated mortalities. Determinants of single cell versus collective dissemination of tumor cells, however, remain elusive. Here, we have analyzed the topology of the network of genes implicated in the collective dissemination of tumor cells. We also investigated the topology of the network of genes reported to be differentially expressed in tumor samples from IBC patients as compared to tumor samples from non-IBC breast cancer patients. Taken together, our analysis suggests that maintenance of the epithelial phenotype in cancer cells disseminating from the primary tumor contributes toward metastasis *via* collective migration of tumor cells as CTC clusters.

Results suggest that the expression of genes differentially expressed in tumor cells migrating as clusters as compared to individually migrating tumor cells (12) exhibits a more hierarchical organization in epithelial cell lines as compared to mesenchymal cell lines among both, immortalized breast cancer cell lines (39) and the cancer cell lines in the NCI60 panel (41, 42).

The importance of expression of such genes involved in cell migration, cell–extracellular matrix interaction, and cell–cell adhesion in the classification of NCI60 cell lines has been observed previously (64). Retention of some epithelial characteristics by cancer cells disseminating from the primary tumor has been reported to contribute toward collective invasion by tumor cells as CTC clusters (12, 65, 66). A more hierarchical organization in the expression of these genes may contribute toward a more robust epithelial phenotype in these cell lines (28–31). Higher hierarchical organization in the expression of these genes is also observed in tumor samples from IBC patients as compared to tumor samples from non-IBC breast cancer patients. This difference may contribute toward the strengthened presentation of epithelial characteristics such as cell–cell adhesion and juxtracrine signaling in tumor cells from IBC patients. The retention of these characteristics can foster the collective migration of tumor cells from the primary breast lesion (65). Further, our results reveal that hierarchical expression of collective dissemination-associated genes is of diagnostic relevance in IBC, thereby strengthening the case for IBC as a model system for the study of collective dissemination of tumor cells (22) and indicating the potential usefulness of mechanistic studies of tumor cell dissemination in determining the principles underlying IBC.

Next, we investigated the hierarchical organization in the expression of genes previously reported to be differentially expressed in tumor samples from IBC patients as compared to tumor samples from non-IBC breast cancer patients (38). The expression of these genes was more hierarchically organized in IBC samples as compared to non-IBC samples across multiple independent datasets. Further, epithelial cell lines exhibited a more hierarchical expression of these genes as compared to mesenchymal cell lines among immortalized breast cell lines (39) and among the cell lines in the NCI60 panel composed of nine different tumor types (41, 42). Thus, both collective dissemination-associated and IBC-associated genes exhibited a similar trend of higher CCC in immortalized breast cell lines or cancer cell lines as well as in tumor samples from IBC patients, adding to the existing evidence on collective dissemination *via* tumor emboli as the predominant mode of IBC metastasis and consequent aggressiveness. Intriguingly, the expression of canonical EMT-inducing transcription factors (52) was more hierarchically organized in non-IBC breast cancer samples as compared to IBC samples. Taken together, these results reinforce the notion that a complete EMT is not involved in IBC metastasis. Rather, it is the collective migration of tumor cells that are able to retain some epithelial characteristics that contributes toward the metastatic aggressiveness of IBC. The results presented here further strengthen the emerging notion that a complete EMT followed by MET is not necessarily as prevalent during cancer metastasis (7, 21) as posited earlier (67).

Both collective dissemination-associated and IBC-associated gene sets exhibited a higher CCC in breast cancer patients with faster posttreatment metastatic relapse as compared to patients with slower posttreatment relapse (53). A similar trend was observed in our calculations of the CCC for patients with SCLC (54), another metastatically aggressive cancer reported to metastasize *via* clusters of CTCs (55–57). These results indicate that a more hierarchical organization in the expression of genes involved in the collective dissemination of tumor cells may contribute toward a more aggressive behavior in metastatically aggressive tumors such as IBC and SCLC, which predominantly metastasize *via* clusters of CTCs. A mechanism-based investigation of the cross-talk between collective dissemination-associated and IBC-associated genes may, therefore, be a promising next step.

Further, samples from breast cancer metastases to lymph nodes and liver (59) exhibited a lower CCC as compared to breast cancer metastases to skin for collective dissemination-associated and IBC-associated gene sets (59). While metastasis of tumor cells to distant organs such as the skin is a complex, multi-step, and highly inefficient process, migration of tumor cells from the primary lesion to the local lymph nodes is likely to be a more facile process and can be brought about by the passive flow of the lymph. Metastasis to the liver is facilitated by the extravasation of migrating tumor cells into the liver *via* the fenestrated hepatic vascular epithelium (58). Correlation of the CCC for both gene sets, collective dissemination-associated and IBC-associated, with a higher rate of and propensity for metastasis to distant organs clearly speaks of the survival advantage afforded to migrating tumor cells by collective dissemination as clusters of CTCs. These advantages include enhanced ability to resist anoikis (cell death upon detachment from the substrate), evasion from immune system recognition, potential polyclonality, and enhanced ability to seed secondary tumors (68). In fact, CTC clusters can include non-tumor cells such as immune cells, platelets, and cancer-associated fibroblasts, thereby reproducing the primary tumor microenvironment conditions. Such an environment may contribute toward the survival of disseminating tumor cells in transit, promoting cancer metastasis (69).

A commonly used approach to determine if an *a priori* defined set of genes is associated with phenotypic differences between two groups is GSEA (70, 71). This method involves finding if the given set of genes is over-represented among genes that are differentially expressed in the two phenotypic groups. To determine if insights similar to those described above can be obtained *via* GSEA for the collective dissemination-associated gene set and for the IBC-associated gene set, we used the GSEA software provided by the Broad Institute (61) to calculate enrichment scores for the two gene sets in the data from Grosse-Wilde et al. (39), i.e., epithelial versus mesenchymal cell lines, and in the data from Iwamoto et al. (45), i.e., IBC versus non-IBC breast cancer patients. While we consistently obtained a higher CCC for collective dissemination-associated and IBC-associated gene sets in epithelial cell lines and in tumor samples from IBC patients, the expression of genes in these sets was not always enriched in epithelial versus mesenchymal cell lines or in IBC versus non-IBC patient samples. Together, these results indicate that the CCC need not correlate with GSEA. In fact, the CCC of a set of genes for two samples with a *k*-fold change in the expression of all genes in the set will be the same. The CCC can thus provide insights in addition to those that may be obtained from a direct analysis of gene expression data by using GSEA. The CCC of a gene network can be a robust metric of functional significance of a set of genes in different phenotypic groups, independent of the enrichment score calculated for the given

gene set. It provides a prognostic measure based on the collective expression of genes in cells exhibiting different phenotypes beyond that provided by GSEA.

The classical view of cancer is that it involves de-differentiation of host cell pathways (36, 72). Since IBC is more metastatically aggressive as compared to non-IBC breast cancer, host cell pathways are likely to be more disrupted in tumor samples from IBC patients. This is indeed observed for breast tumor samples from the study by Iwamoto et al. (45). Of the 100 randomly generated gene sets, 41 exhibited a significantly higher CCC in the non-IBC breast cancer group as compared to the IBC group. This indicates that the host cell pathways are disrupted to a greater extent in IBC as compared to non-IBC breast cancer. However, structure in the pathways involving genes that promote cancer progression may be selected for as the disease advances. We previously showed that the expression of adult acute myeloid leukemia-associated genes is more hierarchically organized in samples from patients in whom the disease relapsed during the follow-up period as compared to patients that underwent complete remission upon treatment (37). Similarly, for breast cancer metastasis-associated genes, hierarchical organization was higher in patients who developed distant metastases during the follow-up period as compared to patients who did not (36). Here, we propose that due to the role of maintenance of an epithelial phenotype in collective dissemination of tumor cells and the subsequent metastatic efficiency of CTC clusters, a hierarchical organization in the expression of these genes may be selected for in metastatically aggressive cancers like IBC. A measure of hierarchical organization, here the CCC, can thus be a useful biomarker in cancer prognosis, particularly in the case of IBC.

CONCLUSION

We have shown that a set of genes previously reported to be associated with the collective dissemination of tumor cells (12) is more hierarchically expressed in epithelial cell lines as compared to mesenchymal cell lines, thereby indicating a role for epithelial characteristics in the collective migration of tumor cells as clusters of CTCs. We further showed that IBC, an aggressive breast cancer subtype that metastasizes primarily *via* CTC clusters, exhibits a more hierarchical organization in the expression of these collective dissemination-associated genes as compared to non-IBC type breast cancer. Along similar lines, we showed that for genes differentially expressed in IBC as compared to non-IBC tumor samples, the expression is more hierarchical in tumor samples from IBC patients and in phenotypically epithelial cell lines, suggesting a a role for the retention of some epithelial traits in the metastatically aggressive nature of IBC. Taken together, our work indicates that at least some maintenance of the epithelial phenotype in disseminating tumor cells during disease progression plays a key role in successful metastasis of cancer to distant organs, and that IBC can be a suitable model system for studying mechanisms of collective migration of tumor cells as CTC clusters. Further, we have introduced the CCC as a quantitative metric for analyzing the collective migration of circulating tumor cell clusters, which can be useful in cancer prognosis, particularly in the case of IBC.

AUTHOR CONTRIBUTIONS

ST designed the study, carried out the analysis, and wrote the manuscript. MKJ designed the study, analyzed the results, and wrote the manuscript. WW and HL analyzed the results and edited the manuscript. MD supervised the study, analyzed the results, and edited the manuscript.

FUNDING

SUPPLEMENTARY MATERIAL

The Supplementary Material for this article can be found online at https://www.frontiersin.org/articles/10.3389/fonc.2018.00244/full#supplementary-material.

FIGURE S1 | Representative collective dissemination-associated gene networks for **(A)** epithelial cell lines and **(B)** mesenchymal cell lines from the study by Grosse-Wilde et al. (39), and for **(C)** tumor samples from IBC patients and **(D)** tumor samples from non-IBC breast cancer patients from the study by Iwamoto et al. (45). The nodes are collective dissemination-associated genes and the weights of the edges between different nodes were defined using Eq. 1.

FIGURE S2 | Normalized CCC of different gene sets calculated for different phenotypic groups using the resistance distance (2). Normalized CCC for 13 epithelial (E) and 11 mesenchymal cell lines from the study by Grosse-Wilde et al. (39), calculated using **(A)** collective dissemination-associated genes and **(B)** IBC-associated genes. Normalized CCC for 11 epithelial (E) and 47 epithelial–mesenchymal hybrid (E/M)+ mesenchymal (M) cell lines from the NCI60 dataset (41, 42), calculated using **(C)** collective dissemination-associated genes and **(D)** IBC-associated genes. Normalized CCC for tumor samples from the study by Iwamoto et al. (45) with 25 IBC and 57 non-IBC breast cancer patients, calculated using **(E)** collective dissemination-associated genes and **(F)** IBC-associated genes. Error bars indicate the SE in the estimate of CCC_{norm} calculated using the bootstrap method. *p-Value < 0.05. The trend in CCC values observed here is same as the trend when calculating CCC using the Euclidean commute time distance, **Figures 1**, **2A**, **3**, and **4A**.

FIGURE S3 | Normalized CCC for estrogen-receptor-positive (ER+) breast cancer patients with metastatic relapse within a 30-month period posttreatment ($T < 30$; $n = 36$) or between 30 and 60 months posttreatment ($T \geq 30$; $n = 44$): **(A)** normalized CCC of the collective dissemination-associated gene network and **(B)** normalized CCC of the IBC-associated gene network. Gene expression data from the study by Wang et al. (53). Error bars indicate the SE in the estimate of CCC_{norm} calculated using the bootstrap method. **p-value < 0.01. There were too few estrogen-receptor-negative (ER−) patients in the data set for similar analysis. The trend here is similar to the trend in **Figure 6A**.

FIGURE S4 | Normalized CCC for breast cancer patients with different estrogen-receptor statuses. Patients with estrogen-receptor-positive status: **(A)** normalized CCC of the collective dissemination-associated gene network and **(B)** normalized CCC of the IBC-associated gene network. In this group, there were 129 patients with no relapse during the 5-year follow-up period and 80 patients with metastatic relapse posttreatment during the follow-up period. Patients with estrogen-receptor-negative status: **(C)** normalized CCC of the collective dissemination-associated gene network and **(D)** normalized CCC of the IBC-associated gene network. In this group, there were 50 patients with no relapse during the 5-year follow-up period and 27 patients with metastatic relapse posttreatment during the follow-up period.

Gene expression data from the study by Wang et al. (53). Error bars indicate the SE in the estimate of CCC_{norm} calculated using the bootstrap method. *p-Value < 0.05 and **p-Value < 0.01. In **(C)**, 10,000 bootstrap samples were drawn to calculate the normalized CCCs, obtain the error bars, and estimate the p-value.

FIGURE S5 | Gene set enrichment analysis on gene expression data for tumor samples from IBC and non-IBC breast cancer patients from the study by Iwamoto et al. (45) using **(A)** genes upregulated in cells in circulating tumor cell clusters, and **(B)** genes downregulated in cells in circulating tumor cell clusters. Genes are ordered from left to right in decreasing order of correlation of

expression with the IBC phenotype. Black bars along the top of each plot indicate the positions of hits to the gene set along the ordered list of genes. Nominal p-values of enrichment are indicated at the bottom of each plot.

FIGURE S6 | Histogram of p-values calculated for the null hypothesis that the normalized CCC of a randomly generated gene set is higher in tumor samples from non-IBC breast cancer patients as compared to samples from IBC patients. Gene expression data from the study by Iwamoto et al. (45). Normalized CCC was calculated for 100 randomly generated gene sets consisting of 83 genes each. The red dotted line indicates p-value = 0.05 while the green dotted line indicates p-value = 0.95.

REFERENCES

1. Gupta GP, Massagué J. Cancer metastasis: building a framework. *Cell* (2006) 127:679–95. doi:10.1016/j.cell.2006.11.001

2. Luzzi KJ, MacDonald IC, Schmidt EE, Kerkvliet N, Morris VL, Chambers AF, et al. Multistep nature of metastatic inefficiency: dormancy of solitary cells after successful extravasation and limited survival of early micrometastases. *Am J Pathol* (1998) 153:865–73. doi:10.1016/S0002-9440(10)65628-3

3. Weiss L. Metastatic inefficiency. *Adv Cancer Res* (1990) 54:159–211. doi:10.1016/S0065-230X(08)60811-8

4. Thiery JP, Acloque H, Huang RYJ, Nieto MA. Epithelial-mesenchymal transitions in development and disease. *Cell* (2009) 139:871–90. doi:10.1016/j.cell.2009.11.007

5. Jolly MK, Ward C, Eapen MS, Myers S, Hallgren O, Levine H, et al. Epithelial–mesenchymal transition, a spectrum of states: role in lung development, homeostasis, and disease. *Dev Dyn* (2018) 247:346–58. doi:10.1002/dvdy.24541

6. Nieto MA, Huang RYYJ, Jackson RAA, Thiery JPP. EMT: 2016. *Cell* (2016) 166:21–45. doi:10.1016/j.cell.2016.06.028

7. Jolly MK, Ware KE, Gilja S, Somarelli JA, Levine H. EMT and MET: necessary or permissive for metastasis? *Mol Oncol* (2017) 11:755–69. doi:10.1002/1878-0261.12083

8. Jolly MK, Boareto M, Huang B, Jia D, Lu M, Ben-Jacob E, et al. Implications of the hybrid epithelial/mesenchymal phenotype in metastasis. *Front Oncol* (2015) 5:155. doi:10.3389/fonc.2015.00155

9. Moore GE, Sandberg AA, Watne AL. The comparative size and structure of tumor cells and clumps in the blood, bone marrow, and tumor imprints. *Cancer* (1960) 13:111–7. doi:10.1002/1097-0142(196001/02)13:1<111::AID-CNCR2820130121>3.0.CO;2-Y

10. Liotta LA, Saidel MG, Kleinerman J. The significance of hematogenous tumor cell clumps in the metastatic process. *Cancer Res* (1976) 36:889–94.

11. Aceto N, Bardia A, Miyamoto DT, Donaldson MC, Wittner BS, Spencer JA, et al. Circulating tumor cell clusters are oligoclonal precursors of breast cancer metastasis. *Cell* (2014) 158:1110–22. doi:10.1016/j.cell.2014.07.013

12. Cheung KJ, Padmanaban V, Silvestri V, Schipper K, Cohen JD, Fairchild AN, et al. Polyclonal breast cancer metastases arise from collective dissemination of keratin 14-expressing tumor cell clusters. *Proc Natl Acad Sci U S A* (2016) 113:201508541. doi:10.1073/pnas.1508541113

13. Hou J-M, Krebs MG, Lancashire L, Sloane R, Backen A, Swain RK, et al. Clinical significance and molecular characteristics of circulating tumor cells and circulating tumor microemboli in patients with small-cell lung cancer. *J Clin Oncol* (2012) 30:525–32. doi:10.1200/JCO.2010.33.3716

14. Camley BA, Zimmermann J, Levine H, Rappel W-J. Collective signal processing in cluster chemotaxis: roles of adaptation, amplification, and co-attraction in collective guidance. *PLoS Comput Biol* (2016) 12:e1005008. doi:10.1371/journal.pcbi.1005008

15. Camley BA, Zimmermann J, Levine H, Rappel W-J. Emergent collective chemotaxis without single-cell gradient sensing. *Phys Rev Lett* (2016) 116:98101. doi:10.1103/PhysRevLett.116.098101

16. Tripathi SC, Peters HL, Taguchi A, Katayama H, Wang H, Momin A, et al. Immunoproteasome deficiency is a feature of non-small cell lung cancer with a mesenchymal phenotype and is associated with a poor outcome. *Proc Natl Acad Sci U S A* (2016) 113:E1555–64. doi:10.1073/pnas.1521812113

17. Yu M, Bardia A, Wittner BS, Stott SL, Smas ME, Ting DT, et al. Circulating breast tumor cells exhibit dynamic changes in epithelial and mesenchymal composition. *Science* (2013) 339:580–4. doi:10.1126/science.1228522

18. Neelakantan D, Drasin DJ, Ford HL. Intratumoral heterogeneity: clonal cooperation in epithelial-to-mesenchymal transition and metastasis. *Cell Adh Migr* (2015) 9:265–76. doi:10.4161/19336918.2014.972761

19. Jeevan DS, Cooper JB, Braun A, Murali R, Jhanwar-Uniyal M. Molecular pathways mediating metastases to the brain via epithelial-to-mesenchymal transition: genes, proteins, and functional analysis. *Anticancer Res* (2016) 36:523–32.

20. Andriani F, Bertolini G, Facchinetti F, Baldoli E, Moro M, Casalini P, et al. Conversion to stem-cell state in response to microenvironmental cues is regulated by balance between epithelial and mesenchymal features in lung cancer cells. *Mol Oncol* (2016) 10:253–71. doi:10.1016/j.molonc.2015.10.002

21. Grigore A, Jolly M, Jia D, Farach-Carson M, Levine H. Tumor budding: the name is EMT. Partial EMT. *J Clin Med* (2016) 5:51. doi:10.3390/jcm5050051

22. Jolly MK, Boareto M, Debeb BG, Aceto N, Farach-Carson MC, Woodward WA, et al. Inflammatory breast cancer: a model for investigating cluster-based dissemination. *NPJ Breast Cancer* (2017) 3:21. doi:10.1038/s41523-017-0023-9

23. Dawood S, Merajver SD, Viens P, Vermeulen PB, Swain SM, Buchholz TA, et al. International expert panel on inflammatory breast cancer: consensus statement for standardized diagnosis and treatment. *Ann Oncol* (2011) 22:515–23. doi:10.1093/annonc/mdq345

24. Woodward WA, Krishnamurthy S, Yamauchi H, El-Zein R, Ogura D, Kitadai E, et al. Genomic and expression analysis of microdissected inflammatory breast cancer. *Breast Cancer Res Treat* (2013) 138:761–72. doi:10.1007/s10549-013-2501-6

25. Warren LEG, Guo H, Regan MM, Nakhlis F, Yeh ED, Jacene HA, et al. Inflammatory breast cancer and development of brain metastases: risk factors and outcomes. *Breast Cancer Res Treat* (2015) 151:225–32. doi:10.1007/s10549-015-3381-8

26. Rodriguez FJ, Lewis-Tuffin LJ, Anastasiadis PZ. E-cadherin's dark side: possible role in tumor progression. *Biochim Biophys Acta Rev Cancer* (2012) 1826:23–31. doi:10.1016/j.bbcan.2012.03.002

27. Mu Z, Wang C, Ye Z, Austin L, Civan J, Hyslop T, et al. Prospective assessment of the prognostic value of circulating tumor cells and their clusters in patients with advanced-stage breast cancer. *Breast Cancer Res Treat* (2015) 154:563–71. doi:10.1007/s10549-015-3636-4

28. Lorenz DM, Jeng A, Deem MW. The emergence of modularity in biological systems. *Phys Life Rev* (2011) 8:129–60. doi:10.1016/j.plrev.2011.02.003

29. Sun J, Deem MW. Spontaneous emergence of modularity in a model of evolving individuals. *Phys Rev Lett* (2007) 99:228107. doi:10.1103/PhysRevLett.99.228107

30. Deem MW. Statistical mechanics of modularity and horizontal gene transfer. *Annu Rev Condens Matter Phys* (2013) 4:287–311. doi:10.1146/annurev-conmatphys-030212-184316

31. Gilarranz LJ, Rayfield B, Liñán-Cembrano G, Bascompte J, Gonzalez A. Effects of network modularity on the spread of perturbation impact in experimental metapopulations. *Science* (2017) 357:199–201. doi:10.1126/science.aal4122

32. Vaupel P. Tumor microenvironmental physiology and its implications for radiation oncology. *Semin Radiat Oncol* (2004) 14:198–206. doi:10.1016/j.semradonc.2004.04.008

33. Tadeo I, Álvaro T, Navarro S, Noguera R. Tumor microenvironment heterogeneity: a review of the biology masterpiece, evaluation systems and therapeutic implications. In: Travascio F, editor. *Composition and Function of the Extracellular Matrix in the Human Body*. London, United Kingdom: InTech (2016). 30 p.

34. Quail DF, Joyce JA. Microenvironmental regulation of tumor progression and metastasis. *Nat Med* (2013) 19:1423–37. doi:10.1038/nm.3394

35. Sokal RR, Rohlf FJ. The comparison of dendrograms by objective methods. *Taxon* (1962) 11:33–40. doi:10.2307/1217208

36. Chen M, Deem MW. Hierarchy of gene expression data is predictive of future breast cancer outcome. *Phys Biol* (2013) 10:56006. doi:10.1088/1478-3975/10/5/056006

37. Tripathi S, Deem MW. Hierarchy in gene expression is predictive of risk, progression, and outcome in adult acute myeloid leukemia. *Phys Biol* (2015) 12:16016. doi:10.1088/1478-3975/12/1/016016

38. Van Laere SJ, Ueno NT, Finetti P, Vermeulen P, Lucci A, Robertson FM, et al. Uncovering the molecular secrets of inflammatory breast cancer biology: an integrated analysis of three distinct affymetrix gene expression datasets. *Clin Cancer Res* (2013) 19:4685–96. doi:10.1158/1078-0432.CCR-12-2549

39. Grosse-Wilde A, D'Hérouël AF, McIntosh E, Ertaylan G, Skupin A, Kuestner RE, et al. Stemness of the hybrid epithelial/mesenchymal state in breast cancer and its association with poor survival. *PLoS One* (2015) 10:e0126522. doi:10.1371/journal.pone.0126522

40. Elenbaas B, Spirio L, Koerner F, Fleming MD, Zimonjic DB, Donaher JL, et al. Human breast cancer cells generated by oncogenic transformation of primary mammary epithelial cells. *Genes Dev* (2001) 15:50–65. doi:10.1101/gad.828901

41. Shoemaker RH. The NCI60 human tumour cell line anticancer drug screen. *Nat Rev Cancer* (2006) 6:813–23. doi:10.1038/nrc1951

42. Park SM, Gaur AB, Lengyel E, Peter ME. The miR-200 family determines the epithelial phenotype of cancer cells by targeting the E-cadherin repressors ZEB1 and ZEB2. *Genes Dev* (2008) 22:894–907. doi:10.1101/gad.1640608

43. Reinhold WC, Sunshine M, Liu H, Varma S, Kohn KW, Morris J, et al. CellMiner: a web-based suite of genomic and pharmacologic tools to explore transcript and drug patterns in the NCI-60 cell line set. *Cancer Res* (2012) 72:3499–511. doi:10.1158/0008-5472.CAN-12-1370

44. Shankavaram UT, Varma S, Kane D, Sunshine M, Chary KK, Reinhold WC, et al. CellMiner: a relational database and query tool for the NCI-60 cancer cell lines. *BMC Genomics* (2009) 10:277. doi:10.1186/1471-2164-10-277

45. Iwamoto T, Bianchini G, Qi Y, Cristofanilli M, Lucci A, Woodward WA, et al. Different gene expressions are associated with the different molecular subtypes of inflammatory breast cancer. *Breast Cancer Res Treat* (2011) 125:785–95. doi:10.1007/s10549-010-1280-6

46. Boersma BJ, Reimers M, Yi M, Ludwig JA, Luke BT, Stephens RM, et al. A stromal gene signature associated with inflammatory breast cancer. *Int J Cancer* (2008) 122:1324–32. doi:10.1002/ijc.23237

47. Saerens M, Fouss F, Yen L, Dupont P. The principal components analysis of a graph, and its relationships to spectral clustering. *Mach Learn ECML 2004* (2004) 3201:371–83. doi:10.1007/978-3-540-30115-8_35

48. Barnett S. *Matrices: Methods and Applications.* Oxford, United Kingdom: Clarendon Press (1990).

49. Sokal MA. Statistical method for evaluating systematic relationships. *Univ Kansas Sci Bull* (1958) 28:1409–38.

50. Klein DJ, Randić M. Resistance distance. *J Math Chem* (1993) 12:81–95. doi:10.1007/BF01164627

51. Chernick MR, González-Manteiga W, Crujeiras RM, Barrios EB. Bootstrap methods. In: Lovric M, editor. *International Encyclopedia of Statistical Science.* Berlin, Heidelberg: Springer (2011).

52. Saunders LR, McClay DR. Sub-circuits of a gene regulatory network control a developmental epithelial-mesenchymal transition. *Development* (2014) 141:1503–13. doi:10.1242/dev.101436

53. Wang Y, Klijn JG, Zhang Y, Sieuwerts AM, Look MP, Yang F, et al. Gene-expression profiles to predict distant metastasis of lymph-node-negative primary breast cancer. *Lancet* (2005) 365:671–9. doi:10.1016/S0140-6736(05)70933-8

54. Rousseaux S, Debernardi A, Jacquiau B, Vitte A-L, Vesin A, Nagy-Mignotte H, et al. Ectopic activation of germline and placental genes identifies aggressive metastasis-prone lung cancers. *Sci Transl Med* (2013) 5:186ra66. doi:10.1126/scitranslmed.3005723

55. Klameth L, Rath B, Hochmaier M, Moser D, Redl M, Mungenast F, et al. Small cell lung cancer: model of circulating tumor cell tumorospheres in chemoresistance. *Sci Rep* (2017) 7:5337. doi:10.1038/s41598-017-05562-z

56. Maulik G, Kijima T, Ma PC, Ghosh SK, Lin J, Shapiro GI, et al. Modulation of the c-Met/hepatocyte growth factor pathway in small cell lung cancer. *Clin Cancer Res* (2002) 8:620–7.

57. Kijima T, Maulik G, Ma PC, Tibaldi EV, Turner RE, Rollins B, et al. Regulation of cellular proliferation, cytoskeletal function, and signal transduction through CXCR4 and c-Kit in small cell lung cancer cells. *Cancer Res* (2002) 62:6304–11.

58. Obenauf AC, Massagué J. Surviving at a distance: organ-specific metastasis. *Trends Cancer* (2015) 1:76–91. doi:10.1016/j.trecan.2015.07.009

59. Kimbung S, Kovács A, Bendahl P-O, Malmström P, Fernö M, Hatschek T, et al. Claudin-2 is an independent negative prognostic factor in breast cancer and specifically predicts early liver recurrences. *Mol Oncol* (2014) 8:119–28. doi:10.1016/j.molonc.2013.10.002

60. Koboldt DC, Fulton RS, McLellan MD, Schmidt H, Kalicki-Veizer J, McMichael JF, et al. Comprehensive molecular portraits of human breast tumours. *Nature* (2012) 490:61–70. doi:10.1038/nature11412

61. Subramanian A, Tamayo P, Mootha VK, Mukherjee S, Ebert BL, Gillette MA, et al. Gene set enrichment analysis: a knowledge-based approach for interpreting genome-wide expression profiles. *Proc Natl Acad Sci U S A* (2005) 102:15545–50. doi:10.1073/pnas.0506580102

62. Colpaert CG, Vermeulen PB, Benoy I, Soubry A, Van Roy F, van Beest P, et al. Inflammatory breast cancer shows angiogenesis with high endothelial proliferation rate and strong E-cadherin expression. *Br J Cancer* (2003) 88:718–25. doi:10.1038/sj.bjc.6600807

63. Kleer CG, van Golen KL, Braun T, Merajver SD. Persistent E-cadherin expression in inflammatory breast cancer. *Mod Pathol* (2001) 14:458–64. doi:10.1038/modpathol.3880334

64. Crescenzi M, Giuliani A. The main biological determinants of tumor line taxonomy elucidated by a principal component analysis of microarray data. *FEBS Lett* (2001) 507:114–8. doi:10.1016/S0014-5793(01)02973-8

65. Boareto M, Jolly MK, Goldman A, Pietilä M, Mani SA, Sengupta S, et al. Notch-jagged signalling can give rise to clusters of cells exhibiting a hybrid epithelial/mesenchymal phenotype. *J R Soc Interface* (2016) 13:20151106. doi:10.1098/rsif.2015.1106

66. Zhang Z, Shiratsuchi H, Lin J, Chen G, Reddy RM, Azizi E, et al. Expansion of CTCs from early stage lung cancer patients using a microfluidic co-culture model. *Oncotarget* (2014) 5:12383–97. doi:10.18632/oncotarget.2592

67. Thiery JP. Epithelial–mesenchymal transitions in tumour progression. *Nat Rev Cancer* (2002) 2:442–54. doi:10.1038/nrc822

68. Tabariès S, Dong Z, Annis MG, Omeroglu A, Pepin F, Ouellet V, et al. Claudin-2 is selectively enriched in and promotes the formation of breast cancer liver metastases through engagement of integrin complexes. *Oncogene* (2011) 30:1318–28. doi:10.1038/onc.2010.518

69. Hong Y, Fang F, Zhang Q. Circulating tumor cell clusters: what we know and what we expect (review). *Int J Oncol* (2016) 49:2206–16. doi:10.3892/ijo.2016.3747

70. Mootha VK, Lindgren CM, Eriksson K-F, Subramanian A, Sihag S, Lehar J, et al. PGC-1α-responsive genes involved in oxidative phosphorylation are coordinately downregulated in human diabetes. *Nat Genet* (2003) 34:267–73. doi:10.1038/ng1180

71. Hung J-H, Yang T-H, Hu Z, Weng Z, DeLisi C. Gene set enrichment analysis: performance evaluation and usage guidelines. *Brief Bioinform* (2012) 13:281–91. doi:10.1093/bib/bbr049

72. Alberts B, Johnson A, Lewis J, Raff M, Roberts K, Walter P, et al. Cancer. *Molecular Biology of the Cell.* 5th ed. New York: Garland Science (2008).

Functional Assay of Cancer Cell Invasion Potential Based on Mechanotransduction of Focused Ultrasound

Andrew C. Weitz[1,2,3,4†], Nan Sook Lee[1,3†], Chi Woo Yoon[1], Adrineh Bonyad[3], Kyo Suk Goo[1], Seaok Kim[1], Sunho Moon[1], Hayong Jung[1], Qifa Zhou[1,4], Robert H. Chow[3*] and K. Kirk Shung[1*]

[1] Ultrasonic Transducer Resource Center, University of Southern California, Los Angeles, CA, United States, [2] Institute for Biomedical Therapeutics, University of Southern California, Los Angeles, CA, United States, [3] Zilkha Neurogenetic Institute, University of Southern California, Los Angeles, CA, United States, [4] USC Roski Eye Institute, University of Southern California, Los Angeles, CA, United States

Cancer cells undergo a number of biophysical changes as they transform from an indolent to an aggressive state. These changes, which include altered mechanical and electrical properties, can reveal important diagnostic information about disease status. Here, we introduce a high-throughput, functional technique for assessing cancer cell invasion potential, which works by probing for the mechanically excitable phenotype exhibited by invasive cancer cells. Cells are labeled with fluorescent calcium dye and imaged during stimulation with low-intensity focused ultrasound, a non-contact mechanical stimulus. We show that cells located at the focus of the stimulus exhibit calcium elevation for invasive prostate (PC-3 and DU-145) and bladder (T24/83) cancer cell lines, but not for non-invasive cell lines (BPH-1, PNT1A, and RT112/84). In invasive cells, ultrasound stimulation initiates a calcium wave that propagates from the cells at the transducer focus to other cells, over distances greater than 1 mm. We demonstrate that this wave is mediated by extracellular signaling molecules and can be abolished through inhibition of transient receptor potential channels and inositol trisphosphate receptors, implicating these proteins in the mechanotransduction process. If validated clinically, our technology could provide a means to assess tumor invasion potential in cytology specimens, which is not currently possible. It may therefore have applications in diseases such as bladder cancer, where cytologic diagnosis of tumor invasion could improve clinical decision-making.

Keywords: cancer invasion, focused ultrasound, calcium imaging, bladder cancer, prostate cancer

INTRODUCTION

Cancer staging determines both patient prognosis and treatment protocol. To stage a biopsied tumor, the pathologist must determine the extent to which the tumor has invaded the surrounding tissue. In many instances, however, the intact tissue needed to assess invasion cannot be obtained from the patient. In such cases, fine-needle aspirations, washings, or brushings can be performed to collect cells from the tumor for cytologic diagnosis. These cells allow the cytopathologist to

determine whether the tumor is benign or malignant, but not whether it is invasive.

The inability to assess invasion can have devastating consequences, for example in the case of bladder cancer. Bladder tumors that have begun to invade the muscle wall must be treated promptly with cystectomy (surgical removal of the bladder), or they may become life-threatening (1). Carcinoma *in situ* (CIS) is an early form of bladder cancer that is considered high grade, as these tumors frequently recur as muscle-invasive disease (2). CIS is normally treated with bacillus Calmette–Guérin (BCG) immunotherapy upon initial diagnosis and recurrence (3). However, BCG inflames the bladder epithelium, making it difficult endoscopically to identify recurrent tumors for biopsy (4). In such cases, bladder wash cytology can be used to detect recurrence, but the invasion status of the recurrent malignancy cannot be determined. The inability to detect invasion precludes the use of preventative cystectomy, which can have fatal consequences if the cancer is indeed invasive. Thus, a method for assessing tumor invasion cytologically (e.g., in bladder washings) would enable appropriate and timely treatments that improve patient outcomes.

Classical cytology relies on examining cell morphology to identify the presence and appearance of malignant cells. Biophysical properties of tumor cells could reveal information about their malignant status that might escape detection in morphological studies. Recent work has revealed a number of biophysical changes that occur during cancer transformation and progression (5). For example, metastatic cells often express voltage-gated ion channels, including the Na$^+$ (6), K$^+$ (7), and Ca^{2+} (8) types, rendering them electrically excitable. Similarly, mechanical properties of metastatic cancer cells differ from those of benign cells; metastatic cells are generally "softer" (9). Because these biophysical changes can serve as diagnostic markers, assays to measure biophysical properties of tumor cells have been proposed and are under development (9–11). These assays are typically intended to differentiate malignant from non-malignant cells in suspension, thus providing information similar to that obtained *via* standard cytological analysis.

Here, we present a new biophysical cancer assay that, to our knowledge, is the first that can assess the invasion potential of isolated tumor cells. The assay leverages the fact that cancer progression is accompanied by remodeling of calcium channels (8, 12, 13) and cellular mechanosensors (14). The assay applies a non-contact, mechanical stimulus—low-intensity focused ultrasound—to probe for presence of these proteins while monitoring their activity *via* calcium imaging. The stimulus elicits marked calcium elevations in invasive cancer cells, but not in non-invasive cells. We previously validated this assay in four breast cancer cell lines and demonstrated its effectiveness in quantifying invasion potential (15). However, analysis was limited to single cells, making the assay impractical for a clinical setting.

In the present study, we show that our assay can be used for high-throughput, functional analysis of cancer invasion in cell populations. A single ultrasound stimulus is applied while monitoring calcium activity in hundreds or thousands of cells simultaneously. We validate the technique in prostate and bladder cancer cell lines while exploring the role of different stimulus parameters. We also investigate the mechanism by which ultrasound elicits calcium elevations in invasive cells. If validated through further testing, this technology may lend itself to cytological assessment of tumor invasion, thus having important implications for diagnosis and management of diseases such as bladder cancer.

MATERIALS AND METHODS

Cell Lines

Six human cancer cell lines were used in this study: four prostate cancer lines (PC-3, DU-145, BPH-1, and PNT1A) and two bladder cancer lines (T24/83 and RT112/84). PC-3 cells were obtained from Frank Markland (University of Southern California), DU-145 and PNT1A from Mitchell Gross (University of Southern California), BPH-1 from Simon Hayward (NorthShore University HealthSystem), and T24/83 and RT112/84 from Sigma. PC-3 and DU-145 cells were cultured in DMEM, PNT1A, and BPH-1 cells in RPMI-1640, T24/83 cells in McCoy's 5A medium, and RT112/84 cells in EMEM. All medium was supplemented with 10% FBS and 2 mM L-glutamine, and RT112/84 medium was additionally supplemented with 1% non-essential amino acids. All cell lines were tested to be free of mycoplasma contamination using a mycoplasma PCR detection kit (Sigma). Cell authentication of all lines was performed with Promega's PowerPlex 16 System within 6 months of use.

PC-3, DU-145, and T24/83 are highly invasive cell lines, while BPH-1, PNT1A, and RT112/84 are weakly invasive (16–19). We confirmed the invasion status of each cell line with Matrigel Boyden chamber assays (20). Invasion potential was measured in BioCoat Matrigel Invasion Chambers (Corning), as described in our previous study (15). In brief, cells ($1–1.5 \times 10^5$) were added to chambers and incubated for 1–2 days at 37°C. Non-invasive cells at the top of the chamber were removed by a cotton swab, and invasive cells that had passed through the Matrigel were stained with 0.2% crystal violet in 10% ethanol. Three independent fields of invasive cells per well were photographed under a microscope.

Preliminary results showed that BPH-1 cells exhibited variable levels of invasiveness over time, as measured by the Matrigel assay (Figure S1 in Supplementary Material) and our ultrasound assay (data not shown). In order to obtain a weakly invasive, homogeneous cell population, BPH-1 cells that passed through the Boyden chamber were removed after 24 h, and cells that did not pass through were selected and propagated. All BPH-1 experiments were performed with the selected cells, which were confirmed to be weakly invasive (see **Figures 2** and **3**). Experiments in the other five cell lines did not require selection, as these lines exhibited consistent levels of invasiveness over time.

Cell Preparation

Cells were plated on 35-mm polystyrene culture dishes to a density of 10^6 cells per dish. In one experiment, the substrate

was coated with Cell-Tak Cell and Tissue Adhesive (Corning) to facilitate immediate cell adhesion. In another experiment, the culture dish substrate was replaced with an acoustically transparent, 50-µm-thick Mylar film (#48-2F-36; CS Hyde Company) to minimize reflection at the surface and eliminate ultrasonic surface waves. All cells were stained with cell-membrane permeant Fluo-4 AM (Thermo Fisher Scientific), a fluorescent reporter of intracellular calcium activity. Staining was performed by incubating dishes with 1 µM Fluo-4 AM for 30–60 min immediately prior to imaging. Following calcium dye loading, cells were washed with and maintained in external buffer solution consisting of 140 mM NaCl, 2.8 mM KCl, 1 mM $MgCl_2$, 2 mM $CaCl_2$, 10 mM HEPES, and 10 mM D-glucose, adjusted to pH 7.3 and 300 mOsm.

Ultrasound Transducers

Single-element, lithium niobate ($LiNbO_3$), press-focused transducers were fabricated in house as described previously (21). A transducer with a center frequency of 38 MHz (f-number = 2, focal length = 8 mm) was used in most experiments (**Figure 1A**); a 3-MHz transducer (f-number = 2, focal length = 6 mm) was also tested. To drive the transducers, sinusoidal bursts from a signal generator (SG382; Stanford Research Systems) were fed to a 50-dB power amplifier (525LA; Electronics & Innovation) whose output was used to excite the transducer. Unless specified otherwise, amplitude was fixed at 16 V_{p-p}, pulse repetition frequency (PRF) at 1 kHz, and duty cycle at 5% (**Figure 1C**).

The acoustic output of the 38-MHz transducer was measured with a needle hydrophone (HGL-0085; Onda). **Figure 1B** shows the two-dimensional intensity beam profile, indicating that the diameter of the ultrasound focus is approximately 150 µm. Using the standard cell stimulation parameters provided above

FIGURE 1 | Cancer cells were stimulated with single-element, $LiNbO_3$, press-focused transducers. **(A)** Photograph of the 38-MHz transducer used in most experiments. **(B)** Two-dimensional beam profile of I_{spta} at the ultrasound focus, as measured by a hydrophone. **(C)** Typical voltage waveform used to drive the transducer. Carrier frequency is 38 MHz, amplitude is 16 V_{p-p}, pulse repetition frequency is 1 kHz, and duty cycle is 5%.

(16 V_{p-p} amplitude, 1 kHz PRF, and 5% duty cycle), the intensity and pressure at the focus were measured by the hydrophone to be 353 mW/cm² spatial-peak temporal-average intensity (I_{spta}), 7.0 W/cm² spatial-peak pulse-average intensity (I_{sppa}), and 394 kPa peak pressure. The mechanical index was measured to be 0.02. These values are below the FDA safety limit for diagnostic ultrasound (22).

Ultrasound Stimulation and Fluorescence Imaging

A custom microscope system was used to image cellular fluorescence while performing simultaneous ultrasonic stimulation (15). Petri dishes containing cells were placed on an inverted epifluorescence microscope (Olympus IX70), and the ultrasound transducer was lowered into the external buffer solution. A motorized three-axis micromanipulator was used to position the transducer in focus with the cell monolayer.

In each experiment, live-cell fluorescence imaging was performed for 300 s, with the ultrasound stimulus being delivered continuously between t = 50 and 200 s. Excitation light was provided by a mercury arc lamp and filtered through an excitation bandpass filter (488 ± 20 nm). Fluorescence emitted from the calcium dye was filtered through an emission bandpass filter (530 ± 20 nm) and recorded at 1 Hz (30% exposure duty cycle) with a digital CMOS camera (ORCA-Flash2.8; Hamamatsu). All imaging was performed at 4× magnification in order to capture activity from hundreds or thousands of cells simultaneously. For each cell line, simulation and imaging experiments were replicated in at least two different dishes of cells, and over least three independent fields of view per dish. (Experiments involving pharmacological blockers were limited to a single field of view per dish.) Figures show representative data obtained from one field of view.

Data Processing

Data were post-processed to determine the calcium response of every imaged cell. Cell locations were identified automatically with CellProfiler image analysis software (23) and used to extract the raw fluorescence intensities of each cell. These intensities were exported to MATLAB (MathWorks) in order to calculate each cell's normalized change in fluorescence ($\Delta F/F$) during every imaging frame. Responding cells were defined as those that exhibited a $\Delta F/F_{max}$ greater than 3.5 times the pre-stimulus root-mean-square noise level.

Two types of plots were generated for each 300-s experiment: a histogram showing the percentage of responding cells over time and a scatter plot indicating the time at which each cell first responded to the stimulus. Responding cells in these plots were arranged with respect to their distance from the transducer focus.

Pharmacology

To investigate the mechanism of ultrasound-induced calcium rise in invasive cancer cells, PC-3 and T24/83 cells were stimulated in the presence of various pharmacological agents. We tested five different blockers, each applied separately (**Table 1**). Blockers were dissolved in the external buffer solution 15–30 min before
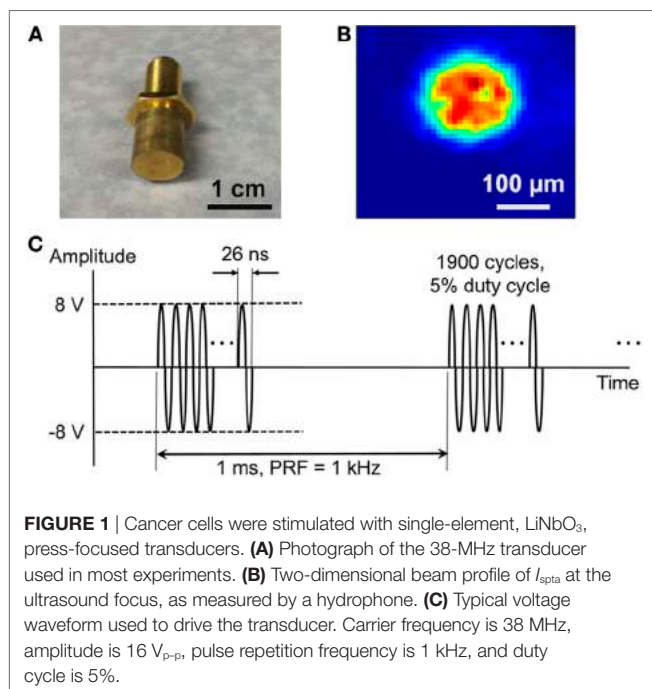
Agent	Effect	Concentration (μM)	Loading time (min)	Reference
2-aminoethoxydiphenyl borate (2-APB)	Transient receptor potential channel blocker; IP_3 receptor antagonist	100	15	(24, 25)
Cadmium chloride ($CdCl_2$)	Voltage-gated Ca^{2+} channel blocker	20	15	(26)
Gadolinium (III) chloride ($GdCl_3$)	Stretch-activated Ca^{2+} channel blocker	10	30	(27)
Iberiotoxin	BK_{Ca} channel blocker	0.1	15	(28)
Streptomycin	Stretch-activated Ca^{2+} channel blocker	200	30	(27)

performing imaging and ultrasound stimulation. Cellular responses were measured before adding the blockers, in the presence of blockers, and after washout.

RESULTS

Matrigel Boyden Chamber Assays

The Matrigel Boyden chamber assay (20) is the standard technique for assessing cancer cell invasion potential in the laboratory setting. We used this assay to measure the invasion potential of four prostate cancer cell lines (PC-3, DU-145, BPH-1, and PNT1A) and two bladder cancer cell lines (T24/83 and RT112/84) with varying levels of invasiveness. As expected, PC-3, DU-145, and T24/83 cells exhibited strong Matrigel invasion, while BPH-1, PNT1A, and RT112/84 cells did not (**Figure 2**; also see Figure S1 in Supplementary Material) (16–19).

Despite the simplicity of the Matrigel Boyden chamber assay, it is not suitable for clinical applications. The assay requires at least 10–25 thousand cells, necessitating time-consuming establishment of cell cultures from tumor biopsies (29, 30), which is not always possible. Furthermore, the Matrigel assay is relatively slow, taking at least 24 h to complete. Our mechanotransduction assay overcomes these limitations, as it can be completed in a matter of minutes and does not require large numbers of cells.

Calcium Responses to Ultrasound Stimulation Differ between Strongly and Weakly Invasive Prostate Cancer Cells

To investigate the use of mechanotransduction for determining the invasion potential of tumor cell populations, we imaged calcium activity of PC-3, DU-145, BPH-1, and PNT1A prostate cancer cells during stimulation with 38-MHz low-intensity focused ultrasound. The stimulus consistently evoked strong calcium responses in highly invasive PC-3 and DU-145 cells, but not in weakly invasive BPH-1 and PNT1A cells (**Figure 3**; Videos S1–S4 in Supplementary Material). In most cases, PC-3 and DU-145 stimulation evoked an intercellular calcium wave that emanated from the transducer focus and spread at a speed of ~50–100 μm/s. The wave began 5–25 s after stimulation onset and persisted for 1–2.5 min. Despite the acoustic focus being localized to an area approximately 150 μm in diameter (see **Figure 1B**), the calcium wave propagated over distances greater than 1 mm. Most cells that responded to ultrasound stimulation exhibited a single calcium transient, though double transients and calcium oscillations were also observed (**Figure 3B**).
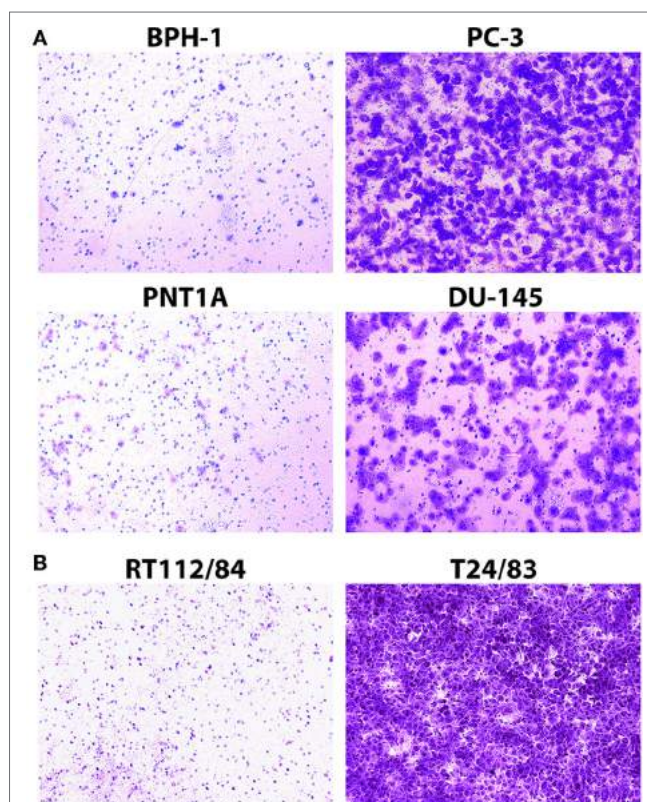
FIGURE 2 | Assessment of prostate cancer **(A)** and bladder cancer **(B)** cell line invasion potential with Matrigel Boyden chamber assays. Cells that passed through the Matrigel barrier were stained with crystal violet. Results indicate that PC-3, DU-145, and T24/83 cells are highly invasive, while BPH-1, PNT1A, and RT112/84 cells are not. **(A)** Photomicrographs showing assay results for BPH-1, PNT1A, PC-3, and DU-145 prostate cancer cells. **(B)** Photomicrographs showing assay results for RT112/84 and T24/83 bladder cancer cells. One representative image for each cell line is shown.

Calcium Responses of Bladder Cancer Cell Lines Mirror Those of Prostate Cancer Cell Lines

As discussed above, a cytological assay of tumor cell invasion potential could have important implications for bladder cancer diagnosis and management. We therefore investigated whether the mechanotransduction assay could be applied to bladder cancer cells. We stimulated T24/83 (highly invasive) and RT112/84 (weakly invasive) bladder cancer cell lines with 38-MHz ultrasound while performing calcium imaging. As shown in **Figure 4A** and

FIGURE 3 | Measuring prostate cancer cell line invasion potential with our mechanotransduction assay. **(A)** BPH-1 (first column), PNT1A (second column), PC-3 (third column), and DU-145 (fourth column) cells were stimulated with 38-MHz low-intensity focused ultrasound while monitoring their activity with calcium imaging. Top row, baseline (pre-stimulation) fluorescence images of the cells. Red asterisks indicate the center position of the ultrasound focus. Scale bar is 500 μm. Second row, background-subtracted fluorescence images revealing all the cells that responded to the ultrasound stimulus (also see Videos S1–S4 in Supplementary Material). Only the PC-3 and DU-145 cells responded strongly, indicating that they are invasive. Third row, two-dimensional histograms showing the percentage of responding cells over time with respect to their distance from the transducer focus. Dotted green and red lines indicate stimulus onset and offset times, respectively. Bottom row, scatter plots showing the time at which each cell first responded to the stimulus (each dot represents a cell). The yellow shaded area indicates the times during which ultrasound was applied. Fitted blue lines indicate the speed of the calcium wave (77 μm/s in PC-3; 106 μm/s in DU-145). The histogram and scatter plots provide an intuitive means to visualize responses of the cell populations over time, making it easy to distinguish responding (invasive) cells from non-responding (non-invasive or weakly invasive) ones. **(B)** Fluorescence responses of three PC-3 cells showing the different types of calcium transients: single (left), double (middle), and oscillating (right).

Videos S5 and S6 in Supplementary Material, the stimulus evoked a calcium wave in T24/83 cells, but no responses were observed in RT112/84 cells. The pattern and timing of T24/83 responses were similar to those of PC-3 prostate cancer cells (see **Figure 3**).

Varying Stimulus Amplitude

We hypothesized that there was an acoustic activation threshold (i.e., intensity) below which invasive cancer cells would not

exhibit calcium responses to ultrasound stimulation. To test for such a threshold, we stimulated T24/83 cells at amplitudes lower than 16 V_{p-p} (the voltage used in all prior experiments; **Figure 5A**). The smallest amplitude we tested, 2 V_{p-p}, did not evoke any detectable calcium activity. At 4 V_{p-p}, the stimulus activated just a few cells in the area where the ultrasound was focused. Stimulation at 8 V_{p-p} also elicited responses near the focus, but more cells responded at this amplitude. Increasing the

FIGURE 4 | Measuring bladder cancer cell line invasion potential with our mechanotransduction assay. **(A)** RT112/84 (left column) and T24/83 (right column) cells were stimulated with 38-MHz low-intensity focused ultrasound while monitoring their activity with calcium imaging. Layout of the plots is the same as in **Figure 3A** (see **Figure 3** caption for descriptions). Results indicate that T24/83 cells are highly invasive, while RT112/84 cells are not. The speed of the calcium wave induced in T24/83 cells was 55 µm/s. See also Videos S5 and S6 in Supplementary Material. **(B)** Fluorescence responses of three T24/83 cells showing the different types of calcium transients: single (left), double (middle), and oscillating (right).

FIGURE 5 | Effect of ultrasound stimulus amplitude on bladder cancer cell calcium responses. Standard stimulus parameters (see Materials and Methods) were used while varying the transducer input voltage. All stated voltages represent peak-to-peak amplitude. Values in parentheses indicate the I_{spta} at each voltage, as measured by a hydrophone. **(A)** Histogram and scatter plots from T24/83 cell stimulation. **(B)** Histogram and scatter plots from RT112/84 cell stimulation.

voltage to 16 V_{p-p} evoked hundreds of responses in the form of an intercellular calcium wave.

Given that RT112/84 bladder cancer cells are weakly invasive ([19]), we hypothesized that they might exhibit calcium responses at intensities greater than 16 V_{p-p}. As shown in **Figure 5B**, stimulation at 16 V_{p-p} did not evoke any calcium activity in these cells (the few data points on the histogram and scatter plots are false positives arising from movement of hyperfluorescent debris in the Petri dish; see Video S5 in Supplementary

Material). At 32 V_{p-p}, three cells at the center of the transducer focus responded. At 48 V_{p-p}, 10–15 cells at the focus responded, but there was still no calcium wave. Amplitudes higher than 48 V_{p-p} were not tested, as they likely would have damaged the ultrasound transducer.

These results reveal a dose–response relationship between stimulus amplitude and the strength of the calcium responses. For a given invasion potential, there appears to be an acoustic activation threshold (inflection point of the dose–response curve)

below which no or a few cells respond to ultrasound stimulation. Given the inverse relationship between acoustic activation threshold and invasion potential, it may be possible to quantify the invasion potential of a tumor cell population by measuring its acoustic activation threshold.

Varying Stimulus Frequency

In this study, we have shown that 38-MHz focused ultrasound evokes calcium responses in invasive cancer cells, and we previously reported a similar effect for 200-MHz ultrasound (15). As shown in **Figure 6**, 3-MHz stimulation was also effective in eliciting calcium responses in invasive cells. Stimulating at 3 MHz evoked a calcium wave that propagated at 101 μm/s, similar to the speed of the calcium waves induced by 38-MHz stimulation (~50–100 μm/s; see **Figures 3A** and **4A**). These results suggest that the mechanism of ultrasound-induced calcium rise in invasive cancer cells is at least partly independent of stimulus frequency.

Mechanism of Ultrasound Stimulation

The fact that our assay can be applied to more than one cancer type (prostate and bladder) implies a conserved mechanism by which invasive cancer cells transduce ultrasound stimuli. To elucidate this mechanism, we applied pharmacological blockers of proteins we suspected were involved in the mechanotransduction process. We stimulated PC-3 and T24/83 cells in the presence of five different blockers, each applied separately (**Table 1**). We blocked voltage-gated Ca^{2+} channels, which are known to be mechanosensitive (31), as well as stretch-activated Ca^{2+} channels. We also blocked BK_{Ca} channels, which are stretch activatable (32) and expressed in PC-3 cells (33). Finally, we applied a drug that blocks both transient receptor potential (TRP) channels and inositol trisphosphate (IP_3) receptors. TRP channels are mechanosensitive, permeable to calcium, and exhibit altered expression levels in several types of cancer (13, 34, 35). IP_3 receptors are found on the endoplasmic reticulum and mediate Ca^{2+} release from intracellular stores.

Of the five blockers we tested (**Table 1**), only 2-aminoethoxydiphenyl borate (2-APB) had an effect on the calcium responses. Application of 2-APB abolished all ultrasound-induced calcium activity, an effect that was partially reversed upon washout of the drug (**Figure 7**). This indicates that TRP channels and/or IP_3 receptors are involved in mediating invasive cancer cell responses to ultrasound stimulation (see Discussion).

Mechanism of the Calcium Waves

Intercellular calcium waves are common biological phenomena that occur in many cell types. They play a role in a variety of cellular activities including migration and mechanotransduction (36). Calcium waves typically occur *via* transmission of an intracellular messenger such as IP_3 through gap junctions (37), or by release of an extracellular messenger such as adenosine
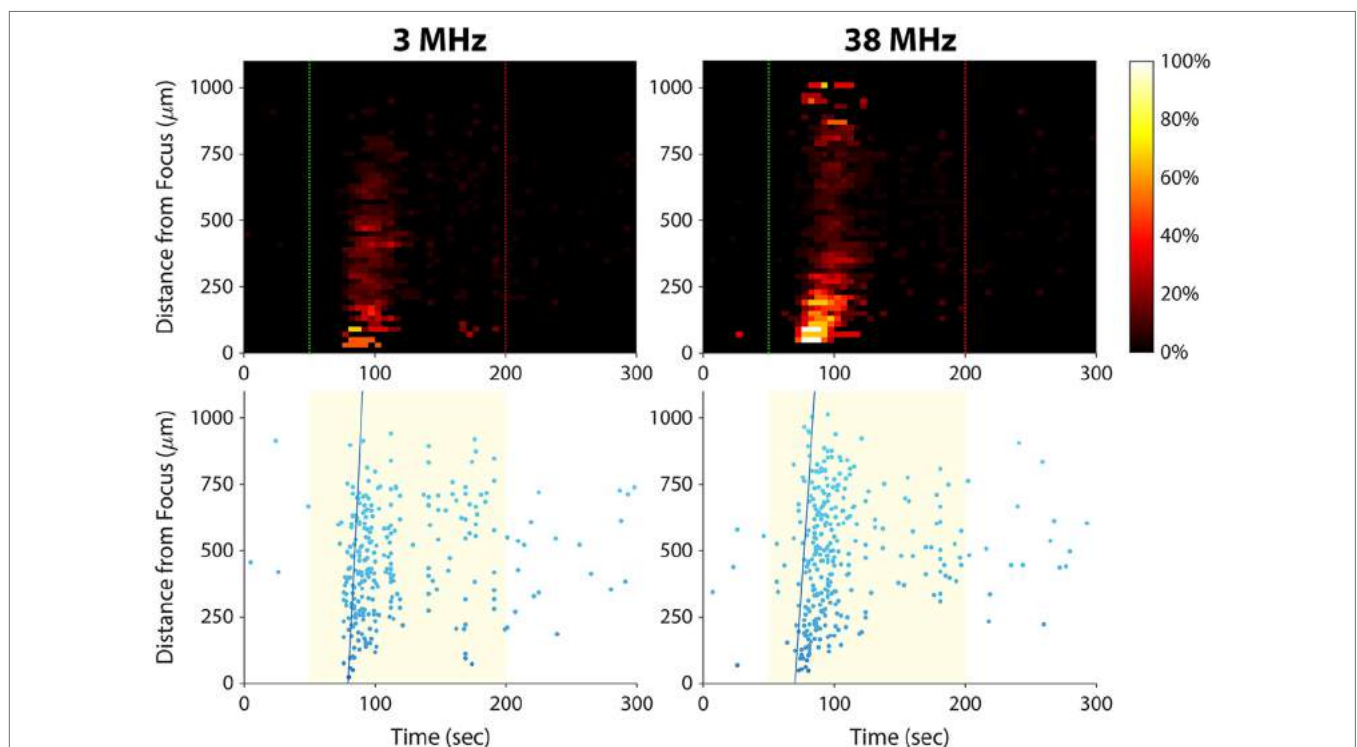
FIGURE 6 | Effect of ultrasound stimulus frequency on prostate cancer cell calcium responses. The same set of PC-3 cells (same imaging field of view) was stimulated with different ultrasound transducers at frequencies of 3 MHz [96 V_{p-p} amplitude, 1 kHz pulse repetition frequency (PRF), 10% duty cycle] and 38 MHz (16 V_{p-p} amplitude, 1 kHz PRF, 5% duty cycle). The speed of the calcium wave induced at each frequency was 101 μm/s at 3 MHz and 73 μm/s at 38 MHz. Slightly fewer cells responded at 3 MHz than at 38 MHz (278 versus 311).

FIGURE 7 | Effect of 2-APB on ultrasound-stimulated calcium responses in PC-3 prostate cancer cells. Left column, the cells exhibited strong calcium responses at baseline, before the drug was applied. Center column, cells were stimulated again 15 min after 2-APB (100 μM) application, and no responses were observed (the few data points on the histogram and scatter plots are false positives arising from movement of hyperfluorescent debris in the Petri dish). Right column, 30 min after 2-APB washout, ultrasound-stimulated calcium responses were partially restored. Results in T24/83 bladder cancer cells were similar.

triphosphate that diffuses to surrounding cells (38). In the case of our experiments, there was a third possibility—that ultrasound energy impinging upon the Petri dish surface was being reflected by the substrate and generating a surface wave that was activating distant cells.

To rule out the possibility of ultrasonic surface wave induced activation, we stimulated PC-3 cells seeded on an acoustically transparent Mylar film, thus minimizing ultrasound reflection by the substrate. As shown in **Figure 8** (left column), the ultrasound stimulus still evoked a calcium wave in these Mylar-seeded cells. This indicates that the wave was likely caused by cell-to-cell signaling, either through gap junctions or *via* release of an extracellular messenger.

To determine whether the calcium wave was propagating through gap junctions, we seeded PC-3 cells on a Petri dish coated with Cell-Tak Cell and Tissue Adhesive, in order to facilitate immediate cell adhesion. We then stimulated the cells within minutes, before they could form gap junctions. The calcium wave was not eliminated under these circumstances (**Figure 8**, center column), ruling out the possibility that it was propagating through gap junctions.

To test whether extracellular signaling molecules were generating the calcium wave, we used a pipette tip to scrape a channel of PC-3 cells off the substrate, leaving two regions of confluent cells separated by a 400-μm gap (**Figure 8**, top right). We then stimulated the cells on one side of the gap with ultrasound. The stimulus evoked a calcium wave that propagated across the gap, eliciting responses in cells on the other side (**Figure 8**, bottom right). These results support the
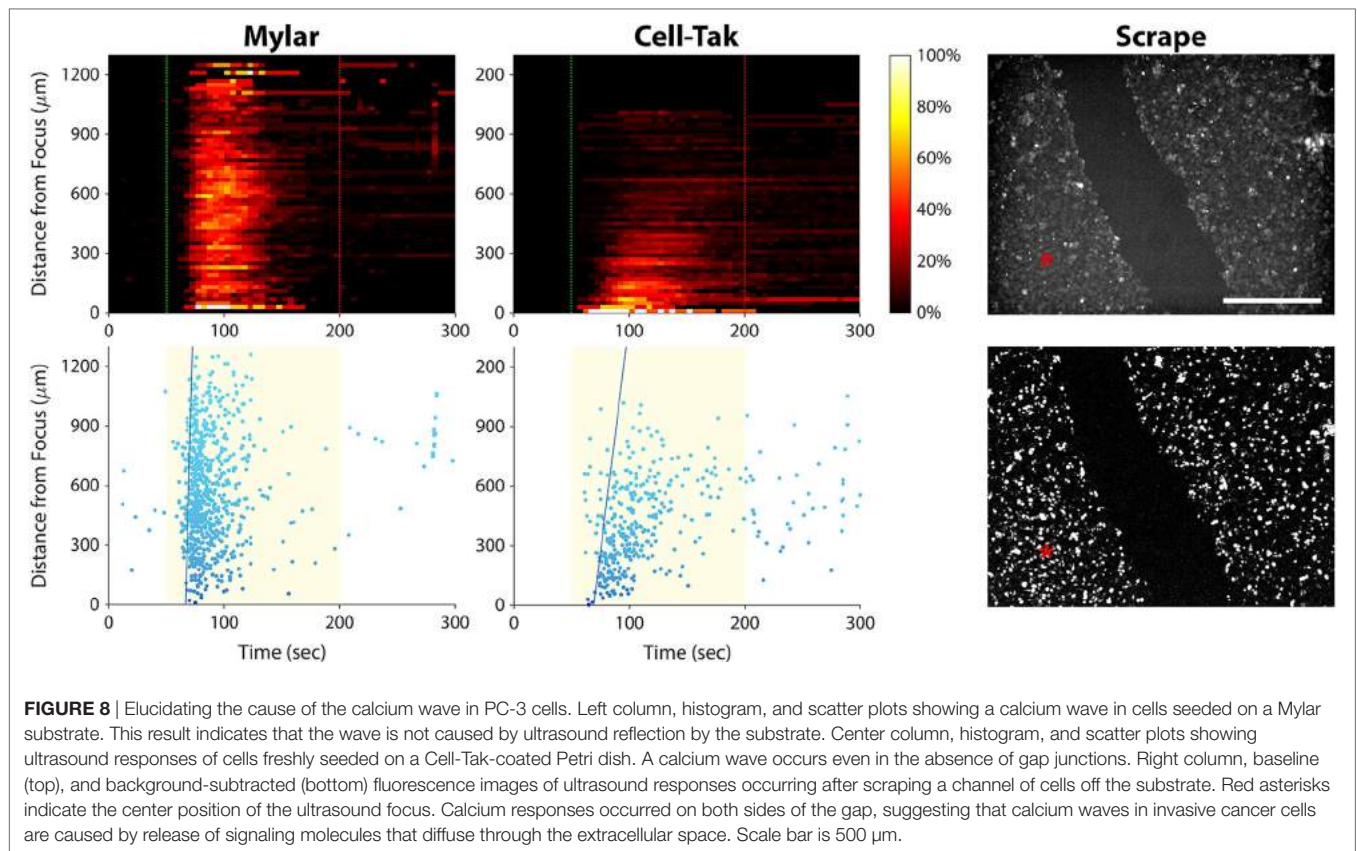
notion that the calcium waves observed in invasive cancer cells are mediated by signaling molecules that diffuse through the extracellular solution.

DISCUSSION

We have demonstrated a new method for assessing the invasion potential of cancer cell populations and have validated the approach in prostate and bladder cancer cell lines. To our knowledge, this is the first technique other than the Matrigel Boyden chamber assay that can assess invasion of isolated tumor cells (as opposed to intact tissue). Unlike the Matrigel assay, our assay is rapid and does not require tens of thousands of cells. It can measure invasion potential of single cells as we have shown previously (15), or as shown in the present study, it can be applied to cancer cell populations.

We are not the first to investigate how low-intensity ultrasound interacts with invasive cancer cells. Tran et al. stimulated invasive MDA-MB-231 breast cancer cells with 1-MHz ultrasound (up to 500 kPa) while using the patch clamp technique to monitor membrane potential (32, 39). The cells immediately became hyperpolarized upon ultrasound application, but only when they were in direct contact with gas-filled microbubbles. By applying the BK_{Ca} channel blocker iberiotoxin, the authors determined that the microbubbles were activating mechanically sensitive BK_{Ca} channels, causing K^+ efflux and consequent hyperpolarization (32).

The BK_{Ca}-based mechanotransduction mechanism reported by the Tran study is fundamentally different from the mechanism

FIGURE 8 | Elucidating the cause of the calcium wave in PC-3 cells. Left column, histogram, and scatter plots showing a calcium wave in cells seeded on a Mylar substrate. This result indicates that the wave is not caused by ultrasound reflection by the substrate. Center column, histogram, and scatter plots showing ultrasound responses of cells freshly seeded on a Cell-Tak-coated Petri dish. A calcium wave occurs even in the absence of gap junctions. Right column, baseline (top), and background-subtracted (bottom) fluorescence images of ultrasound responses occurring after scraping a channel of cells off the substrate. Red asterisks indicate the center position of the ultrasound focus. Calcium responses occurred on both sides of the gap, suggesting that calcium waves in invasive cancer cells are caused by release of signaling molecules that diffuse through the extracellular space. Scale bar is 500 µm.

observed in our study: We observed ultrasound responses in invasive cancer cells without using microbubbles. Furthermore, we found that PC-3 and T24/83 responses were not affected by iberiotoxin (**Table 1**), thus excluding involvement of BK_{Ca} channels in the mechanotransduction process. Instead, we found that the drug 2-APB blocked ultrasound-induced calcium activity (**Figure 7**), implicating a role of TRP channels and/or IP_3 receptors. We also observed a delay of several seconds between stimulus onset and the calcium responses, suggesting a second messenger effect.

Several lines of evidence support the possibility that TRP channels are mediating the ultrasound responses observed in our study. TRP channels are a family of non-selective cation channels that can be activated by mechanical force, either directly or through a second messenger pathway (34). They have been implicated in several types of cancer including prostate (40) and bladder (41) cancer, regulating behaviors such as proliferation, differentiation, and migration [see Ref. (13, 35) for review]. Invasive and metastatic cancers are known to overexpress certain TRP channel isoforms, and silencing expression of these isoforms in cell lines significantly reduces migration and invasion (42, 43). It was recently reported that TRP-4, the *C. elegans* TRP channel homolog, transduces low-pressure ($\leq$900 kPa) ultrasound stimuli in this model organism [though only in the presence of microbubbles; Ref. (44)].

Because 2-APB blocks both TRP channels and IP_3 receptors, it is possible, however, that IP_3 receptors are involved in transducing the ultrasound stimulus (instead of or in addition to TRP channels). IP_3 and its receptors play a dominant role in transducing external stimuli into calcium signals by evoking Ca^{2+} release from intracellular stores. They are also known to mediate oscillatory changes in cytosolic calcium concentration (45), such as those observed in this study (see **Figures 3B** and **4B**). In ongoing work, we aim to determine the precise mechanism of ultrasound-induced calcium rise *via* small interfering RNA-mediated downregulation of IP_3 receptors versus TRP channels.

Although we found that ultrasound stimulation consistently evoked calcium waves in invasive cancer cells, the timing of those waves was somewhat variable. Calcium waves typically began 5–25 s after stimulation onset, traveled at a speed of ~50–100 µm/s, and persisted for 1–2.5 min. Though the reason for this variability is not clear, it is possible that the calcium wave timing correlates with invasion potential (for example, a faster wave could indicate greater invasion potential). In support of this theory, we did observe spontaneous variations in the degree of PC-3 and T24/83 Matrigel invasiveness that occurred during passaging in culture (data not shown). Likewise, others have reported that prostate and bladder cancer cells undergo cyclical, population-wide changes in tumorigenicity as they are passaged (46). Future studies will explore whether these changes in tumorigenicity and Matrigel invasiveness correlate with the pattern of ultrasound responses (such as calcium wave speed, percentage of responding cells, etc.).

If validated using clinical specimens, our mechanotransduction assay could provide pathologists with a means to detect tumor invasion in cytology specimens, a feat that is not currently possible. At present, pathologists can assess invasion only through histological analysis of biopsied tissue. However, there are many instances when intact tissue cannot be obtained from the patient. In such cases, diagnosis often relies exclusively on cytology, which cannot assess invasion. This can have devastating consequences, for example in the case of recurrent bladder cancer. As discussed above, recurrent invasive bladder malignancies sometimes go undetected by cystoscopy, which can be life-threatening (1, 4). An assay for identifying invasion in bladder wash cytology specimens could inform treatment decisions that improve patient outcomes. Esophageal carcinoma is another disease that could benefit from cytological assessment of tumor invasion. Detecting invasion in cells collected from esophageal brushings could limit the need for endoscopic tumor biopsies, which carry the serious risk of esophageal perforation (47).

In addition to assessing invasion potential, our technology could also be as a high-throughput optical screen for drugs that target the mechanotransduction pathway (48). Cells could be placed in multiwell plates, treated with different drugs, and then stimulated with ultrasound while imaging calcium activity. Drug effects would be indicated by any changes induced in the pattern of ultrasound responses.

A functional assay of cancer cell invasion potential, as demonstrated herein, could provide key advantages over other types of cancer diagnostic assays. Genomic tests, for example, are intended to predict tumor aggression or recurrence and have gained widespread use in recent years. These tests are limited, however, in that they provide information about nucleic acid expression, rather than protein expression/translation or protein functional state, which can be altered post-translationally. Protein activity is what controls a tumor's behavior, including its ability to invade and metastasize (5). By probing cell function as a measure of invasion potential, our assay may provide a more precise measure of a tumor's propensity to spread.

It may eventually be possible to develop an *in vivo* version of the assay that could mitigate the need for tumor biopsies. In the case of bladder cancer, a confocal laser endoscope (49) with an integrated ultrasound transducer could deliver calcium dye to the tumor, stimulate it with ultrasound, and image cellular responses. For other types of solid cancers, the tumor could be stimulated percutaneously with ultrasound while using calcium-sensitive MRI contrast agents (50) to image the response. This approach would provide an entirely non-invasive means to assess tumor invasion potential.

AUTHOR CONTRIBUTIONS

AW, NL, CY, AB, KG, SM, and HJ collected and analyzed data. SK analyzed data. AW, NL, CY, QZ, RC, and KS designed the research. AW and NL wrote the manuscript. All authors read, contributed to, and approved the final manuscript.

SUPPLEMENTARY MATERIAL

The Supplementary Material for this article can be found online at http://journal.frontiersin.org/article/10.3389/fonc.2017.00161/full#supplementary-material.

FIGURE S1 | Matrigel Boyden chamber assays of BPH-1 cells at different time points. Cells that passed through the Matrigel barrier were stained with crystal violet. As cells were passaged in culture, their level of invasiveness changed spontaneously over time. To obtain a weakly invasive homogeneous population for use in ultrasound stimulation experiments, BPH-1 cells that did not pass through the Boyden chamber were selected and propagated (see Materials and Methods).

VIDEO S1 | Calcium responses of weakly invasive BPH-1 prostate cancer cells to stimulation with 38-MHz low-intensity focused ultrasound (video corresponds to images in **Figure 3**, first column). The red asterisk indicates the center position of the ultrasound focus; its appearance and disappearance coincide with stimulation onset and offset, respectively. Video is played back at 60× real-time speed.

VIDEO S2 | Calcium responses of weakly invasive PNT1A prostate cancer cells to stimulation with 38-MHz low-intensity focused ultrasound (video corresponds to images in **Figure 3**, second column). The red asterisk indicates the center position of the ultrasound focus; its appearance and disappearance coincide with stimulation onset and offset, respectively. Video is played back at 60× real-time speed.

VIDEO S3 | Calcium responses of strongly invasive PC-3 prostate cancer cells to stimulation with 38-MHz low-intensity focused ultrasound (video corresponds to images in **Figure 3**, third column). The red asterisk indicates the center position of the ultrasound focus; its appearance and disappearance coincide with stimulation onset and offset, respectively. Video is played back at 60× real-time speed.

VIDEO S4 | Calcium responses of strongly invasive DU-145 prostate cancer cells to stimulation with 38-MHz low-intensity focused ultrasound (video corresponds to images in **Figure 3**, fourth column). The red asterisk indicates the center position of the ultrasound focus; its appearance and disappearance coincide with stimulation onset and offset, respectively. Video is played back at 60× real-time speed.

VIDEO S5 | Calcium responses of weakly invasive RT112/84 bladder cancer cells to stimulation with 38-MHz low-intensity focused ultrasound (video corresponds to images in **Figure 4**, left column). The red asterisk indicates the center position of the ultrasound focus; its appearance and disappearance coincide with stimulation onset and offset, respectively. Video is played back at 60× real-time speed.

VIDEO S6 | Calcium responses of strongly invasive T24/83 bladder cancer cells to stimulation with 38-MHz low-intensity focused ultrasound (video corresponds to images in **Figure 4**, right column). The red asterisk indicates the center position of the ultrasound focus; its appearance and disappearance coincide with stimulation onset and offset, respectively. Video is played back at 60× real-time speed.

REFERENCES

1. Stein JP, Lieskovsky G, Cote R, Groshen S, Feng A-C, Boyd S, et al. Radical cystectomy in the treatment of invasive bladder cancer: long-term results in 1,054 patients. *J Clin Oncol* (2001) 19:666–75. doi:10.1200/JCO.2001.19.3.666

2. Sylvester RJ, van der Meijden APM, Oosterlinck W, Witjes JA, Bouffioux C, Denis L, et al. Predicting recurrence and progression in individual patients with stage Ta T1 bladder cancer using EORTC risk tables: a combined analysis of 2596 patients from seven EORTC trials. *Eur Urol* (2006) 49:466–77. doi:10.1016/j.eururo.2005.12.031

3. Alexandroff AB, Jackson AM, O'Donnell MA, James K. BCG immunotherapy of bladder cancer: 20 years on. *Lancet* (1999) 353:1689–94. doi:10.1016/S0140-6736(98)07422-4

4. Kriegmair M, Baumgartner R, Knuchel R, Stepp H, Hofstadter F, Hofstetter A. Detection of early bladder cancer by 5-aminolevulinic acid induced porphyrin fluorescence. *J Urol* (1996) 155:105–10. doi:10.1097/00005392-199601000-00038

5. Djamgoz MBA. Biophysics of cancer: cellular excitability ("CELEX") hypothesis of metastasis. *J Clin Exp Oncol* (2014) S1. doi:10.4172/2324-9110.S1-005

6. Fraser SP, Diss JKJ, Chioni A-M, Mycielska ME, Pan H, Yamaci RF, et al. Voltage-gated sodium channel expression and potentiation of human breast cancer metastasis. *Clin Cancer Res* (2005) 11:5381–9. doi:10.1158/1078-0432.CCR-05-0327

7. Wang Z. Roles of K^+ channels in regulating tumour cell proliferation and apoptosis. *Pflügers Archiv* (2004) 448:274–86. doi:10.1007/s00424-004-1258-5

8. Monteith GR, Davis FM, Roberts-Thomson SJ. Calcium channels and pumps in cancer: changes and consequences. *J Biol Chem* (2012) 287:31666–73. doi:10.1074/jbc.R112.343061

9. Cross SE, Jin Y-S, Rao J, Gimzewski JK. Nanomechanical analysis of cells from cancer patients. *Nat Nanotechnol* (2007) 2:780–3. doi:10.1038/nnano.2007.388

10. Tse HTK, Gossett DR, Moon YS, Masaeli M, Sohsman M, Ying Y, et al. Quantitative diagnosis of malignant pleural effusions by single-cell mechanophenotyping. *Sci Transl Med* (2013) 5:212ra163. doi:10.1126/scitranslmed.3006559

11. Conti M. Targeting ion channels for new strategies in cancer diagnosis and therapy. *Curr Clin Pharmacol* (2007) 2:135–44. doi:10.2174/157488407780598153

12. Chen YF, Chen YT, Chiu WT, Shen MR. Remodeling of calcium signaling in tumor progression. *J Biomed Sci* (2013) 20:23. doi:10.1186/1423-0127-20-23

13. Santoni G, Farfariello V. TRP channels and cancer: new targets for diagnosis and chemotherapy. *Endocr Metab Immune Disord Drug Targets* (2011) 11:54–67. doi:10.2174/187153011794982068

14. Jaalouk DE, Lammerding J. Mechanotransduction gone awry. *Nat Rev Mol Cell Biol* (2009) 10:63–73. doi:10.1038/nrm2597

15. Hwang JY, Lee NS, Lee C, Lam KH, Kim HH, Woo J, et al. Investigating contactless high frequency ultrasound microbeam stimulation for determination of invasion potential of breast cancer cells. *Biotechnol Bioeng* (2013) 110:2697–705. doi:10.1002/bit.24923

16. Davila M, Frost AR, Grizzle WE, Chakrabarti R. LIM kinase 1 is essential for the invasive growth of prostate epithelial cells. *J Biol Chem* (2003) 278:36868–75. doi:10.1074/jbc.M306196200

17. Mamoune A, Kassis J, Kharait S, Kloeker S, Manos E, Jones DA, et al. DU145 human prostate carcinoma invasiveness is modulated by urokinase receptor (uPAR) downstream of epidermal growth factor receptor (EGFR) signaling. *Exp Cell Res* (2004) 299:91–100. doi:10.1016/j.yexcr.2004.05.008

18. Collins AT, Berry PA, Hyde C, Stower MJ, Maitland NJ. Prospective identification of tumorigenic prostate cancer stem cells. *Cancer Res* (2005) 65:10946–51. doi:10.1158/0008-5472.CAN-05-2018

19. Davies G, Jiang WG, Mason MD. Cell-cell adhesion molecules and their associated proteins in bladder cancer cells and their role in mitogen induced cell-cell dissociation and invasion. *Anticancer Res* (1998) 19:547–52.

20. Albini A, Iwamoto Y, Kleinman HK, Martin GR, Aaronson SA, Kozlowski JM, et al. A rapid *in vitro* assay for quantitating the invasive potential of tumor cells. *Cancer Res* (1987) 47:3239–45.

21. Lam KH, Hsu HS, Li Y, Lee C, Lin A, Zhou Q, et al. Ultrahigh frequency lensless ultrasonic transducers for acoustic tweezers application. *Biotechnol Bioeng* (2013) 110:881–6. doi:10.1002/bit.24735

22. Nelson TR, Fowlkes JB, Abramowicz JS, Church CC. Ultrasound biosafety considerations for the practicing sonographer and sonologist. *J Ultrasound Med* (2009) 28:139–50. doi:10.7863/jum.2009.28.2.139

23. Carpenter AE, Jones TR, Lamprecht MR, Clarke C, Kang IH, Friman O, et al. CellProfiler: image analysis software for identifying and quantifying cell phenotypes. *Genome Biol* (2006) 7:R100. doi:10.1186/gb-2006-7-10-r100

24. Iwasaki H, Mori Y, Hara Y, Uchida K, Zhou H, Mikoshiba K. 2-Aminoethoxydiphenyl borate (2-APB) inhibits capacitative calcium entry independently of the function of inositol 1,4,5-trisphosphate receptors. *Receptors Channels* (2000) 7:429–39.

25. Maruyama T, Kanaji T, Nakade S, Kanno T, Mikoshiba K. 2APB, 2-aminoethoxydiphenyl borate, a membrane-penetrable modulator of Ins(1,4,5)P_3-induced Ca^{2+} release. *J Biochem* (1997) 122:498–505. doi:10.1093/oxfordjournals.jbchem.a021780

26. Swandulla D, Armstrong CM. Calcium channel block by cadmium in chicken sensory neurons. *Proc Natl Acad Sci U S A* (1989) 86:1736–40. doi:10.1073/pnas.86.5.1736

27. Nishitani WS, Saif TA, Wang Y. Calcium signaling in live cells on elastic gels under mechanical vibration at subcellular levels. *PLoS One* (2011) 6:e26181. doi:10.1371/journal.pone.0026181

28. Galvez A, Gimenez-Gallego G, Reuben JP, Roy-Contancin L, Feigenbaum P, Kaczorowski GJ, et al. Purification and characterization of a unique, potent, peptidyl probe for the high conductance calcium-activated potassium channel from venom of the scorpion *Buthus tamulus*. *J Biol Chem* (1990) 265:11083–90.

29. Cobbs C, Khan S, Matlaf L, McAllister S, Zider A, Yount G, et al. HCMV glycoprotein B is expressed in primary glioblastomas and enhances growth and invasiveness via PDGFR-alpha activation. *Oncotarget* (2014) 5:1091–100. doi:10.18632/oncotarget.1787

30. Miyazaki H, Patel V, Wang H, Ensley JF, Gutkind JS, Yeudall WA. Growth factor-sensitive molecular targets identified in primary and metastatic head and neck squamous cell carcinoma using microarray analysis. *Oral Oncol* (2006) 42:240–56. doi:10.1016/j.oraloncology.2005.07.006

31. Ben-Tabou S, Keller E, Nussinovitch I. Mechanosensitivity of voltage-gated calcium currents in rat anterior pituitary cells. *J Physiol* (1994) 476:29–39.

32. Tran TA, Le Guennec JY, Bougnoux P, Tranquart F, Bouakaz A. Characterization of cell membrane response to ultrasound activated microbubbles. *IEEE Trans Ultrason Ferroelectr Freq Control* (2008) 55:43–9. doi:10.1109/TUFFC.2008.615

33. Wu SN, Chen BS, Hsu CL, Peng H. The large-conductance Ca^{2+}-activated K^+ channel: a target for the modulators of estrogen receptors. *Curr Top Biochem Res* (2008) 10:93–101.

34. Lin S-Y, Corey DP. TRP channels in mechanosensation. *Curr Opin Neurobiol* (2005) 15:350–7. doi:10.1016/j.conb.2005.05.012

35. Prevarskaya N, Zhang L, Barritt G. TRP channels in cancer. *Biochim Biophys Acta* (2007) 1772:937–46. doi:10.1016/j.bbadis.2007.05.006

36. Sanderson MJ, Charles AC, Boitano S, Dirksen ER. Mechanisms and function of intercellular calcium signaling. *Mol Cell Endocrinol* (1994) 98:173–87. doi:10.1016/0303-7207(94)90136-8

37. Boitano S, Dirksen ER, Sanderson MJ. Intercellular propagation of calcium waves mediated by inositol trisphosphate. *Science* (1992) 258:292–5. doi:10.1126/science.1411526

38. Sauer H, Hescheler J, Wartenberg M. Mechanical strain-induced Ca^{2+} waves are propagated via ATP release and purinergic receptor activation. *Am J Physiol Cell Physiol* (2000) 279:C295–307.

39. Tran TA, Roger S, Le Guennec JY, Tranquart F, Bouakaz A. Effect of ultrasound-activated microbubbles on the cell electrophysiological properties. *Ultrasound Med Biol* (2007) 33:158–63. doi:10.1016/j.ultrasmedbio.2006.07.029

40. Tsavaler L, Shapero MH, Morkowski S, Laus R. *Trp-p8*, a novel prostate-specific gene, is up-regulated in prostate cancer and other malignancies and shares high homology with transient receptor potential calcium channel proteins. *Cancer Res* (2001) 61:3760–9.

41. Caprodossi S, Lucciarini R, Amantini C, Nabissi M, Canesin G, Ballarini P, et al. Transient receptor potential vanilloid type 2 (TRPV2) expression in normal urothelium and in urothelial carcinoma of human bladder: correlation with the pathologic stage. *Eur Urol* (2008) 54:612–20. doi:10.1016/j.eururo.2007.10.016

42. Dhennin-Duthille I, Gautier M, Faouzi M, Guilbert A, Brevet M, Vaudry D, et al. High expression of transient receptor potential channels in human breast cancer epithelial cells and tissues: correlation with pathological parameters. *Cell Physiol Biochem* (2011) 28:813–22. doi:10.1159/000335795

43. Meng X, Cai C, Wu J, Cai S, Ye C, Chen H, et al. TRPM7 mediates breast cancer cell migration and invasion through the MAPK pathway. *Cancer Lett* (2013) 333:96–102. doi:10.1016/j.canlet.2013.01.031

44. Ibsen S, Tong A, Schutt C, Esener S, Chalasani SH. Sonogenetics is a non-invasive approach to activating neurons in *Caenorhabditis elegans*. *Nat Commun* (2015) 6:8264. doi:10.1038/ncomms9264

45. Zhang S, Fritz N, Ibarra C, Uhlén P. Inositol 1,4,5-trisphosphate receptor subtype-specific regulation of calcium oscillations. *Neurochem Res* (2011) 36:1175–85. doi:10.1007/s11064-011-0457-7

46. He K, Xu T, Goldkorn A. Cancer cells cyclically lose and regain drug-resistant highly tumorigenic features characteristic of a cancer stem-like phenotype. *Mol Cancer Ther* (2011) 10:938–48. doi:10.1158/1535-7163. MCT-10-1120

47. Chirica M, Champault A, Dray X, Sulpice L, Munoz-Bongrand N, Sarfati E, et al. Esophageal perforations. *J Visc Surg* (2010) 147:e117–28. doi:10.1016/j.jviscsurg.2010.08.003

48. Compton JL, Luo JC, Ma H, Botvinick E, Venugopalan V. High-throughput optical screening of cellular mechanotransduction. *Nat Photonics* (2014) 8:710–5. doi:10.1038/nphoton.2014.165

49. Kiesslich R, Goetz M, Vieth M, Galle PR, Neurath MF. Technology insight: confocal laser endoscopy for *in vivo* diagnosis of colorectal cancer. *Nat Clin Pract Oncol* (2007) 4:480–90. doi:10.1038/ncponc0881

50. Atanasijevic T, Shusteff M, Fam P, Jasanoff A. Calcium-sensitive MRI contrast agents based on superparamagnetic iron oxide nanoparticles and calmodulin. *Proc Natl Acad Sci U S A* (2006) 103:14707–12. doi:10.1073/pnas.0606749103

Check for updates

The Expression and Prognostic Impact of Immune Cytolytic Activity-Related Markers in Human Malignancies: A Comprehensive Meta-analysis

Constantinos Roufas[1,2], Dimitrios Chasiotis[1], Anestis Makris[1], Christodoulos Efstathiades[2], Christos Dimopoulos[2] and Apostolos Zaravinos[1]*

[1] Department of Life Sciences, Biomedical Sciences Program, School of Sciences, European University Cyprus, Nicosia, Cyprus, [2] The Center for Risk and Decision Sciences (CERIDES), Department of Computer Sciences, School of Sciences, European University Cyprus, Nicosia, Cyprus

Background: Recently, immune-checkpoint blockade has shown striking clinical results in different cancer patients. However, a significant inter-individual and inter-tumor variability exists among different cancers. The expression of the toxins granzyme A (GZMA) and perforin 1 (PRF1), secreted by effector cytotoxic T cells and natural killer (NK) cells, were recently used as a denominator of the intratumoral immune cytolytic activity (CYT). These levels are significantly elevated upon CD8+ T-cell activation as well as during a productive clinical response against immune-checkpoint blockade therapies. Still, it is not completely understood how different tumors induce and adapt to immune responses.

Methods: Here, we calculated the CYT across different cancer types and focused on differences between primary and metastatic tumors. Using data from 10,355, primary tumor resection samples and 2,787 normal samples that we extracted from The Cancer Genome Atlas and Genotype-Tissue Expression project databases, we screened the variation of CYT across 32 different cancer types and 28 different normal tissue types. We correlated the cytolytic levels in each cancer type with the corresponding patient group's overall survival, the expression of several immune-checkpoint molecules, as well as with the load of tumor-infiltrating lymphocytes (TILs), and tumor-associated neutrophils (TANs) in these tumors.

Results: We found diverse levels of CYT across different cancer types, with highest levels in kidney, lung, and cervical cancers, and lowest levels in glioma, adrenocortical carcinoma (ACC), and uveal melanoma. GZMA protein was either lowly expressed or absent in at least half of these tumors; whereas PRF1 protein was not detected in almost any of the different tumor types, analyzing tissue microarrays from 20 different tumor types. CYT was significantly higher in metastatic skin melanoma and correlated significantly to the TIL load. In TCGA-ACC, skin melanoma, and bladder cancer, CYT was associated with an improved patient outcome and high levels of both GZMA and PRF1 synergistically affected patient survival in these cancers. In bladder, breast, colon,

esophageal, kidney, ovarian, pancreatic, testicular, and thyroid cancers, high CYT was accompanied by upregulation of at least one immune-checkpoint molecule, indicating that similar to melanoma and prostate cancer, immune responses in cytolytic-high tumors elicit immune suppression in the tumor microenvironment.

Conclusion: Overall, our data highlight the existence of diverse levels of CYT across different cancer types and suggest that along with the existence of complicated associations among various tumor-infiltrated immune cells, it is capable to promote or inhibit the establishment of a permissive tumor microenvironment, depending on the cancer type. High levels of immunosuppression seem to exist in several tumor types.

INTRODUCTION

In normal cells, the role of cytotoxic T lymphocyte antigen-4 (CTLA-4 or CD152), programmed death-1 (PD-1 or CD279), or other similar immune-checkpoint molecules is to inhibit an autoimmune response and restrict an immune cell-mediated tissue damage. Cancer cells on the other hand, regularly use these immune-checkpoint molecules to escape from being detected and eliminated by the cells of the immune system (1–3).

Cytotoxic T cells (CTLs) and natural killer (NK) cells release perforin 1 (PRF1), granzymes, and granulysin, upon their expose to infected or dysfunctional somatic cells. The first cytotoxin polymerizes and creates a channel in the membrane of the target cell. Through these pores, granzymes will then enter the cytoplasm and trigger a caspase cascade, composed of cysteine proteases that will ultimately lead to apoptosis (4, 5). However, apoptosis can also be induced *via* cell–surface interaction between the CTL and the infected cell. Upon the activation of a CTL, the FAS ligand (FasL or CD95L) is expressed on its surface, and it binds to Fas (CD95) being expressed on the target cell (6). Furthermore, the TNF-related apoptosis-inducing ligand (TRAIL) and its receptors (TRAILR1/2) constitute another important axis of immune cytolytic activity (CYT) that leads to apoptosis (7).

Apart from tumor cells, the tumor microenvironment contains many different immune cell types, including neutrophils, macrophages, dendritic cells (DCs), NK cells, T and B cells (8–10). Spontaneous tumor immunity due to the infiltration of such immune cells to the tumor site (11) and immunotherapy can be used to predict the patient outcome in cancer (12–14). However, it is now known that these nonmalignant tumor-infiltrating immune cells can also contribute to cancer by taking part in the modulation of the tumor microenvironment together with other nonimmune stromal cells, including fibroblasts and endothelial cells (15–17).

Immunotherapies that depend on the blockade of such immune-checkpoint molecules can stimulate an anticancer response (18–21). Among them, PD-1 targeting drugs (Pembrolizumab and Nivolumab) or PD-L1 (Atezolizumab, Avelumab, and Durvalumab), and CTLA-4 inhibitors (Ipilimumab) can benefit treatment of several cancer types, comprising skin melanoma, non-small cell lung cancer, kidney cancer, bladder cancer, head and neck cancer, and Hodgkin lymphoma (22–24). Nevertheless, success rate varies from one tumor type to other and some cancers do not respond to therapy or they gradually develop resistance to it.

The interactions between cancer cells and cells of the immune system can be further understood using high-dimensional genomic and transcriptomic datasets stored in online repositories. One such publically available repository is The Cancer Genome Atlas (TCGA),[1] which contains comprehensive, multidimensional maps of the key genomic changes in 33 different cancer types. Latest analysis of the TCGA datasets has linked the genomic landscape of tumors with tumor immunity, implicating neoantigen load in driving T-cell responses (25), and identifying somatic mutations associated with immune infiltrates (26). The Human Protein Atlas (HPA)[2] (27–30) is another open access platform that provides a map to all the human proteins in cells, tissues, and organs, and integrates different "omics" technologies, such as antibody-based imaging, mass spectrometry-based proteomics, transcriptomics, and systems biology.

Here, we have used a large number of TCGA and HPA datasets containing thousands of solid tumor samples to understand how different cancers induce and adapt to immune responses. RNA-seq data for the genes of interest were extracted from different datasets in Fragments Per Kilobase Million (FPKM) and subsequently transformed to Transcripts Per Kilobase Million (TPM) values using the formula $TPMi = FPKMi/sum(FPKMj) \times 10^6$. We have further supported the RNA-level information using protein-level data across all cancer datasets. The CYT from each dataset has been further associated with the corresponding patient group's overall survival. To associate the CYT with patient survival both in primary and metastatic cancers, we have focused our attention on skin melanoma, breast, and thyroid cancers. We have also evaluated the density of tumor-infiltrating lymphocytes (TILs) and tumor-associated neutrophils (TANs) using hematoxylin and eosin (H&E)-stained sections of primary and metastatic tumors and made associations of their load with patient survival in each type of cancer.

---

[1]https://cancergenome.nih.gov/.
[2]https://www.proteinatlas.org/.

MATERIALS AND METHODS

Cancer Datasets

Using the Genomic Data Commons (GDC) Data Portal (The Cancer Genome Atlas, TCGA program[3]) and the GTEx web portal (Genotype-Tissue Expression project[4]), we extracted data from a total of 10,355 tumor resection samples and 2,935 normal samples and screened the variation of CYT across these 32 different cancer types and 28 different normal solid tissue types. TCGA-derived data represent mainly untreated primary tumors ($n = 9,913$). In addition, we extracted 47 recurrent and 395 metastatic cancer cases. The Skin Cutaneous Melanoma (SKCM) dataset included the majority of these metastatic cases ($n = 368$). Patients who received neoadjuvant therapy were excluded from the analysis. Where available, TCGA tumor samples were paired with their corresponding normal tissues, providing a germline reference.

In specific, the following tumor types were selected: diffuse large B-cell lymphoma (DLBCL, $n = 48$), kidney clear cell cancer (KIRC, $n = 539$), kidney papillary cancer (KIRP, $n = 289$), kidney chromophobe cancer (KIRCH, $n = 65$), testicular germ cell cancer (TGCT, $n = 156$), lung adenocarcinoma (LUAD, $n = 535$), lung squamous cell carcinoma (LUSC, $n = 502$), cervical squamous cell carcinoma and endocervical adenocarcinoma (CESC, $n = 306$), thymoma (THYM, $n = 119$), (SKCM, $n = 471$), acute myeloid leukemia (LAML, $n = 151$), head and neck squamous cell carcinoma (HNSC, $n = 502$), pleural mesothelioma (MESO, $n = 86$), sarcoma (SARC, $n = 263$), stomach adenocarcinoma (STAD, $n = 375$), colorectal cancer (COAD, $n = 480$), and rectum adenocarcinoma (READ, $n = 167$), uterine corpus endometrial carcinoma (UCEC, $n = 552$), uterine carcinosarcoma (UCS, $n = 56$), bladder cancer (BLCA, $n = 414$), pancreatic cancer ($n = 178$), breast cancer (BRCA, $n = 1109$), bile duct cancer ($n = 36$), ovarian serous cystadenocarcinoma (OV, $n = 379$), liver hepatocellular carcinoma (LIHC, $n = 374$), thyroid carcinoma (THCA, $n = 510$), esophageal cancer ($n = 162$), prostate adenocarcinoma (PRAD, $n = 499$), glioblastoma (GBM, $n = 169$), brain lower grade glioma (LGG, $n = 529$), pheochromocytoma and paraganglioma (PCPG, $n = 183$), adrenocortical carcinoma (ACC, $n = 79$), and uveal melanoma (UVM, $n = 80$) (where each acronym denotes the corresponding project's code and "n" is the number of cancer tissue samples).

"Level 3" mRNA-Seq expression data of the genes of interest, along with the corresponding patient clinical information for each disease type (tumors and normals) were extracted from TCGA public access web portal [launch data portal[3]] and GTEx[4] (for normal samples only). Gene expression data were additionally accessed from the Fantom5 Consortium[5] and were used to evaluate gene expression markers.

We also retrieved protein expression data derived from antibody-based protein profiling using immunohistochemistry (IHC) from the Tissue Atlas of The Human Protein Atlas (HPA)

(27–29). Information regarding the cellular distribution of each cytolytic protein (GZMA and PRF1) was also retrieved across all major cancers from the same repository. In total, we extracted IHC data from 19 different tumor types, among them BRCA ($n = 12$), cervical cancer ($n = 11$), colorectal cancer ($n = 11$), endometrial cancer ($n = 12$), glioma ($n = 12$), head and neck cancer ($n = 3$), liver cancer ($n = 11$), lung cancer ($n = 12$), lymphoma ($n = 12$), melanoma ($n = 12$), ovarian cancer ($n = 12$), pancreatic cancer ($n = 10$), prostate cancer ($n = 10$), renal cancer ($n = 11$), skin cancer ($n = 11$), stomach cancer ($n = 11$), testis cancer ($n = 9$), thyroid cancer ($n = 4$), and urothelial cancer ($n = 11$).

Calculation of CYT Followed by Downstream RNA-seq and Protein Profiling Analyses

We calculated the CYT (or "cytolytic index") as the geometric mean of GZMA and PRF1, as formerly defined (31). Briefly, we divided the total raw read counts per gene by the gene's maximum transcript length to signify a coverage depth estimate. Coverage estimates were then scaled to sum to a total depth of $1e^6$ per sample and inferred as Transcripts Per Kilobase Million (TPM). We compared the cytolytic index between metastatic and non-metastatic (primary) cancers, wherever a sufficient number of metastatic tumor cases were available (TCGA-BRCA, TCGA-SKCM, and TCGA-THCA datasets). We also calculated the expression of several other CTL/NK or non-CTL/NK expressing genes, including immunosuppressive factors, the C1Q complex, and interferon-stimulated chemokines, all of which were previously shown to associate with an increased CYT in cancer. We further correlated the cytolytic index with the expression of immune-checkpoint molecules, including CTLA-4, PD-1, CD274 (PD-L1), PDCD1LG2 (PD-L2), LAG3, IDO1, CD73 (NT5E), and ENTPD1 (CD39), across all TCGA datasets. The p-values from the comparisons of the CYT between tumor and normal samples or between metastatic and primary cancer samples were FDR-adjusted. Loess regression was applied to diminish the noise of the variables during correlation analysis.

We also extracted GZMA and PRF1 protein expression data from the Tissue Atlas of HPA, and further analyzed them. GZMA was stained with an anti-GZMA antibody produced in rabbit (HPA054134, 1:200 dilution, Sigma-Aldrich) and PRF1 using two different antibodies produced in rabbit (either HPA037940, 1:29 dilution, or CAB002436, 1:10 dilution, Sigma-Aldrich) (27–29).

Overall Survival and Synergistic Target Analysis on the TCGA Datasets

We performed Kaplan–Meier curves analysis to calculate the overall survival of each TCGA-dataset's patient group, based on their cytolytic index, TIL, and TAN load, or specific tumor subtype (e.g., triple negative vs triple positive BRCA). In total, we assessed overall survival data of patients suffering from 25 different cancer types (37 TCGA-datasets). Analysis was performed using the log-rank (Mantel Cox) test with a statistical significance at the 95% level ($p < 0.05$). We further tested the synergistic effect of the genes PRF1 and GZMA on each dataset's patient survival outcome, using SynTarget (32).

Detection and Quantification of Lymphocyte and Neutrophil Infiltration among Primary and Metastatic Cancers

We extracted digital slide images with H&E-stained histological slides of skin melanoma, breast, and thyroid cancer from The Cancer Digital Slide Archive (CDSA)[6] and compared the load of TILs and TANs between metastatic and primary cancers. TILs were distinguished by the typical features of lymphocytes (33), including size, shape, and staining of the nucleus. The percentage (%) of lymphocyte and neutrophil infiltration was compared to the information extracted from the corresponding datasets at the GDC Data Portal. We further compared the percentage of necrosis between primary and metastatic cancers, as well as the percentage of tumor, normal, and stromal cells. We correlated the levels of immune CYT (TPM counts) with the load of TILs and TANs, as well as with the percentage of necrosis found among metastatic and non-metastatic breast, skin melanoma, and thyroid cancers, using Pearson's correlation test.

RESULTS

Immune CYT across Different Tumor Types

To assess the intratumoral immune cytolytic T-cell activity across various tumor types, we quantified the transcript levels of GZMA and PRF1, as previously done by Rooney et al. (31). GZMA is a tryptase leading to apoptosis through the caspase pathway, whereas PRF1 is a pore-forming enzyme facilitating the entrance of granzymes into the target cells. Both effector molecules are considerably overexpressed upon CD8+ T-cell activation (34) and during productive clinical responses to anti-CTLA-4 or anti-PD-L1 immunotherapy (12, 13). CTL/NK cells can kill cancer cells by overexpressing GZMA and PRF1. We now know that effector T cells at the tumor site are good predictors of a favorable outcome across various cancer types (35–40).

Although Rooney et al. previously measured the immune CYT of the local immune infiltrate across various tumor types (31), some datasets did not contain enough data at the time (e.g., there were only three normal cervix samples in the TCGA-CESC dataset). Given the increased number of tumor samples in the TCGA platform since 2014, we have now significantly enlarged the total number of different cancer types, from 18 to 32. We have also considerably increased the sample number in many datasets, thus providing an opportunity to better estimate the different cytolytic levels across diverse tumors.

Consistent with previous findings (31, 41), we found that the cytolytic index was highest in the kidney (in clear cell and papillary renal cell carcinoma, but not in chromophobe carcinoma), lung, and cervical cancers. Importantly, we show for the first time that DLBCL and testicular cancer also rank among the top cytolytic active tumors, with DLBCL exhibiting even higher cytolytic levels compared to KIRC (>100 TPM). In addition, melanoma and head and neck cancer exhibited significantly higher CYT

---

[6]http://cancer.digitalslidearchive.net/.

compared to the corresponding normal tissues. Acute myeloid leukemia, pleural mesothelioma, sarcoma, and stomach cancer, also exhibited high tendency in CYT. On the contrary, ovarian, liver, thyroid, esophageal, and prostate cancers, as well as glioblastoma, glioma, pheochromocytoma and paraganglioma, adrenocortical carcinoma and uveal melanoma, exhibited the lowest cytolytic indexes (**Figure 1A**).

Although most normal tissues (11 tissues from TCGA or GTEx) showed significantly lower CYT compared to their corresponding tumors, some of them exhibited significantly higher activity. Specifically, lung cancer, thymoma, stomach, colorectal, uterine, bladder, breast, liver, and thyroid cancers, all exhibited lower CYT compared to their corresponding normal tissues. In the cases of lung adenocarcinoma, colorectal, uterine, liver, and thyroid cancers, the differences between cancer, and the normal tissues were statistically significant (**Figure 1A**). The vast range in CYT across different cancers and compared to their corresponding normal tissues reveals the existence of a combination of tissue- and tumor-specific mechanisms that control local immunity. In line with their synchronized roles, the expression of GZMA and PRF1 was strongly coordinated across the different cancer samples (Spearman rank correlation, rho = 0.87) (**Figure 1B**).
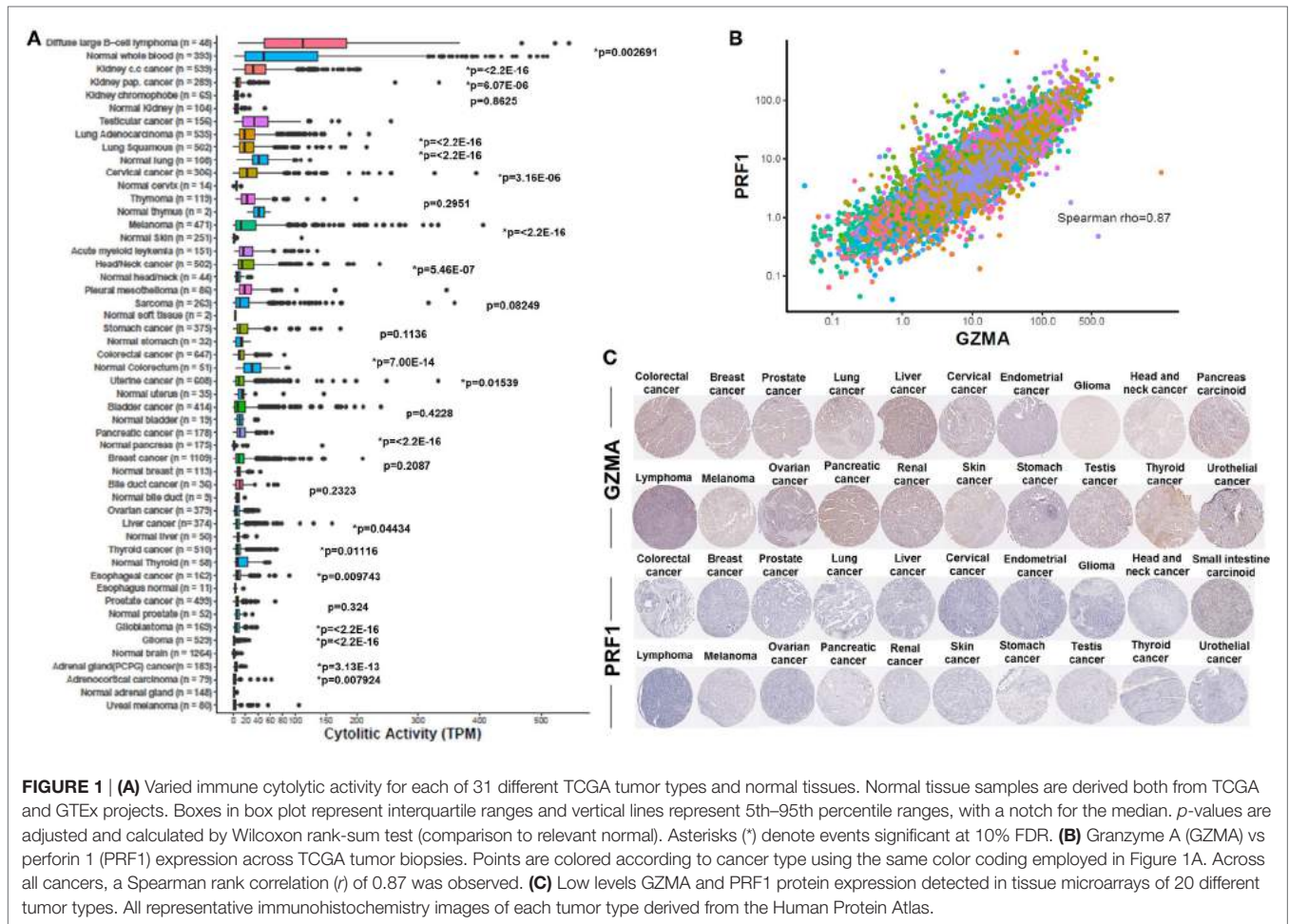
At the protein level, we analyzed tissue microarray (TMA) data from 20 different tumor types, and found that GZMA was either lowly expressed or absent in at least half of these tumors, whereas, PRF1 was not detected in almost any of the different tumor types (**Figure 1C**). GZMA exhibited medium protein expression in the majority of the pancreatic cancers (70%), in <35% of breast, cervical, liver, ovarian, prostate, renal, stomach, testis, and urothelial cancers, as well as in <10% of lymphomas and melanomas. These data are consistent with the low TPM values derived from our RNA-seq analysis (**Table 1**). Further information regarding anti-GZMA and anti-PRF1 antibody staining, intensity, quantity, and location are provided in Table S1 in Supplementary Material.

Immune CYT in Primary and Metastatic Cancers

Next, we focused our attention on whether the cytolytic index differs between primary and metastatic cancers. Among all TCGA datasets, the metastatic tumors were composed of 368 SKCM, seven BRCA, eight THCAs, one PRAD, two cervical cancers (CESC), one colorectal adenocarcinoma (COAD), one esophageal carcinoma (ESCA), two HNSCs, one pancreatic adenocarcinoma (PAAD), two PCPGs, one PRAD, and one sarcoma (SARC) sample. Therefore, since the majority of metastatic tumors were composed mainly of skin melanomas, breast and thyroid carcinomas we focused our downstream analysis on the corresponding datasets of these tumors.

To assess the cytolytic index in them, we obtained RNA-seq data from TCGA for 103 primary and 368 metastatic skin resection melanomas, 1,102 primary and seven metastatic BRCAs, as well as for 502 primary and eight metastatic THCAs. Although all metastatic tumors had higher CYT compared to their corresponding primary tumors, the difference was statistically significant only for the skin melanoma dataset. This is obviously due to the significantly higher number of metastatic melanoma cases (*n* = 368) (**Figure 2**).

FIGURE 1 | **(A)** Varied immune cytolytic activity for each of 31 different TCGA tumor types and normal tissues. Normal tissue samples are derived both from TCGA and GTEx projects. Boxes in box plot represent interquartile ranges and vertical lines represent 5th–95th percentile ranges, with a notch for the median. *p*-values are adjusted and calculated by Wilcoxon rank-sum test (comparison to relevant normal). Asterisks (*) denote events significant at 10% FDR. **(B)** Granzyme A (GZMA) vs perforin 1 (PRF1) expression across TCGA tumor biopsies. Points are colored according to cancer type using the same color coding employed in Figure 1A. Across all cancers, a Spearman rank correlation (*r*) of 0.87 was observed. **(C)** Low levels GZMA and PRF1 protein expression detected in tissue microarrays of 20 different tumor types. All representative immunohistochemistry images of each tumor type derived from the Human Protein Atlas.

Similarly, we investigated the expression of various suppressive factors previously shown to be associated with CYT, and compared their expression levels between metastatic and primary tumors. These genes included the immune-checkpoint molecules, CTLA-4, PD-1 (PDCD1), PD-L1 (CD274), PD-L2 (PDCD1LG2), LAG3, CD73 (NT5E)/CD39 (ENTPD1), IDO1/2, DOK3, the GMCSF receptors (CSF2RA, CSF2RB) (42), CD70, UBD, DOC3, NKG7, PLA2G2D, and the C1Q complex. We also included interferon-stimulated chemokines that attract T cells (CXCL9, CLCL10, and CXCL11) (11). We further investigated the expression of alternative genes through which T cells can induce cytolysis of cancer cells, including CD95-CD95L (FAS-FASLG) and TRAIL-TRAILR (TNFSF10, TNFRSF10A/B). Among the investigated genes, CD247, GZMK, GZMH, NKG7, PRF1, GZMA, GZMB, GZMH, GZMK, CD3E, and CD2 are expressed in CTL/NK cells; whereas CSF2RB, LTA, DOK3, PDCD1LG2, IDO1, PLA2G2D, CXCL9, CXCL10, CXCL11, CXCL13, UBD, C1QA, C1QB, C1QC, BATF2, and CSF2RA are expressed in non-CTL/NK cells (31).

In TCGA-SKCM, all genes (apart from CD70) exhibited significantly higher levels in metastatic skin melanomas compared to primary tumors. We also noticed a similar, but non-significant trend in datasets TCGA-BRCA and TCGA-THCA, presumably due to the small sample number of metastatic cases (**Figures 3**–**5**).

Kaplan–Meier and Synergistic Survival Analysis of GZMA and PRF1 across TCGA-Datasets

We next performed Kaplan–Meier survival analysis on 37 TCGA-datasets deriving from 25 different cancer types in order to estimate the risk of individual and/or simultaneous high (or low) PRF1 and GZMA expression on patient overall survival.

In TCGA-ACC, non-metastatic cutaneous melanoma ("m0" TCGA-SKCM), and bladder urothelial carcinoma (TCGA-BLCA but not the GSE32894 dataset), both individual and simultaneous high levels of PRF1 and GZMA were significantly associated with better prognosis. On the reverse, simultaneous low expression of both genes led to a significant shift toward negative effect vs all other ACC (or SKCM) patients. As expected, metastatic melanoma sufferers succumbed much earlier than non-metastatic skin melanoma patients did. These data provide significant evidence that high expression of both cytolytic genes in these cancer types, synergistically affects patient survival (**Figure 6A**).

TABLE 1 | Protein expression profiles of granzyme A (GZMA) and perforin 1 (PRF1) across 19 different cancer types, using antibody-based protein profiling data from immunohistochemistry (the Human Protein Atlas).

	Tumor patients expressing cytolytic genes							
	GZMA				PRF1			
Tumor	High	Medium	Low	Not detected	High	Medium	Low	Not detected
breast cancer	0/12 (0)	4/12 (33)	7/12 (58)	1/12 (8)	1/10 (0)	1/10 (0)	1/10 (0)	10/10 (100)
cervical cancer	0/11 (0)	3/11 (27)	5/11 (45)	3/11 (27)	0/11 (0)	0/11 (0)	1/11 (9)	10/11 (91)
colorectal cancer	0/11 (0)	0/11 (0)	3/11 (27)	8/11 (73)	0/12 (0)	0/12 (0)	0/12 (0)	12/12 (100)
endometrial cancer	0/12 (0)	0/12 (0)	1/12 (8)	11/12 (92)	0/11 (0)	0/11 (0)	0/11 (0)	11/11 (100)
glioma	0/12 (0)	0/12 (0)	0/12 (0)	12/12 (100)	0/12 (0)	0/12 (0)	0/12 (0)	12/12 (100)
head and neck cancer	0/3 (0)	0/3 (0)	1/3 (33)	2/3 (67)	0/4 (0)	0/4 (0)	0/4 (0)	4/4 (100)
liver cancer	0/11 (0)	3/11 (27)	1/11 (9)	7/11 (64)	0/12 (0)	0/12 (0)	0/12 (0)	12/12 (100)
lung cancer	0/11 (0)	0/12 (0)	4/11 (33)	8/12 (67)	0/12 (0)	0/12 (0)	0/12 (0)	12/12 (100)
lymphoma	0/12 (0)	1/12 (8)	1/12 (8)	10/12 (83)	0/11 (0)	0/11 (0)	0/11 (0)	11/11 (100)
melanoma	0/12 (0)	1/12 (8)	6/12 (50)	5/12 (42)	0/11 (0)	0/11 (0)	0/11 (0)	11/11 (100)
ovarian cancer	0/12 (0)	3/12 (25)	2/12 (17)	7/12 (58)	0/10 (0)	0/10 (0)	0/10 (0)	10/10 (100)
pancreatic cancer	0/10 (0)	7/10 (70)	2/10 (20)	1/10 (10)	0/12 (0)	0/12 (0)	0/12 (0)	12/12 (100)
prostate cancer	0/10 (0)	3/10 (30)	6/10 (60)	1/10 (10)	0/11 (0)	0/11 (0)	0/11 (0)	11/11 (100)
renal cancer	0/11 (0)	2/11 (18)	3/11 (27)	6/11 (55)	0/12 (0)	0/12 (0)	0/12 (0)	12/12 (100)
skin cancer	0/11 (0)	0/11 (0)	4/11 (36)	7/11 (64)	0/12 (0)	0/12 (0)	0/12 (0)	12/12 (100)
stomach cancer	0/11 (0)	2/11 (18)	6/11 (55)	3/11 (27)	0/12 (0)	0/12 (0)	0/12 (0)	12/12 (100)
testis cancer	0/9 (0)	2/9 (22)	2/9 (22)	5/9 (56)	0/12 (0)	0/12 (0)	0/12 (0)	12/12 (100)
thyroid cancer	0/4 (0)	0/4 (0)	2/4 (50)	2/4 (50)	0/4 (0)	0/4 (0)	0/4 (0)	4/4 (100)
urothelial cancer	0/11 (0)	3/11 (27)	5/11 (45)	3/11 (27)	0/11 (0)	0/11 (0)	0/11 (0)	11/11 (100)

Numbers indicate the tumor patients expressing each gene out of the total number (percentage, %).

In TCGA-LIHC, only the individual high levels of PRF1 and GZMA were significantly associated with a positive effect on patient survival. A similar non-significant association of (individual or simultaneous) high GZMA and PRF1 expression with better effect on patient survival could also be observed in TCGA-MESO, ovarian cancer (GSE13876 and GSE49997), TCGA-STAD, TCGA-THCA, and TCGA-UCEC (Figure S1 in Supplementary Material). These data suggest that high CYT is widely associated with an improved prognosis among the above-mentioned cancer types.
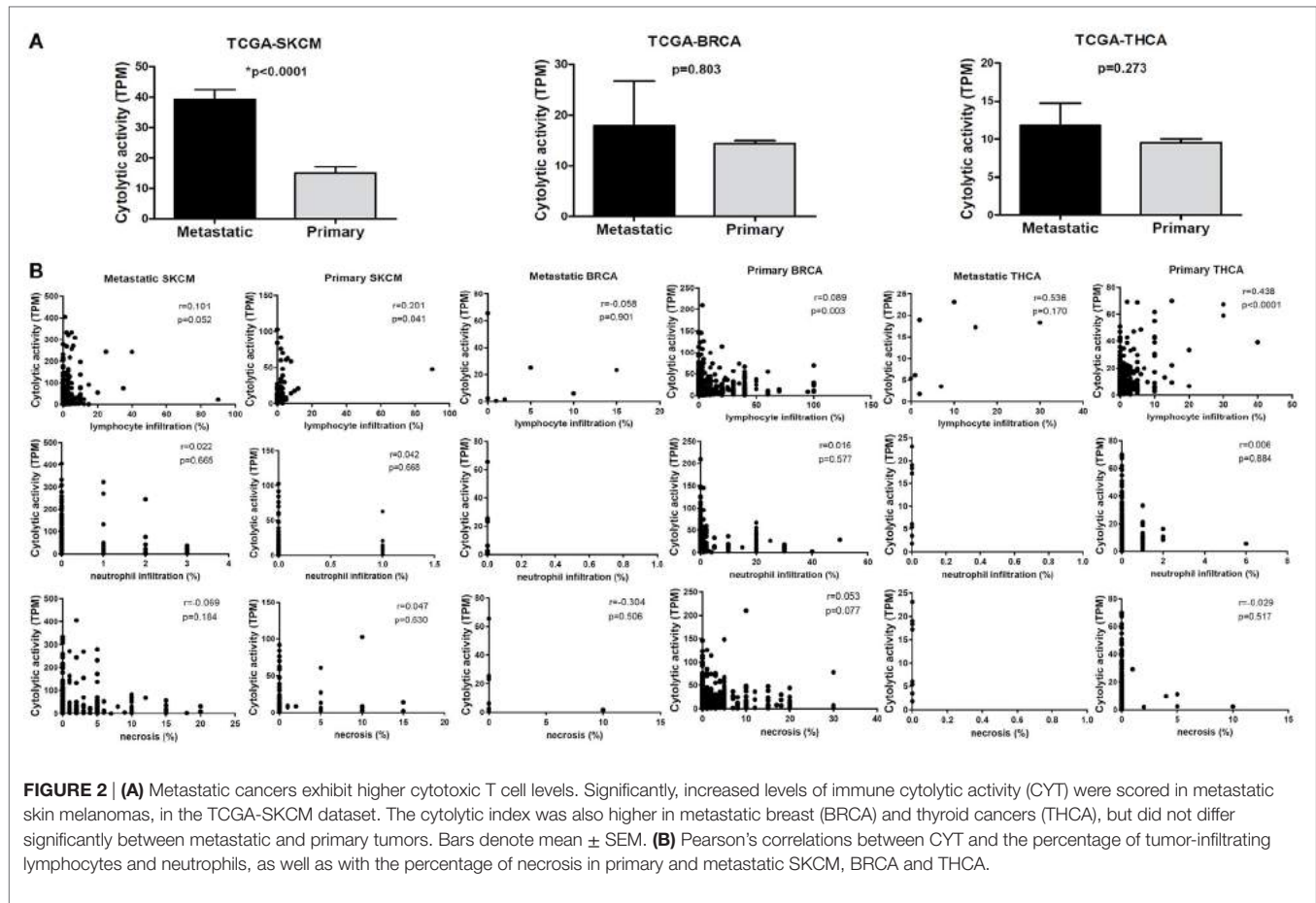
On the contrary, across TCGA-LGG, BRCAs (GSE25066), and TCGA-THYM, both individual and simultaneous high levels of GZMA and PRF1 were significantly associated with a worse prognosis, whereas the simultaneous low levels of both genes led to a significant shift toward positive effect (**Figure 6B**). Regarding BRCA, though, we could not confirm these results using the independent datasets METABRIC and TCGA-BRCA, which revealed a tendency for the opposite effects of both cytolytic genes on patient survival. Regarding the METABRIC dataset, we separated BRCA patients who were subjected to hormonal therapy plus radiotherapy (HT/RT) ($n = 605$) from the untreated patients; however, an association of high levels of GZMA and PRF1 with a worse prognosis could not be confirmed (Figure S6 in Supplementary Material).

Analogous non-significant associations of (individual or simultaneous) high cytolytic levels with worse effect on patient survival were also observed in lung cancer (GSE30219, TCGA-LUAD, and TCGA-LUSC), TCGA-PAAD, TCGA-PRAD and GSE16560, and TCGA-READ (Figure S2 in Supplementary Material).

In colon cancer, neither the individual nor the simultaneous high levels of the two genes were associated with a better prognosis, although simultaneous low levels of GZMA and PRF1 tended to shift toward a negative effect. Depending on the probe used, it seemed that a combination of high PRF1 and low GZMA levels yields a better patient outcome (GSE39582, TCGA-COAD, TCGA-COADREAD). Among metastatic colon cancer patients ("M1" patients in the TCGA-COAD dataset), simultaneous high levels of both genes were marginally significantly associated with worse prognosis, but simultaneous low levels of both genes could not provide the reverse trend (Figure S3 in Supplementary Material). We did not notice the same trend in the TCGA-COADREAD colorectal cancer patient cohort, though, implying that the aforementioned results are specific for colon (but not rectum) cancers.

Among clear-cell (TCGA-KIRC) and papillary renal cell carcinomas (TCGA-KIRP), we could not deduce any similar association among metastatic or non-metastatic tumors. In chromophobe renal carcinoma (TCGA-KICH) though, individual and simultaneous high levels of both genes tended to associate with better patient survival. On the other hand, concurrent low levels of both cytolytic genes, tended to associate with a worse prognosis. Interestingly, in the TCGA-KIPAN dataset, both the individual and synchronized high levels of GZMA and PRF1 significantly connected with worse patient survival. The simultaneous low expression of both genes exhibited reverse outcome (Figure S4 in Supplementary Material).

In DLBCL (GSE10846, and GSE32918), using various combinations of distinct molecular probes for the two cytolytic genes (PRF1, 214617_AT, 1553681_A_AT, or ILMN_1740633; GZMA, 205488_AT, or ILMN_1779324), we could not provide any

FIGURE 2 | **(A)** Metastatic cancers exhibit higher cytotoxic T cell levels. Significantly, increased levels of immune cytolytic activity (CYT) were scored in metastatic skin melanomas, in the TCGA-SKCM dataset. The cytolytic index was also higher in metastatic breast (BRCA) and thyroid cancers (THCA), but did not differ significantly between metastatic and primary tumors. Bars denote mean ± SEM. **(B)** Pearson's correlations between CYT and the percentage of tumor-infiltrating lymphocytes and neutrophils, as well as with the percentage of necrosis in primary and metastatic SKCM, BRCA and THCA.

significant association with patient survival. A similar absence of significant associations was also detected in glioblastoma (GSE4271, GSE13041, and TCGA-GBM) and non-metastatic HNSCs. We could not deduce any further association or trend between the expression of both cytolytic genes and the survival of TCGA-TGCT and uterine carcinosarcoma patients (Figure S5 in Supplementary Material).

Infiltration of Lymphocytes and Neutrophils in Primary and Metastatic TCGA-Datasets

We further evaluated the infiltration of lymphocytes (TILs) and neutrophils (TANs) to the tumor site of primary and metastatic cancer samples across the TCGA-SKCM, TCGA-BRCA, and TCGA-THCA datasets, using the Cancer Digital Slide Archive (see text footnote 6). TILs contained both stromal- and intratumoral-compartment lymphocytes, as previously defined (43). Both of them were mainly composed of T cells and a smaller number of B cells, NK cells, and macrophages (44, 45).

In the TCGA-BRCA dataset, the number of TILs appeared enriched in the stroma of the primary tumors compared to the corresponding areas on the slide of the metastatic BRCAs. However, this might probably be due to the higher number of stroma cells detected in the primary breast tumors (percentage

of stromal cells in primary vs metastatic BRCA, 21.15 ± 0.520 vs 7.143 ± 3.595; $p = 0.032$).

Although the number of TILs and neutrophils was higher in several cases of primary BRCA, the overall difference was not statistically significant (mean% of TILs ± SD in primary vs metastatic BRCAs, 6.102 ± 0.403 vs 4.714 ± 2.179; $p = 0.78$ and mean% of neutrophil infiltration ± SD in primary vs metastatic BRCAs, 1.625 ± 0.167 vs 0 ± 0; $p = 0.44$). Among primary tumors, comparing between triple negative (ER−, PR−, Her2/neu−, or TNBC), and triple positive (ER+, PR+, Her2/neu+, or TPBC) BRCAs, the load of TILs (and TANs) was not significantly different and was not significantly associated with a worse outcome, in argument with previous observations (46–48). In addition, the percentage of necrosis did not differ between metastatic and primary skin melanoma (<2%) (**Figure 7**).

In the TCGA-SKCM dataset, although in several cases the number of TILs was more enriched in the stroma of primary melanomas (as opposed to metastatic cancers), the overall load of TIL and TAN did not differ significantly between them. It is also worth noticing that the number of stroma cells counted in metastatic melanomas was higher compared to primary skin tumors (percentage of stromal cells in primary vs metastatic melanoma, 5.835 ± 1.083 vs 9.043 ± 0.571; $p = 0.009$). In addition, the rate of necrosis was marginally higher in metastatic skin melanoma
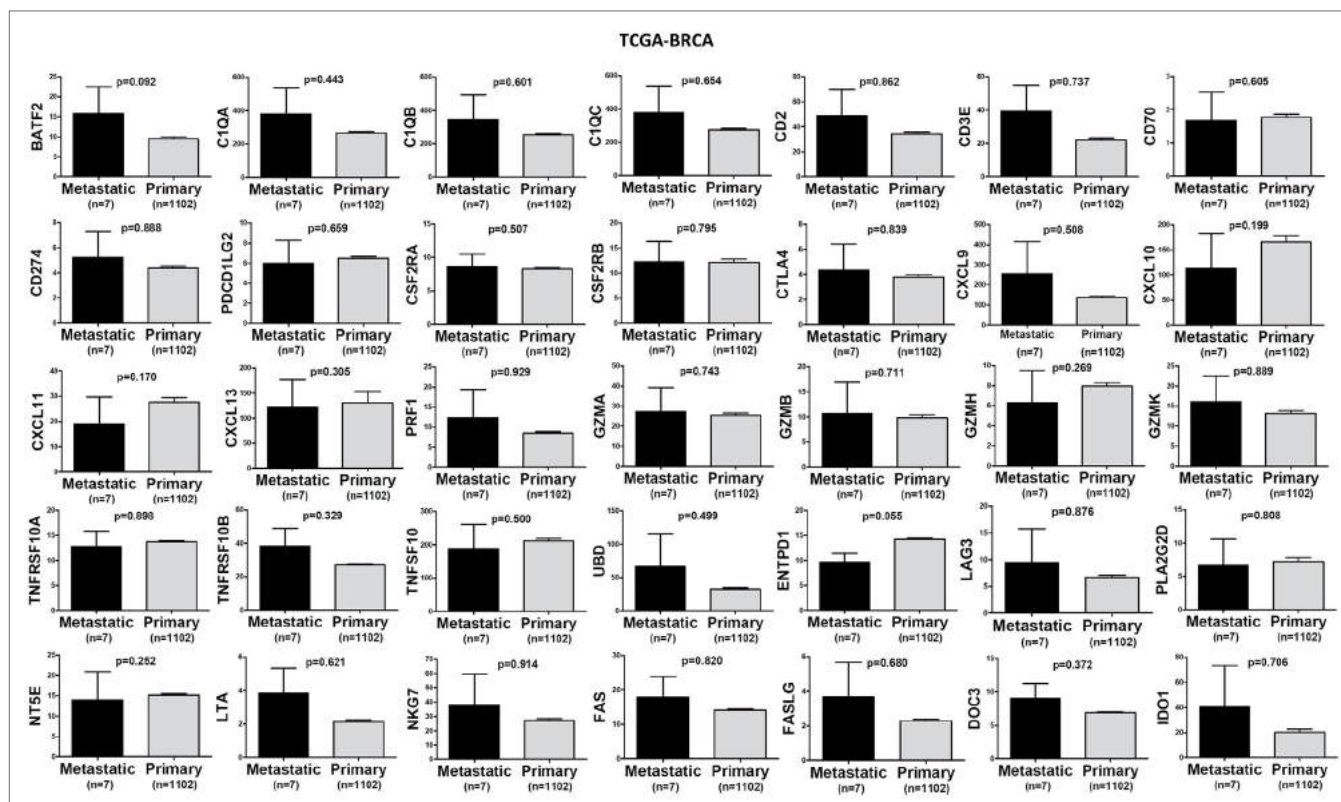
FIGURE 3 | A trend for higher expression (TPM) of a group of genes being expressed in cytotoxic T cell/natural killer (CTL/NK) and non-CTL/NK cells and correlating with cytolytic activity (CYT) in metastatic breast cancers compared to primary tumors. Bars denote mean ± SEM.

compared to primary tumors ($p = 0.042$). The overall survival did not differ between high TIL load (>1% TILs) or low TIL load (<1% TILs) in primary skin melanoma patients. However, among metastatic patients, a high percentage of lymphocytic infiltration shifted toward a better prognosis (**Figure 8**). According to recent data, the number of TILs in stage III metastatic melanoma associates with the response to Ipilimumab once these patients progress to stage IV disease (49).

In the TCGA-THCA dataset, the infiltration of lymphocytes was significantly higher in metastatic thyroid tumors and the high TIL load (>2% TILs) was associated with a better prognosis within the primary tumor group (mean% of TILs ± SD in primary vs metastatic cancers, 1.597 ± 0.160 vs 8.375 ± 3.59, $p < 0.0001$). The infiltration of neutrophils was minor (<0.1%) and did not differ between primary and metastatic THCAs. The necrotic rate was equally low between the two groups (**Figure 9**).

Correlation of the Cytolytic Index with Immune-Checkpoint Molecules and TILs in Primary and Metastatic TCGA-Datasets

In order to understand the context of PRF1/GZMA deregulation relative to the expression of various immune-checkpoint molecules, we correlated the cytolytic index with the expression of CTLA-4, PD-1, CD274 (PD-L1), PDCD1LG2 (PD-L2), LAG3, IDO1, CD73 (NT5E), and CD39 (ENTPD1) across all TCGA

datasets (Figure S7 in Supplementary Material). In the majority of the cancers, a high cytolytic index was accompanied by upregulation of at least one immune-checkpoint molecule, indicating that similar to melanoma (42) and prostate cancer (41), immune response in CYT-high tumors elicits multiple host and tumor mechanisms of immune suppression in the tumor microenvironment (Figure S7 in Supplementary Material). For example, in TCGA-BRCA, CTLA-4, and PD-1 expression was significantly associated with a high cytolytic index (CTLA-4, $p = 8.75e{-}199$, Pearson's rho = 0.75; PD-1, $4.09e{-}309$, Pearson's rho = 0.85). As expected, this correlation was 20 times stronger compared to the normal breast, due to absence of immunosuppression in the latter (CTLA-4, $p = 2.44e{-}12$, Pearson's rho = 0.60; PD-1, $1.12e{-}14$, Pearson's rho = 0.65). Importantly, this association was even stronger among metastatic melanomas, suggesting the existence of a more intense immunosuppression in these tumors (e.g., in primary melanoma, PD-1, $p = 1.14e{-}35$, Pearson's rho = 0.887; LAG3, $p = 1.03e{-}45$, Pearson's rho = 0.930; IDO1, $p = 3.05e{-}08$, Pearson's rho = 0.513. In metastatic melanoma, PD-1, $p = 1.48e{-}148$, Pearson's rho = 0.917; LAG3, $p = 4.28e{-}163$, Pearson's rho = 0.931; IDO1, $p = 2.38e{-}53$, Pearson's rho = 0.690) (Figure S8 in Supplementary Material).

The cytolytic index was significantly correlated with lymphocyte infiltration in BRCA, thyroid cancer, and skin melanoma. The association between a high TIL load and CYT was stronger among primary breast and THCAs, but not in melanomas.
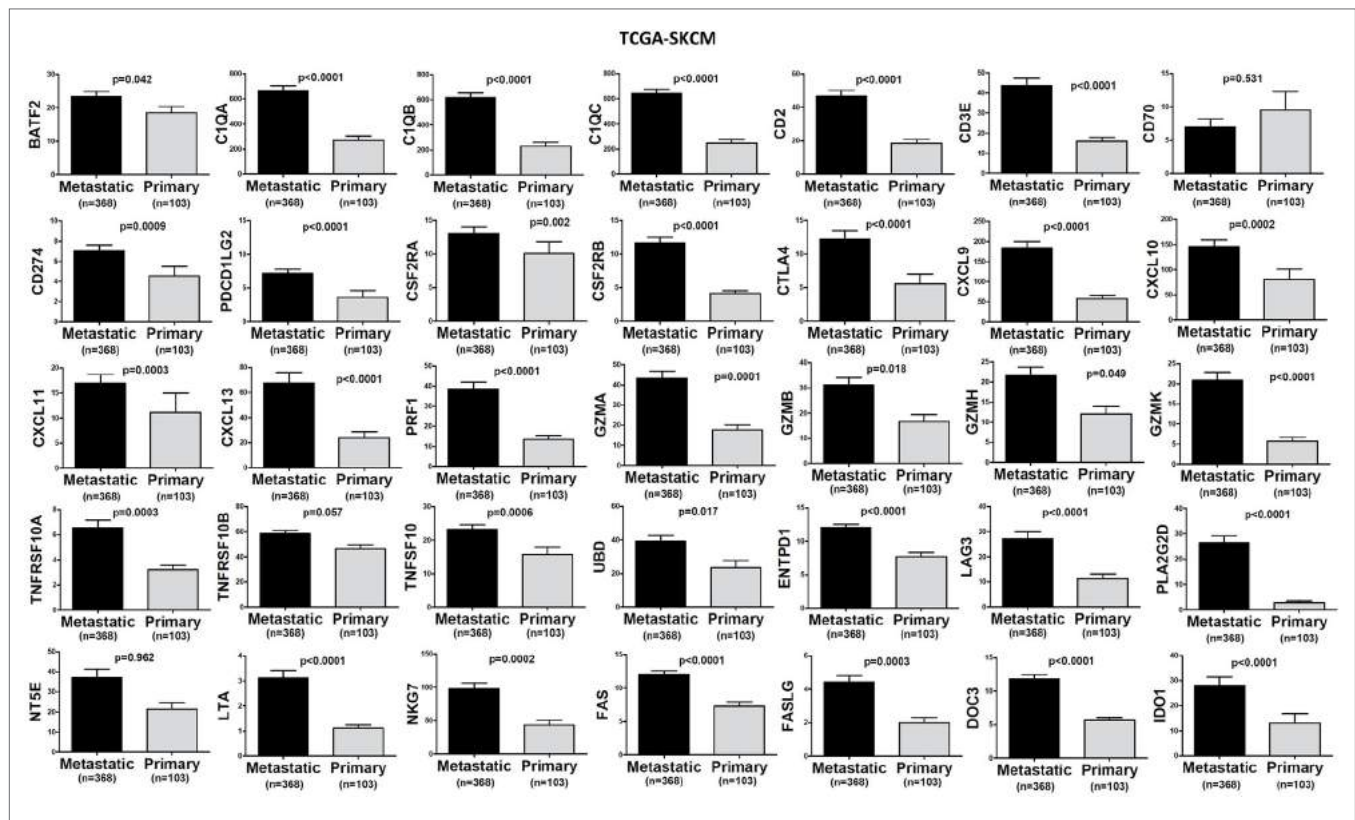
FIGURE 4 | Significantly higher expression (TPM) of a group of genes being expressed in cytotoxic T cell/natural killer (CTL/NK) and non-CTL/NK cells and correlating with cytolytic activity (CYT) in metastatic skin melanomas compared to primary tumors. Bars denote mean ± SEM.

Consistent with the fact that apoptosis is a hallmark of CYT, we scored no further correlation between CYT and necrosis or between CYT and infiltration of neutrophils (**Figure 2B**).

Number of Tumor and Normal Cells across Metastatic and Non-Metastatic TCGA-Datasets

Expression analysis can be hampered due to a different number of cells within each tumor, thus reducing the ability to confidently measure the cytolytic index and correlate it with the expression of immune-checkpoint molecules in each dataset, as well as to compare gene expression between primary and metastatic cancers. To address this, we calculated the number of tumor and normal cells within each tumor. Overall, the primary and metastatic cancer samples across the three datasets contained an equal number of tumor cells (70–90% tumor cells, $p > 0.05$) (**Figures 7–9**). Thus, the detected differences should not be the result of enrichment in tumor cells in one group or the other. Similarly, the percentage in normal cells did not differ between primary and metastatic BRCAs (3.48 ± 0.26, in primary cancers vs 7.86 ± 3.56, in metastatic cancers; $p = 0.188$). On the other hand, primary melanomas had higher percentage of normal cells compared to metastatic tumors (7.485 ± 1.263 vs 1.155 ± 0.313, $p < 0.001$), and metastatic THCAs had a higher percentage of normal cells compared

to their primary counterparts (8.125 ± 8.125 vs 2.126 ± 0.305, $p = 0.021$).

DISCUSSION

In this study, we quantified the cytolytic index based on the expression of GZMA and PRF1, both of which mediate cytolysis. This index is strongly associated with CTLs, plasmacytoid dendritic cells, counter-regulatory Tregs, and known T-cell co-inhibitory receptors (31).

In agreement with Rooney et al. (31), we found a great variation in the immune CYT across different types of cancer, which possibly reflects the existence of merged tissue- and tumor-specific mechanisms orchestrating the local immunity. Cancers of the ovaries, liver, thyroid, esophagus, and prostate, as well as glioblastoma, glioma, pheochromocytoma and paraganglioma, adrenocortical carcinoma and uveal melanoma all exhibited minimal levels of CYT. On the contrary, DLBCL, clear-cell renal cell carcinoma, testicular cancer, cervical cancer, skin melanoma, and head and neck carcinoma exhibited increased levels of CYT.

The tumor-intrinsic resistance to CYT has been suggested to be due to different mechanisms. Among them, recurrent mutations in immune-related genes have been proposed, such as B2M, HLA-A, -B, and -C, and CASP8, as well as copy number aberrations in loci containing immunosuppressive factors, including
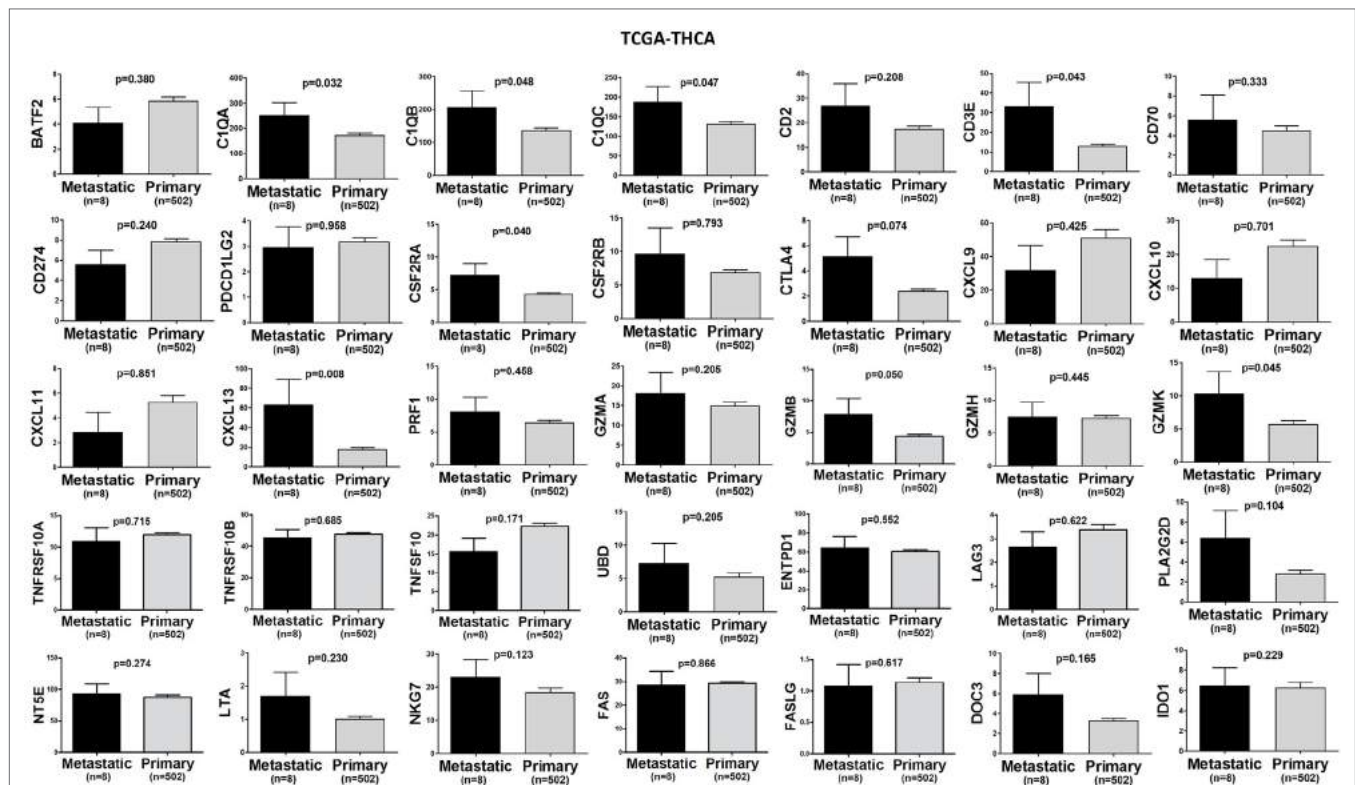
FIGURE 5 | A trend for higher expression (TPM) of a group of genes being expressed in cytotoxic T cell/natural killer (CTL/NK) and non-CTL/NK cells and correlating with cytolytic activity (CYT) in metastatic thyroid cancers compared to primary tumors. Bars denote mean ± SEM.

the receptors PD-L1/2 and CTLA-4 (31). PD-1 is transiently induced in activated T cells (50) and its expression is preserved in TILs (51–53). PD-L1 expression is high in several human malignancies, such as skin melanoma, lung, head and neck, and ovarian cancers (54, 55). PD-L1 expression is also correlated with a bad prognosis among patients with esophageal, colon, ovarian, or kidney cancer (56–60). The PD-1/PD-L1 axis is significant in tumor-induced immune evasion and both molecules are hopeful target candidates for immunotherapy. Actually, recent clinical trials have demonstrated that blockage of this signaling can benefit patients with advanced melanoma, kidney, or non-small cell lung cancer (2, 61–63). In metastatic melanoma, PD-L1 expression on peripheral T cells was recently shown to be prognostic on overall and progression-free survival (64).
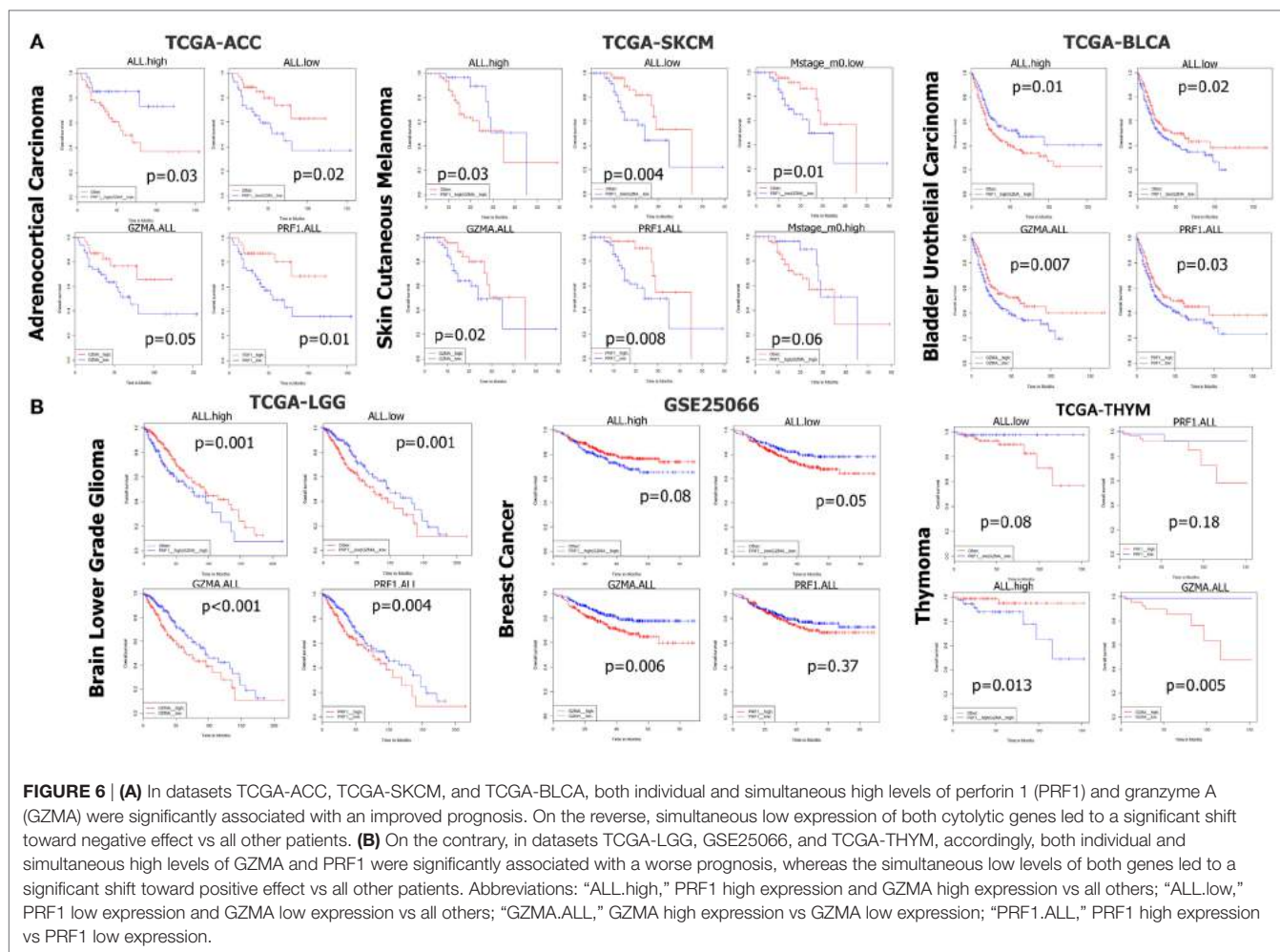
CTLA-4 expression levels are low on resting T cells, but increase upon T-cell activation. In acute infection, CTLA-4 is transiently induced and binds to B7-1/2, thus competing with CD28 and weakening the T-cell response (65). On the other hand, CTLA-4 is constitutively expressed in T cells during chronic infection and cancer due to chronic antigen exposure. CTLA-4 is also constitutively expressed on antigen-experienced memory CD4+ and CD8+ T cells, as well as Tregs (65). Similarly, B7-1 is not expressed on resting antigen-presenting cells (APCs) (as opposed to B7-2) and is induced after APC activation. Anti-CTLA-4 therapy (Ipilimumab) was shown to induce cancer

regression in metastatic kidney cancer (22, 66) and melanoma (67–70). Importantly, CTLA-4 blockade was reported to associate with bowel inflammation in melanoma patients (71), signifying that its signaling is crucial for the preservation of immune homeostasis in the gut.

Another example of immune-inhibitory molecule is indoleamine-pyrrole 2,3-dioxygenase (IDO). This molecule is constitutively expressed in the tumor microenvironment either by tumor cells or by host immune cells and is stimulated by inflammatory cytokines as IFN-γ, leading to host immune inhibition through increased Treg and effector T-cell proliferation blockade. A combination of IDO inhibition and immune-checkpoint blockade are currently under clinical investigation, with promising results (72).

Arginase is also an immune-inhibitory metabolic enzyme being expressed by both tumor cells as well as infiltrating myeloid cells (73). Both IDO and arginase inhibit immune responses by locally depleting the essential amino acids for anabolic functions in T cells or synthesizing specific natural ligands for cytosolic receptors, which can change the functions of lymphocytes. Inhibition of both IDO and arginase can enhance intratumoral inflammation (74, 75).

We found that high levels of several immune-checkpoint molecules, including CTLA-4, PD-1, PD-L1/2, LAG3, IDO1, CD73, and CD39 are associated with an increased cytolytic

FIGURE 6 | **(A)** In datasets TCGA-ACC, TCGA-SKCM, and TCGA-BLCA, both individual and simultaneous high levels of perforin 1 (PRF1) and granzyme A (GZMA) were significantly associated with an improved prognosis. On the reverse, simultaneous low expression of both cytolytic genes led to a significant shift toward negative effect vs all other patients. **(B)** On the contrary, in datasets TCGA-LGG, GSE25066, and TCGA-THYM, accordingly, both individual and simultaneous high levels of GZMA and PRF1 were significantly associated with a worse prognosis, whereas the simultaneous low levels of both genes led to a significant shift toward positive effect vs all other patients. Abbreviations: "ALL.high," PRF1 high expression and GZMA high expression vs all others; "ALL.low," PRF1 low expression and GZMA low expression vs all others; "GZMA.ALL," GZMA high expression vs GZMA low expression; "PRF1.ALL," PRF1 high expression vs PRF1 low expression.

index, across many cancers; and we expect that a combinatorial targeting of such immune-checkpoint molecules can provide a synergistic effect in cancer immunotherapy. Garg et al. found that predictive biomarkers of responsiveness to immune-checkpoint inhibitors in glioblastoma (GBM) exhibited inconsistent patterns among patients, predicting either resistance or susceptibility to therapeutic targeting of CTLA-4 or IDO1 (76).

Furthermore, different levels of tumor-intrinsic resistance to CYT can be attributed to the diverse levels of neoepitopes in these tumor types. Neoepitopes are tumor-specific antigens produced from DNA mutations occurring in cancer cells. Such mutations can be missense mutations, indels (insertions/deletions), and/or gene fusions. Increasing evidence shows that neoepitope-specific antitumor immune responses occur naturally in cancer cells and have great potentials as immunotherapeutic agents (77). Theoretically, immune responses to neoepitopes are not diminished by host central tolerance in the thymus and cannot trigger an autoimmune reaction (77, 78). These neoepitopes were lately shown to facilitate recognition of a tumor as foreign (78, 79), and an increased load of them is associated with effective immune responses to immune-checkpoint therapy (80). Currently,

strategies to selectively enhance T-cell reactivity against genetically defined neoepitopes are under development (78, 81–84). Furthermore, recent findings identified target neoepitopes which can be helpful in the design of a vaccine against murine melanoma (85). Importantly, the immunogenicity and specificity of these neoepitopes was validated *in vivo*, after administering mice either mutated or wild type synthetic peptides. Further advance in the field was made by Verdegaal et al. who analyzed the stability of neoantigen-specific T-cell responses and the antigens they recognize in melanoma patients treated by adoptive T-cell transfer. This study demonstrated that T cells mediate neoantigen immunoediting, indicating that the therapeutic induction of broad neoantigen-specific T-cell responses should be used to avoid tumor resistance (86).

In comparison to melanoma, the immune CYT in breast cancer, the burden of nonsynonymous mutations, and the predicted load of neoepitopes were previously found to be relatively modest, suggesting that a combination of immune agents with nonredundant mechanisms of action should be of high-priority (87). Recently, Vonderheide et al. highlight the critical steps that need to be followed for a more successful immunotherapy
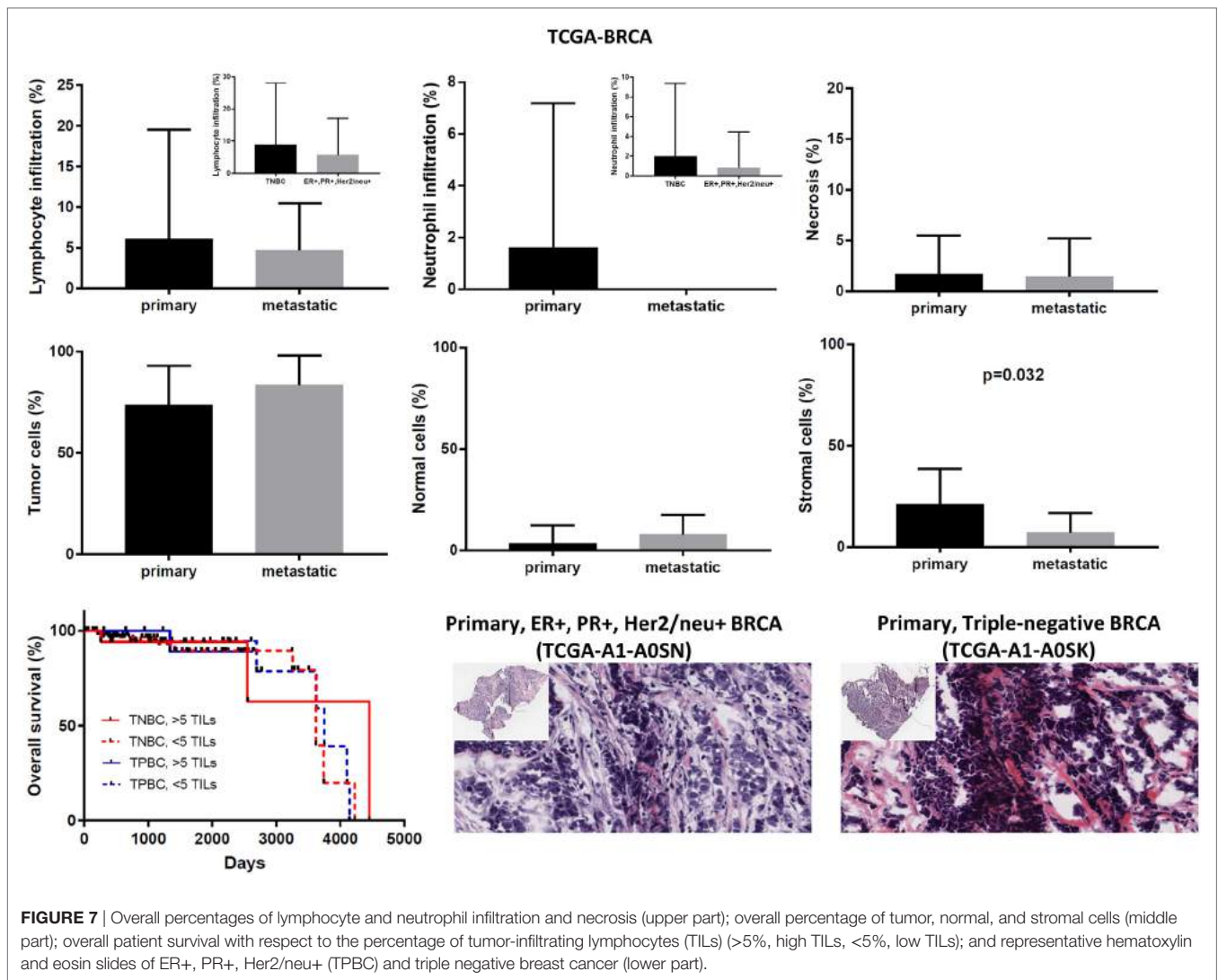
FIGURE 7 | Overall percentages of lymphocyte and neutrophil infiltration and necrosis (upper part); overall percentage of tumor, normal, and stromal cells (middle part); overall patient survival with respect to the percentage of tumor-infiltrating lymphocytes (TILs) (>5%, high TILs, <5%, low TILs); and representative hematoxylin and eosin slides of ER+, PR+, Her2/neu+ (TPBC) and triple negative breast cancer (lower part).

in breast cancer, including immune suppression in the tumor microenvironment and failed or suboptimal T-cell priming (87).

Also Chen et al. (88) categorized the tumor microenvironment into four types, depending on the expression of PD-L1, as well as the ratio CD8A/CYT, and proposed that this classification can serve the design of more suitable immunotherapeutic strategies.

A very interesting improvement in the field was further made by Riaz et al. (89), who showed that the mutation burden in melanoma patients decreases with successful anti-PD-1 blockade therapy, suggesting that the selection against mutant neoepitopes is a critical mechanism of action of this immunotherapy.

All these advances, show that neoepitopes can be used as biomarkers to predict the clinical response to immunotherapy and the outcome, as well as to serve as immunotherapy targets (25, 90). Besides epitope selection, the reduction of gene expression heterogeneity within tumor cells, the definition of the optimum number of simultaneously targeted neoantigens, of the patient profile that can benefit from neoantigen-based immunotherapy and escape the risk of adverse effects, and a synergistic combination

of immune-checkpoint blockade and/or adoptive T-cell therapy, are all issues that need to be successfully addressed in order to select potent neoantigens for cancer immunotherapy (77).

Adding to the variability in cytolytic levels that we detected among different cancer types, CYT has also been previously shown to correlate with oncogenic viruses in certain tumor types. For example, CYT is associated with HPV infection in cervical cancer, and head and neck cancer, with EBV infection in stomach cancer, and with HBV and HCV infection in liver cancer (31). Overall, it seems that CYT is part of an inflammatory environment in a premalignant state of certain tumor types, whereas, in others, oncogenic mutations, copy number aberrations, or viral infection can induce a tumor-promoting inflammatory microenvironment, within which complex interactions between different cell types regulate cancer development and metastasis (91, 92).

In the context of metastasis, we observed that CYT was significantly higher in metastatic skin melanoma compared to primary skin tumors. The increased cytolytic levels could be

FIGURE 8 | Overall percentages of lymphocyte and neutrophil infiltration and necrosis (upper part); overall percentage of tumor, normal, and stromal cells (middle part); overall patient survival with respect to tumor-infiltrating lymphocytes and representative hematoxylin and eosin slides of primary and metastatic skin melanomas (lower part).
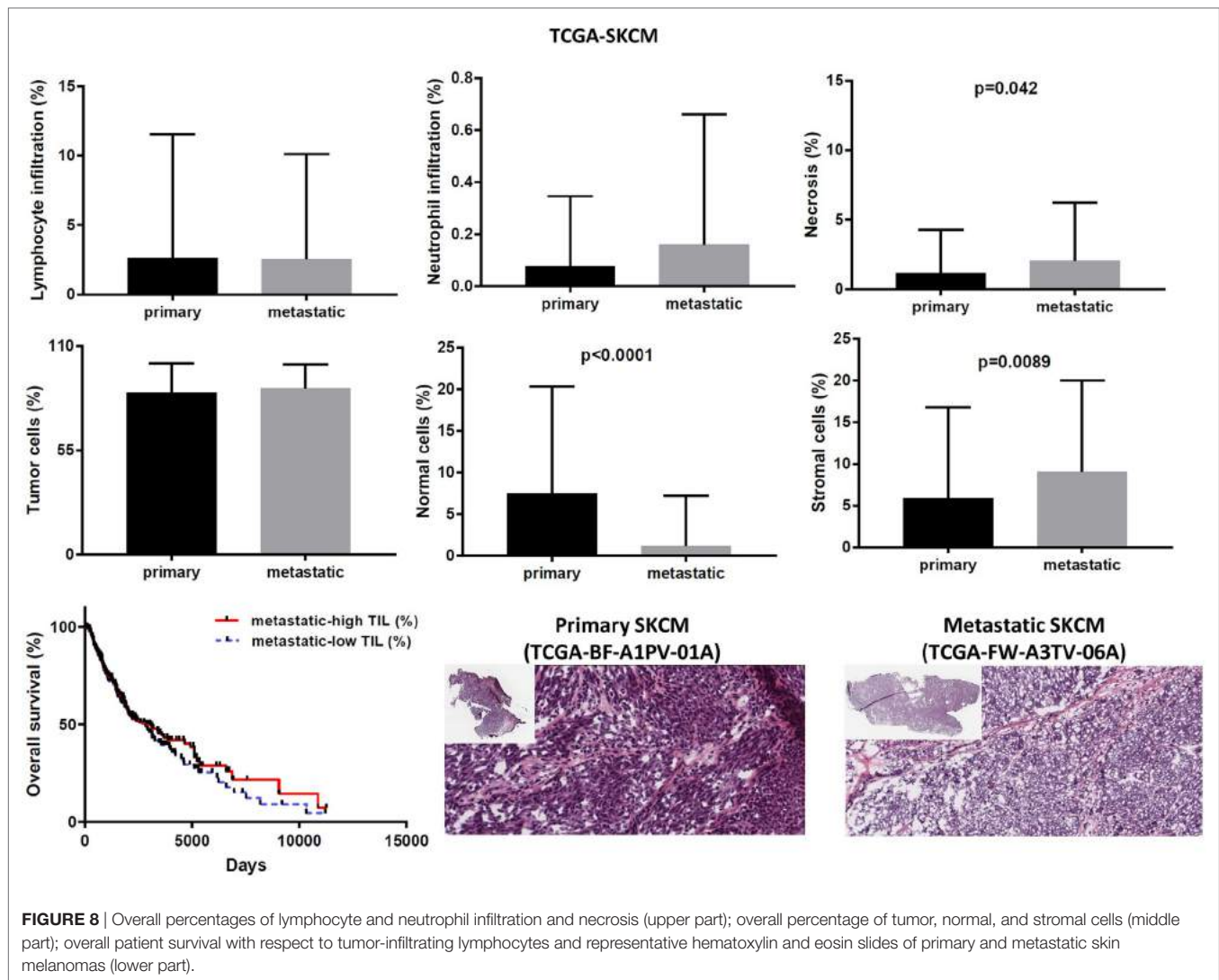
further observed in metastatic breast and thyroid cancers suggesting that although initially regarded as an indicator of a failed immune response, CTLs/NK cells (among other inflammatory cells) also support tumor development (93, 94). This observation is in agreement with previous reports supporting that regardless of the tumor's origin, an inflamed tumor microenvironment has many tumor-promoting effects (91, 92). In line with this, we found significantly elevated expression of various suppressive factors, correlating with a high cytolytic index, in metastatic skin melanomas, breast, and thyroid cancers. For example, high levels of CTLA-4, PD-1, PD-L1/2, LAG3, and IDO1 that we detected in metastatic melanoma, were many fold times more significantly associated with high cytolytic levels, pointing towards the existence of immunosuppression in these metastatic tumors (Figure S8 in Supplementary Material).

The above-mentioned vast range in the CYT and the different levels of infiltration of inflammatory cells (T cells and neutrophils) is best reflected by the different survival curves produced among different types of cancer. In some tumor types

(ACC, SKCM, BLCA, LIHC, MESO, OV, STAD, THCA, and UCEC), high CYT was associated with an improved outcome; whereas in others (LGG, BRCA, THYM, LUAD/LUSC, PAAD, PRAD, and READ) it is correlated with a worse outcome. Among LGG, THYM, and BRCA, we showed that both individual and simultaneous high levels of GZMA and PRF1 were significantly associated with a worse prognosis, whereas the simultaneous low levels of both cytolytic genes led to a significant shift toward a positive effect. Nevertheless, we could not observe this across different breast cancer datasets. Furthermore, contrasting results mentioning a worse effect of PRF1 on survival of BRCA patients were also recently reported in another large-scale meta-analysis (95). The difference between the two studies might be due to cohort-specific bias or power-related discrepancies. Of interest, among certain tumor types including ACC, SKCM and BRCA, the simultaneous expression of both cytolytic genes synergistically affected patient survival.

Tumor-infiltrating lymphocytes are mononuclear cells of the immune system that intrude the tumor tissue, and their presence
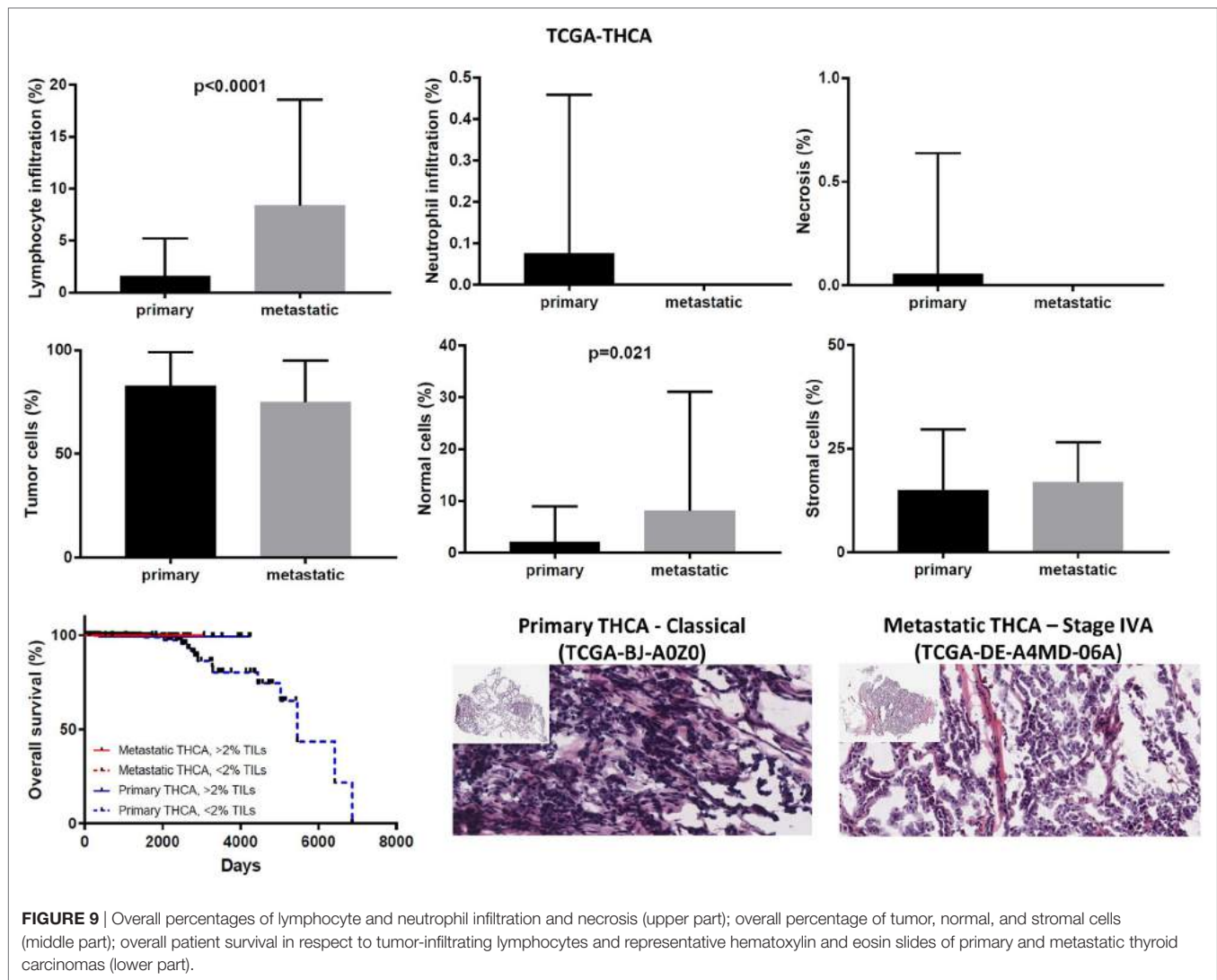
FIGURE 9 | Overall percentages of lymphocyte and neutrophil infiltration and necrosis (upper part); overall percentage of tumor, normal, and stromal cells (middle part); overall patient survival in respect to tumor-infiltrating lymphocytes and representative hematoxylin and eosin slides of primary and metastatic thyroid carcinomas (lower part).

has been reported in solid tumors, such as breast, colon, lung, and cervical cancers, as well as in melanoma (43, 96–98). Low levels of CD8+ TILs are related with the likelihood of response and may escalate during therapy in responding tumors (2, 99). Further, the location of CD8+ TILs at the invasive margin of tumors may indicate an effective immune response (42, 99, 100). The tumor microenvironment may limit extravasation of effector T cells into the tumor, diminish their expansion, or reduce their viability (101). In BRCA, an increased TIL load in the stroma of the tumor was reported to associate with a higher prospect of therapy in early stage TNBC and Her2+ patients (98). Assessing light microscopy data of tissue slides, we found a higher TIL load in primary BRCA compared to the metastatic counterparts, but the differences were not significant ($p > 0.05$). These lymphocytic infiltrates mirror favorable host antitumor immune responses within these samples. Although the presence of high TIL levels has been previously linked with a more favorable prognosis in patients with Her2+ and early stage TNBC (46–48), we found no significant difference in the outcome of TNBC or TPBC between high and low TIL load.

Tumor-associated neutrophils also compose a significant part of the inflammatory cell infiltrate in several tumor types (102–105), but the mechanisms by which they affect tumor progression are only now being investigated. Recent studies point toward the tumor-promoting effects of neutrophils. Histologic studies performed on a variety of tumor types have shown that the increased TAN load correlates with unfavorable recurrence-free, cancer-specific and overall patient survival in kidney cancer, skin melanoma, colorectal cancer, and head and neck cancer (106). It has also been suggested that TANs can drive the metastasis of breast cancer cells to the liver or the lung (107, 108), activating angiogenesis (109, 110). In contrast, older reports suggested that neutrophils have antitumoral effects, by inducing direct cytotoxicity of target cells, and decreasing the size and the number of lung metastatic foci (111–113). Interestingly, the anticancer activity of TANs was reported to mostly culminate into anticancer activity *via* oxidative burst (114, 115). Despite the heavily debated role in favor or against cancer, the latest research shows that TANs do play a key role in various aspects of tumor development, from malignant transformation to tumor progression, modification

of the extracellular matrix, angiogenesis, cell migration, and immunosuppression (116–121). Due to their contradictory roles in cancer, neutrophils are now classified into two subpopulations, antitumor and pro-tumor TANs (117). We detected very low percentage of TANs in primary breast and thyroid carcinomas and almost null levels in their metastatic counterparts. We noticed higher neutrophilic infiltration in TNBC compared to TPBC, but without reaching statistical significance ($p > 005$). In skin melanoma, we noticed even less neutrophilic infiltration, being slightly higher in the metastatic tumors.

Overall, the multiple crosstalks among different tumor-infiltrating immune cells, including TILs and TANs, was suggested to promote or inhibit the establishment of a permissive tumor microenvironment (17). A better understanding of the role of these cells will provide opportunities for the immunomodulation and the improvement of the existing antitumor therapies.

To conclude, we have measured the CYT in terms of RNA and protein levels in a large number of TCGA datasets, in order to understand how different cancers induce and adapt to immune responses. We associated each cancer's CYT with patient survival both in primary and metastatic cases and evaluated the tumor-infiltration of lymphocytes and neutrophils in H&E-stained sections of the same tumors. Our data suggest that the cytolytic index along with the existence of complicated associations among various tumor-infiltrated immune cells is capable to promote evasion from immunosurveillance in certain cancers.

SUPPLEMENTARY MATERIAL

The Supplementary Material for this article can be found online at http://www.frontiersin.org/articles/10.3389/fonc.2018.00027/full#supplementary-material.

REFERENCES

1. Swart M, Verbrugge I, Beltman JB. Combination approaches with immune-checkpoint blockade in cancer therapy. *Front Oncol* (2016) 6:233. doi:10.3389/fonc.2016.00233

2. Topalian SL, Hodi FS, Brahmer JR, Gettinger SN, Smith DC, McDermott DF, et al. Safety, activity, and immune correlates of anti-PD-1 antibody in cancer. *N Engl J Med* (2012) 366:2443–54. doi:10.1056/NEJMoa1200690

3. Postow MA, Callahan MK, Wolchok JD. Immune checkpoint blockade in cancer therapy. *J Clin Oncol* (2015) 33(17):1974–82. doi:10.1200/JCO.2014.59.4358

4. Peters PJ, Borst J, Oorschot V, Fukuda M, Krähenbühl O, Tschopp J. Cytotoxic T lymphocyte granules are secretory lysosomes, containing both perforin and granzymes. *J Exp Med* (1991) 173:1099–109. doi:10.1084/jem.173.5.1099

5. Trapani JA, Smyth MJ. Functional significance of the perforin/granzyme cell death pathway. *Nat Rev Immunol* (2002) 2:735–47. doi:10.1038/nri911

6. Suda T, Takahashi T, Golstein P, Nagata S. Molecular cloning and expression of the Fas ligand, a novel member of the tumor necrosis factor family. *Cell* (1993) 75:1169–78. doi:10.1016/0092-8674(93)90326-L

7. Johnstone RW, Frew AJ, Smyth MJ. The TRAIL apoptotic pathway in cancer onset, progression and therapy. *Nat Rev Cancer* (2008) 8:782–98. doi:10.1038/nrc2465

8. Quail DF, Joyce JA. Microenvironmental regulation of tumor progression and metastasis. *Nat Med* (2013) 19:1423–37. doi:10.1038/nm.3394

9. Joyce JA, Pollard JW. Microenvironmental regulation of metastasis. *Nat Rev Cancer* (2009) 9:239–52. doi:10.1038/nrc2618

10. Kerkar SP, Restifo NP. Cellular constituents of immune escape within the tumor microenvironment. *Cancer Res* (2012) 72:3125–30. doi:10.1158/0008-5472.CAN-11-4094

11. Bindea G, Mlecnik B, Tosolini M, Kirilovsky A, Waldner M, Obenauf AC, et al. Spatiotemporal dynamics of intratumoral immune cells reveal the immune landscape in human cancer. *Immunity* (2013) 39:782–95. doi:10.1016/j.immuni.2013.10.003

12. Herbst RS, Soria J-C, Kowanetz M, Fine GD, Hamid O, Gordon MS, et al. Predictive correlates of response to the anti-PD-L1 antibody MPDL3280A in cancer patients. *Nature* (2014) 515:563–7. doi:10.1038/nature14011

13. Ji RR, Chasalow SD, Wang L, Hamid O, Schmidt H, Cogswell J, et al. An immune-active tumor microenvironment favors clinical response to ipilimumab. *Cancer Immunol Immunother* (2012) 61:1019–31. doi:10.1007/s00262-011-1172-6

14. Chan TA, Wolchok JD, Snyder A. Genetic basis for clinical response to CTLA-4 blockade in melanoma. *N Engl J Med* (2015) 373:1984. doi:10.1056/NEJMc1508163

15. Swierczak A, Mouchemore KA, Hamilton JA, Anderson RL. Neutrophils: important contributors to tumor progression and metastasis. *Cancer Metastasis Rev* (2015) 34:735–51. doi:10.1007/s10555-015-9594-9

16. Kim J, Bae JS. Tumor-associated macrophages and neutrophils in tumor microenvironment. *Mediators Inflamm* (2016) 2016:6058147. doi:10.1155/2016/6058147

17. Shaul ME, Fridlender ZG. Neutrophils as active regulators of the immune system in the tumor microenvironment. *J Leukoc Biol* (2017) 102:343–9. doi:10.1189/jlb.5MR1216-508R

18. Miller DM, Flaherty KT, Tsao H. Current status and future directions of molecularly targeted therapies and immunotherapies for melanoma. *Semin Cutan Med Surg* (2014) 33:60–7. doi:10.12788/j.sder.0081

19. Yi Q. Novel immunotherapies. *Cancer J* (2009) 15:502–10. doi:10.1097/PPO.0b013e3181c51f0d

20. Galluzzi L, Vacchelli E, Pedro J-MB-S, Buqué A, Senovilla L, Baracco EE, et al. Classification of current anticancer immunotherapies. *Oncotarget* (2014) 5:12472–508. doi:10.18632/oncotarget.2998

21. Hinrichs CS, Rosenberg SA. Exploiting the curative potential of adoptive T-cell therapy for cancer. *Immunol Rev* (2014) 257:56–71. doi:10.1111/imr.12132

22. Pardoll DM. The blockade of immune checkpoints in cancer immunotherapy. *Nat Rev Cancer* (2012) 12:252–64. doi:10.1038/nrc3239

23. Li Y, Li F, Jiang F, Lv X, Zhang R, Lu A, et al. A mini-review for cancer immunotherapy: molecular understanding of PD-1/ PD-L1 pathway &

translational blockade of immune checkpoints. *Int J Mol Sci* (2016) 17:E1151. doi:10.3390/ijms17071151

24. Zou W, Wolchok JD, Chen L. PD-L1 (B7-H1) and PD-1 pathway blockade for cancer therapy: mechanisms, response biomarkers, and combinations. *Sci Transl Med* (2016) 8:rv4–328. doi:10.1126/scitranslmed.aad7118

25. Brown SD, Warren RL, Gibb EA, Martin SD, Spinelli JJ, Nelson BH, et al. Neo-antigens predicted by tumor genome meta-analysis correlate with increased patient survival. *Genome Res* (2014) 24:743–50. doi:10.1101/gr.165985.113

26. Caleb Rutledge W, Kong J, Gao J, Gutman DA, Cooper LAD, Appin C, et al. Tumor-infiltrating lymphocytes in glioblastoma are associated with specific genomic alterations and related to transcriptional class. *Clin Cancer Res* (2013) 19:4951–60. doi:10.1158/1078-0432.CCR-13-0551

27. Thul PJ, Åkesson L, Wiking M, Mahdessian D, Geladaki A, Ait Blal H, et al. A subcellular map of the human proteome. *Science* (2017) 356:eaal3321. doi:10.1126/science.aal3321

28. Uhlén M, Fagerberg L, Hallström BM, Lindskog C, Oksvold P, Mardinoglu A, et al. Proteomics. Tissue-based map of the human proteome. *Science* (2015) 347:1260419. doi:10.1126/science.1260419

29. Uhlen M, Zhang C, Lee S, Sjöstedt E, Fagerberg L, Bidkhori G, et al. A pathology atlas of the human cancer transcriptome. *Science* (2017) 357:eaan2507. doi:10.1126/science.aan2507

30. Uhlen M. A human protein atlas for normal and cancer tissues based on antibody proteomics. *Mol Cell Proteomics* (2005) 4:1920–32. doi:10.1074/mcp.M500279-MCP200

31. Rooney MS, Shukla SA, Wu CJ, Getz G, Hacohen N. Molecular and genetic properties of tumors associated with local immune cytolytic activity. *Cell* (2015) 160:48–61. doi:10.1016/j.cell.2014.12.033

32. Amelio I, Tsvetkov PO, Knight RA, Lisitsa A, Melino G, Antonov AV. SynTarget: an online tool to test the synergic effect of genes on survival outcome in cancer. *Cell Death Differ* (2016) 23:912. doi:10.1038/cdd.2016.12

33. Kaushansky K, Lichtman M, Beutler E, Kipps T, Prchal J, Seligsohn U. *Williams Hematology*. The McGraw-Hill Companies, Inc (2010).

34. Johnson BJ, Costelloe EO, Fitzpatrick DR, Haanen JBAG, Schumacher TNM, Brown LE, et al. Single-cell perforin and granzyme expression reveals the anatomical localization of effector CD8+ T cells in influenza virus-infected mice. *Proc Natl Acad Sci U S A* (2003) 100:2657–62. doi:10.1073/pnas.0538056100

35. Pagès F, Berger A, Camus M, Sanchez-Cabo F, Costes A, Molidor R, et al. Effector memory T cells, early metastasis, and survival in colorectal cancer. *N Engl J Med* (2005) 353:2654–66. doi:10.1056/NEJMoa051424

36. Pagès F, Kirilovsky A, Mlecnik B, Asslaber M, Tosolini M, Bindea G, et al. In situ cytotoxic and memory T cells predict outcome in patients with early-stage colorectal cancer. *J Clin Oncol* (2009) 27:5944–51. doi:10.1200/JCO.2008.19.6147

37. Sato E, Olson SH, Ahn J, Bundy B, Nishikawa H, Qian F, et al. Intraepithelial CD8+ tumor-infiltrating lymphocytes and a high CD8+/regulatory T cell ratio are associated with favorable prognosis in ovarian cancer. *Proc Natl Acad Sci U S A* (2005) 102:18538–43. doi:10.1073/pnas.0509182102

38. Schumacher K, Haensch W, Röefzaad C, Schlag PM. Prognostic significance of activated CD8+ T cell infiltrations within esophageal carcinomas. *Cancer Res* (2001) 61:3932–6.

39. Kawai O, Ishii G, Kubota K, Murata Y, Naito Y, Mizuno T, et al. Predominant infiltration of macrophages and CD8+ T cells in cancer nests is a significant predictor of survival in stage IV nonsmall cell lung cancer. *Cancer* (2008) 113:1387–95. doi:10.1002/cncr.23712

40. Hendry S, Salgado R, Gevaert T, Russell PA, John T, Thapa B, et al. Assessing tumor-infiltrating lymphocytes in solid tumors. *Adv Anat Pathol* (2017) 24(5):235–51. doi:10.1097/PAP.0000000000000161

41. Balli D, Rech AJ, Stanger BZ, Vonderheide RH. Immune cytolytic activity stratifies molecular subsets of human pancreatic cancer. *Clin Cancer Res* (2017) 23:3129–38. doi:10.1158/1078-0432.CCR-16-2128

42. Spranger S, Spaapen RM, Zha Y, Williams J, Meng Y, Ha TT, et al. Up-regulation of PD-L1, IDO, and Tregs in the melanoma tumor microenvironment is driven by CD8+ T cells. *Sci Transl Med* (2013) 5:200ra116. doi:10.1126/scitranslmed.3006504

43. Salgado R, Denkert C, Demaria S, Sirtaine N, Klauschen F, Pruneri G, et al. The evaluation of tumor-infiltrating lymphocytes (TILS) in breast cancer: recommendations by an International TILS Working Group 2014. *Ann Oncol* (2015) 26:259–71. doi:10.1093/annonc/mdu450

44. Tuaillon E, Valea D, Becquart P, Al Tabaa Y, Meda N, Bollore K, et al. Human milk-derived B cells: a highly activated switched memory cell population primed to secrete antibodies. *J Immunol* (2009) 182:7155–62. doi:10.4049/jimmunol.0803107

45. Gu-Trantien C, Loi S, Garaud S, Equeter C, Libin M, de Wind A, et al. CD4+ follicular helper T cell infiltration predicts breast cancer survival. *J Clin Invest* (2013) 123:2873–92. doi:10.1172/JCI67428

46. Yamaguchi R, Tanaka M, Yano A, Tse GM, Yamaguchi M, Koura K, et al. Tumor-infiltrating lymphocytes are important pathologic predictors for neoadjuvant chemotherapy in patients with breast cancer. *Hum Pathol* (2012) 43:1688–94. doi:10.1016/j.humpath.2011.12.013

47. Loi S, Sirtaine N, Piette F, Salgado R, Viale G, Van Eenoo F, et al. Prognostic and predictive value of tumor-infiltrating lymphocytes in a phase III randomized adjuvant breast cancer trial in node-positive breast cancer comparing the addition of docetaxel to doxorubicin with doxorubicin-based chemotherapy: BIG 02-98. *J Clin Oncol* (2013) 31:860–7. doi:10.1200/JCO.2011.41.0902

48. Ali HR, Provenzano E, Dawson S-J, Blows FM, Liu B, Shah M, et al. Association between CD8+ T-cell infiltration and breast cancer survival in 12,439 patients. *Ann Oncol* (2014) 25:1536–43. doi:10.1093/annonc/mdu191

49. Diem S, Hasan Ali O, Ackermann CJ, Bomze D, Koelzer VH, Jochum W, et al. Tumor infiltrating lymphocytes in lymph node metastases of stage III melanoma correspond to response and survival in nine patients treated with ipilimumab at the time of stage IV disease. *Cancer Immunol Immunother* (2017) 67(1):39–45. doi:10.1007/s00262-017-2061-4

50. Barber DL, Wherry EJ, Masopust D, Zhu B, Allison JP, Sharpe AH, et al. Restoring function in exhausted CD8 T cells during chronic viral infection. *Nature* (2006) 439:682–7. doi:10.1038/nature04444

51. Ahmadzadeh M, Johnson LA, Heemskerk B, Wunderlich JR, Dudley ME, White DE, et al. Tumor antigen-specific CD8 T cells infiltrating the tumor express high levels of PD-1 and are functionally impaired. *Blood* (2009) 114:1537–44. doi:10.1182/blood-2008-12-195792

52. Fourcade J, Kudela P, Sun Z, Shen H, Land SR, Lenzner D, et al. PD-1 is a regulator of NY-ESO-1-specific CD8+ T cell expansion in melanoma patients. *J Immunol* (2009) 182:5240–9. doi:10.4049/jimmunol.0803245

53. Mumprecht S, Schürch C, Schwaller J, Solenthaler M, Ochsenbein AF. Programmed death 1 signaling on chronic myeloid leukemia-specific T cells results in T-cell exhaustion and disease progression. *Blood* (2009) 114:1528–36. doi:10.1182/blood-2008-09-179697

54. Dong H, Strome SE, Salomao DR, Tamura H, Hirano F, Flies DB, et al. Tumor-associated B7-H1 promotes T-cell apoptosis: a potential mechanism of immune evasion. *Nat Med* (2002) 8(8):793–800. doi:10.1038/nm730

55. Strome SE, Dong H, Tamura H, Voss SG, Flies DB, Tamada K, et al. B7-H1 blockade augments adoptive T-cell immunotherapy for squamous cell carcinoma. *Cancer Res* (2003) 63:6501–5.

56. Hamanishi J, Mandai M, Iwasaki M, Okazaki T, Tanaka Y, Yamaguchi K, et al. Programmed cell death 1 ligand 1 and tumor-infiltrating CD8+ T lymphocytes are prognostic factors of human ovarian cancer. *Proc Natl Acad Sci U S A* (2007) 104:3360–5. doi:10.1073/pnas.0611533104

57. Ohigashi Y, Sho M, Yamada Y, Tsurui Y, Hamada K, Ikeda N, et al. Clinical significance of programmed death-1 ligand-1 and programmed death-1 ligand-2 expression in human esophageal cancer. *Clin Cancer Res* (2005) 11:2947–53. doi:10.1158/1078-0432.CCR-04-1469

58. Song M, Chen D, Lu B, Wang C, Zhang J, Huang L, et al. PTEN loss increases PD-L1 protein expression and affects the correlation between PD-L1 expression and clinical parameters in colorectal cancer. *PLoS One* (2013) 8(6):e65821. doi:10.1371/journal.pone.0065821

59. Gandini S, Massi D, Mandalà M. PD-L1 expression in cancer patients receiving anti PD-1/PD-L1 antibodies: a systematic review and meta-analysis. *Crit Rev Oncol Hematol* (2016) 100:88–98. doi:10.1016/j.critrevonc.2016.02.001

60. Wang X, Teng F, Kong L, Yu J. PD-L1 expression in human cancers and its association with clinical outcomes. *Onco Targets Ther* (2016) 9:5023–39. doi:10.2147/OTT.S105862

61. Kyi C, Postow MA. Checkpoint blocking antibodies in cancer immunotherapy. *FEBS Lett* (2014) 588:368–76. doi:10.1016/j.febslet.2013.10.015

62. Farkona S, Diamandis EP, Blasutig IM. Cancer immunotherapy: the beginning of the end of cancer? *BMC Med* (2016) 14:73. doi:10.1186/s12916-016-0623-5

63. Topalian SL, Drake CG, Pardoll DM. Immune checkpoint blockade: a common denominator approach to cancer therapy. *Cancer Cell* (2015) 27:451–61. doi:10.1016/j.ccell.2015.03.001

64. Jacquelot N, Roberti MP, Enot DP, Rusakiewicz S, Ternès N, Jegou S, et al. Predictors of responses to immune checkpoint blockade in advanced melanoma. *Nat Commun* (2017) 8. doi:10.1038/s41467-017-00608-2

65. Wang D, DuBois RN. Immunosuppression associated with chronic inflammation in the tumor microenvironment. *Carcinogenesis* (2015) 36:1085–93. doi:10.1093/carcin/bgv123

66. Yang JC, Hughes M, Kammula U, Royal R, Sherry RM, Topalian SL, et al. Ipilimumab (anti-CTLA4 antibody) causes regression of metastatic renal cell cancer associated with enteritis and hypophysitis. *J Immunother* (2007) 30:825–30. doi:10.1097/CJI.0b013e318156e47e

67. Camacho LH, Antonia S, Sosman J, Kirkwood JM, Gajewski TF, Redman B, et al. Phase I/II trial of tremelimumab in patients with metastatic melanoma. *J Clin Oncol* (2009) 27:1075–81. doi:10.1200/JCO.2008.19.2435

68. Ribas A. Anti-CTLA4 antibody clinical trials in melanoma. *Update Cancer Ther* (2007) 2:133–9. doi:10.1016/j.uct.2007.09.001

69. Ribas A, Kefford R, Marshall MA, Punt CJA, Haanen JB, Marmol M, et al. Phase III randomized clinical trial comparing tremelimumab with standard-of-care chemotherapy in patients with advanced melanoma. *J Clin Oncol* (2013) 31:616–22. doi:10.1200/JCO.2012.44.6112

70. Ribas A, Hanson DC, Noe DA, Millham R, Guyot DJ, Bernstein SH, et al. Tremelimumab (CP-675,206), a cytotoxic T lymphocyte associated antigen 4 blocking monoclonal antibody in clinical development for patients with cancer. *Oncologist* (2007) 12:873–83. doi:10.1634/theoncologist.12-7-873

71. Berman D, Parker SM, Siegel J, Chasalow SD, Weber J, Galbraith S, et al. Blockade of cytotoxic T-lymphocyte antigen-4 by ipilimumab results in dysregulation of gastrointestinal immunity in patients with advanced melanoma. *Cancer Immun* (2010) 10:11.

72. Ott PA, Hodi FS, Kaufman HL, Wigginton JM, Wolchok JD. Combination immunotherapy: a road map. *J Immunother Cancer* (2017) 5:16. doi:10.1186/s40425-017-0218-5

73. Rodríguez PC, Ochoa AC. Arginine regulation by myeloid derived suppressor cells and tolerance in cancer: mechanisms and therapeutic perspectives. *Immunol Rev* (2008) 222:180–91. doi:10.1111/j.1600-065X.2008.00608.x

74. Qian F, Villella J, Wallace PK, Mhawech-Fauceglia P, Tario JD, Andrews C, et al. Efficacy of levo-1-methyl tryptophan and dextro-1-methyl tryptophan in reversing indoleamine-2,3-dioxygenase-mediated arrest of T-cell proliferation in human epithelial ovarian cancer. *Cancer Res* (2009) 69:5498–504. doi:10.1158/0008-5472.CAN-08-2106

75. Reisser D, Onier-Cherix N, Jeannin JF. Arginase activity is inhibited by L-NAME, both in vitro and in vivo. *J Enzyme Inhib Med Chem* (2002) 17:267–70. doi:10.1080/1475636021000006252

76. Garg AD, Vandenberk L, Van Woensel M, Belmans J, Schaaf M, Boon L, et al. Preclinical efficacy of immune-checkpoint monotherapy does not recapitulate corresponding biomarkers-based clinical predictions in glioblastoma. *Oncoimmunology* (2017) 6(4):e1295903. doi:10.1080/2162402X.2017.1295903

77. Shigehisa Kitano AI. Cancer neoantigens: a promising source of immunogens for cancer immunotherapy. *J Clin Cell Immunol* (2015) 6:2. doi:10.4172/2155-9899.1000322

78. Schumacher TN, Schreiber RD. Neoantigens in cancer immunotherapy. *Science* (2015) 348:69–74. doi:10.1126/science.aaa4971

79. Riaz N, Morris L, Havel JJ, Makarov V, Desrichard A, Chan TA. The role of neoantigens in response to immune checkpoint blockade. *Int Immunol* (2016) 28:411–9. doi:10.1093/intimm/dxw019

80. McGranahan N, Furness AJS, Rosenthal R, Ramskov S, Lyngaa R, Saini SK, et al. Clonal neoantigens elicit T cell immunoreactivity and sensitivity to immune checkpoint blockade. *Science* (2016) 351:1463–9. doi:10.1126/science.aaf1490

81. Tran E, Turcotte S, Gros A, Robbins PF, Lu Y, Dudley ME, et al. Cancer immunotherapy based on mutation-specific CD4+ T cells in a patient with epithelial cancer. *Science* (2014) 344:641–5. doi:10.1126/science.1251102

82. Kreiter S, Vormehr M, Van De Roemer N, Diken M, Löwer M, Diekmann J, et al. Mutant MHC class II epitopes drive therapeutic immune responses to cancer. *Nature* (2015) 520:692–6. doi:10.1038/nature14426

83. Carreno BM, Magrini V, Becker-Hapak M, Kaabinejadian S, Hundal J, Petti AA, et al. A dendritic cell vaccine increases the breadth and diversity of melanoma neoantigen-specific T cells. *Science* (2015) 348:803–8. doi:10.1126/science.aaa3828

84. Gubin MM, Zhang X, Schuster H, Caron E, Ward JP, Noguchi T, et al. Checkpoint blockade cancer immunotherapy targets tumour-specific mutant antigens. *Nature* (2014) 515:577–81. doi:10.1038/nature13988

85. Castle JC, Kreiter S, Diekmann J, Löwer M, Van De Roemer N, De Graaf J, et al. Exploiting the mutanome for tumor vaccination. *Cancer Res* (2012) 72:1081–91. doi:10.1158/0008-5472.CAN-11-3722

86. Verdegaal EME, De Miranda NFCC, Visser M, Harryvan T, Van Buuren MM, Andersen RS, et al. Neoantigen landscape dynamics during human melanoma-T cell interactions. *Nature* (2016) 536:91–5. doi:10.1038/nature18945

87. Vonderheide RH, Domchek SM, Clark AS. Immunotherapy for breast cancer: what are we missing? *Clin Cancer Res* (2017) 23:2640–6. doi:10.1158/1078-0432.CCR-16-2569

88. Chen YP, Zhang Y, Lv JW, Li YQ, Wang YQ, He QM, et al. Genomic analysis of tumor microenvironment immune types across 14 solid cancer types: immunotherapeutic implications. *Theranostics* (2017) 7(14):3585–94. doi:10.7150/thno.21471

89. Riaz N, Havel JJ, Makarov V, Desrichard A, Urba WJ, Sims JS, et al. Tumor and microenvironment evolution during immunotherapy with nivolumab. *Cell* (2017) 171:934.e–49.e. doi:10.1016/j.cell.2017.09.028

90. Snyder A, Makarov V, Merghoub T, Yuan J, Zaretsky JM, Desrichard A, et al. Genetic basis for clinical response to CTLA-4 blockade in melanoma. *N Engl J Med* (2014) 371(23):2189–99. doi:10.1056/NEJMoa1406498

91. Mantovani A, Allavena P, Sica A, Balkwill F. Cancer-related inflammation. *Nature* (2008) 454:436–44. doi:10.1038/nature07205

92. Candido J, Hagemann T. Cancer-related inflammation. *J Clin Immunol* (2013) 33(Suppl 1):S79–84. doi:10.1007/s10875-012-9847-0

93. Coussens LM, Werb Z. Inflammation and cancer. *Nature* (2002) 420:860–7. doi:10.1038/nature01322

94. Grivennikov SI, Greten FR, Karin M. Immunity, inflammation, and cancer. *Cell* (2010) 140:883–99. doi:10.1016/j.cell.2010.01.025

95. Garg AD, De Ruysscher D, Agostinis P. Immunological metagene signatures derived from immunogenic cancer cell death associate with improved survival of patients with lung, breast or ovarian malignancies: a large-scale meta-analysis. *Oncoimmunology* (2016) 5(2):e1069938. doi:10.1080/2162402X.2015.1069938

96. Underwood JC. Lymphoreticular infiltration in human tumours: prognostic and biological implications: a review. *Br J Cancer* (1974) 30:538–48. doi:10.1038/bjc.1974.233

97. Tsuyuguchi I, Shiratsuchi H, Fukuoka M. T-lymphocyte subsets in primary lung cancer. *Jpn J Clin Oncol* (1987) 17:13–7.

98. Savas P, Salgado R, Denkert C, Sotiriou C, Darcy PK, Smyth MJ, et al. Clinical relevance of host immunity in breast cancer: from TILs to the clinic. *Nat Rev Clin Oncol* (2015) 13:228–41. doi:10.1038/nrclinonc.2015.215

99. Tumeh PC, Harview CL, Yearley JH, Shintaku IP, Taylor EJM, Robert L, et al. PD-1 blockade induces responses by inhibiting adaptive immune resistance. *Nature* (2014) 515:568–71. doi:10.1038/nature13954

100. Chen PL, Roh W, Reuben A, Cooper ZA, Spencer CN, Prieto PA, et al. Analysis of immune signatures in longitudinal tumor samples yields insight into biomarkers of response and mechanisms of resistance to immune checkpoint blockade. *Cancer Discov* (2016) 6:827–37. doi:10.1158/2159-8290.CD-15-1545

101. Joyce JA, Fearon DT. T cell exclusion, immune privilege, and the tumor microenvironment. *Science* (2015) 348:74–80. doi:10.1126/science.aaa6204

102. Wislez M, Rabbe N, Marchal J, Milleron B, Crestani B, Mayaud C, et al. Hepatocyte growth factor production by neutrophils infiltrating bronchioloalveolar subtype pulmonary adenocarcinoma: role in tumor progression and death. *Cancer Res* (2003) 63:1405–12.

103. Jensen HK, Donskov F, Marcussen N, Nordsmark M, Lundbeck F, Von Der Maase H. Presence of intratumoral neutrophils is an independent prognostic factor in localized renal cell carcinoma. *J Clin Oncol* (2009) 27:4709–17. doi:10.1200/JCO.2008.18.9498

104. Trellakis S, Bruderek K, Dumitru CA, Gholaman H, Gu X, Bankfalvi A, et al. Polymorphonuclear granulocytes in human head and neck cancer: enhanced

inflammatory activity, modulation by cancer cells and expansion in advanced disease. *Int J Cancer* (2011) 129:2183–93. doi:10.1002/ijc.25892

105. Donskov F. Immunomonitoring and prognostic relevance of neutrophils in clinical trials. *Semin Cancer Biol* (2013) 23:200–7. doi:10.1016/j.semcancer.2013.02.001

106. Shen M, Hu P, Donskov F, Wang G, Liu Q, Du J. Tumor-associated neutrophils as a new prognostic factor in cancer: a systematic review and meta-analysis. *PLoS One* (2014) 9(6):e98259. doi:10.1371/journal.pone.0098259

107. Tabariès S, Ouellet V, Hsu BE, Annis MG, Rose AA, Meunier L, et al. Granulocytic immune infiltrates are essential for the efficient formation of breast cancer liver metastases. *Breast Cancer Res* (2015) 17:45. doi:10.1186/s13058-015-0558-3

108. Wculek SK, Malanchi I. Neutrophils support lung colonization of metastasis-initiating breast cancer cells. *Nature* (2015) 528:413–7. doi:10.1038/nature16140

109. Nozawa H, Chiu C, Hanahan D. Infiltrating neutrophils mediate the initial angiogenic switch in a mouse model of multistage carcinogenesis. *Proc Natl Acad Sci U S A* (2006) 103:12493–8. doi:10.1073/pnas.0601807103

110. Tazzyman S, Niaz H, Murdoch C. Neutrophil-mediated tumour angiogenesis: subversion of immune responses to promote tumour growth. *Semin Cancer Biol* (2013) 23:149–58. doi:10.1016/j.semcancer.2013.02.003

111. Ishihara Y, Fujii T, Iijima H, Saito K, Matsunaga K. The role of neutrophils as cytotoxic cells in lung metastasis: suppression of tumor cell metastasis by a biological response modifier (PSK). *In Vivo* (1998) 12:175–82.

112. Granot Z, Henke E, Comen EA, King TA, Norton L, Benezra R. Tumor entrained neutrophils inhibit seeding in the premetastatic lung. *Cancer Cell* (2011) 20:300–14. doi:10.1016/j.ccr.2011.08.012

113. López-Lago MA, Posner S, Thodima VJ, Molina AM, Motzer RJ, Chaganti RSK. Neutrophil chemokines secreted by tumor cells mount a lung antimetastatic response during renal cell carcinoma progression. *Oncogene* (2013) 32:1752–60. doi:10.1038/onc.2012.201

114. Finisguerra V, Di Conza G, Di Matteo M, Serneels J, Costa S, Thompson AAR, et al. MET is required for the recruitment of anti-tumoural neutrophils. *Nature* (2015) 522:349–53. doi:10.1038/nature14407

115. Garg AD, Vandenberk L, Fang S, Fasche T, Van Eygen S, Maes J, et al. Pathogen response-like recruitment and activation of neutrophils by sterile immunogenic dying cells drives neutrophil-mediated residual cell killing. *Cell Death Differ* (2017) 24:832–43. doi:10.1038/cdd.2017.15

116. Granot Z, Jablonska J. Distinct functions of neutrophil in cancer and its regulation. *Mediators Inflamm* (2015) 2015:701067. doi:10.1155/2015/701067

117. Sionov RV, Fridlender ZG, Granot Z. The multifaceted roles neutrophils play in the tumor microenvironment. *Cancer Microenviron* (2015) 8:125–58. doi:10.1007/s12307-014-0147-5

118. Coffelt SB, Wellenstein MD, de Visser KE. Neutrophils in cancer: neutral no more. *Nat Rev Cancer* (2016) 16:431–46. doi:10.1038/nrc.2016.52

119. Treffers LW, Hiemstra IH, Kuijpers TW, van den Berg TK, Matlung HL. Neutrophils in cancer. *Immunol Rev* (2016) 273:312–28. doi:10.1111/imr.12444

120. Liang W, Ferrara N. The complex role of neutrophils in tumor angiogenesis and metastasis. *Cancer Immunol Res* (2016) 4:83–91. doi:10.1158/2326-6066.CIR-15-0313

121. Mishalian I, Bayuh R, Levy L, Zolotarov L, Michaeli J, Fridlender ZG. Tumor-associated neutrophils (TAN) develop pro-tumorigenic properties during tumor progression. *Cancer Immunol Immunother* (2013) 62:1745–56. doi:10.1007/s00262-013-1476-9

Advantages of publishing in Frontiers

OPEN ACCESS
Articles are free to read
for greatest visibility
and readership

FAST PUBLICATION
Around 90 days
from submission
to decision

HIGH QUALITY PEER-REVIEW
Rigorous, collaborative,
and constructive
peer-review

TRANSPARENT PEER-REVIEW
Editors and reviewers
acknowledged by name
on published articles

Frontiers
Avenue du Tribunal-Fédéral 34
1005 Lausanne | Switzerland

Visit us: www.frontiersin.org
Contact us: info@frontiersin.org | +41 21 510 17 00

**REPRODUCIBILITY OF
RESEARCH**
Support open data
and methods to enhance
research reproducibility

DIGITAL PUBLISHING
Articles designed
for optimal readership
across devices

FOLLOW US
@frontiersin

IMPACT METRICS
Advanced article metrics
track visibility across
digital media

EXTENSIVE PROMOTION
Marketing
and promotion
of impactful research

LOOP RESEARCH NETWORK
Our network
increases your
article's readership